

PREDICTION OF AXISYMMETRIC CHEMICALLY-
REACTING COMBUSTOR FLOWFIELDS

By

JERRY WAYNE SAMPLES

Bachelor of Science in Chemical Engineering
Clarkson College of Technology
Potsdam, New York
1969

Master of Science
Oklahoma State University
Stillwater, Oklahoma
1979

Submitted to the Faculty of the Graduate College
of the Oklahoma State University
in partial fulfillment of the requirements
for the Degree of
DOCTOR OF PHILOSOPHY
May, 1983

Thesis
1983D
S192p
cop. 2



PREDICTION OF AXISYMMETRIC CHEMICALLY-
REACTING COMBUSTOR FLOWFIELDS

Thesis Approved:

David G. Dille

Thesis Adviser

J. W. Maxwell

A. J. Ghajar

J. W. Maxwell

Norman N. Durham

Dean of the Graduate College

ACKNOWLEDGMENTS

The author wishes to express his appreciation to his major advisor, Dr. David G. Lilley, for his guidance and valuable assistance throughout this study. Appreciation is also expressed to the other committee members, Dr. Afshin J. Ghajar, Dr. James W. Maxwell and Dr. John A. Wiebelt, for their invaluable assistance in the preparation of the final manuscript.

A note of thanks is given to Colonel Robert M. Wilson and Colonel Michael A. Paolino of the United States Military Academy for their assistance and encouragement during the entire study. Thanks are also extended to Miss C. Snyder of the West Point Library for her assistance in obtaining many of the references cited herein. Thanks are also extended to Mrs. Neisa Lock for the excellence of the final copy and her response to many short suspenses.

Finally, special gratitude is expressed to my wife, Kathy, our sons Christopher and Steven, for their understanding, encouragement and countless sacrifices.

TABLE OF CONTENTS

| Chapter | Page |
|--|------|
| I. INTRODUCTION | 1 |
| 1.1 Combustion Phenomena and Design Problems | 1 |
| 1.2 Analytical Needs and the Present Research | 2 |
| 1.3 Theoretical Investigations | 4 |
| 1.4 The Present Contribution | 6 |
| II. REVIEW OF PREVIOUS AXISYMMETRIC COMBUSTOR STUDIES | 7 |
| 2.1 Previous Work in Nonreacting Flows | 7 |
| 2.2 Turbulence Models in Combustor Flows | 9 |
| 2.3 Numerical Prediction Methods | 11 |
| 2.4 Experimental Measurements in Reacting Flows | 14 |
| III. RADIATION HEAT TRANSFER | 17 |
| 3.1 Background | 17 |
| 3.2 Radiation Models Available for Numerical Simulation | 18 |
| 3.3 Present Approach | 21 |
| 3.3.1 Choice of Radiation Model | 21 |
| 3.3.2 Finite Difference Formulation of the Mathematical Model | 26 |
| 3.3.3 Assessment of the Model | 29 |
| IV. COMBUSTION MODELING AND CARBON MONOXIDE PRODUCTION | 32 |
| 4.1. Background | 32 |
| 4.2. Combustion Models Available for Numerical Simulation | 34 |
| 4.2.1 Simple One-Step Chemical Reaction Model | 34 |
| 4.2.2 Two-Step Global Model | 38 |
| 4.2.3 Complex Global Models, Quasi- global | 40 |
| 4.3 Present Approach | 43 |
| 4.3.1 Choice of Combustion Model | 43 |
| 4.3.2 Finite Difference Formulation of the Mathematical Model | 45 |
| 4.3.3 Assessment of the Models | 49 |

| Chapter | Page |
|--|------|
| V. MODELING OF NO PRODUCTION IN COMBUSTORS | 51 |
| 5.1 Background | 51 |
| 5.2 Nitrogen Oxide Models Available for Numerical Simulation | 53 |
| 5.2.1 Thermal NO | 53 |
| 5.2.2 Fuel NO | 54 |
| 5.2.3 Prompt NO | 55 |
| 5.2.4 Evaluation of the NO Models | 56 |
| 5.3 Present Approach | 58 |
| 5.3.1 Choice of a Nitrogen Oxide Model | 58 |
| 5.3.2 Finite Difference Formulation of the Mathematical Model | 60 |
| 5.3.3 Assessment of the Model | 61 |
| VI. PREDICTIVE TECHNIQUE | 63 |
| 6.1 Scope and Method of Approach | 63 |
| 6.2 Mathematical Model | 63 |
| 6.2.1 Governing Equations | 63 |
| 6.2.2 Solution Techniques and Finite Difference Formulation | 65 |
| 6.2.3 Boundary Conditions | 67 |
| 6.2.4 Solution Procedure | 68 |
| 6.3 Operation of STRAC | 70 |
| 6.3.1 General Arrangement | 70 |
| 6.3.2 Major Variables | 71 |
| 6.3.3 MAIN Subprogram | 72 |
| 6.3.3.1 Introduction | 72 |
| 6.3.3.2 CO Preliminaries | 72 |
| 6.3.3.3 C1 Parameters and Control Indices | 74 |
| 6.3.3.4 C2 Initial Operations | 74 |
| 6.3.3.5 C3 Iteration Loop | 74 |
| 6.3.3.6 C4 Final Operations and Output | 75 |
| 6.4 Closure | 75 |
| VII. RESULTS AND ANALYSIS | 76 |
| 7.1 Complex Chemical Kinetic Model | 76 |
| 7.2 Radiation Heat Transfer | 80 |
| 7.3 General Predictions | 82 |
| 7.4 Recirculation Zone Lengths | 88 |
| 7.5 Reliability of Predictions | 89 |

| Chapter | Page |
|--|------|
| VIII. CONCLUSIONS | 91 |
| REFERENCES. | 93 |
| APPENDIXES | 102 |
| APPENDIX A - TABLES | 103 |
| APPENDIX B - FIGURES | 117 |
| APPENDIX C - DEVELOPMENT OF THE SECOND-ORDER RADIATION FLUX EQUATIONS | 148 |
| APPENDIX D - DEVELOPMENT OF THE FINITE DIFFERENCE | 154 |
| APPENDIX E - STRAC CODE LISTING | 163 |
| APPENDIX F - MAJOR FORTRAN VARIABLES | 231 |

LIST OF TABLES

| Table | Page |
|---|------|
| I. Extended C-H-O Chemical Kinetic Reaction Mechanism (Reference 10) | 104 |
| II. Nitrogen Reactions from Mellor (Reference 74) | 105 |
| III. Source Terms and Exchange Coefficients Used in the General Equation of Φ | 106 |
| IV. The Form of the Components of the Linearized Source Term | 108 |
| V. Subroutine Tasks | 109 |
| VI. Principle Dependent Variables and Controlling Parameters | 112 |
| VII. Effect of Radiation Heat Transfer on Radial Temperature Distribution at Axial Locations; Swirl Number = 0.332 | 114 |
| VIII. Effect of Radiation Heat Transfer on Radial Temperature Distribution at Axial Locations; Swirl Number = 0.721 | 115 |
| IX. Effect of Radiation Heat Transfer on Nitrogen Oxide Concentrations; Swirl Number = 0.720 | 116 |

LIST OF FIGURES

| Figure | Page |
|---|------|
| 1. Structure of a Numerical Model | 118 |
| 2. Radiant Energy Balance in a Specified Direction | 119 |
| 3. Flux Model for Cylindrical Coordinates | 120 |
| 4. Radiation Balance at an Inside Combustor Wall | 121 |
| 5. Irregularly Spaced Grid System with Flow Domain Fitted Inside | 122 |
| 6. Staggered Grid and Notation for the Rectangular Computational Mesh | 123 |
| 7. The Three Control Volumes Associated with Points of the Three Grids | 124 |
| 8. Flow Chart of Computer Program Showing the Subroutine Arrangement | 125 |
| 9. Axial Velocity Profiles for $S = 0.721$ | 126 |
| 10. Swirl Velocity Profiles for $S = 0.721$ | 127 |
| 11. Temperature Profiles for $S = 0.721$ | 128 |
| 12. Axial Velocity Profiles for $S = 1.980$ | 129 |
| 13. Swirl Velocity Profiles for $S = 1.980$ | 130 |
| 14. Temperature Profiles for $S = 1.980$ | 131 |
| 15. Axial Velocity Profiles for $S = 0.0$ and Pressure at 3.8 atm. | 132 |
| 16. Temperature Profiles for $S = 0.0$ and Pressure at 3.8 atm. | 133 |
| 17. Nitrogen Oxide Profiles for $S = 0.0$ and Pressure at 3.8 atm. | 134 |
| 18. Axial Velocity Profiles for $S = 0.3$ and Pressure at 3.8 atm. | 135 |

| Figure | Page |
|--|------|
| 19. Temperature Profiles for $S = 0.3$ and Pressure at 3.8 atm. | 136 |
| 20. Nitrogen Oxide Profiles for $S = 0.3$ and Pressure at 3.8 atm. | 137 |
| 21. Temperature Profiles for $S = 0.53$ | 138 |
| 22. Nitrogen Oxide Profiles for $S = 0.53$ | 139 |
| 23. Carbon Monoxide Profiles for $S = 0.53$ | 140 |
| 24. Axial Velocity Profiles for $S = 0.0$ | 141 |
| 25. Temperature Profiles for $S = 0.0$ | 142 |
| 26. Axial Velocity Profiles for $S = 0.52$ | 143 |
| 27. Swirl Velocity Profiles for $S = 0.52$ | 144 |
| 28. Temperature Profiles for $S = 0.52$ | 145 |
| 29. Predicted Central Toroidal Recirculation Zone for Hot and Cold Cases | 146 |
| 30. Predicted Corner Recirculation Zone for Hot and Cold Cases. . | 147 |

LIST OF SYMBOLS

| | |
|---------------------------|---|
| a | - Absorption coefficient |
| a_j | - Coupling coefficient for some cell face |
| A | - Area |
| AX | - Number of carbon atoms |
| $^{\circ}C$ | - Degrees Celsius |
| C_{EBU} | - Eddy-break-up constant |
| C_{g1}, C_{g2} | - Fuel fluctuating concentration constants |
| C_p | - Specific heat |
| $C_0, C_1, C_2,$ C_u | - Constants |
| D | - Diameter |
| D_w | - Diffusion coefficient, western cell face |
| E | - Eastern neighbors |
| E_B | - Blackbody emissive power |
| E/R | - Activation energy |
| f | - Under-relaxation factor |
| g | - Component of fuel fluctuations |
| h | - Enthalpy |
| H_{CO} | - Heating value of carbon monoxide |
| H_{fu} | - Heating value of fuel component |
| i | - Stoichiometric ratio |
| I | - Radiation flux in the direction of positive x |
| I, J | - Mesh Point |

| | |
|------------------|---|
| J | - Radiation flux in the direction of negative x |
| k | - Kinetic energy of turbulence |
| K | - Radiation flux in the direction of positive r or Kelvin degrees |
| \bar{K} | - Equilibrium constant |
| L | - Radiation flux in the direction of negative r |
| M_{CO} | - Mass fraction of carbon monoxide |
| M_{fu} | - Mass fraction of fuel |
| M_{NO} | - Mass fraction of nitrogen oxide |
| M_{OX} | - Mass fraction of oxygen |
| M_{pr} | - Mass fraction of products |
| N | - Northern neighbors |
| p | - Pressure |
| P | - Kinetic reaction constant |
| PPM | - Parts per million |
| Q | - Total heat flux |
| r | - Radius or Radial direction |
| R | - Residual source term |
| R_{CO} | - Carbon monoxide reaction rate |
| R_{fu} | - Fuel reaction rate |
| R_{f1}, R_{f2} | - Nitrogen oxide forward reaction rate |
| R_{NO} | - Composite nitrogen oxide reaction rates |
| R_r | - Radial component of radiation flux |
| R_{r1}, R_{r2} | - Nitrogen oxide reverse reaction rates |
| R_x | - Axial component of radiation flux |
| s | - Scattering coefficient |
| S | - Southern neighbor or swirl number |

| | |
|-----------|---------------------------------------|
| S_ϕ | - Source term of the general variable |
| t | - Time |
| T | - Temperature |
| u | - Axial velocity component |
| u_o | - Inlet axial velocity |
| v | - Radial velocity component |
| V | - Volume |
| \bar{V} | - Velocity vector |
| w | - Swirl velocity component |
| W | - Western neighbor |
| W_{CO} | - Molecular weight of carbon monoxide |
| W_{fu} | - Molecular weight of fuel |
| x | - Axial direction |

Greek Letters

| | |
|------------|--|
| α | - Absorptivity |
| Γ | - Exchange coefficient |
| ϵ | - Emissivity or dissipation rate of turbulence |
| μ | - Effective viscosity |
| ρ | - Time-mean density or reflectivity |
| σ | - Prandtl-Schmidt number or Stefan-Boltzman constant |
| τ | - Transmissivity |
| ϕ | - Dependent variable |
| ψ | - Stream function |
| ω | - Vorticity |

Superscripts

- n+1 - Next iteration value
- n - Present iteration value

Subscripts

- j - n, s, e, w cell faces
- o - Outer radius
- r - Radial component
- w - Wall
- x - Axial component or number of carbon atoms
- y - Number of hydrogen atoms

CHAPTER I

INTRODUCTION

1.1 Combustion Phenomena and Design Problems

The continuous flow combustor of a gas turbine engine contains a high energy combustion process which is simultaneously turbulent and strongly backmixed. Such flows are classified as complex because of the complicated fluid dynamics and chemistry (1). Consideration of convective mass transfer, thermodynamics, thermal radiation and dissociation kinetics have caused combustor design to develop as an art, based on restricted experimental data, rather than a science. The consequence is that the design of most combustion chambers is far from optimum (2). Strict pollutant controls established by the 1972 EPA Aircraft Emission Standards further complicate the design procedure (3). The designer must develop economic, efficient and pollutant free combustion systems; the task being to provide a route which leads to the accomplishment of design objectives more quickly and less expensively than current practice permits (4).

In design situations, costly and time consuming experimental procedures must be supplemented with mathematical models. These models bring benefits, and entail costs; a good model is one with a high ratio of benefit to cost. Benefits include knowing quantitatively, in advance, what will be the performance of equipment which has not yet been built, or which has not yet been operated in the manner under

investigation (5). The mathematical model (numerical simulation of the governing partial differential equations) cannot stand alone, but through its use and coupled with carefully selected experiments, experimental costs can be drastically reduced. These advanced tools (mathematical models), while still in their incipient stages, offer the potential of reducing the design and development time required for gas turbine combustors. At the same time, the analytical models serve to increase the understanding of the phenomena affecting combustor performance and provide the basis for designing better combustors (6).

1.2 Analytical Needs and the Present Research

The combustion engineering designer faces a myriad of problems in developing a computational model to approximate the complex aerothermochemistry of the gas turbine combustor. The task is to provide a route which optimizes the path between irreconcilable alternatives of, for example, efficiency and pollution. Some combustor modeling problems are:

1. Physical process - turbulence, radiation, combustion, pollution formation and multiphase effects.
2. Computer programs - 0-, 1-, 2-, and 3- dimensional approaches in steady state and transient cases.
3. Unresolved problems - effect of swirl and wall proximity on turbulence, turbulence-reaction interaction and multiphase simulation (7). Further emphasis on numerical simulation of the physical process of chemical kinetics, pollutant formation mechanisms and thermal radiation stresses their importance to the combustor designer (2, 8).

Practical combustors, such as those in gas turbines, consume fuel through a complex series of chemical reactions. Models of the combustion process are envisioned which contain 39 species entering into over 1000 reactions (9). Such models would tax the storage capacity of even larger computers and would be impractical from an economic standpoint. However, because of the coupling of the heat release with the chemical reaction mechanism, the details of the reaction must be modeled accurately (10). The designer must choose an accurate model which exhibits sufficient computational economy for practical application.

Public concern regarding pollutant emissions has made the problem of modeling flames an absolute requirement for the definition of the relationships between the combustion and pollutant formation mechanisms. Coupling of the relevant processes governing the degree of completion of combustion and the formation of pollutants must be included into the numerical scheme (11). Like the reaction mechanism, numerous pollution formation mechanisms are available in varying degrees of complexity. The chemical kinetic influence on NO_x production is an area in need of concentrated research and is a major problem for combustion designers.

Many combustors are large enough in size for thermal radiation to be important (2). The magnitude and validity of this statement has been debated (12, 13). Combustor designers are faced with a formidable task when including radiation theory. With at least four methods available for modeling the radiation physics, the designer must choose the one which is both economic and accurate. Accuracy is further complicated due to insufficient information concerning absorptivities, emissivities and scattering coefficients.

The present research work is concerned with a numerical simulation of the physical process occurring in a combustion chamber. The specific problem is to develop a two-dimensional axisymmetric combustion model for steady, turbulent, reacting, swirling flow in a combustor with the physical processes fully installed. The flow may have swirl induced by swirl vanes at the inlet. Interior flowfield domains may have various degrees of recirculation including a central toroidal recirculation zone around the center line, and a corner recirculation zone due to sudden chamber expansion. Significant heat release may cause pollutant formation in the recirculation zone which is perpetuated into the exhaust region. Of particular interest is interaction of the reactions model and the pollution formation mechanism, together with the net effect of radiation heat transfer. The need exists for a two-dimensional model capable of accurate flowfield prediction of the physical process with reasonable computational economy.

1.3 Theoretical Investigation

Numerical simulation of combustor systems has been a viable option since the advent of enhanced systems and numerical models of the partial differential equations associated with combustion. The mathematical model should provide results more cheaply, quickly, and accurately than is possible through experimentation. In order to achieve this, the model should simulate the flowfield in all respects (geometry, boundary conditions, physical properties of gases, turbulence, etc.) and provide a means for solving the governing equations. Two areas of difficulty are clearly evident: the simulation of the physical processes and solution of the multi-dimensional flowfield (14).

Further, the model must be candidly assessed by comparison with reliable experimental data.

The availability of reliable data for verification of the numerical model is but one of the problems associated with good predictions. The designer is faced with a formidable set of variable inputs, all of which must be carefully analyzed to determine the overall accuracy of the final product. Examination of the structure of the numerical model, as seen in Figure 1 of Appendix B, reveals that the model comprises a set of component models covering the chemistry, turbulence, multiphase flow, geometry, radiation and flow approximations. These components are used within the context of a set of governing equations which, with the specification of a set of initial and boundary conditions form a well-posed problem which is solved by means of some equation solving technique to ultimately yield a prediction. In attempting to resolve the question of how good a prediction is, prior to using the overall model in a design analysis, the accuracy of the experimental data being used to judge the model must be known, as must the accuracy of the equation solver. A comprehensive study of the available predictive techniques and an analysis of their predictive capabilities is available in a recent work (15).

A predictive procedure based on the TEACH code, a numerical model which solves the governing equations, has been developed. Details of this program are found in Chapter VI of this study. Additionally, a brief discussion of the turbulence modeling problem can be found in Chapter II.

1.4 The Present Contribution

The main objective of the present investigation is to develop a numerical simulation which compliments the hydrodynamics by including the physical processes of combustion, pollutant formation and radiation heat transfer. The theoretical investigation results in a two-dimensional axisymmetric swirl flow reacting model which is used to predict flowfield variables including, temperature, velocity, species concentration and radiation heat transfer. Detailed background analysis of available models and a preferred method of including each physical process are found in Chapter III thru V. Fundamental operation of the computer code is formalized in Chapter VI.

Numerous experimental results and associated predictions, when available, are used to validate the applicability of the resulting simulation. Comparisons of velocity, temperature and pollutant concentration used in the validation process are discussed in Chapter VII. Here, the value of the code is substantiated. Finally, Chapter VIII summarizes the conclusions of the present work and gives recommendations for future work.

CHAPTER II

REVIEW OF PREVIOUS AXISYMMETRIC COMBUSTOR STUDIES

Previous experimental and theoretical studies in axisymmetric recirculating flows provide valuable insight for this investigation. Publications concerning reacting, turbulent flows have been carefully studied. Included in the following summary are the significant results which emphasize reacting turbulent flows, with and without swirl. Information pertaining specifically to complex chemical kinetics, radiation heat transfer and pollution formation mechanisms are addressed in subsequent chapters.

2.1 Previous Work in Nonreacting Flows

The effect of expansion angle was experimentally investigated by Chaturvedi (16) to determine the general characteristics of axisymmetric flow at abrupt expansions of 15°, 30°, 45° and 90°. Mean motion and turbulence, together with the patterns of separation, were determined. Further, the boundary proximity to the separation surface is seen to have almost no effect on the maximum intensity attained by the turbulence, but its effect on the production and diffusion of turbulence is striking.

Owen (17) studied the initial mixing regions of free and confined coaxial airjets with recirculation. Both jets exhibited recirculation in the mixing regions, with the confined jet exhibiting an additional

corner recirculation zone. Measurements of the axial and radial mean velocity profiles show that the time-average characteristics of the two flowfields are substantially different. Significant increases in both the longitudinal and lateral extent of the recirculation zone for the confined case were confirmed.

Habib and Whitelaw (18) investigated velocity characteristics of confined coaxial jets with and without swirl. Swirl numbers of 0.0 and 0.23 were compared through measurement of axial and radial velocities. They found that as the swirl number is increased from zero, a region of recirculation on the centerline tends to grow while the jet spreads more rapidly away from the centerline. Their results were compared with calculations based on the solution of finite-difference forms of the steady, Navier-Stokes equations. It was shown that the nonswirling case could be adequately represented while the swirling case was less adequate.

Turbulent flows with separation were studied by Durst and Rastogi (19), both experimentally and theoretically. A square obstacle was placed in a two-dimensional channel to create a separated flow and associated turbulence. Laser Doppler anemometer measurements were taken to characterize the flowfield. They used a recirculating flow program to produce theoretical results for comparison with their experimental data. They concluded that streamline patterns outside the separation zone could be adequately predicted, but more work was needed on the turbulence model to obtain accurate calculations in the separated flow region.

Kubo and Gouldin (20) developed a numerical technique for solving axisymmetric, incompressible turbulent swirling flow problems. They utilized a stream function-vorticity approach coupled with a $k-\epsilon$

turbulence model. This numerical technique was applied to turbulent swirling flow inside a simplified combustor with a diameter ratio of four to one. They reported the effect of inner and outer swirl, axial velocity ratio and Reynolds number on the formation, size and location of the recirculation zone.

A form of the TEACH code was developed by Green and Whitelaw (21) to compare calculations with measurements of isothermal flow in axisymmetric models of combustor geometries. Measurements were obtained, with water flowing in a plexiglass arrangement, by laser Doppler anemometry. They reported reasonable agreement between calculations and measurements except in regions affected by recirculation, where discrepancies rise to 25 percent. Also, downstream regions not in direct contact with the recirculation zone had discrepancies of approximately 10 percent.

Rhode et al. (22) investigated swirling nonreacting flow similar to that found in a conventional gas turbine combustor. They utilized numerical computations for a two-dimensional axisymmetric flowfield including a conventional $k-\epsilon$ turbulence model and realistic accommodation of swirl effects. Their results include recirculation zone characterization and predicted mean streamline patterns. Comparison of the nonswirling case with measurements exhibits good qualitative agreement. They demonstrate the validity of their computations by comparing predicted mean streamline patterns with pathlines traced out by soap bubbles in flow visualization experiments they conducted.

2.2 Turbulence Models in Combustor Flows

A variety of turbulence models were investigated by Lilley (23) in an effort to predict inert turbulent swirl flows. The models include:

mixing length extensions, energy-length models, stress models and algebraic stress models. A numerical finite-difference procedure was utilized to generate results for comparison with experimental data. The simpler mixing length model provided adequate predictions as did the energy-length model, however the latter was deemed more universally applicable.

Launder and Spalding (24) studied the application of the $k-\epsilon$ turbulence model to nine substantially different kinds of turbulent flow. They present three different two-equation turbulence models and support their adoption of the $k-\epsilon$ model. Predictions generated by the $k-\epsilon$ model are compared with experimental data and other turbulence model predictions for each of the nine flow situations. They conclude that the $k-\epsilon$ model is the simplest model that permits prediction of both near-wall and free-shear-flow phenomena without adjustments to constants or functions and its use led to accurate predictions of flows with recirculation as well as those of the boundary layer kind.

Three turbulence models were used by Tennankore and Steward (25) to predict flow patterns within confined jets. Numerical solutions of the differential equations governing isothermal and nonisothermal flows were compared with experimental data. Their investigation shows that the $k-\epsilon$ model is superior when predicting velocity and temperature profiles in nonisothermal confined jets. However, in isothermal flows, in the absence of measured values of k at the entrance, the $k-\epsilon$ model is less effective than the mixing length model. Also, the constants associated with these models are not universal.

Giberling et al. (26) utilized the $k-\epsilon$ model in a three-dimensional combustor flow analysis. They determined that since k and ϵ are used

only to specify the turbulent viscosity, the k - ϵ equations can be solved after determination of the flowfield for a given iteration. This allows for a substantial savings in computer time compared with two other turbulence models tested.

Novick et al. (27) simulated turbulence by way of the two-equation k - ϵ model in their theoretical combustor model of swirling, inert and reacting, turbulent, recirculating flows. They studied the effect of swirl on a combustor configuration which included a central hub and a sudden expansion in the main chamber. Their model was successful not only in predicting a valid solution but also in its economy. They concluded that the model was useful in predicting experimental results with reasonable trendwise accuracy.

2.3 Numerical Prediction Methods

Numerical procedures for predicting combustion chamber flows are reviewed by Lilley (4). Marching methods are associated with parabolic boundary-layer flows with relaxation methods being used for elliptic recirculating flows. Two- and three-dimensional geometries are discussed for each method. Flowfield variables are the stream function-vorticity, ψ - ω or primitive pressure-velocity, p - u - v formulation where the latter exhibits easy transition from two- to three-dimensions. The difficulties of modeling aerothermochemistry and developments attained are discussed. Sample predictions demonstrate the capabilities of the numerical models.

Spalding (28) discusses the difficulties in producing mathematical models for multi-dimensional flow situations such as those in continuous combustors. Computational procedures are presented for solving two-

and three-dimensional steady flow problems, both with and without swirl. Lilley (29) presented a similar work for combustor swirl flows. Both felt that difficulties exist in combining physical and mathematical models, but they felt that computation models were capable of predicting flowfield characteristics.

An example of a time-dependent numerical technique was presented by Hirt et al. (30). SOLA, a simplified version of the Marker and Cell method was developed for use by persons with little experience in numerical fluid dynamics. Sample computations demonstrate the utility of the code.

Manheimer-Timnat (31) develops a parabolic boundary-layer code using the stream function-vorticity variable set. Two different flow situations are considered. Peck and Samuelson (32) also use the ψ - ω approach and demonstrate favorable qualitative correlation with experimental observations. Both applications are for two-dimensional flows.

A primitive pressure-velocity code was developed by Lilley (33) for two-dimensional, inert and reacting recirculating flows with strong swirl. Detailed formulation of the governing differential equations and adaptation into finite-difference form was provided. Swirl number effects on mean axial and swirl velocities were presented along with streamline and recirculation zone predictions. Results demonstrated trend conformity with experimental results and proved the applicability of this prediction method.

Khalil et al. (34) utilized the primitive pressure-velocity approach to investigate local flow properties in two-dimensional furnaces. Comparison of calculations and experiments are provided to

determine the overall precision of the model. They concluded that general agreement is demonstrated although some deficiencies do exist. Also, agreement is sufficient to justify calculations for many engineering purposes. Model comparisons of temperature, axial and swirl velocities are provided to support their conclusions.

Computer simulation of liquid-fueled combustors was investigated by Gosman and Ioannides (35). They used the same model as Lilley (33) and Khalil (34) with the addition of a droplet model for liquid sprays. They found the model adequate for studying the effects of turbulent dispersion of droplets in combustors.

Although three-dimensional models are not specifically addressed in this investigation, they are included for completeness. Works by Patankar and Spalding (36), Ellail et al. (2), Serag-Elden and Spalding (37), Pan (38), Mongia and Reynolds (39), and Srivatsa (6) provide valuable insight in both mathematical and physical modeling. Patankar and Spalding (36) introduce many physical realities including radiation heat transfer to their model and present results of computations. Fast kinetic models, advanced radiation methods and comparison of computational and experimental works are presented by Ellail et al. (2). Mongia and Reynolds (39) produced an advanced fully three-dimensional model for reacting flowfields in gas turbine combustors. They included an eddy-break-up chemical reaction model, radiation heat transfer and fuel spray droplet phenomena to increase the quality of their predictions. Good results were obtained for a number of complex combustion systems. Srivatsa (6) expanded the program of Mongia and Reynolds (39) to include a four-step chemical reaction scheme. The result was a marked increase in predictive capability as compared with

the two-step chemical reaction model. A major discrepancy in predicting H_2 was reported.

Other works pertaining to gas turbine combustion systems are available (40, 41, 42, 43, 44). An excellent summary of combustion modeling in two- and three-dimensional systems is presented by McDonald (15).

2.4 Experimental Measurements in Reacting Flows

Validation of computational results must be accomplished through comparison with experimental measurements. Khalil et al. (45) conducted an experimental study using a 2 meter long, 0.2 meter diameter furnace fitted with swirl vanes with angles of 70° , 60° , 52° and 45° . They measured axial and swirl velocities along with temperature profiles for two swirl numbers. Their experiment was conducted to provide data for comparison with numerical computations which they produced. Thus, their data is particularly important to other theoretical studies.

Owen et al. (46) used a 12.2 cm diameter axisymmetric combustor to study combustion of natural gas. Replaceable swirl vanes were used to achieve swirl numbers of 0.0, 0.3 and 0.6. Measurements included near axial and mean tangential velocities, temperature, hydrocarbon and NO concentrations. They concluded that swirl, pressure, and fuel/air velocities produce major changes in the time-mean flowfield within a turbulent flame combustor and that this significantly influences pollutant formation.

Temperature and species concentration measurements were made by Owen (47) for swirling combustion. The effects of swirl on the combustion are discussed. Particularly important are the concentration

measurements of CO and NO which are easily compared to temperature fields.

Scheefer and Sawyer (48) studied premixed fuel lean combustion in an opposed jet combustor. Temperature and chemical concentrations are presented for equivalence ratios of 0.45 and 0.625. Experimental and analytical results showed fair agreement. A discussion of chemical kinetic reactions is included.

A similar investigation was performed by McDonnell et al. (49). They studied species concentration and temperature in a reverse flow jet with recirculations. They reported CO, O₂, NO and NO_x concentrations as a function of temperature. It was apparent that NO and NO_x concentrations were strongly temperature dependent but also depend on recirculation zone size and mixing. Similarly CO concentrations are temperature dependent but in an inverse relation. Cooler temperatures producing more CO. Flow visualization studies demonstrate the recirculation effects.

Measurements of three velocity components in a model furnace with and without combustion were made by Baker et al. (50). They used swirl numbers of 0.0 and 0.52 to study the effect of swirl in an expansion chamber. Comparison of hot and cold flows revealed larger forward velocities in the combusting flows and correspondingly larger regions of recirculation. Swirl was observed to reduce the length of the flame.

Sawyer (51) measured composition and temperature in a model gas turbine. This effort was devoted to understanding the processes controlling the emissions of CO, HC and NO. Of particular note was the determination that NO levels are determined by kinetic levels which are strongly influenced by the maximum local temperatures. Also, sig-

nificant NO formation begins at the critical temperature range of 1900-2000°K and that NO once formed does not go away. The conclusion is that NO is most easily controlled by limiting the maximum local temperature.

Sadakata and Beer (52) used an experimental apparatus to calculate the formation rates of NO. Temperature and NO concentrations are compared to NO formation rates predicted by using the Zeldovich kinetic model. Temperature fluctuations and superequilibrium atom concentrations are considered in their calculations.

Other experimental studies of lesser importance to this study are available (53, 54, 55, 56).

CHAPTER III

RADIATION HEAT TRANSFER

3.1 Background

Numerical solution of the complex fluid dynamics and chemical reactions which occur in combustor systems are often simplified by excluding many of the physical processes, such as radiation, from the model. As the foundations for computer models were laid, authors commented that physical processes must be included in future simulations (14, 28) and that radiation, along with chemical kinetics and others, must appear in the next generation of computer models (4, 8, 29, 37, 57). It has been argued that in many flames, heat transfer by radiation is as important as that by turbulent mixing (12), however, others indicate that radiative heat transfer has only nominal importance as compared to the combustion reaction itself (13). Inclusion of a radiation model into a computer simulation should provide support for one of these opinions.

Three primary methods exist for inclusion of radiation heat transfer into the numerical simulation of a combustion system. These methods are the "zone method", the Monte Carlo method and the radiation flux method. Each method has strengths and weaknesses which must be considered when choosing one for application. Economy and accuracy are critical when building a simulation which includes many of the physical

processes.

Finally, there are many unknowns when dealing with radiation in furnaces and combustors. Absorptivities are often guessed or calculated using approximations. Unless soot production is included in the model, scattering coefficients are assigned based on experimental data. Experience has provided workable data and estimations which have merit but are not absolutes. Even with the best models, these variations make them subject to error.

3.2 Radiation Models Available for Numerical Simulation

The first method is the "zone method" of Hottel (58) which is based on the division of the surface area and gas volume, in the combustion chamber, into zones and the evaluation of their mutual exchange of heat and mass. These zones must be small enough to approximate isothermal regions, thus allowing for energy balances on each zone. An extensive series of integro-differential equations are introduced which, when solved numerically, result in a dense matrix requiring much computer storage area. Consequently, the computer model is cumbersome and expensive to operate, but it has been proven to be very accurate.

Accuracy is an advantage of the "zone method," but there are several disadvantages. Beer (59) points out that the starting point is an assumed knowledge of the patterns of flow, chemical heat release, and radiating gas concentrations within the furnace. Hottel (60) formulates the three-dimensional problem including five unknowns; the temperature, the gas concentration, and three components of velocity. Equations are written about the zones with the energy balance, radia-

tive transfer included, being the focal point. This produces a formidable set of simultaneous equations, five for each gas zone, and one for the surface where only energy is transferred. The simultaneous solution of these equations being an immense undertaking.

The problem is immediately simplified by assuming a cold flow solution of the mass concentrations and velocity components, leaving the energy equation alone to be solved for the "hot flow" case. Success in cold flow jet modeling and apparent agreement with hot flow solutions of the mass and velocity components is cited as an assumption. The resulting set of nonlinear equations are solved for the temperature in each zone, with the corresponding heat fluxes being obtained by inserting these temperatures into the energy equation. The accuracy of the model is excellent based on the listed assumptions. Even so, the computer model remains cumbersome and expensive.

It is apparent that a hot flow solution incorporating variation of all five unknowns would be difficult to manipulate. Additional difficulty arises due to incompatibility of the numerical techniques for the fluid flow simulation and the energy equation from the zone method. A further consideration is the addition of chemical kinetics and pollution calculations which would require additional temperature dependent equations. The previous five unknowns would immediately double, as a minimum. Thus, in the final analysis, the zone method and its inherent accuracy must be weighed carefully against ease of solution and computational costs.

The second method is the Monte Carlo technique. This method is considered the most flexible of the available procedures; however, it has not been extensively developed or tested, and its computational

efficiency is no better than that of the "zone method" (61). For these reasons, the Monte Carlo method will not be considered further.

The third method is the radiation flux method which attempts to replace the exact integro-differential equations of radiative transfer by approximate differential ones. The two- and three-dimensional models now being utilized are extensions by Patankar and Spalding (36) of an earlier one-dimensional model which was rendered applicable to heat transfer by Hamaker (62). Gosman et al. (61) and Lockwood et al. (63) have advanced the flux model to its present form. A recent work by Mongia and Reynolds (39) indicates that the accuracy of flux models is within 20% of measured values. Mongia, however, has chosen not to pursue his model to improve the accuracy of the predictions since he offers some concern about the accuracy of the measured data. The Lockwood model, an improvement on the original flux model, expands the number of equations to be solved and takes into account directional intensity at each point in the combustion chamber.

The basis of the flux model is the establishment of positive and negative flux vectors about the calculation point at discretized angles, usually orthogonal, to produce 2, 4, and 6 fluxes for 1-, 2-, and 3-dimensional problems, respectively. First-order differential equations for the fluxes are formulated and second-order differential equations are derived by summing flux pairs. This procedure reduces the number of differential equations to one per dimension required. Thus, in a two-dimensional problem, there are two differential equations required to determine the radiation flux. These equations are easily solved using finite differencing techniques.

The flux method offers two distinct advantages; first, it yields a sparse finite difference matrix where the temperature of the node is related to only its immediate neighbors, and second, the finite difference equations are of the same form as those solved for mass and the velocity components in momentum (61). The latter allows for immediate inclusion in computer codes such as TEACH (Teaching Elliptic Axisymmetric Characteristics Heuristically) and STARPIC (Swirling Turbulent Axisymmetric Recirculating flow in Practical Isothermal Combustor geometries) (64) and insures a more economical solution than with the zone method. The one disadvantage is the lack of proven accuracy. Since the flux method is a differential approximation to a complicated physical situation there exists considerable room for error. Lockwood, et al. (63) have attempted to remove some of this uncertainty by dividing the combustor into six angular zones and concentrating on the directional intensity about each node. They claim good agreement with experimental results but admit that more work is required. Thus, the flux method is still under close scrutiny since it has not been actively compared to measured radiation fluxes on an extensive basis.

3.3 Present Approach

3.3.1 Choice of Radiation Model

A physically realistic combustor simulation can be achieved by introducing radiation heat transfer via the flux method. The flux models inclusion into TEACH in two-dimensional axisymmetric form is facilitated by its differential form. Development of the mathematical model from the physical situation is included to facilitate under-

standing.

The flux method divides the radiation into three primary directions with positive and negative fluxes acting on gas volumes in each direction. The physical situation from which the basic radiation flux equations are derived is depicted in Figure 2 (65). Here a small volume element is exposed to incident radiation. Some of this energy is transmitted, absorbed, scattered out and some energy is scattered in from other elements. This process is simultaneously occurring in other volumes. This basic formulation is then expanded into the axisymmetric four flux model where the fluxes acting on the volumes are considered in both the negative and positive directions (61). The physical situation is demonstrated in cylindrical coordinates in Figure 3.

The differential equations describing the fluxes in the axial and radial directions are:

$$\frac{dI}{dx} = -(a + s)I + aE_B + \frac{S}{4}(I + J + K + L)$$

(i) (ii) (iii) (iv)

$$\frac{dJ}{dx} = (a + s)J - aE_B - \frac{S}{4}(I + J + K + L) \quad (3.1)$$

$$\frac{1}{r} \frac{d(rK)}{dr} = -(a + s)K + \frac{L}{r} + aE_B + \frac{S}{4}(I + J + K + L)$$

$$\frac{1}{r} \frac{d(rL)}{dr} = (a + s)L + \frac{L}{r} - aE_B - \frac{S}{4}(I + J + K + L)$$

where

I - radiation flux in the direction of positive x

J - radiation flux in the direction of negative x

K - radiation flux in the direction of positive r

- L - radiation flux in the direction of negative r
 a - absorption coefficient
 s - scattering coefficient
 $E_B = \sigma T^4$ - black emissive power at the fluid temperature
 σ - Stefan-Boltzman constant

Utilizing equation 3.1, term (i) represents the gradient of intensity in the specified direction; term (ii) is the reduction in intensity due to absorption within the volume, and the scattering of radiation into other volumes, which is in the specified direction upon arrival at these volumes; term (iii) is the increase in intensity due to emissions from the volume; and term (iv) is the increase in intensity due to scattering into the specified direction of radiation, which is incident upon the volume from all other directions. In Equation 3.1, the appearance of the L/r term is a consequence of cylindrical geometry and requires the assumption of isotropic distribution of radiation intensity.

Each pair of first-order equations in Equation (3.1) are combined to yield second-order equations which are then cast into finite difference form for use in the TEACH code. Axial and radial forms of the second-order equations are:

$$\frac{d}{dx} \left[\Gamma_x \frac{dR_x}{dx} \right] + a (E_B - R_x) + \frac{s}{2} (R_r - R_x) = 0$$

and

$$\frac{1}{r} \frac{d}{dr} \left[r \left(\Gamma_r \frac{dR_r}{dr} \right) \right] + a (E_B - R_r) + \frac{s}{2} (R_x - R_r) = 0$$

(3.2)

With the composite fluxes defined by:

$$R_x = \frac{1}{2} (I + J)$$

$$R_r = \frac{1}{2} (K + L)$$
(3.3)

and exchange coefficients, Γ , defined as:

$$\Gamma_x = \frac{1}{(a + s)}$$

$$\Gamma_r = \frac{1}{(a + s + \frac{1}{r})}$$
(3.4)

Development of these equations can be found in Appendix C.

Equation (3.2) forms the basis of the four-flux model. Application of the axisymmetric assumption has reduced the number of first-order differential equations from six to four. Scattering azimuthally (θ direction) is being disregarded; it is being supposed that any loss of radiant energy in the sideward direction is compensated for by an equal contribution from the neighboring section of the layer under observation (62). Essentially, there is no variation with respect to θ . Thus, in the axisymmetric combustion chamber, the four-flux model will be utilized to represent the radiation heat transfer in lieu of the six-flux model.

The boundary conditions are developed from the physical situation. Consider the outer shell of the combustion chamber subject to incident radiation and recall that

$$\rho + \alpha + \tau = 1$$
(3.5)

where

ρ = reflectivity

α = absorptivity

τ = transmissivity.

Since the wall is solid, $\tau = 0$. Assuming that $\alpha = \epsilon$, ϵ being the emissivity, Equation (3.5) becomes

$$\rho + \epsilon = 1. \quad (3.6)$$

Equation (3.6) is applied to gray surfaces such as the inside of the chamber. Recall the definitions of K and L , the radial radiation fluxes in the positive and negative directions respectively. Figure 4 demonstrates the physical situation at the wall where some amount of the incoming radiation is reflected and some radiation is emitted due to the wall temperature. The total radiation coming from the wall is

$$L_w = (1 - \epsilon_w) K_w + \epsilon_w E_w \quad (3.7)$$

As seen in Appendix C, this equation yields the following differential boundary condition for the north wall

$$\left[\Gamma_r \frac{dR_r}{dr} + \frac{\epsilon_w}{2 - \epsilon_w} (R_r - E_B) \right]_w = 0 \quad (3.8)$$

Similar boundary conditions are developed for each wall. The equivalent expression for the axial direction, eastern wall is

$$\left[\Gamma_x \frac{dR_x}{dx} + \frac{\epsilon_w}{2 - \epsilon_w} (R_x - E_B) \right]_w = 0 \quad (3.9)$$

Note that both the gradient and magnitude of the dependent variable are specified (66).

Both the basic flux equation and the associated boundary conditions are now specified. The next step is to determine an appropriate format for inclusion of these equations into the TEACH code.

3.3.2 Finite Difference Formulation of the Mathematical Model

Inclusion of the radiative heat transfer equations into the computer model is broken down into four areas which are tightly coupled. These areas include:

- a. The effect of radiative transfer on the solution of the energy equation by way of the enthalpy source term.
- b. Development of a procedure for including the radiative heat transfer equations into the basic code, which will be compatible with the general finite difference scheme.
- c. Treatment of boundary conditions to supplement (b) above.
- d. Use of a solution technique, such as the tri-diagonal matrix algorithm, to solve the difference equations. Each of these problems must be carefully considered to insure accurate solution of this model. The method of solution will be discussed separately for each case.

The coupling of the radiation fluxes with the enthalpy equations is via the enthalpy source term, S_h . In the absence of the radiation fluxes, the source term is set identically equal to zero. Each treatment of the radiative flux equations; four-flux, six-flux, or the enhanced Lockwood model, result in a slightly different representation of the enthalpy source. For the case addressed here, the four-flux model, the source term is represented by (61)

$$S_h = 2a(R_x + R_r - 2E) \quad (3.10)$$

Note that in the four-flux model only the axial and radial flux sums are present in the enthalpy term. Little further discussion is warranted since Equation (3.10) is cast directly into the code as it is seen here.

A significant part of the problem is to take Equation (3.2) from differential form to finite difference form. Since there are no convective terms and only one diffusion term it is necessary to modify the existing tri-diagonal-matrix algorithm to accomodate these differences. Additionally, since the radiation fluxes are directional in nature, the new tri-diagonal matrix algorithm will progress through the grid system in a different manner.

Before the flux equations can be cast into finite difference form they must be rearranged so as to identify the source terms. Rearrangement of Equation (3.2) provides the source term for the axial flux situation,

$$\frac{d}{dx} \left[\Gamma_x \frac{dR_x}{dx} \right] = a(R_x - E_B) + \frac{S}{2} (R_x - R_r) \quad (3.11)$$

where the source term is

$$S_x = a(R_x - E_B) + \frac{S}{2} (R_x - R_r) \quad (3.12)$$

In a similar manner the radial source term, S_r , is defined as

$$S_r = a(R_r - E_B) + \frac{S}{2} (R_r - R_x) \quad (3.13)$$

Equation (3.2) now becomes

$$\frac{d}{dx} \left[\Gamma_x \frac{dR_x}{dx} \right] = S_x \quad (3.14)$$

and

$$\frac{1}{r} \frac{d}{dr} \left[r \left(\Gamma_r \frac{dR_r}{dr} \right) \right] = S_r,$$

and will be cast into finite difference form.

An alternate approach to prescribing the flux equations prior to inclusion in the TEACH code is that of Felton, et al. (67). They begin with the general differential equation

$$\frac{\partial \beta \phi}{\partial t} + \text{div} (\beta \vec{V} \phi - \Gamma \text{ grad } \phi) = S_2 \quad (3.15)$$

where ϕ is the variable in question and $\beta = 0$ for the radiation terms, thus eliminating convection. For the axisymmetric case the axial radiation flux equation becomes

$$\frac{\partial}{\partial x} \left[\Gamma_x \frac{\partial R_x}{\partial x} \right] + \frac{1}{r} \left[\frac{\partial}{\partial r} (r \Gamma_x \frac{\partial R_x}{\partial r}) \right] = S_2 \quad (3.16)$$

where

$$S_2 = a(R_x - E_B) + \frac{s}{2} (R_x - R_r) + \frac{1}{r} \left[\frac{\partial}{\partial r} (r \Gamma_x \frac{\partial R_x}{\partial r}) \right] \quad (3.17)$$

Note that both sides of the equation contain the second partial derivative of the ϕ variable, R_x , with respect to r . Addition of these false terms does not change the value of the equation, however, treatment of the source term is difficult and requires great care. Several efforts were made to include this information into the TEACH code with little success. A problem was encountered whereby this addition to the source term caused the solution to diverge. After many attempts to modify the code to prevent divergence proved unsuccessful, this approach was abandoned in favor of the general method utilized by Mongia and Reynolds (39). Appendix D contains the transition of this differential model into the finite difference form.

The boundary conditions previously described are unusual because they contain both the gradient and values of the radiation flux variable. An implicit formulation is used to apply the boundary conditions to the basic flow field specification. Appendix D contains the finite difference formulation for the boundary conditions.

As seen in Appendix D, the finite difference equations are easily obtained from the differential form. These new equations are placed into code using the general TEACH format. A discussion of the code is found in Chapter VI.

3.3.3 Assessment of the Model

The various methods which can be used in modeling the radiative heat transfer were presented earlier. The enormous amounts of computer storage and incompatibility with the hydrodynamics of the combustor have eliminated the "zone method" from further consideration. The Monte Carlo method, which requires considerable computer storage without significant improvements in accuracy, has also been eliminated. The remaining flux model, available in several forms, appears to be the most useful, although possibly not the most accurate of the three. The basic multi-flux model proposed by Gosman and Lockwood (61) and used by both Mongia and Reynolds (39) and Felton, et al. (67) is the easiest to use while requiring the least computer storage. The improved model of Lockwood and Shah (63), considered to be a more accurate flux model, requires six additional equations to support the basic flux model, thus increasing the computational time and storage capacity. The decision as to which model should be used depends on many factors which must be carefully weighed against the desired and actual results.

Considering the magnitude of the computational task of predicting what is actually happening inside the combustion chamber, it is evident that some assumptions and approximations must be made. As previously stated, some experts in the field feel that the radiation effect is minimal and may not be worth a large amount of effort (13). Others feel that we must model every detail, especially radiation since it plays such an important part in the combustor (12). The choice has been to include radiation and determine its effect. But which model should be used.

In looking at the models, the cost of computational time must be considered. This consideration has been the grounds for eliminating both the Monte Carlo technique and the "zone method". Use of these methods require large computational facilities. This leaves the flux models as the primary candidates for future use. Which of these should be used.

In looking at the flux models many additional considerations must be weighed. A key factor is the eventual use of the information gained through their application. If the required data is the heat flux at the wall then a more accurate model, one which treats each segment of the wall separately, may be in order. Whereas if the desired result is an adequate temperature profile to predict pollution emissions, then a less vigorous model may be used. In either case, a primary result of calculating the radiative fluxes is the enthalpy source term. Unless these fluxes are quite large, it appears that the source term will have only a small effect on the final calculation of the temperature field. The temperature field is strongly dependent on the combustion heat release and may be weakly dependent on the radiation. Radiation

may serve only to smooth the temperature fluctuations in the combustion zone. Although this is important, it does not seem to justify a complicated, expensive model. Preliminary results support this conclusion, keeping in mind that the model used was the least extensive of the group. Considering the complexity of the situation, it does not appear economical to use the improved Lockwood and Shah model (63).

It is for these reasons that the basic multi-flux model has been chosen here. It has been shown to be fairly accurate (39). It is economical and provides input which can be useful in flow field temperature prediction. Coupled with the other assumptions made in the overall program, it should not detract appreciably from the overall result.

CHAPTER IV

COMBUSTION MODELING AND CARBON MONOXIDE PRODUCTION

4.1 Background

Choice of a combustion model is an important step in developing a numerical model which will accurately predict velocities, temperature, heat transfer and species concentration. Since the combustion model interacts with all other variables it is the driving force behind the numerical simulation. Many models have been proposed, most of which have survived validation testing, and are considered viable in application. It is left to the researcher to choose the model which satisfies requirements of accuracy and economy.

The questions of accuracy and economy must be viewed in light of the overall complexity of the numerical model for the entire combustor. Consider the large number of variables such as: three velocities, two radiation fluxes, temperature, pressure, turbulent kinetic energy, and dissipation, which must be included along with the combustion model to be chosen. It becomes necessary to consider economy early on. Accuracy is important to insure validation when compared to experimental results. Accuracy does not necessarily mean complexity but does mean absolute simulation of the physical process of combustion.

The combustion models available vary widely in complexity. The initial model is the simplified process whereby



This model, although simple, has been used extensively (32, 68-72). Increasing complexity is introduced through the two-step global fuel consumption reaction of the type



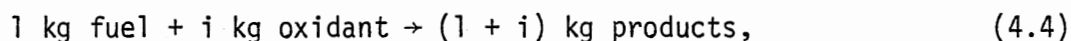
The ability of this model to predict the combustion reaction and demonstrate CO emissions has been demonstrated (32, 39, 40, 48). Quasi-global models have no limit. Models are envisioned which contain 39 species entering into over 1000 reactions or more nominally 25 species involved in 322 reactions (9). Others have used less ambitious extensions of the quasi-global model (10, 73-76).

It is apparent that with the inclusion of the combustion reaction it is possible to create a numerical simulation which is extremely large. Here, claims of accuracy must be weighed against economy of solution. Gosman, et al. (43) state that some 200 intermediate species have been identified in the combustion of typical hydrocarbon fuels. Further, any attempt to simulate all these species would precipitate a computational catastrophe. Care must be taken to insure that computational economy is carefully considered.

4.2 Combustion Models Available for Numerical Simulation

4.2.1 Simple One-Step Chemical Reaction Model

The one-step chemical reaction model has been in use for several years. Gosman, et al. (77) proposed the use of the single-step reaction mechanism



in their discussion of numerical modeling of combustor systems. They realized that during the combustion process hundreds of distinct chemical species are present in the combustor. However, the lack of thermodynamic, transport, and chemical-kinetic properties of a majority of the species would defeat any possibility of including them into the model. An additional problem of computational limits was a strong condition which favored the simplified model. This engineering assumption was the basis for other assumptions, all of which simplified the problem without unnecessary degradation of results.

This same model has been used continuously and appears in recent works (2, 42, 72, 78). Primary among the uses of this model is its ability to reliably predict the heat release. Hence, the net heat release can be obtained for the combustor in an economical way. Heat release information is also coupled, through the energy equation, to property evaluation and velocity calculations used to predict flowfield variables. Measured success in these areas support the use of this model (72).

Application of the simplified combustion model is normally via the turbulent flux (Reynolds) equation which for the general variable ϕ is

$$\frac{1}{r} \left[\frac{\partial}{\partial x} (\rho u r \phi) + \frac{\partial}{\partial r} (\rho u r \phi) - \frac{\partial}{\partial x} (r \Gamma_{\phi} \frac{\partial}{\partial x}) - \frac{\partial}{\partial r} (r \Gamma_{\phi} \frac{\partial}{\partial r}) \right] = S_{\phi} \quad (4.5)$$

In order to solve this model, two ϕ variables are considered. The fuel mass fraction m_{fu} , whose source term is the fuel consumption rate which will be discussed at length later. The other variable is the conserved property $m_{ox} - im_{fu}$, where m_{ox} is oxygen mass fraction and the associated source term is zero. The exchange coefficient Γ_{ϕ} is based on the Schmidt number which is assumed to be unity.

The apparent success of the simple combustion model is due in part to the treatment of the fuel consumption rate R_{fu} , which is actually S_{ϕ} for the case where ϕ is mass fraction of fuel. Gosman, et al. (77) used chemical kinetics to provide the rate of creation or conversely consumption of the specie in question. Thus, the specie concentration was uncoupled from the hydrodynamics of the problem. Spalding as referenced by Khalil, et al. (34) recognized that the hydrodynamics must be included in calculating the rate of fuel consumption. The model proposed was the eddy-break-up (EBU) model which attempts to incorporate the turbulent mixing effects into the reaction rate formulation. Spalding (12) illustrates the development of the EBU model to include the mixing length, $k-\epsilon$ and scale reduction versions.

Primary among the functions of the EBU model is to account for mixing caused by the break-up of large eddies in the combustion region. It is felt that the combustion may not be kinetically controlled in these regions but may be limited by the breakdown of the eddies (28). Thus a so-called second limit is introduced into the combustion process (70), and it is the fuel concentration dissipation rate which controls the reaction rate.

The EBU model accounts for the turbulent effects by introducing a new variable, g , the mean square fuel concentration fluctuating component, expressed algebraically

$$g = \frac{C_{g1}}{C_{g2}} \frac{\mu k}{\rho \epsilon} \left[\left(\frac{\partial m_{fu}}{\partial r} \right)^2 + \left(\frac{\partial m_{fu}}{\partial x} \right)^2 \right] \quad (4.6)$$

where $C_{g1} = 3.0$ and $C_{g2} = 0.132$ (32). Through the use of g , fluctuations of temperature and oxygen concentrations can be directly correlated to fuel fluctuations. The final fuel consumption rate expression for the EBU model is

$$R_{fu} = - C_{EBU} g^{1/2} \epsilon / k \quad (4.7)$$

where $C_{EBU} = 0.53$.

While the EBU model considers turbulent mixing, the Arrhenius model concentrates on the molecular process of combustion. Generally the Arrhenius rates are time-mean values bearing no relation to the fluctuating values of temperature or species concentration. A form of the Arrhenius reaction rate is

$$R_{fu} = - P p^2 m_{fu} m_{ox} \exp (-E/RT) \quad (4.8)$$

where P is a constant, p is the pressure, and E/R is the activation energy. Values for the activation energy are generally obtained from kinetic data.

Combination of the EBU and Arrhenius reaction rates allows consideration of both molecular and turbulence controlled combustion. Generally, this is accomplished by utilizing the minimum value of the EBU and Arrhenius fuel consumption rates (32, 72). Other possibilities exist such as the use of only the EBU rates when both are of the same

order of magnitude (70).

The combined EBU - Arrhenius model is often used with the single-step combustion model, however, other methods are available. Khalil, et al. (34) use a model which is physically controlled and does not allow fuel and oxygen to coexist and only one equation for mixture fraction needs to be solved. Their second model is an infinitely fast one-step where fuel and oxygen can coexist at different times. Here both the mixture fraction and fluctuations equations must be solved. Khalil (42) proposes another model where the mixture fraction varies randomly and assumes a Gaussian form for the probability density function. These alternate models, with the exception of the physically controlled model of Khalil (34), have performed well.

Evaluation of the simple one-step reaction model reveals some strengths and weaknesses. One primary strength is the economy exhibited. Since only two additional variables are used, the model is not computationally limited. Another strength is its ease of use in predicting heat release information (2). This information then allows evaluation of other properties. Coupling of the EBU and Arrhenius model is a plus for this model, but it is also available in other, more precise, kinetic models and will not be considered a strength here. Several weaknesses do exist. The primary weakness is the inability to predict CO concentration. Coupled with this is mean gas temperature which may be 40K low (78). In constructing a model for heat release alone, this problem is non-existent, but most work now underway includes pollutant prediction. Thus, the inability of the model to predict CO is a severe shortcoming. The value of the simple one-step reaction model depends on the intended use. If pollution emission data is desired, the model

is of little use.

4.2.2 Two-Step Global Model

The two-step global model is the next level of sophistication and represents an intermediate level of complexity. Predictions of local mass fractions of fuel, CO_2 , CO , H_2O , and O_2 can be accomplished with relative ease. The general form of the two-step model is (79)



Three differential transport equations are required, one each for fuel, CO , and $m_{\text{ox}} - i m_{\text{fu}}$. Additional algebraic equations for the atomic balance of C, H, and O are used to completely specify the problem. The differential equations used are of the general form of equation (4.5) where the genral variable ϕ is the species concentration.

Equation (4.9) implies that the reaction goes to completion and that the mixture of fuel and air are stoichiometric (80). Concern about the stoichiometric condition in the combustor brought about more complicated models which will be addressed later. Present consideration will be with the two-step model as shown.

The two-step global model has received attention from several authors (32, 39, 40, 48, 80). Samuelsen (81) uses this model, adapted for methane oxidation, to demonstrate the applicability of numerical methods to predict continuous combustion flow. The results of this work were later presented by Peck and Samuelsen (82). They determined that an adequate description of the combustor could be obtained.

Unfortunately they did not address the details of the computer application.

Gosman, et al. (43) discuss the use of the same model utilizing the TEACH-T code. They indicate that the Arrhenius and EBU models may be used to determine fuel consumption rates. They also investigate several other models to determine their applicability. Mongia and Reynolds (39) present a clearer picture of the use of the two-step model. Here they utilize a three-dimensional code, similar in format to the TEACH code. They solve the three basic differential equations, one each for fuel-mass fraction, CO, and a composite fuel fraction. Reaction rates are addressed at some length. These include a kinetically controlled fuel reaction, and turbulent controlled reaction rates for fuel and oxidant. These turbulent reaction rates are not the same eddy-break-up model used previously, therefore they do not include the fluctuation terms. Mongia and Reynolds use the lower value of the reaction rates as the controlling mechanism, be it turbulent or kinetic. They claim good agreement with experiment using this system.

Scheefer and Sawyer (83) used the two-step global reaction mechanism in the analysis of a propane fired opposed reacting jet combustor. They had fair qualitative agreement with experimental results. Discrepancies were due to the turbulence model and the propane consumption rate derived. Ramos (40) also used the two-step model; however, he used differential equations for fuel-mass fraction, CO and CO₂. He showed generally good agreement throughout his combustor.

It appears that this model has exhibited reasonable success in modeling combustor reactions. An obvious advantage of the two-step model is its ability to predict CO concentrations. This could not be

accomplished with the simple one-step mechanism. Ramos (40) claims temperature predictions to within 6 percent. Gosman et al. (43) show generally fair agreement with all variables for many test cases. A second advantage is the overall economy of the model. The relatively small computational cost of one additional differential and several algebraic expressions to complete the C-H-O atom balances is reasonable since CO is being predicted.

The primary problem associated with this model is the stoichiometric assumption which allows the reaction to go to completion (80). The rather brief residence time in the combustor and failure of oxidant and fuel to exist at the stoichiometric ratio cause the problem. A second problem is the lack of EBU models which take into account the fuel fluctuations and appropriate oxygen fluctuations. Mongia and Reynolds (39) have turbulent rate equations in their model but these too do not account for turbulent fluctuations of fuel concentration. An additional problem arises in the area of fuel kinetics which can occupy many steps. In the case of longer chain hydrocarbons the number and type of intermediate reactions are often unknown.

4.2.3 Complex Global Models, Quasi-global

Srivatsa (6) introduced the four-step kinetic scheme to account for the essential features of hydrocarbon oxidation. Valid for any aliphatic hydrocarbons, this extension contains ethene, carbon monoxide and hydrogen intermediate reactions. Demonstrated results are good, but the aliphatic restriction eliminates some fuels. Additionally, prediction of the mean time between fuel disappearance, and a significant rise in temperature is not possible as with the more elaborate models. The four-step model is an intermediate step in the development of the quasi-

global model.

Edelman and Harsha (9), in reviewing the status of mathematical modeling of combustors, recommended the use of the multi-step reaction scheme in the form of the quasi-global model for higher hydrocarbons. The necessity for such a model comes from uncertainty about the application of equilibrium conditions for most species in a combustor (10). Super-equilibrium levels of intermediate atoms and free radicals have fostered interest in complex kinetic mechanisms for the combustion process. Extension of the two-step mechanism to include detailed oxidation reactions leads to a formidable series of chemical reactions. Table I in Appendix A depicts such a kinetic scheme. Note that the scheme also includes nitrogen-related equations to be addressed separately.

The quasi-global approach starts with a single equation such as Equation 1 on Table I. This is the basic fuel reaction, similar in format to the two-step global equation. Other forms of this equation further complicates matters by dividing H atom conservation between H_2 and H_2O (72). The same basic set of reaction equations can be used here also. The degree of complexity is dependent on the researcher's desires. Odgers (76) uses a slightly different kinetic scheme with only fourteen equations and lists several other kinetic schemes containing from six to twenty-four reactions. Other possibilities include a mechanism with a detailed breakdown of the hydrocarbon fuel (10). This possibility is viable for methane which has been extensively studied but data is not readily available for most hydrocarbons.

Implementation of the kinetic scheme into the combustor model is another area of interest. Mongia and Reynolds (39) used a parabolic formulation for their pollutant emissions model which was separated

from their combustor performance (heat release) model. Rate reactions were the kinetic mechanisms for forward and backward reactions. Caretto (72) discusses well-stirred and simple-stirred models to introduce combustion and mixing into the overall combustor model and adds that many authors use these methods. Caretto also discusses the direct solution techniques which he claims are viable only if sufficient computational power is available. Further the interaction of turbulence and chemical reactions rates is not completely understood. Thus, this method is not on firm footing. Edelman and Harsha (10) also reference stirred reactor theory as a means of introducing the complex kinetic mechanism theory. Felton et al. (83) use well-stirred reactor to introduce their kinetic scheme. Likewise, Osgerby (64) uses the well-stirred reactor theory.

The obvious advantage of the quasi-global model is that with the detailed kinetics, the equilibrium assumption can be avoided. Since there is some concern as to the validity of equilibrium assumptions, this first result is important. Secondly, if kinetic data are available, the precision enjoyed by the quasi-global method can aid in obtaining precise predictions. Here accuracy is a definite advantage of the basic model.

There are several disadvantages to the quasi-global model. Since there seems to be reasonable agreement that finite difference codes are most suited to dump combustors, application of kinetic models should be adapted to support these methods (9). Fitting the full kinetic scheme into the general variable differential equation, previously discussed, would create a program, the cost of which, would be prohibitive. The quasi-global method attempts to circumvent this problem; however, comp-

utational costs are still fairly high. Use of well-stirred reactors appears to lessen the computational burden, but tends to create other problems. For example, use of the well-stirred reactor model is quite different from the method currently used for elliptic flows. Coupling of these models by solving flow and turbulence field variables in order to provide information to the stirred network is required. Although good results are obtained, this is somewhat cumbersome to operate. Lastly, there are many intermediate reactions and data are not available for all of them. Knowing which model to use, and how complicated it needs to be, is an additional variable. As previously noted, reaction mechanisms vary widely in complexity and the researcher must insure that the model chosen approximates the combustion process in question.

4.3 Present Approach

4.3.1 Choice of Combustion Model

The model of choice for this work is the two-step global combustion mechanism. Careful consideration of the available models and variations of these models has produced this decision. The details and application of this decision are discussed below.

The two-step global model provides a mechanism for predicting both the consumption of fuel and the presence of carbon monoxide. Subsequent oxidation of the CO provides carbon dioxide data. As a result of these reactions, heat release data is available which is used extensively to predict other flowfield variables such as temperature, velocity, and pressure. Since the two-step global mechanism is capable of predicting CO concentration along with heat release data, it is infinitely more acceptable than the single-step model which merely lumps all products

into a single variable. As stated in the previous section, the capabilities of this model have been tested by several authors. In each case, the numerical predictions compared favorably with experimental results.

The second advantage of this model is the economy afforded by its size. Since there is only one additional differential equation to be solved, as compared to the single-step mechanism, the computational burden is minimized. When compared to the capabilities of the model, the extra computational effort is no problem. Of course, there are several algebraic relations which must be considered, but generally these represent only a small portion of the overall program. These additions are minimal when compared to the computational effort which would be required when using the quasi-global model. Further, if differential relationships were added for only the most important quasi-global constituents, the resulting program would be enormous.

The major disadvantage is the equilibrium assumption inherent in the two-step global representation. Occurrence of other than stoichiometric conditions seem to be limited to the primary zone of the combustor. Thus it appears that the equilibrium assumption is objectionable primarily in this zone. While there is active criticism of this assumption by the quasi-global proponents, those who utilize the two-step model feel quite comfortable with the results obtained. Most authors feel that turbulent effects are the main problem and that these need immediate attention.

A second and smaller disadvantage is that of kinetic and turbulent interaction in computing fuel consumption rates. As shown previously, little has been done to include turbulent fluctuations into the fuel consumption rates for this model. Turbulence was included by one

author but not in the same way as documented in the use of the EBU reaction rate model.

In sum, the advantage of reliable predictions and computational economy outweigh the disadvantages listed. It is felt that the two-step global model is capable of producing results which can be used in the simulation of combustor systems. Thus the two-step global model will be utilized in this application.

4.3.2 Finite Difference Formulation of the Mathematical Model

The two-step model requires differential solution for fuel-mass fraction, CO mass fraction and $m_{ox} - i m_{fu}$. Each of these variables will be substituted into an equation such as Equation (4.5) where ϕ will be the variable in question. There will be three differential equations solved which will be in the general equation format of Equation (D.3) Appendix D.

Solution will be as in TEACH-T utilizing the tri-diagonal-matrix-algorithm (TDMA). The source terms, S_u and S_p will be functions of the rate of consumption of the generalized variable ϕ . Lilley (64) explains the manner of solution for these generalized variables and a detailed explanation is similarly available in the radiation section. Further considerations here will be limited to explanation of source terms, variations caused by the implementation of the two-step reaction model, algebraic relations required for atomic balances, and boundary conditions to be specified.

Consider first, the consumption of the hydrocarbon fuel. The fuel-mass fraction, m_{fu} , is specified early-on and is the value used to

initialize the flowfield. Determination of the source term follows with the computation of the fuel consumption rate at each grid node being accomplished. The present model utilizes the consumption rate equations of Mongia and Reynolds (39). They have developed an Arrhenius (chemical) form and a turbulent kinetic form for fuel and oxidant. Application and testing of the model reveals that the turbulent kinetic oxidant equation has negligible effect on the problem solution. For this reason it has been excluded. The Arrhenius and turbulent kinetic fuel rates are

$$RFUARR = 3.3 \text{ E}14 \rho^{1.5} m_{ox} m_{fu}^{1/2} \exp (-27000/T) \quad (4.11)$$

and

$$RFUEBU = 3.0 \rho m_{fu} \epsilon/k \quad (4.12)$$

respectively. Here the name RFUEBU is used for convenience and ϵ is the turbulent dissipation rate and k is the kinetic energy of turbulence. The resulting fuel consumption rates are compared, with the minimum value being utilized in the source term for m_{fu} . Actually, the negative value or fuel depletion rate is utilized in the code. Source term modifications at the boundary are not necessary since fuel is neither supplied nor consumed there.

The conserved property, $m_{ox} - i m_{fu}$, or the fuel-oxygen proportion is calculated next. Here the source term is zero, the variable being a conserved property. The critical variable is the stoichiometric fuel to oxygen ratio which is determined in the early stages of the code, and is a function of the C-H-O concentration in the hydrocarbon fuel. For this problem this ratio is

$$i = \frac{32(\frac{x}{2} + \frac{y}{4})}{(12x + y)}, \quad (4.13)$$

where x and y are the number of carbon and hydrogen atoms respectively. Again, the source term at the boundary is zero.

The final step is the calculation of the CO concentration in the combustor. CO concentrations are initialized to zero early-on. Again, the calculation of production and consumption rates is the important step here. The rate of creation of CO is related to the rate of consumption of fuel with an adjustment for differences in molecular weights and the number of carbon atoms in the hydrocarbon fuels. The correction factor, RAT4, is the number of carbon atoms times the molecular weight of CO divided by the molecular weight of the fuel and is

$$RAT4 = AX * WCO/WFU \quad (4.14)$$

Thus through the fuel consumption rate, the production of CO can be determined and is applied to the problem via the source term.

The consumption rate of CO is again a pair of rates, one each for chemical kinetics (Arrhenius) and turbulent consumption (39). Here the third rate expression, kinetic oxidant rate, has been eliminated. The Arrhenius and turbulent reaction rates are

$$RFUARR = 6.0 \text{ E}8 \rho^2 \text{ CO exp } (-12500/T) \quad (4.15)$$

and

$$RFUEBU = 4.00 \rho \text{ CO } \epsilon/k \quad (4.16)$$

respectively. As before, the minimum value will be utilized as the con-

sumption. Source terms at the boundary are zero as discussed earlier.

Upon completion of the calculation of m_{fu} and CO, several important calculations must be accomplished. Calculation of temperature being the most important. Temperature is calculated via the definition of enthalpy which is also calculated using the general equation. The stagnation enthalpy must be adjusted by the amount of energy available in the unburned fuel and CO. This correction is made by subtracting the mass fraction of fuel times the heat of formation, HFU, and the mass fraction of CO times its heat of formation, HCO, from the total energy. HFU and HCO are input variables read in during the initial steps of execution. After the correction is made, the temperature at each grid node is obtained by dividing the enthalpy at that node by the mixture specific heat.

The specific heat of the mixture is the sum of products of the mass fraction of each species times the variable specific heat of that specie. Introduction of variable specific heat was necessary due to the wide range of temperature associated with the combustion chamber. A first-order equation was utilized to determine the value of the specific heat for each chemical species using constants which applied to the temperature range of 400-1600 K (95). Although this range falls below the maximum temperature expected in the combustor it was determined that these constants provided an accurate representation of the specific heat until the temperature reached 2200 K. This determination was made by plotting the 1600-2500 K range utilizing constants for both the 400-1600 K and 1600-6000 K ranges and comparing the resulting curves. In general, these curves were within 5 percent up to 2200 K. Since the majority of the combustor temperature were in the lower range, the

lower temperature constants were used.

During each iteration these variable specific heats are updated utilizing temperatures from the previous iteration. Since the enthalpy value is generally increasing due to fuel consumption and since fuel consumption is based on local temperatures, a natural dampening is in effect which reduces the change of divergence.

Lastly, the calculation of CO_2 can be made via an atom balance. By assuming that all the consumed fuel goes to CO_2 and subtracting the amount of CO predicted, CO_2 concentrations are resolved. A similar procedure is used for H_2O which is directly related to the amount of fuel consumed.

4.3.3 Assessment of the Models

The various methods which can be used in modeling the combustion process were presented earlier. The inability of the single-step model to predict CO concentrations immediately eliminates it from further consideration. But the two-step and quasi-global models have this capability. However, the quasi-global model has two disadvantages. First, the intermediate reaction steps, although well known for methane combustion, are generally not available for other fuels. Secondly, the enormous amounts of computer storage required by the myriad of species present is prohibitive.

The required degree of sophistication has been decided and the two-step model was chosen. The disadvantage is that the calculation of the fluctuating fuel concentration and corresponding fluctuation of oxygen concentration have been eliminated. Attempts to utilize the

EBU model containing this capability have proven fruitless. With this model in place and using the minimum reaction rate of fuel consumption, the reaction does not proceed to completion. Thus, the use of the EBU model has been abandoned.

To its advantage, the two-step model provides a mechanism for predicting fuel consumption and CO concentration. This coupled with nominal increases in storage requirements makes this model very desirable.

CHAPTER V

MODELING OF NO PRODUCTION IN COMBUSTORS

5.1 Background

One of the primary pollutants of concern for the combustor modeler is the formation of oxides of nitrogen, NO_x . The 1972 EPA Aircraft Emissions Standards called for strict control of the levels of unburned hydrocarbons (UHC), carbon monoxide (CO), oxides of nitrogen (NO_x) and smoke (3). High combustion efficiency, stimulated by swirl in the reaction zone, reduces the amount of UHC, CO and, in turn, smoke. With better efficiency often comes higher temperatures throughout the combustor. This presents a problem since NO_x production is a strong function of temperature and increased temperature means increases in NO_x (84). Goals of the combustor designer include lowering of temperatures and removal of "hot spots" from the reaction zone. These solutions, however, usually lead to increases in CO and UHC release. Thus, appropriate tradeoffs must be made by the designer. Lowes, et al. (85) indicate that a mathematical model which could accurately predict NO_x emission levels would certainly aid the combustor designer in his quest for a clean engine.

Lilley (4) conducted a literature review concentrating on practical combustors. Various two- and three-dimensional combustor prediction methods are presented with NO_x being discussed at some length. Many prediction methods are presented, as are their pros and cons. Lilley

concludes that only time will determine which methods are best. Edelman and Harsha (9) recommend a quasi-global approach for predicting all reaction species in the combustor, Table I. The NO_x question is a complex one and requires much thought prior to the selection of a kinetic model for use in a numerical prediction.

The term NO_x includes nitrogen oxide, NO, nitrogen dioxide, NO_2 , and others. Nitrogen oxide is the primary pollutant mentioned in most theoretical studies. Nitrogen dioxide is quite a different story. Sawyer (51) conducted experimental studies using a can-type combustor and found that measurable quantities, 5 PPM or greater, were never detected while NO concentrations were greater than 100 PPM. He is careful to state that this occurred in his experiment and that this may not be conclusive. Owen, et al. (47) conducted a series of measurements in a swirl-stabilized combustor. They reasoned that some NO_2 is present but, that large amounts of NO_2 can be attributed to probe reactions. Heap, et al. (86) address only the presence of NO in the combustor flow field. Caretto (75) reasoned that NO is the primary pollutant and spent most of his effort on modeling its formation, NO_2 being an additional reaction. Many authors represent all nitrogen oxides as NO_x and make no determination as to the molecular make-up of the oxides being modeled. Kinetic equations for NO and NO_2 are used but the results are lumped together into NO_x . The possible presence of NO_2 is a problem which must be resolved in time, however, for now, efforts will be confined to NO modeling.

As previously stated, NO formation is strongly temperature dependent. The production of thermal NO comes from reactions of N_2 with oxygen in the combustor (87). NO can also be produced from nitrogen-

containing fuel components. This method is called fuel NO. Lastly, prompt NO is a result of reactions of fuel-derived radicals with N_2 which lead to NO. Each of these mechanisms will be addressed separately.

5.2 Nitrogen Oxide Models Available for Numerical Simulation

5.2.1 Thermal NO

The fundamental model for the production of nitrogen oxide is the Zeldovich mechanism (82)



Here Equation (5.1) is the rate limiting step since the second reaction cannot proceed until the first is completed. Adoption of a simplifying assumption that O/O_2 is in equilibrium produces a series of kinetic equations which are easily modeled. The Zeldovich mechanism has been widely used for predicting NO concentrations in combustion system (32, 40, 52, 81, 88). Additionally, in most cases, equilibrium oxygen has been utilized. Steady-state assumptions for N atom concentrations (40).

$$\frac{d[N]}{dt} = 0 \quad (5.3)$$

completes the kinetic specification. Caretto, et al. (88) utilize a slightly different assumption, that of equal reaction rates for Equations (5.1) and (5.2) to produce a reaction mechanism such as Equation (5.4). Details of [N] and [O] production are found in 5-3-1.



This same mechanism is also used by Osgerby (73). Obviously, this is a simplification of the basic Zeldovich mechanism.

The utility of the Zeldovich reaction scheme has been demonstrated for gas turbine combustors. Ramos (40) states that this mechanism over predicts NO concentrations by a factor related to the over prediction of temperature. Caretto (88) states that NO concentrations are low in the combustion zone. Mellor (74) completes a comprehensive study of gas turbines by stating that the Zeldovich mechanism is probably appropriate, especially in fuel lean primary zones.

5.2.2 Fuel NO

Nitrogen oxide produced through reaction with fuel components has been attributed to Fenimore (89). Here, reactions such as



and



provides a route for NO formation in the primary zone of flame reaction. Edelman and Harsha (10) discuss, at some length, the fuel NO problem. They conclude that Fenimore's contention may have merit; however, they feel that the quasi-global model itself is a valid approach to NO production without including fuel NO. Caretto (89) claims that Fenimore's assumption of fuel NO should be attributed to super-equilibrium concen-

trations of oxygen in the combustor instead. Caretto (75) states that nitric oxide formation from fuel nitrogen is limited due to the complexity of the chemical steps. Nitrogen bound to fuel elements should be handled as a portion of detailed fuel consumption, should such a model be developed.

5.2.3 Prompt NO

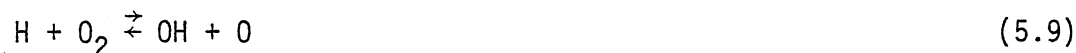
As a result of the chemical reaction, various radicals which contain oxygen are available in the combustor. These radicals combine with nitrogen atoms present to form NO via the so-called prompt mechanism. The Zeldovich mechanism is the primary NO production system and is extended to include the prompt NO via (89)



This reaction is normally used in lieu of a super-equilibrium oxygen concentration. Utilization of this reaction is seen in many cases (10, 39, 67, 75, 79, 80, 90-93). In some of these models this additional equation is the only extension of the Zeldovich mechanism (39, 75, 89, 91-93) whereas others use more extensive models which include NO₂ (10, 79, 90) and N₂ (67, 80). Generally good agreement with measured data result from the single extension model (75, 89, 91, 92). The more expansive models also show promise. Scheefer and Sawyer (48) and Peck and Samuelson (32) have formulated super-equilibrium models by assuming that the reactions



and



are in equilibrium. Reasonable agreement with measured values were obtained with this method. Here O concentrations are directly related to CO/CO₂ concentrations and knowledge of OH concentration is not required. Values for CO and CO₂ concentrations come from combustion reactions previously completed. Odgers (76) includes a single termolecular reaction as the necessary extension to the Zeldovich mechanism. No results are discussed.

5.2.4 Evaluation of the NO Models

There are many models which are applicable to the prediction of NO concentrations in combustors. Fuel NO will be eliminated from the discussion since little is actually known about this mechanism. Further, the complex fuel kinetics for hydrocarbons other than methane are unknown. Thus, this discussion will be limited to thermal and prompt NO production.

The reliability of the Zeldovich model for predicting NO concentrations in combustors has fostered the prompt NO mechanism. Iverach, et al. (93) concludes that the Zeldovich mechanism is applicable in both flame and post-flame regions when the equivalence ratio is less than 1.15. For cases where the equivalence ratio is larger, super-equilibrium oxygen should be considered. Jones and Pridden (91) utilize the extended Zeldovich model and note over prediction of NO. Bowman and Seery (92) note that equations (5.1) and (5.2) are the principal NO formation reactions, with Equation (5.7) being of minor importance for fuel-rich mixtures. Further, for modern gas turbines which operate with

lean primary zone equivalence ratios, the Zeldovich mechanism is probably appropriate.

If this is the case, extended mechanisms such as those of Caretto (75), Edelman and Harsha (10), and Swithenbank et al. (79) may not be necessary. Table I demonstrates the complexity of the full set of nitrogen reactions. Note that only reactions 14 through 24 pertain to nitrogen production. As with the combustion kinetics, excessively complex models lead to large computer programs. Application of the Zeldovich mechanism would require one additional partial differential equation along with several algebraic relations. Thus, computational economy is a consideration which must be weighed. The combustion model utilized is a factor which must be considered when choosing a NO mechanism. Unless OH concentrations are available from the combustion reactions, Equation (5.7) cannot be used. In this event, the inclusion of super-equilibrium can be via the method of Peck and Samuelsen (32). It is important to consider the combustion model prior to inclusion of the NO model.

Mellor (74) discusses the various NO, NO₂, and N₂O formation reactions and comments on their applicability. He presents a listing of these reactions, part of which are seen in Table II. He states that many authors conclude that reactions 21-25 are not necessary because this oxide does not form in appreciable amounts in combustors. Further, reactions involving N₂O, 26-28, have also been shown unimportant or negligible by others. The conditions used to reach these conclusions correspond roughly to gas turbine combustors. In general, reactions 17-20 have also been shown unimportant for various combustion situations. His final conclusion that the Zeldovich mechanism is probably

appropriate in gas turbines was previously stated.

5.3 Present Approach

5.3.1 Choice of a Nitrogen Oxide Model

The nitrogen oxide model of choice in this work is the Zeldovich mechanism. Mellor's comments above indicate that this model can be used to successfully predict NO concentrations within the combustor. This coupled with the computational economy afforded by it make the Zeldovich mechanism an appealing choice. Further, by applying super-equilibrium assumptions, this model can be applied even in cases when the equivalence ratio increases. Documentation of its ability to predict NO concentrations supports inclusion into this work.

An important factor which leads to this choice was the combustion model previously chosen. The two-step global model does not produce many of the radical concentrations required by many of the extended NO mechanisms. Basically the two-step model provides the temperature field which is used to drive the NO mechanism to solution. By providing CO and CO₂ concentration data, this model can aid in predicting the super-equilibrium oxygen concentration levels, if such a need arises. This coupling of the two models supports the inclusion of both into this work.

As previously noted the Zeldovich mechanism consists of the reactions seen below:



and



where R_{f1} and R_{f2} are the forward rates and R_{r1} and R_{r2} are the reverse rates. Assuming that the problem is steady state for N concentrations produced

$$\frac{d[\text{N}]}{dt} = 0 \quad (5.12)$$

and after some algebraic manipulations the N concentration was determined as (40)

$$[\text{N}] = [\text{O}] \frac{R_{f1} [\text{N}_2] + R_{r2} [\text{NO}]}{R_{f2} [\text{O}_2] + R_{r1} [\text{NO}]} \quad (5.13)$$

Since the O-atom concentration is considered to be in equilibrium with O_2 , unless otherwise specified (or as a result of super-equilibrium requirements) then

$$[\text{O}] = \bar{K} [\text{O}_2]^{1/2} \quad (5.14)$$

where \bar{K} is the equilibrium constant (52). The rate of reaction of NO is given by

$$\frac{d[\text{NO}]}{dt} = R_{f1} [\text{N}_2][\text{O}] - R_{r1} [\text{NO}][\text{N}] + R_{f2} [\text{N}][\text{O}_2] - R_{r2} [\text{NO}][\text{O}] \quad (5.15)$$

Equation (5.15) provides the rate of creation of NO which will be utilized in the finite difference formulation.

5.3.2 Finite Difference Formulation of the Mathematical Model

The Zeldovich model requires the solution of one differential equation for NO concentration. This equation is the general partial differential equation

$$\frac{1}{r} \left[\frac{\partial}{\partial x} (\rho u r \phi) + \frac{\partial}{\partial r} (\rho v r \phi) - \frac{\partial}{\partial x} (r \Gamma_{\phi} \frac{\partial \phi}{\partial x}) - \frac{\partial}{\partial r} (r \Gamma_{\phi} \frac{\partial \phi}{\partial r}) \right] = S_{\phi} \quad (5.16)$$

where ϕ is the general variable, NO in this case. Additional algebraic relations will be used to determine the O and N atom concentrations. The differential equation is cast into the general equation format of Equation (D.3), Appendix D. S_{ϕ} is the source term and will include forward and reverse reaction rates determined from the Zeldovich reactions, Equations (5.10) and (5.11). Note that the reverse rates are negative and contain expressions for the variable NO. These can be fit nicely into the source term S_p^{ϕ} whereas the forward rates fit into S_u^{ϕ} . Forward and reverse reaction rates for the Zeldovich reactions are from Odgers (76) and the oxygen equilibrium constant is from Sadakata and Beer (52). Variations of the units are considered in the mixture fraction portions of the code. Solution will be as in TEACH-T utilizing the tri-diagonal matrix algorithm.

Calculation of NO follows the same pattern as all other variables in the code. The field variables of NO, O, and N are initialized to zero. Determination of the source term follows the calculation of the forward and reverse reaction rates. These are highly temperature dependent and do not have significant effect until the temperature reaches 1500K. The forward and reverse reaction rates are

$$R_{f_1} = 5.192 \text{ E } 10 (T)^{0.1} \exp (-37888/T)/28 \quad (5.17)$$

$$R_{f_2} = 6.43 \text{ E } 06 (T) \exp (-3150/T)/14 \quad (5.18)$$

$$R_{r_1} = 3.1 \text{ E } 10 \exp (-168.2/T) \quad (5.19)$$

and

$$R_{r_2} = 3.661 \text{ E } 05 (T)^{1.16} \exp (-19077/T) \quad (5.20)$$

Application of mixture fraction relationships are used in Equations (5.19) and (5.20) to fix the units. Care must be exercised when dealing the large negative exponent in Equation (5.17) since it can easily exceed the limits of the computer.

Boundary conditions are similar to those in the combustion model with no reaction taking place at the wall of the combustor. Because of this restriction, source term modifications are not necessary on the boundary. Boundary conditions are applied by breaking the link in the algebraic representation of the differential equation; setting the coupling coefficient equal to zero.

5.3.3. Assessment of the Model

The various methods available for predicting NO production have been presented. The Zeldovich mechanism has the advantage of computational economy and compatibility with the previously chosen combustion model. The problem of over prediction or under prediction of NO concentration is primarily a function of the accuracy of the temperature profiles. Accurate profiles have produced good NO predictions.

The only disadvantage of the Zeldovich models is that it cannot predict other oxides. This problem is negated by presuming that NO_2 is not a measurable pollutant as was previously stated. With this problem aside, the Zeldovich mechanism, with the possibility of adding super-equilibrium oxygen, appears to be sufficient.

CHAPTER VI

PREDICTIVE TECHNIQUE

6.1 Scope and Method of Approach

The economic design of a combustor system is dependent upon a viable predictive technique capable of detailed flowfield prediction. A computer code has been developed as an extension of the TEACH (Teaching Elliptic Axisymmetric Characteristics Heuristically) code of Gosman and Pun (94) for this purpose. This new code, STRAC (Swirling Turbulent Reacting Axisymmetric Combustion), includes the two-step combustion model, radiation heat transfer and pollution mechanisms. A listing of STRAC is found in Appendix E.

This chapter emphasizes the addition of the reacting portion of the code and includes a synopsis of the overall operation of STRAC. A similar nonreacting code is extensively discussed by Lilley and Rhode (64) and can be used to supplement this description. Sufficient detail is included to insure adequate comprehension of this complex simulation.

6.2 Mathematical Model

6.2.1 Governing Equations

The turbulent Reynolds equations for conservation of mass, momentum, stagnation enthalpy, chemical species mass fraction, radiation flux, turbulent kinetic energy and turbulent dissipation rate, govern the two-

dimensional steady flow of the turbulent reacting multi-component combustion reaction (64). Each of these equations, with the exception of radiation which was addressed in Chapter III, contain similar terms for the convection and diffusion of the flowfield variables along with a source term S_ϕ for the general variable ϕ . The general form of the differential equation to be solved is

$$\frac{1}{r} \left\{ \frac{\partial}{\partial x} (\rho u r \phi) + \frac{\partial}{\partial r} (\rho v r \phi) - \frac{\partial}{\partial x} (r \Gamma_\phi \frac{\partial \phi}{\partial x}) - \frac{\partial}{\partial r} (r \Gamma_\phi \frac{\partial \phi}{\partial r}) \right\} = S_\phi \quad (6.1)$$

where ϕ is any of the dependent variables; $u, v, w, h, m_{fu}, m_{ox} - m_{fu}, m_{co}, m_{NO}, R_x, R_r, K$ and ϵ . Each variable has an associated source term which is linearized and divided into two portions, S_p and S_u . To aid in convergence the S_p term contains only negative values while S_u is positive. Introduction of turbulent exchange coefficients Γ_ϕ , and their stress ~ rate of strain relationships allows each variable to fit Equation (6.1). Table III is a listing of source terms and exchange coefficients for each variable.

The hydrodynamic solution is as in STARPIC and utilizes the two equation $k-\epsilon$ turbulence model to specify the turbulent viscosity where

$$\mu_t = C_\mu \rho k^2 / \epsilon \quad (6.2)$$

and

$$\mu = \mu_{eff} = \mu_{lam} + \mu_t \quad (6.3)$$

Two different equations are solved for the k and ϵ turbulence quantities listed in Table III. Values of the parameters are given by $C_\mu = 0.09$, $C_0 = 1.00$, $C_1 = 1.44$, $C_2 = 1.92$, $\sigma_k = 1.00$ and $\sigma_\epsilon = 1.21$ (71).

Algebraic relations are used to specify mass fraction conservation and to define the enthalpy. Here the mass fractions are set to unity

$$m_{fu} + m_{ox} + m_{pr} = 1 \quad (6.4)$$

Similar mass fraction relationships exist throughout the program with m_{pr} being the sum of the individual specie products. Enthalpy is specified by

$$h = C_{p_{mix}} T + H_{fu} m_{fu} + H_{co} m_{co} \quad (6.5)$$

and is solved in a partial differential equation where the source term is a function of the radiative flux. The radiative heat transfer formulation was discussed in Chapter III.

The combination of partial differential and algebraic equations provide a high degree of non-linearity and make the numerical analysis of the combustion process a difficult task. Coupled with the above equations must be initial and boundary conditions which will be discussed separately. Difficulty in solution is found in the linkage between the various ϕ variables. Enthalpy and heat release via the combustion kinetics requires the knowledge of flowfield temperature profiles. Successful solution of these variables is accomplished through successive adjustment of one variable after another to form a convergent sequence.

6.2.2 Solution Techniques and Finite Difference

Formulation

Solution of the hydrodynamics was via the primitive pressure-velocity approach incorporated into the TEACH format and utilizing TDMA (tri-diagonal matrix algorithm) as the starting point in this investigation.

investigation. Additional variables were incorporated which, with the exception of radiation heat transfer, were solved in the TDMA format. The radiation solution used a modified TDMA for solution of the equations developed in Appendix D.

The finite difference equations were solved on a two-dimensional grid system applicable to the axisymmetric condition where variations in the θ direction are set to zero. Figure 5 depicts the irregularly spaced mesh which covers the flow domain (33). Note that the grid crosses the boundaries of the domain. Figure 6 depicts the staggered grid which was used throughout the mesh. All variables except u - and v -velocities are stored at the central grid nodes (crossing of the solid lines), whereas the velocities, denoted by arrows, are stored midway between nodes. A boomerang-shaped envelop encloses a triad of points denoted by a single letter $P(I,J)$. For example, $U(I,J)$ is the axial velocity at reference location (I,J) even though it actually represents the velocity positioned at $(I-1/2,J)$. The advantages of the system are: first, it places the u - and v -velocities between the pressure nodes which drive them; and secondly, the velocities are directly available for calculation of the convective fluxes across the boundaries of the control volume surrounding the grid node.

Figure 7 depicts single cells which show the locations of the u - and v -velocities, respectively. Since the grid mesh overlaps the physical boundaries of the combustor, the normal velocities are situated directly on them, while the tangential velocities are displaced by one-half cell inside the solution domain. This aided in specifying the requisite boundary conditions.

The finite difference equations for each ϕ variable were formed by integrating Equation (6.1) over the cell control volume and expressing the result in terms of neighboring grid point values. Convective and diffusive terms become surface integrals by applying Gauss' divergence theorem thus allowing cell areas to specify the domain. This procedure as well as the linearization of the source terms, is demonstrated in Appendix D. Although only the diffusive terms are expanded in Appendix D, the convective terms can be easily developed (64). Table IV contains the components of the linearized sources.

When all portions of the governing partial differential equation, Equation (6.1), have been integrated the following equation is obtained:

$$a_P^\phi = \sum_j a_j^\phi \phi_j + S_u^\phi \quad (6.6)$$

where

$$a_P^\phi = \sum_j a_j^\phi - S_P^\phi \quad (6.7)$$

and \sum_j = sum over the N, S, E, and W neighbors, thus linking each ϕ -value at a point P with its neighbors. Special care is required when dealing with ϕ as u- and v-velocities and pressure. Equation (6.6) is the form which is solved utilizing the TDMA.

6.2.3 Boundary Conditions

Application of boundary conditions are discussed extensively in STARPIC (64), however, some additional comments are necessary.

The series of finite difference equations used to solve each variable require modification when cells come in contact with boundaries. Insertion of correct boundary conditions requires amendment of

the finite difference formulation and is usually accomplished by breaking the link (via the coupling coefficient, i.e. a_e^ϕ) with the value at the external point. In the case of the western wall boundary for example, the normal P-W link is broken by setting, $a_w^\phi = 0$ with the correct expression inserted as a false source term in S_u^ϕ and S_p^ϕ . Both Neumann and Dirichlet condition can be specified via this method.

Several different types of boundary conditions must be considered. Inlet conditions are normally specified as some fixed value such as the inlet u-velocity. Similar fixed quantities are prescribed for mass fractions of fuel, air and radiation flux. Velocities normal to walls are given zero values with the link also being broken. Tangential velocities result in shear-stress calculations. Other near wall occurrences are handled via the introduction of wall functions. These link velocities, k and ϵ to those in the logarithmic region. Radiation conditions are discussed in Appendix C. Chemical kinetic boundary conditions are specified by breaking the link at the boundary and setting the normal component equal to zero.

Care must be exercised in specifying boundary conditions. Inadvertent errors lead to instabilities which can cause divergence of the solution. Additionally, false source terms must correspond to the rule which stipulates that all negative values be included in the S_p^ϕ term.

6.2.4 Solution Procedure

With the finite difference equations and boundary conditions, a series of equations is obtained for each variable within the flow domain. Solution of the strongly coupled simultaneous algebraic equations requires cyclic integration as follows (33):

(i) guess the value of all variables including a pressure approximation. Calculate other variables such as density, viscosity, etc;

(ii) solve the axial and radial momentum equations to obtain first guesses of u and v velocities;

(iii) solve the pressure correction equation (Poissons Equation) and obtain a corrected pressure;

(iv) calculate the pressure and the corrected velocities, u and v ;

(v) solve equations like Equation (6.6) for all other ϕ variables successively, and

(vi) treat the new values of each variable as improved guesses and return to step i.

The process is now repeated until convergence is complete.

The TDMA is used to solve the algebraic equations for each variable. Generally, TDMA is applied along vertical grid lines and from left to right in the solution domain. At each point there are three unknowns, except at the first and last points where there are two. The procedure is used for all variables except for the radiative heat transfer where the fluxes are directional. Here a new TDMA is necessary and may proceed as discussed above, or solution may be along horizontal grid lines and from bottom to top. These changes do not affect the validity of the TDMA but are required to assure a solution of the flux variables.

Convergence is supplemented by including some degree of under-relaxation when solving Equation (6.6). Under-relaxation influences

the solution by taking the weighted average of newly calculated values and the previous values at each gridpoint when solving the difference equation. The under-relaxation factor f ($0 < f \leq 1$) is applied directly to obtain the under-relaxation value ϕ_p^{n+1} via

$$(a_p^\phi/f)\phi_p^{n+1} = \sum_j a_j^\phi \phi_j^n + [S_u^\phi + (1 - f) \frac{a_p^\phi}{f} \phi_p^n] \quad (6.8)$$

The effect of the under-relaxation factor is to increase the rate of conversion. Unacceptably slow convergence or divergence of the solution is obtained if factors are too low or too high, respectively. Large pressure corrections arise which produce large u - and v -velocity corrections. If these corrections are too large, the nonlinearity of the finite difference equations causes divergence (64).

Final convergence is determined by examining residual source terms, essentially the exactness of ϕ at the point P . The residual sources are defined by

$$R_p^\phi = a_p^\phi \phi_p - \sum_j a_j^\phi \phi_j - S_u^\phi \quad (6.9)$$

When these terms become smaller than a predetermined value the finite difference equations are considered solved.

6.3 Operation of STRAC

6.3.1 General Arrangement

The STRAC program is outlined in the flow chart at Figure 8. Fortran 4 is utilized to allow easy amendment at the expense of computer time. The MAIN subprogram is the operator and contains those values which characterize the combustor flow situation. PROMOD (problem modification) is a subroutine used to specify boundary conditions for each

variable. The various subroutines are described briefly in Table V. Detailed explanation of the operation of these subroutines is available in (64, 77) with the exception of subroutines EQUAL, CALCRX, CALCRR, TEMPND, SOLVERX, SOLVRR, CALCQ, FIXBND, and TRPRINT. Adequate description of these subroutines is contained in Table V.

For the user, the most important section of the program is MAIN. Main controls the iterative solution procedure with calls to INIT (initialization), PROPS (properties) and PRINT (output of all variables). Control of the iterative process requires repeated calls to the various CALC subroutines for calculation of ϕ variables, PROPS and PRINT (after convergence or when MAXIT, maximum iterations is achieved). Each CALC subroutine calls PROMOD to modify boundaries. Subroutine LISOLV (or SOLVRX and SOLVRR for radiation heat transfer) is called by the CALC subroutines to update the flowfield variables by sweeping through the flow domain using TDMA. The number of sweeps through the domain for each variable is specified (NSWPU times for the case of u-velocity calculations).

6.3.2 Major Variables

Appendix E contains a listing of the entire code. Only the significant FORTRAN variables are discussed here; while other variables yield their meaning by inspection of their context and mnemonics. A glossary of Fortran variables is found in Appendix F. Table VI lists principal dependent variables and controlling parameters.

6.3.3 MAIN Subprogram

6.3.3.1 Introduction. The importance of MAIN necessitates a detailed explanation of its intricacies. Since MAIN is divided into chapters, this discussion will be in chapter format.

6.3.3.2 CO Preliminaries. Dimension, common and data blocks are followed by user input of logical and algebraic variables which set the program into operation. LABRPT is used to specify the type of expansion at the combustor inlet. A value of .FALSE. requires a sloping boundary. Specification of NSWPU (number of sweeps for U velocity) etc. and input variables are located here. Input variables are both logical and algebraic and specify the type of problem (reacting or nonreacting) to be solved. Card 1: this specifies INCOLD as true or false through specification of the first read alphanumeric character as T or F. A true value is used in the code to allow zero heat release resulting in an isothermal flow situation. Card 2: this specifies INCOOL as true or false through specification of the first read alphanumeric character as T or F. A true value is used in the code to severely reduce the value of heat release from the fuel, thereby predicting a very cool flow situation. Card 3: this specifies INFUPR as 1, 2, or 3 to determine the inlet fuel profile to be used at the entrance region. A uniform profile is specified by setting INFUPR to 1, while various peak profiles are specified by setting INFUPR to 2 or 3. Card 4: this specifies the type of hydrocarbon fuel being burned, the associated heat release, the percent stoichiometric air and the fuel flow rate. These are specified by setting; the number of carbon atoms (AX), the number of hydrogen atoms (AY), the production of hydrogen is controlled by setting (AO = AY) thus eliminating hydrogen,

the heat released through fuel consumption (HFU), the heat release through carbon monoxide consumption (HCO), the percent stoichiometric air (PERSTO), and the inlet fuel flow rate (FUIN). Card 5: this specifies the inlet temperature (TIN) and the maximum wall boundary temperature (TWALL). Card 6: this specifies INOTPT as true or false through specification of the first read alphanumeric character as T or F. A true value allows intermediate output which is monitored during each iteration. Card 7: this specifies INLET as true or false through specification of the first read alpha-numeric character as T or F. A true value allows a printout prior to calculation. Cards 8 through 39: these specify alphanumeric headings for various output variables. Input variables are seen below for a methane combustion problem.

```

F
F
1
1., 4., 4., 45000000., 94000000., 1.00, 0.041
500., 700
F
F

```

```

U VELOCITY
V VELOCITY
W VELOCITY
PRESSURE
TEMPERATURE
NON DIMENSIONAL TEMPERATURE
TURBULENCE KINETIC ENERGY
ENERGY DISSIPATION
VISCOSITY
KPLUS=TE*RHO/TAUN
LENGTH SCALE
STAGNATION ENTHALPY
FUEL MASS FRACTION
OXYGEN FUEL RATIO
OXYGEN MASS FRACTION
PRODUCT MASS FRACTION
DENSITY
EDDY BREAK UP MODEL
ARRHENIUS MODEL
HEDFUP
X DIRECTION RADIATION
R DIRECTION RADIATION
CO2 MASS FRACTION

```

```

H2O MASS FRACTION
CO MASS FRACTION
H2 MASS FRACTION
O MASS FRACTION
N MASS FRACTION
NO MASS FRACTION
NON DIMENSIONAL U VELOCITY
NON DIMENSIONAL V VELOCITY
NON DIMENSIONAL W VELOCITY

```

6.3.3.3 C1 Parameters and Control Indices. This chapter specifies the flowfield domain to be solved. INDCOS=2 implies that the problem is axisymmetric and that cylindrical coordinates will be used. The grid system is marked and boundaries are specified through initialization of variables such as JSTEP and ISTEP. The total geometry is specified by appropriate choice of integers NI, NJ, IHUB, JHUB, RLARGE ($=D/2$), ALTOT ($=$ total length), JCON and ICON. Dependent variables to be solved are selected (setting .TRUE. or .FALSE. to INCALCU etc.), while fluid properties (Prandtl/Schmidt numbers), physical constants, boundary values, species concentration, pressure calculation and program control and monitor points are specified.

6.3.3.4 C2 Initial Operations. Here geometric quantities are calculated and now 2-D array variables are set to zero or to obvious initial values by way of subroutine INIT. Inlet swirl velocity is determined using VANB or SWNB for flat or solid body rotation according to whether NSBR (number for solid body rotation) is 0 or 1. Other interior variables are specified as required or are modified for inlet conditions. Finally, wall functions are determined for use in boundary specification.

6.3.3.5 C3 Iteration Loop. In this section of MAIN, variables are updated through repeated calls to subroutines such as CALCU when the

appropriate INCAL logical variable is set equal to .TRUE.. Each iteration is counted by NITER (number of iterations) until convergence is verified or a maximum number of iterations is reached. Maximum iterations (MAXIT) is specified in Chapter I and updated in III. Other functions performed include; update of variables, update of properties, and print out of intermediate source terms and flowfield values at a monitored location (IMON, JMON).

6.3.3.6 C4 Final Operations and Output, Upon termination of the iteration process final flowfield variables are printed. The current problem is finished, however, if LFS (loop for swirl) is less than the maximum value LFSMAX then LFS is increased by 1. The inlet swirl values are recalculated for the new case and the iteration process begins again. If LFS is the maximum value, the program is terminated.

6.4 Closure

Users should confine changes in the program to specification of the flow domain in Chapter I of Main. Here, geometric variations can be applied for different problems. Inlet values, grid spacing, logical variable specification and certain properties can be given here also. This section of the MAIN subprogram must be amended carefully prior to running the computer program on a new problem.

Subroutines used to initialize variables (INIT), calculate properties (PROPS), update variables (CALCU for example), specify boundaries (PROMOD) and solve the algebraic equations (LISOLV, SOLVRX, SOLVRR) should remain intact. These subroutines represent the power of the numerical simulation whereas MAIN is the operator.

CHAPTER VII

RESULTS AND ANALYSIS

The STRAC computer code has been developed by supplementing the hydrodynamics of the TEACH code with complex chemical kinetics, radiation heat transfer and pollution formation mechanisms. The need for a predictive model which incorporates these physical processes has been established (2, 8). The results of this investigation are presented by comparison of numerical predictions with experimental data and/or other predictions when available. Justification for inclusion of the physical processes is presented to substantiate their need and to discuss their effect on the results obtained.

7.1 Complex Chemical Kinetic Model

The STRAC code has been employed to predict the swirling, reacting case investigated experimentally by Khalil et al. (45). They conducted an experiment using a cylindrical combustion chamber with variable guide vane cascade swirlers to vary the swirl intensity from a swirl number of 0.721 to 1.980. The experiment was conducted expressly for comparison with mathematical models, to show aerodynamic and thermodynamic conditions which exist in the firing test section. Kerosene was burned in a water cooled combustion section which was 200 cm in length and 20 cm in diameter. Axial and tangential (swirl) velocities, and temperature data were reported.

Two numerical predictions were accomplished using a nonuniform mesh of size 40×15 arranged over the combustion section. Inlet values of temperature, velocity, fuel flow rates and theoretical air were determined from initial conditions provided. STRAC accounted for one of the numerical predictions whereas a separate code incorporating the one-step reaction mechanism provided the second set of predictions. Except for the difference in reaction mechanisms, these codes were identical.

The numerical results, Figures 9-11, show comparisons of experimental data with the two levels of predictive capability. Various axial stations are denoted by their nondimensional distance x/D with the radial location determined by r/D . Information plotted includes velocities normalized with respect to a fixed quantity U_0 (inlet velocity) and temperatures normalized with respect to the maximum field temperature T_{\max} .

Figures 9-11 represent the case with a swirl number of 0.721. Figure 9 demonstrates the ability of the STRAC code to accurately predict the axial velocity trends. At the first two stations, $x/D = 0.55$ and 1.2 , the predictions are in excellent agreement with experimental values. Notice, however, that at the next two stations, $x/D = 1.9$ and 2.6 , strong centerline capability is evident but some difficulty is exhibited at the outside wall where velocities are overpredicted. This variance appears to be a result of dampened recirculation effects in the downstream portion of the model. The predictions made using the one-step reaction mechanism are poor and are neither qualitatively nor quantitatively accurate. Strong coupling of the hydrodynamics and thermodynamics may provide insight into the inadequacy of the axial

velocity predictions of the one-step combustion model.

Predictions of the normalized swirl velocity, Figure 10, further illustrate the dampened recirculation effects. Here, qualitative results of both predictions are good with slightly better quantitative predictions in the case of the two-step global mechanisms. At station, $x/D = 0.55$, maximum swirl effects in the experimental study occur at $r/D = 0.37$ whereas the predictions are maximized at $r/D = 0.25$ and leads to overprediction at the outer wall. Further downstream, the near centerline predictions are good but the outer wall region is again overpredicted, never returning to zero. Notice that in each case, the predictions made using the two-step global mechanism provide better qualitative results than does the other prediction. Notice also that the maximum swirl velocity is moving closer to the outer wall. In general, these predictions are considered to be good.

Figure 11 demonstrates the superiority of the two-step global mechanism in predicting the normalized temperature distribution. In general the STRAC code produces excellent quantitative results except at $x/D = 1.2$ and $x/D = 1.9$ where rapid temperature growth overpredicts the experimental results. Temperature reductions such as those reported in this experiment have not been observed elsewhere. At all other stations, the current model predictions and experimental results exhibit close correlation. Also, the one-step mechanism predictions are extremely poor, especially at the first three stations.

Analysis of Figures 9-11 demonstrates the need for inclusion of the two-step global mechanism to adequately predict the velocity and temperature profiles in the combustion section. Overall quantitative results are good to excellent, with minor exceptions as noted.

Additional predictions using the STRAC code have been compared with the experimental data of Khalil et al. (45) when the swirl number is 1.980 and are seen in Figures 12-14. Predictions of normalized axial velocity are presented in Figure 12. At the first two stations the predictions are quantitatively good except at $x/D = 1.2$ where the central toroidal recirculation zone length is underpredicted. This trend is perpetuated in the next two stations where the velocity is over predicted at the centerline and underpredicted as r/D becomes longer. For the axial velocity, the predictions are considered fair to good. Swirl velocities are shown on Figure 13. Here, as with the smaller swirl number, recirculation effects are dampened from $r/D = 0.3$ to the outer-wall resulting in overprediction of the swirl velocities at the outer-wall. These results are disappointing quantitatively but are qualitatively useful.

Normalized temperatures are compared to experimental results in Figure 14. At $x/D = 0.55$ the temperature profiles are quite satisfying, as the prediction are in excellent agreement with experimental data. At the next station the temperatures are slightly overpredicted from the centerline to $r/D = 0.3$. This represents an excessive use of fuel in this region which affects the predictions at the last three stations. Notice that in each case the temperatures are underprediction along the entire radius of the combustor. The maximum underprediction is approximately 225°C , at the last station. In general the predictions are qualitatively good and quantitatively fair to excellent.

The improved predictive capability of the two-step global mechanism has been demonstrated in Figures 9-11. Predictions of axial and swirl velocities along with temperature are substantially better using

this process as compared with the simple one-step mechanism. While there are variations between predicted and experimental velocities, the temperature profiles produced exhibit excellent correlation with experimental data throughout the combustion zone. Based on this evidence, the inclusion of the two-step global mechanism is necessary for adequate prediction of the combustion process.

7.2 Radiation Heat Transfer

Radiative heat transfer has been included in the STRAC code via the four-flux model. Tables VII and VIII illustrate the effect of radiation heat transfer on radial temperature distributions at various axial stations. Comparisons are made with and without radiation for swirl numbers of 0.332 and 0.720 using the two-step global reaction model to produce heat release information.

Table VII represents the effect of radiation heat transfer with a swirl number of 0.332. Radial temperature profiles are presented at various axial stations with and without the inclusion of radiation effects. At $x/D = 1.078$ the temperatures are generally higher with radiation included and reach a maximum differential of $+329^{\circ}\text{C}$ at $r/r_0 = 0.35$. Also, radial flame spread is quite evident. At $x/D = 1.948$, radiation generally causes the flame to be cooler except at the outer boundary where radial flame spread causes a dramatic increase in temperature with the differential being $+335^{\circ}\text{C}$. At $x/D = 4.742$ radiation causes the temperature to be cooler at each radial location, often by as much as 60°C . These variations illustrate the effect of radiation on the temperature profiles, however, without comparison to experimental data this information is speculative.

Table VIII represents the effect of radiation heat transfer with a swirl number of 0.721 and corresponds to the results shown in Figure 11. The profiles presented in Figure 11 demonstrate good to excellent predictive capability using the two-step global combustion model. Variations previously discussed would have been more severe without the inclusion of radiation heat transfer in the overall model. Study of Table VIII reveals that $x/D = 1.078$ radiation has reduced temperatures from $r/r_0 = 0$ to 0.50 then increases the temperatures as the outer boundary is approached. Thus, the predicted profile at $x/D = 1.2$ on Figure 11 would be moved farther to the right (greater quantitative error) without radiation. Similar radial temperature reductions are seen at $x/D = 1.948$ when radiation is included. Farther downstream at $x/D = 4.742$, all radial temperature values have been increased by the inclusion of radiation. The effect is the excellent prediction displayed at $x/D = 5.85$ on Figure 11. Notice that throughout the combustion section, radiation heat transfer has provided significant temperature variations which have increased the quantitative accuracy of the predictive technique.

The justification for including radiation heat transfer is evident. Improved predictive capability has been the net effect. An additional consideration is the degree of temperature variation which radiation produces. Differentials from 20°C to 335°C have been observed in the combustion zone. Since temperature is the primary consideration in the production of nitrogen oxide, radiation heat transfer will also affect the predictive capability of the pollution formation mechanism. Table IX demonstrates the radiation heat transfer effect on NO prediction for the case when the swirl number is 0.720.

Notice that without radiation the downstream predictions are between 40 and 75 percent higher than the values predicted with radiation included. Thus, from the information presented here, radiative heat transfer is an important physical process which impacts on the predictive capability of the combustion model and must be included.

7.3 General Predictions

Owen et al. (46) conducted an experimental evaluation utilizing a water cooled, axisymmetric combustor fueled by natural gas (96% CH₄) mixed with heated input air. Recirculation was produced in the combustion region by imparting a swirl component into the air flow. Investigations were made for various swirl numbers, pressures, mass flow rates and inlet temperatures. Cases where the swirl numbers were 0.0 and 0.3, and the inlet pressure was 3.8 atmospheres have been used for comparison with the present predictive model. Also, the zero swirl case has been compared with the predictions of Jones and Whitelaw (44).

Figures 15 and 16 show the experimental results compared with the two predictive techniques. Figure 15 contains the normalized axial velocity profiles at various axial stations. At $x/D = 0.5$ both predictive techniques overpredicted the velocity field and exhibited a recirculation zone that was considerably shorter than in the experimental case. A slight reduction of the inlet velocity increases the recirculation zone length but also reduced the maximum velocity obtained in the combustion zone. In this case an estimated inlet velocity of 17 m/s allowed attainment of the maximum velocity and provided excellent downstream results. At $x/D = 1.0$ the predictions

of Jones and Whitelaw (44) are quantitatively good except at the outer wall region, while the present predictions are qualitatively good. The velocity profiles at $x/D = 1.5$ and 2.0 are essentially the same with some exceptions. At $x/D = 1.5$, the current model is more accurate from the centerline to $r/D = 0.25$ and the overall variance is less than the previous predictions (44). At $x/D = 2.0$, the outer wall capability of the present model and the overall quantitative agreement demonstrates excellent predictive capability. In general both models appear adequate with the present model exhibiting good results in the downstream regions.

The quality of either technique cannot be assessed on the basis of predicted axial velocity only. Figure 16 shows the normalized temperature profiles at three axial stations. Clearly the capability of the present model is superior in this case. At each x/D station, the previous predictions exhibit significant errors. Also, their maximum temperature is approximately 200°C lower than that obtained by Owen et al. (46). These are serious shortcomings since Owen et al. proceed to obtain nitrogen oxide concentrations. The present model produces good results at $x/D = 1.0$ although temperatures are over-predicted by 10 percent. This overprediction may cause acceleration of the flowfield thus shortening the recirculation zone at $x/D = 0.5$ (Figure 15). This effect is felt downstream until $x/D = 2.0$ where both the temperature and velocity profiles align themselves with the experimental results. At this station and at $x/D = 3.0$ the normalized temperature predictions of the present model are excellent.

Figure 17 compares experimental predictions of nitrogen oxide with predictions from the current model. Predicted NO concentrations

compare favorably with experimental results except that maximum and minimum concentrations occur at different radial locations. Study of Figure 16 reveals small but significant temperature variations at centerline locations. Overpredictions of 50°C at these locations causes overprediction of NO concentrations due to the sensitivity of the pollutant mechanism to temperature variations. Similarly, although the nondimensionalized temperature profiles are essentially the same at $x/D = 2.0$ and 3.0 , the maximum experimental temperature is some 20-30°C greater than the predicted values. Above 1900°C this small variation can cause rapid increases in NO production and is the case at r/D equal to or greater than 0.25. This explains the shift in the maximum NO production when comparing the experimental and predictive results. Notice, however, that the predictions are reasonably accurate.

Predictions for a swirl number of 0.30 are shown in Figures 18-20. Notice in Figure 18 that the experiment contains a recirculation zone which is off the centerline whereas the prediction has a central torroidal recirculation zone. Here the hydrodynamics may be dominated by the large temperature surge seen at $x/D = 1.0$ on Figure 19. These higher temperatures and the associated density increases cause velocity accelerations, either recirculations or axial thrusts, such as those observed in Figure 18. Normalized temperature profiles at $x/D = 2.0$ and 3.0 show excellent agreement with experimental, however at the latter, the maximum velocity is some 50°C too low. This results in NO prediction at $x/D = 3.0$ on Figure 20, which are substantially lower than the experimental result. Again, NO production is strongly coupled to temperature. Notice that the NO production is off by a

factor of 2. Small temperature variations around 2000 K cause significant changes in predicted NO concentrations. Ramos (40) encountered a similar problem during his investigation. Thus, accurate NO prediction is dependent on, among other things, extremely accurate temperature predictions.

Oven et al. (47) conducted an experimental evaluation of a swirl-stabilized combustor. A 10.2 cm steel section, six diameters in length was used to study co- and counter-swirl effects on combustion. Two concentric swirling jet flows were established with an inner swirl number of 0.493 and outer swirl number of 0.559. This combination was approximated by a single swirl number of 0.53. Similarly, inner and outer equivalence ratios were defined, however only the inner equivalence ratio was used since the combustion appeared to be controlled by this inner value. A mean entrance axial velocity of 24 m/s was used to approximate the experimental conditions.

The normalized temperature profiles are seen in Figure 21. Predicted and experimental maximum temperatures were within 2%, thus these normalized profiles are excellent representations of the predictive capability. Near the centerline the predictions are excellent but as r/D passes 0.25 the low equivalence ration and low ignition temperatures cause a dramatic temperature reduction in the experimental case, whereas the predicted temperatures remain quite high. The result is a slightly higher predicted rate of NO production in this region. Comparison of NO concentration in Figure 22 shows excellent agreement between experimental and predicted results. Thus, when the temperatures are essentially equal, the ability to predict NO concentrations is excellent.

Oven et al. (47) also present carbon monoxide concentrations which are compared to predicted levels in Figure 23. Experimental results show high levels of CO concentration near the centerline with negligible concentrations beyond r/r_0 greater than 0.6. The reason is that dilution by the outer jet of pure air coupled with vigorous mixing preclude the combustion of this CO and reduces lateral propagation. The predictions indicate the opposite, high efficiency and lateral propagation at both axial stations. This difference is caused by the simplicity of the model in combining the two jet flows into a single inlet flow. The validity of the CO concentration profile is supported by the accuracy of previous temperature predictions, although the high combustion efficiency of the model may account for over prediction of temperatures below $x/D = 1.0$ in several cases. Experimental evidence of Scheefer and Sawyer (48) demonstrates a two order of magnitude increase in CO concentrations as r/r_0 moves to the outer wall. This supports the results presented in Figure 23 and indicates that the two jet simulation must be exactly modeled to obtain accurate predictions of CO concentrations.

Khalil et al. (34) conducted a series of predictive comparisons with experimental data from other authors. Comparisons contained in Figures 24 through 28 will include their choice of experimental data and their "model 2" predictions along with current model predictions. Here, comparisons are made for swirl number of 0.0 and 0.52 however, a shortfall exists in that no experimental temperature data are available.

Figures 24 and 25 represent the swirl case with a swirl number of 0.0. Axial velocities are shown in Figure 24. Notice that both

both predictive techniques adequately represent the experimental data, although the predictions of Khalil et al. are quantitatively more accurate. The current predictions are underpredicted especially at the centerline where a recirculation flow is evident. Khalil et al. overpredict the centerline axial velocities, but are generally in good agreement. Figure 25 shows a large variation between the temperature predictions, however, without experimental data, it is difficult to assess their worth. Khalil et al. have a large radial spread which is more often seen in a swirling case. The current predictions show a cool centerline with some radial spread. The cool region may be a result of the recirculation noted earlier. Temperature predictions will be discussed later.

Figures 26-28 represent the swirl case with a swirl number of 0.52. The recirculation zone of the current model is vastly overpredicted at $x/D = 1.0$ on Figure 26, the outer velocity values coincide with the experimental data. Here, the coupling of hydrodynamics and heat release at the centerline have caused a rapid acceleration of the axial velocity. At $x/D = 1.5$ the axial velocity is underpredicted at all radial stations. These results are disappointing although they have qualitative value. Swirl velocity comparison in Figure 27 again demonstrate the ability of the model of Khalil et al. Here, current predictions are generally good except in the region of r/D greater than 0.35. In this region, swirl velocities are slightly overpredicted. Temperature predictions in Figure 28 are again speculative but demonstrate a degree of compatibility. Notice that centerline variation of temperature at $x/D = 1.0$ is significant enough to affect the hydrodynamics.

The temperature predictions of Khalil et al. are obtained by using a "Model 2" which they developed. This model was adopted because it demonstrated reasonable agreement with other experimental results. A noted shortcoming is its inability to accurately predict centerline temperature values. Also, it exhibits errors in the range of 100-300°C depending on the radial location and especially at upstream locations. While it is the best of the models used by Khalil et al., they recognize its shortcomings. For this reason, the predictive capability of the present model will be determined by comparison with previous results.

7.4 Recirculation Zone Lengths

Swirl is introduced into the combustion process to aid in flame stabilization. In cases where swirl is weak, variations in axial flow patterns are minimal, however, as the swirl strength increases adverse pressure gradients cause recirculation zones to form. Recirculation zones may form in corners adjacent to the combustor inlet or along the centerline of the combustion section, or both. Figures 29 and 30 illustrate the strength of these recirculation zones for hot and cold flows under varying swirl conditions.

Figure 29 demonstrates the effect of increased swirl strength on the length of the central toroidal recirculation zone for hot and cold flows. Notice that until the swirl number is greater than 0.3 both the cold and hot flows exhibit small, stable recirculation zones. Notice also, that as the swirl number is increased to 0.52, both flows exhibit recirculation zone length enlargement. Here the hot flow recirculation zone length enlargement is significant.

The corner recirculation zone behaves differently as shown in Figure 30. While both hot and cold flows have decreased corner recirculation with increased swirl, the hot flow reduction is more dramatic. The corner recirculation zone of the cold flow remains stable until the stronger swirl is achieved, while the hot flow corner recirculation zone immediately begins a rapid decline in length as the swirl increases from 0.0. Comparison of these results with the experimental results provided by Khalil et al. (34) verifies these trends. Thus, as central toroidal recirculation zones increase in size, corner recirculation zones tend to be smaller.

7.5 Reliability of Predictions

The finite difference mesh size was chosen to be 40×15 for many of the predictions contained in this investigation. Computational cost and flowfield resolution must be considered when choosing the grid density for such applications. Reduction to a 30×15 mesh reduced the storage requirement and computational effort by approximately 25 percent and resulted in velocity and temperature variation of less than 1 percent throughout the domain.

Paramount in solution accuracy are reliable kinetic reaction rates for fuels consumed in the combustor, accurate inlet conditions derived from experimental studies, and a reliable turbulence model applicable to the recirculating flows found in the combustion test section. Reasonable kinetic data are available for methane and propane fuels, however considerable work is required if other fuels, are to be consumed. With expanded quasi-global models, the degree of uncertainty surrounding intermediate reaction rates increases the probability of

error. Certainly this is the case when considering the pollutant formation mechanisms of Nitrogen oxide and other nitrogen oxides. Concern over equilibrium assumptions for monatomic oxygen production points out possible errors here also. Many experimental reports omit vital inlet data which must be determined by the designer to begin the numerical simulation. Assumed initial conditions can lead to erroneous conclusions. Reconciliation of these problems is a must to assure accurate predictions.

Accuracy of prediction is divided into two levels; qualitative and quantitative. Qualitative accuracy indicates predictions useful in describing trends within the flowfield. Quantitative accuracy indicates that the prediction can be used to specify information that the predictions can be used to specify information concerning the flowfield variables. Various degrees of quantitative accuracy are discussed, including; fair, good and excellent. Excellent results are normally within 5 percent of the experimental data, while good results are in the range of 5-20 percent in the case of velocities. In the case of temperatures, a 20 percent error could be 400 K high or low, and would be considered poor. Likewise, a good NO prediction is within a factor of two. Thus these quantitative measures must be weighed with respect to the variable being discussed. The results presented herein were interpreted based upon accepted practice in the combustion field.

CHAPTER VIII

CONCLUSION

The present research was concerned with the two-dimensional axisymmetric approximation of the three-dimensional combustion problem as it occurs in combustors such as those in gas turbine engines. The primitive pressure-velocity two-dimensional axisymmetric finite difference TEACH computer code was extensively modified to produce a turbulent reacting computer code. Radiation heat transfer was simulated by way of a second-order flux method, appropriate to axisymmetric flows. Heat release information was obtained via a two-step global reaction mechanism, which includes prediction of local carbon monoxide levels and temperatures local and global heat release because of incomplete combustion. The importance of heat release is realized when dealing with oxides of nitrogen which are extremely temperature sensitive. Included were discussions of predictive methods available for radiation, heat release and nitrogen oxide production.

Many factors affect the production of pollutants in the combustion section of the gas turbine engine. Predictions made with the code demonstrated the ability to predict four different flow situations with good to excellent correlation. Significant is the importance of radiation heat transfer in tempering the overall energy balance in the combustion section of the combustor. The two-step global reaction mechanism shows good agreement with experiment. The requirement for accurate heat

release data can be seen when comparing predicted nitrogen oxide concentrations with experimental results. Significant concentration errors are seen with small temperature variations when temperatures above 1900 K are obtained. Coupling of the chemical kinetics and radiation heat transfer provides good heat release data and nitrogen oxide predictions.

REFERENCES

1. Wuerer, J. E. and G. S. Samuelson. "Predictive Modeling of Back-mixed Combustor Flows: Mass and Momentum Transport," AIAA Paper No. 79-215, New Orleans, La., January 15-17, 1969.
2. Ellail, M. M. M. Abou, A. D. Gosman, F. C. Lockwood and I. E. A. Megahed. "Description and Validation of a Three-Dimensional Procedure for Combustion Chamber Flows." Journal of Energy, Vol. 2, No. 2, March-April 1978, pp. 71-80.
3. Jones, Robert E. "Gas Turbine Engine Emissions--Problems, Progress and Future." Progress in Energy and Combustion Science, Vol. 4, Pergamon Press, LTD, 1978, pp. 73-113.
4. Lilley, D. G. "Flowfield Modeling in Practical Combustors: A Review." Journal of Energy, Vol. 3, July-August 1979, pp. 193-210.
5. Patankar, S. V. and D. B. Spalding. "Mathematical Models of Fluid Flow and Heat Transfer in Furnaces: A Review" Journal of the Institute of Fuel, September 1973, pp. 279-283.
6. Srivatsa, S. K. "Computations of Soot and NO_x Emissions from Gas Turbine Combustors". NASA CR-167930, Garrett Turbine Engine Company, Phoenix, Arizona, 1982.
7. Lilley, D. G. "Fluid Dynamic Combustor Research Problems." Presented at DOD Colloquium on Gas Turbine Combustor Modeling, Purdue University, West Lafayette, Indiana, September 5-6, 1979.
8. Lilley, D. G. "Swirl Flows in Combustion: A Review," AIAA Journal, Vol. 15, August 1977, pp. 1063-1078.
9. Edelman, R. B. and P. T. Harsha. "Analytical Modeling of Sudden Expansion Burners," Chemical Propulsion Information Agency Publication 298, June 1977.
10. Edelman, R. B. and P. T. Harsha. "Laminar and Turbulent Gas Dynamics in Combustion - Current Status." Progress in Energy and Combustion Science, Vol. 4, Pergamon Press, 1978, pp. 1-62.
11. Edelman, R. B., O. Fortune and G. Weilerstein. "Some Observations on Flows Described by Coupled Mixing and Kinetics", In Emissions from Continuous Combustion Systems, Edited by

Walter Cornelius and William G. Agnew, Plenum Press, N. Y., 1972, pp. 55-87.

12. Spalding, D. B. "Mathematical Models of Turbulent Flames: A Review," Combustion Science and Technology, Vol. 13, 1976, pp. 3-25.
13. Odgers, J. Personal Communication, Hartford, Connecticut, June 30, 1979.
14. Lilley, D. G., D. L. Rhodes and J. W. Samples. "Prediction of Swirling Reacting Flow in Ramjet Combustors." AIAA Paper No. 81-1485. Colorado Springs, Colo., July 25-27, 1981.
15. McDonald, H. "Combustion Modeling in Two and Three Dimensions - Some Numerical Considerations." Progress in Energy and Combustion Science, Vol. 5, (1979) pp. 97-122.
16. Chaturvedi, M. C. "Flow Characteristics of Axisymmetric Expansions". Journal of the Hydraulics Division, Proceedings ASCE. Vol. 89, No. HY3 (1963). pp. 61-92.
17. Owen, R. K. "Measurements and Observations of Turbulent Recirculating Jet Flows." AIAA Journal, Vol. 14, No. 11, Nov. 1976, pp. 1556-1562.
18. Habib, M. A. and J. H. Whitelaw. "Velocity Characteristics of Confined Coaxial Jets With and Without Swirl." ASME Paper No. 79-WA/FE-21. New York, New York, December 2-7, 1979.
19. Durst, F. and A. K. Rastogi. "Theoretical and Experimental Investigations of Turbulent Flows with Separation". ASME/Pennsylvania State University Symposium on Turbulent Shear Flows. University Park, PA, April 18-20, 1977, pp. 18.1-18.9.
20. Kubo, I. and F. C. Gouldin. "Numerical Calculations of Turbulent Swirling Flow". Presented at the Joint Fluids Conference (Combustion Symposium). Montreal, Canada. May 13-15, 1974.
21. Green, A. and J.H. Whitelaw. "Measurements and Calculations of the Isothermal Flow in Axisymmetric Models of Combustor Geometries". Journal of Mechanical Engineering Science, Vol. 22, No. 3, 1980, pp. 7-12.
22. Rhode, D. L., D. G. Lilley, and D. K. McLaughlin. "On the Prediction of Swirling Flowfields Found in Axisymmetric Combustor Geometries". Proceedings, ASME Symposium on Fluid Mechanics of Combustion Systems. Boulder, Colo., June 22-24, 1983, pp. 257-266.
23. Lilley, D. G. "Prediction of Inert Turbulent Swirl Flows". AIAA Journal. Vol. 11, No. 7, July 1973, pp. 955-960.

24. Launder, B. E. and D. B. Spalding. "The Numerical Computation of Turbulent Flows". Computer Methods in Applied Mechanics and Engineering. North-Holland Publishing Company. (1974), pp. 269-289.
25. Tennakore, K. N. and F. R. Steward. "Comparison of Several Turbulence Models for Predicting Flow Patterns with Confined Jets". ASME/Pennsylvania State University Symposium on Turbulent Shear Flows. University Park, PA, April 18-20, 1977, pp. 10.9-10.16.
26. Gibeling, H. J. H. McDonald and W. R. Briley. "Development of a Three-Dimensional Combustor Flow Analysis. Volume II: Theoretical Studies." Technical Report AFAPL-TR-75-59. United Technologies Research Center. East Hartford, Connecticut, October 1, 1976.
27. Novick, A. S., G. A. Miles and D. G. Lilley. "Modeling Parameter Influences in Gas Turbine Combustor Design". AIAA Paper No. 79-0354. New Orleans, La., January 15-17, 1979.
28. Spalding, D. B. "Mathematical Models of Continuous Combustion." In Emissions from Continuous Combustion Systems, edited by Walter Cornelius and William G. Agnew, Plenum Press, N. Y., 1972, pp. 3-16.
29. Lilley, D. G. "Modeling of Combustor Swirl Flows." Acta Astronautica, Vol. 1, 1974, pp. 1129-1147.
30. Hirt, C. W., B. D. Nichols and N. C. Romero. "SOLA - A Numerical Solution Algorithm for Transient Fluid Flows". Report No. LA-5852, Los Alamos Scientific Laboratory, Los Alamos, New Mexico, 1975.
31. Manheimer-Timnat, Y. "Numerical Methods for Calculating the Performance of Air-Breathing Combustion Chambers." International Symposium on Air-Breathing Engines, 3rd Proc., Munich, Germany. Rtsch Ges Luft und Raumfahrt, Cologne Germany, March 7-12, 1976, pp. 473-487.
32. Peck, R. E. and G. S. Samuelsen. "Analytical and Experimental Study of Turbulent Methane - Fired Blackmixed Combustion". AIAA Paper 75-1268, Anaheim, California, Sept. 29-Oct. 1, 1975.
33. Lilley, D. G., "Primitive Pressure - Velocity Code for the Computation of Strongly Swirling Flows". AIAA Journal, Vol. 14, June 1976, pp. 749-756.
34. Khalil, E. E., D. B. Spalding and J. H. Whitelaw. "The Calculation of Local Flow Properties in Two-Dimensional Furnaces." International Journal of Heat and Mass Transfer, Vol. 18, 1975, pp. 755-791.

35. Gosman, A. D. and E. Ioannides. "Aspect of Computer Simulation of Liquid-Fuelled Combustors". AIAA Paper No. 81-0323, St. Louis, Missouri, January 12-15, 1981.
36. Patankar, S. V. and D. B. Spalding. "A Computer Model for Three-Dimensional Flow in Furnaces", 14th Symposium (Int.) on Combustion, Penn State, PA, Aug. 20-25, 1972, pp. 605-615.
37. Serag-Eldin, M. A. and D. B. Spalding. "Computations of Three-Dimensional Gas Turbine Combustion Chamber Flows". Transactions of the ASME, Vol. 101, July 1979, pp. 326-336.
38. Pan, Y. S. "The Development of a Three-Dimensional Partially Elliptic Flow Computer Program for Combustion Research". NASA Contractor Report 3057, Pittsburgh Energy Research Center, Pittsburgh, Pa., 1978.
39. Mongia, H. C. and R. S. Reynolds. "Combustor Design Criteria Validation, Vol. III - User's Manual". Report USARTL-TR-78-55C, U. S. Army Research and Technology Laboratory, Ft. Eustis, Va., February 1979.
40. Ramos, J. I. "Exhaust Gas Emissions from a Swirl Stabilized Combustor". AICHE Symposium Series, R. P. Stein, ed. Vol. 177, No. 208, (1981), pp. 393-399.
41. Ramos, J. I. "The Numerical Modeling of Swirling Flows in a Gas Turbine Combustor". International Symposium on Refined Modeling of Flows, Paris, 1982.
42. Khalil, E. E. "Assessment of Numerical Computation of Flow Properties in an Axisymmetric Reversed Flow Furnance". Applied Mathematical Modeling, Vol. 3, No. 1, Feb. 1979. pp. 25-31.
43. Gosman, A. D., F. C. Lockwood and A. P. Salooja. "The Prediction of Cylindrical Furnaces Gaseous Fueled with Premixed and Diffusion Burners". 17th Symposium on Combustion, The Combustion Institute, 1978, pp. 747-759.
44. Jones, W. P. and J. H. Whitelaw. "Calculation Methods for Reacting Turbulent Flows". Paper in Prediction of Turbulent Reacting Flows in Practical Systems, presented at the Fluids Engineering Conference, Boulder, Co., June 22-29, 1981, pp. 9-27.
45. Khalil, K. H., F. M. El-Mahallawy, and H. A. Moneib. "Effect of Combustion Air Swirl on the Flow Pattern in a Cylindrical Oil Fired Furnace". Sixteenth Symposium (International) on Combustion, The Combustion Institute, 1977.
46. Owen, F. K., L. J. Spadaccine, and C. T. Bowman. "Pollutant Formation and Energy Release in Confined Turbulent Diffusion Flames". Sixteenth Symposium (International) on Combustion, The Combustion Institute, 1977.

47. Oven, M. J., F. C. Gouldin and W. J. McLean. "Temperature and Species Concentration Measurements in a Swirl-Stablized Combustor." Seventeenth Symposium on Combustion, The Combustion Institute, 1978, pp. 363-374.
48. Scheefer, R. W. and R. F. Sawyer. "Lean Premixed Recirculating Flow Combustion for Control of Oxides of Nitrogen". Sixteenth Symposium (International) on Combustion, The Combustion Institute, 1977.
49. McDannel, M. D., P. R. Peterson and G. S. Samuelson. "Species Concentration and Temperature Measurements in a Lean Premixed Flow Stablized by a Reverse Jet". Combustion Science and Technology, Vol. 28, (1982), pp. 211-224.
50. Baker, R. J., P. Hutchinson, E. E. Khalil and J. H. Whitelaw. "Measurements of Three Velocity Components in a Model Furnace With and Without Combustion". Fifteenth Symposium (International) on Combustion, The Combustion Institute, (1975), pp. 553-559.
51. Sawyer, R. F. "Experimental Studies of Chemical Processes in a Model Gas Turbine Combustor". Paper in Emissions from Continuous Combustion Systems, (Cornelius, W. and W. G. Agnew, eds.), Plenum Press, N. Y., (1972), pp. 243-252.
52. Sadakata, M. and J. M. Beer. "Spatial Distribution of Nitric Oxide Formation Rates in a Swirling Turbulent Methane-Air Flame". Sixteenth Symposium (International) on Combustion, The Combustion Institute, (1977), pp. 93-101.
53. Tuteja, A. D. and H. K. Newhall. "Nitric Oxide Formation in Laminar Diffusion Flames". Paper in Emissions from Continuous Combustion Systems, (Cornelius, W. and W. G. Agnew, eds), Plenum Press, N.Y., (1972), pp. 108-118.
54. Khalil, E. E. and J. H. Whitelaw. "Aerodynamic and Thermodynamic Characteristics of Kerosene - Spray Flames". Sixteenth Symposium (International) on Combustion, The Combustion Institute, (1977), pp. 569-575.
55. Chigier, N. A. and K. Dvorak. "Laser Anemometer Measurements in Flames with Swirl". Fifteenth Symposium (International on Combustion, The Combustion Institute (1975), pp. 573-582.
56. Anasoulis, R. F. and H. McDonald. "Development of a Combustor Flow Analysis - Part II; Experimental Studies". AFAPL-TR-73-98, Part II, United Aircraft Research Labs, East Hartford, Connecticut, Feb. 28, 1974.
57. Chigier, N. A., "Application of Model Results to Design of Industrial Flames". Paper from the Fourth Symposium on Flames and Industry, British Flame Research Committee and the Institute of Fuel, Sept. 19-20, 1972.

58. Hottel, H. C. and E. S. Cohen. "Radiant Heat Exchange in a Gas Filled Enclosure: Allowance for Non-uniformity of Gas Temperature." AICHE Journal, Vol. 4 #1, March 1958.
59. Beer, J. M. "Methods for Calculating Radiative Heat Transfer from Flames in Combustors and Furnaces," Heat Transfer in Flames, edited by N. Afgan and J. Beer, Scripta, Wash. 1974.
60. Hottel, H. C. and A. F. Sarofim. Radiative Transfer, p. 470, McGraw Hill, (1967).
61. Gosman, A. D. and F. C. Lockwood. "Incorporation of a Flux Model for Radiation into a Finite Difference Procedure for Furnace Calculation." Proc. 14th Symposium on Combustion, Combustion Institute, (1972), pp. 661-671.
62. Hamaker, H. C. "Radiation and Heat Conduction in Light Scattering Material." Philips Research Report #2, 55-67, 1947.
63. Lockwood, F. C. and N. G. Shah. "An Improved Flux Model for the Calculation of Radiation Heat Transfer in Combustion Chambers." ASME Paper 76-HT-55, Aug. 9-11, 1976.
64. Lilley, D. G., and D. L. Rhode. A Computer Code for Swirling Turbulent Axisymmetric Recirculating Flows in Practical Isothermal Combustor Geometries. Report NASA Cr-3442, Feb., 1982.
65. Siddal, R. G. "Flux Methods for the Analysis of Radiant Heat Transfer." Paper presented at the Fourth Symposium on Flames and Industry, 1972.
66. Lockwood, F. C. and D. B. Spalding. "Prediction of a Turbulent Reacting Duct Flow with Significant Radiation." Journal De Physique, Colloquo D'Evia De La Societe Francais De Physique. May 25-29, 1971, pp. 27-31.
67. Felton, P. G., J. Swithenbank, and A. Turan. "Progress in Modeling Combustors." Report No. AFOSR-TR-77-1297, University of Sheffield, Sheffield, England, (1977).
68. Patankar, S. V. "Numerical Prediction of Three-Dimensional Flows." Paper in Studies in Convection: Theory, Measurement, and Applications, (Launder, B. E., ed.), Vol. 1, Academic Press, London, 1975, pp. 1-78.
69. Serag-Eldin, M. A. and D. B. Spalding. "Prediction of the Flow and Combustion Processes in a Three-Dimensional Combustion Chamber." International Symposium on Air-Breathing Engines, 3rd Proc. Munich, Germany, Dtsch Ges Luft und Raumfahrt, Cologne, Germany, March 7-12, 1967, pp. 489-514.

70. Lilley, D. G. "Turbulent Swirling Flame Prediction." AIAA Journal, Vol. 12, February 1974, pp. 219-223.
71. Novick, A. S., G. A. Miles, and D. G. Lilley. "Numerical Simulations of Combustor Flow Fields." AIAA Paper 78-949, Las Vegas, Nevada, July 25-27, 1978.
72. Boysan, F., W. H. Ayers, J. Swithenbank, and Z. Pan. "Three Dimensional Model of Spray Combustion in Gas Turbine Combustors." AIAA Paper No. 81-0324. Presented at AIAA 19th Aero Science Meeting, St. Louis, Missouri, January 1981, pp. 12-15.
73. Osgerby, I. T. "An Efficient Numerical Method for Stirred Reactor Calculations." Report No. AFOSR-TR-72-0910, Arnold Engineering Development Center, Tennessee, 1971.
74. Mellor, A. M. "Current Kinetic Modeling Techniques for Continuous Flow Combustors." Paper in Emissions From Continuous Combustion Systems (W. Cornelius and W. G. Agnew, eds.), Plenum Press, N. Y., 1972.
75. Caretto, L. S. "Mathematical Modeling of Pollutant Formation." Progress in Energy and Combustion Science, Vol. 1, (1976), pp. 47-71.
76. Odgers, J. "Current Theories of Combustion within Gas Turbine Chambers." 15th Symposium (Int.) on Combustion, The Combustion Institute, Pittsburgh, Pennsylvania, (1975), pp. 1321-1339.
77. Gosman, Pun, Runchal, Spalding, and Wolfshtein, Heat and Mass Transfer in Recirculating Flows, Academic Press, London, 1969.
78. Khalil, E. E. and J. S. Truelove. "Calculation of Radiative Heat Transfer in a Large Gas-Fired Furnace." Letters in Heat and Mass Transfer, Vol. 4, pp. 353-365, 1977.
79. Swithenbank, J. A. Turan, and P. G. Felton. "Three Dimensional Two-Phase Mathematical Modeling of Gas Turbine Combustors," Gas Turbine Combustor Design Problems, A. H. LeFebvre, ed., Hemisphere Publishing Corp., N. Y., 1980.
80. Anasoulis, R. F., H. McDonald, and R. C. Buggeln. "Development of a Combustor Flow Analysis - Part I: Theoretical Studies." Report Number AFAPL-TR-73-98, United Aircraft Research Labs, East Hartford, Connecticut, 1973.
81. Samuelson, G. S. "Mechanisms of Exhaust Pollutant and Plume Formation in Continuous Combustion," Report No. UCI-ART-76-10, UCI Combustion Laboratory, Irvine, California, 1976.

82. Peck, R. E. and G. S. Samuelson. "Eddy Viscosity Modeling in the Prediction of Turbulent, Backmixed Combustion Performance," Proc. 16th Symposium on Combustion, Combustion Institute, 1976.
83. Felton, P. G., J. Swithenbank, and A. Turan. "Progress in Modeling Combustors," Report No. AFOSR-TR-77-1297, University of Sheffield, Sheffield, England, 1977.
84. LeFebvre, A. H. "Pollution Control in Continuous Combustion Engines." 15th Symposium on Combustion. The Combustion Institute, Pittsburgh, Pennsylvania, (1975), pp. 1169, 1179.
85. Lowes, T. M., M. P. Heap, S. Michelfelder, and B. R. Pai. "Mathematical Modeling of Combustion Chamber Performance." Paper from the Fourth Symposium on Flames and Industry, British Flame Research Committee and the Institute of Fuel, Sept. 19-20, (1972) pp. 47-54.
86. Heap, M. P., T. M. Lowes, and R. Walmsley. "Emission of Nitric Oxide from Large Turbulent Diffusion Flames." 14th Symposium (Int.) on Combustion, Aug. 20-25, 1972, Penn State.
87. Khalil, E. E. Modeling of Furnaces and Combustors. Abacus Press, Tunbridge Wells, England. 1982 (In Press).
88. Caretto, L. S., L. J. Muzio, R. F. Sawyer, and E. S. Starkman. "The Role of Kinetics in Engine Emission of Nitric Oxide." Combustion Science and Technology, (1971), Vol. 3, pp. 53-61.
89. Caretto, L. S. "Modeling Pollutant Formation in Combustion Processes." 14th Symposium (Int.) on Combustion, Aug. 20-25, 1972, Penn State.
90. Edelman, R. B. and P. T. Harsha. "Mixing and Combustion in High Speed Air Flows." AFOSR-TR-78-0878, Science Applications, Inc., April 1978.
91. Jones, W. P. and C. H. Pridden. "Predictions of the Flow Field and Local Gas Composition in Gas Turbine Combustors." 17th Symposium on Combustion, The Combustion Institute, 1978.
92. Bowman, C. T., and D. J. Seery. "Investigation of NO Formation Kinetics in Combustion Processes: The Methane-Oxygen-Nitrogen Reaction." Paper in Emissions from Continuous Combustion Systems (Eds. W. Cornelius and W. G. Agnew), Plenum Press, N.Y., (1972), pp. 123-135.
93. Iverach, D. K., S. Basden, and N. Y. Kirov. "Formation of Nitric Oxide in Fuel Lean and Fuel Rich Flames." 14th Symposium (Int.) on Combustion, Aug. 20-25, 1972, Penn State.
94. Gosman, A. D. and W. M. Pun. Calculation of Recirculating Flows." Report No. HTS/74/2, Dept. of Mechanical Engineering, Imperial College, London, 1974.

95. Campbell, A. S. Thermodynamic Analysis of Combustion Engines, John Wiley and Sons, New York, 1979.

APPENDIXES

APPENDIX A

TABLES

TABLE I
EXTENDED C-H-O CHEMICAL KINETIC REACTION MECHANISM

| $k_f = AT^b \exp(-E/RT)$ | | | | | | |
|---|-----------------------|-------------------|----------------|---------------------|---------------------|--|
| Reaction | A | Forward | E | R | | |
| | Long chain | Cyclic | b | Long chain | Cyclic | |
| 1. $C_nH_m + \frac{n}{2}O_2 \rightarrow \frac{m}{2}H_2 + nCO^*$ | 6.0×10^4 | 2.8×10^7 | 1 | 12.2×10^3 | 19.65×10^3 | |
| 2. $CO + OH = H + CO_2$ | 5.6×10^{11} | | 0 | 0.543×10^3 | | |
| 3. $CO + O_2 = CO_2 + O$ | 3×10^{12} | | 0 | 25.0×10^3 | | |
| 4. $CO + O + M = CO_2 + M$ | 1.8×10^{19} | | -1 | 2×10^3 | | |
| 5. $H_2 + O_2 = OH + OH$ | 1.7×10^{13} | | 0 | 24.7×10^3 | | |
| 6. $OH + H_2 = H_2O + H$ | 2.19×10^{13} | | 0 | 2.59×10^3 | | |
| 7. $OH + OH = O + H_2O$ | 5.75×10^{12} | | 0 | 0.393×10^3 | | |
| 8. $O + H_2 = H + OH$ | 1.74×10^{13} | | 0 | 4.75×10^3 | | |
| 9. $H + O_2 = O + OH$ | 2.24×10^{14} | | 0 | 8.45×10^3 | | |
| 10. $M + O + H = OH + M$ | 1×10^{16} | | 0 | 0 | | |
| 11. $M + O + O = O_2 + M$ | 9.38×10^{14} | | 0 | 0 | | |
| 12. $M + H + H = H_2 + M$ | 5×10^{15} | | 0 | 0 | | |
| 13. $M + H + OH = H_2O + M$ | 1×10^{17} | | 0 | 0 | | |
| 14. $O + N_2 = N + NO$ | 1.36×10^{14} | | 0 | 3.775×10^4 | | |
| 15. $N_2 + O_2 = N + NO_2$ | 2.7×10^{14} | | -1.0 | 6.06×10^4 | | |
| 16. $N_2 + O_2 = NO + NO$ | 9.1×10^{24} | | -2.5 | 6.46×10^4 | | |
| 17. $NO + NO = N + NO_2$ | 1.0×10^{10} | | 0 | 4.43×10^4 | | |
| 18. $NO + O = O_2 + N$ | 1.55×10^9 | | 1.0 | 1.945×10^4 | | |
| 19. $M + NO = O + N + M$ | 2.27×10^{17} | | -0.5 | 7.49×10^4 | | |
| 20. $M + NO_2 = O + NO + M$ | 1.1×10^{16} | | 0 | 3.30×10^4 | | |
| 21. $M + NO_2 = O_2 + N + M$ | 6.0×10^{14} | | -1.5 | 5.26×10^4 | | |
| 22. $NO + O_2 = NO_2 + O$ | 1×10^{12} | | 0 | 2.29×10^4 | | |
| 23. $N + OH = NO + H$ | 4×10^{13} | | 0 | 0 | | |
| 24. $H + NO_2 = NO + OH$ | 3×10^{13} | | 0 | 0 | | |
| 25. $CO_2 + N = CO + NO$ | 2×10^{11} | | $-\frac{1}{2}$ | 4×10^3 | | |
| 26. $CO + NO_2 = CO_2 + NO$ | 2×10^{11} | | $-\frac{1}{2}$ | 2.5×10^3 | | |

* $-(dC_{C_nH_m}/dt) = AT^b P^{-3} C_{C_nH_m}^{1/2} C_{O_2} \exp[-E/RT]$; $[C] = \text{g moles/cc}$, $[T] = ^\circ\text{K}$, $[P] = \text{atm}$ $[E] = \text{k cal/mole}$. Reverse reaction rate, k_r , is obtained from k_f and the equilibrium constant, K_e .

Source: R. B. Edelman and P. T. Harsha. "Laminar and Turbulent Gas Dynamics in Combustion - Current Status." Progress in Energy and Combustion Science, Vol. 4, Pergamon Press, 1978, pp. 1-62.

TABLE II
NITROGEN REACTIONS FROM MELLOR

| | | |
|----------------------------------|---|--|
| VI. NO Formation* | | |
| 15. | $O + N_2 \rightleftharpoons NO + N$ | |
| 16. | $N + O_2 \rightleftharpoons NO + O$ | |
| 17. | $N + O + M \rightleftharpoons NO + M$ | |
| 18. | $N + OH \rightleftharpoons NO + H$ | |
| 19. | $N_2 + O_2 \rightleftharpoons NO + NO$ | |
| 20. | $N_2 + OH \rightleftharpoons NO + NH$ | |
| VII. Involving NO ₂ | | |
| 21. | $N_2 + O_2 \rightleftharpoons N + NO_2$ | |
| 22. | $NO + NO \rightleftharpoons N + NO_2$ | |
| 23. | $NO_2 + M \rightleftharpoons O + NO + M$ | |
| 24. | $NO_2 + M \rightleftharpoons O_2 + N + M$ | |
| 25. | $NO + O_2 \rightleftharpoons NO_2 + O$ | |
| VIII. Involving N ₂ O | | |
| 26. | $H + N_2O \rightleftharpoons N_2 + OH$ | |
| 27. | $O + N_2O \rightleftharpoons N_2 + O_2$ | |
| 28. | $O + N_2O \rightleftharpoons NO + NO$ | |

* Zeldovich Mechanism = Reactions 15 + 16

Source: A. M. Mellor. "Current Kinetic Modeling Techniques for Continuous Flow Combustors." Paper in Emissions From Combustion Systems (W. Cornelius and W. G. Agnew, eds.), Plenum Press, N.Y., 1972.

TABLE III
SOURCE TERMS AND EXCHANGE COEFFICIENTS USED IN THE
GENERAL EQUATION OF ϕ

| ϕ | Γ_ϕ | S_ϕ |
|--------------------|-----------------------------------|--|
| 1 | 0 | 0 |
| u | μ | $-\frac{\partial p}{\partial x} + S^u$ |
| v | μ | $-\frac{\partial p}{\partial r} + \frac{\rho w^2}{r} - \frac{2}{r^2} v + S^v$ |
| w | μ | $-\frac{\rho v w}{r} - \frac{w}{r^2} \frac{\partial}{\partial r} (r\mu) + S^w$ |
| h | μ/σ_h | S_h |
| m_{fu} | μ/σ_m | R_{fu} |
| $m_{ox} - im_{fu}$ | μ/σ_f | 0 |
| k | μ/σ_k | $G - C_d \rho \epsilon$ |
| ϵ | μ/σ_e | $(C_1 \epsilon G - C_2 \rho \epsilon^2)/k$ |
| m_{co} | μ/σ_c | $R_{fu} - R_{co}$ |
| m_{NO} | μ/σ_n | R_{NO} |
| R_x | $\frac{1}{(a + s)}$ | $a(\sigma T^4 - R_x) + \frac{s}{2} (R_r - R_x)$ |
| R_r | $\frac{1}{(a + s + \frac{1}{r})}$ | $a(\sigma T^4 - R_r) + \frac{s}{2} (R_x - R_r)$ |

In this table certain quantities are defined as follows:

$$S^u = \frac{\partial}{\partial x} \left(\mu \frac{\partial u}{\partial x} \right) + \frac{1}{r} \frac{\partial}{\partial r} \left(r\mu \frac{\partial v}{\partial x} \right)$$

$$S^v = \frac{\partial}{\partial x} \left(\mu \frac{\partial u}{\partial r} \right) + \frac{1}{r} \frac{\partial}{\partial r} \left(r\mu \frac{\partial v}{\partial r} \right)$$

$$S^w = 0$$

TABLE III (Continued)

$$S^h = 0 \text{ or if radiation included } S^h = 2a (R_x + R_r - 2\sigma T^4)$$

$$G = \mu [2 \{ (\frac{\partial u}{\partial x})^2 + (\frac{\partial v}{\partial r})^2 + (\frac{v}{r})^2 \} + (\frac{\partial u}{\partial r} + \frac{\partial v}{\partial x})^2 + \{ r \frac{\partial}{\partial r} (\frac{w}{r}) \}^2 + (\frac{\partial w}{\partial x})^2]$$

TABLE IV
THE FORM OF THE COMPONENTS OF THE LINEARIZED SOURCE TERM*

| ϕ | Γ_ϕ | S_p^ϕ | S_u^ϕ/V |
|--------------------|-----------------------------------|---------------------------|--|
| 1 | 0 | 0 | 0 |
| u | μ | 0 | $S^u - \frac{\partial p}{\partial x}$ |
| v | μ | $-2 \frac{\mu}{r^2}$ | $S^v + \frac{\rho w^2}{r} - \frac{\partial p}{\partial r}$ |
| w | μ | 0 | $-\frac{\rho v w}{r} - \frac{w}{r^2} \frac{\partial}{\partial r} (r\mu)$ |
| h | μ/σ_h | 0 | $2a(R_x + R_r - 2\sigma T^4)$ |
| m_{fu} | μ/σ_m | $-R_{fu}/m_{fu}$ | 0 |
| $m_{ox} - im_{fu}$ | μ/σ_f | 0 | 0 |
| k | μ/σ_k | $-C_\mu C_D \rho^2 K/\mu$ | G |
| ϵ | μ/σ_ϵ | $-C_2 \rho \epsilon/K$ | $C_1 C_\mu G \rho K/\mu$ |
| m_{CO} | μ/σ_C | $-R_{CO}/m_{CO}$ | R_{fu} |
| m_{NO} | μ/σ_n | 0 | R_{NO} |
| R_x | $\frac{1}{(a + s)}$ | $a + s$ | $a\sigma T^4 + \frac{s}{2} (R_x + R_r)$ |
| R_r | $\frac{1}{(a + s + \frac{1}{r})}$ | $a + s$ | $a\sigma T^4 + \frac{s}{2} (R_x + R_r)$ |

In this table, certain quantities are defined as follows:

S^u , S^v , and G are as in TABLE III

R_{fu} , R_{CO} , and R_{NO} are rates of formation or consumption of fuel, carbon monoxide and nitrogen oxide respectively. (-indicates consumption.)

* In this TABLE, V stands for the cell control volume and $\mu = \mu_{eff}$.

TABLE V
SUBROUTINE TASKS

| <u>Subroutine</u> | <u>Task</u> |
|-------------------|---|
| MAIN | Controls and monitors the entire sequence of calculations: initialization, properties and initial output; and iteration loop with calls to update main variables, other mixture properties and intermediate output; and, after termination of the iteration loop, final output, an increment in inlet degree of swirl and a return to the beginning again. |
| INIT | Sets values to the numerous geometric quantities concerned with grid structure, and initializes most variables to zero or other reference value. |
| PROPS | Updates the fluid properties via calculation of turbulent viscosity, under-relaxed using its previous value. In nonisothermal flows, perhaps with chemical reaction, additional species' mass fractions, temperature, density and variable specific heat are also calculated here, with appeals to FIXBND to establish boundary temperatures and to PROMOD (1) for any other modifications. |
| PRINT | Prints out an entire variable field according to a standard format. |
| TPRINT | Prints out only the temperature and non-dimensional temperature fields according to a format which includes boundary conditions. |
| CLACU and CALCV | Calculates coupling coefficients of finite difference equation for axial velocity u^* and radial v^* , calls PROMOD (2) and PROMOD (3) for boundary modifications and LISOLV for entire field of variables to be updated to get u^* and v^* fields. |
| CALCP | Calculates coupling coefficients of finite difference equation for pressure correction p' ; calls PROMOD (4) for boundary modifications and LISOLV to obtain p' field. The subroutine closes with p^* , u^* and v^* being 'corrected' with p' , u' and v' . |

TABLE V (Continued)

| | |
|------------------------|---|
| CALCH | Calculates coupling coefficients of finite difference equation for stagnation enthalpy, h , calls PROMOD(5) for boundary modifications and LISOLV to obtain h field. Also determines the requirement to update enthalpy via the radiation flux variation. |
| CALCRX and CALCRR | Calculates coupling coefficients of finite difference equation for x- and r-directional radiation flux; calls PROMOD(11) for boundary modifications and SOLVRX or SOLVRR respectively to obtain solution of the flux field. The directionality of the flux variables require specialized solution routines. |
| Other CALC Subroutines | Calculates coupling coefficients of appropriate finite difference equation, calls appropriate part of PROMOD and then LISOLV for complete update of the variable in question. |
| EQUAL | Determines the specie concentration of atomic nitrogen and oxygen for use in CALCNO. |
| CALCQ | Calculates the net radiation flux based on the directional fluxes previously calculated. |
| PROMOD | Modifies the values of the finite difference equation coefficients, or the variables, near walls or other boundaries where particular conditions apply. The subroutine is divided into chapters, each handling a particular variable and being called from a CALC subroutine, and each chapter considers all the boundaries around the solution domain. |
| FIXBND | Modifies the boundary temperature in a progressive manner to achieve the maximum boundary condition based on the interior temperature profile. Prevents early specification of boundary temperatures from driving the solution. |

TABLE V (Continued)

| | |
|-------------------|---|
| LISOLV | Updates entire field of a particular variable, by applying TDMA (tridiagonal matrix algorithm) to all the lines in the r-direction sequentially from left to right of the integration domain. |
| SOLVRX and SOLVRR | Updates the axial and radial radiation flux variables respectively, by applying a modified TDMA. Integration is directional and depends on the variable being solved. |

TABLE VI
PRINCIPAL DEPENDENT VARIABLES AND CONTROLLING PARAMETERS

| Algebraic Variable | Fortran Variable | Alphanumeric Heading | Logical Variable | Inlet Value | CALC Subroutine | Underrelax- ation Factor | Number of Sweeps of LISOLV per iteration | Prandtl/Schmidt Number | Residual Source Term |
|---------------------|------------------|----------------------|------------------|-------------|-----------------|-----------------------------|--|------------------------|---------------------------------------|
| u | U | HEDU | INCALU | UIN | CALCU | URFU | NSWPU | - | RESORU |
| v | V | HEDV | INCALW | VIN | CALCW | URFV | NSWPV | - | RESORV |
| w | W | HEDW | INCALW | WIN | CALCW | URFW | NSWPW | PRW | RESORW |
| k | TE | HEDK | INCALK | TEIN | CALCTE | URFK | NWSPK | PRTE | RESORK |
| ϵ | ED | HEDD | INCALD | EDIN | CALCED | URFE | NSWPD | PRED | RESORE |
| p' | PP | HEDP | INCALP | - | CALCP | URFP | NSWPP | - | (RESORM for mass calculated in CALCP) |
| μ | VIS | HEDVIS | INPRO | - | PROPS | URFVIS | - | - | - |
| h | H | HEDH | INCALH | HIN | CALCH | URFH | NSWPH | PRH | RESORH |
| T | T | HEDTEM | INPRO | TIN | PROPS | - | - | - | - |
| M_N | FU | HEDFU | INCALF | FUIN | CALCFU | URFF | NSWPF | PRFU | RESORF |
| ox-im _{Fu} | OF | HEDOF | INCALO | OFIN | CALCOF | URFO | NSWPO | PROF | RESORO |
| CO | CO | HEDCO | INCALC | - | CALCCO | URFCO | NSWPC | PRCO | RESORC |

TABLE VI (Continued)

| Algebraic Variable | Fortran Variable | Alphanumeric Heading | Logical Variable | Inlet Value | CALC Subroutine | Underrelax- ation Factor | Number of Sweeps of LISOLV per iteration | Prandtl/ Schmidt Number | Residual Source Term |
|--------------------|------------------|----------------------|------------------|-------------|-----------------|-----------------------------|---|-------------------------------|----------------------------|
| NO | AND | HEDNO | INCLNO | - | CALCNO | URFNO | NSWPNO | PRNO | RESRNO |
| R _x | RADX | HEDRX | INCLRX | RADIN | CALCRX | URFRX | NSWPRX | - | RESORX |
| R _r | RADR | HEDRR | INCLRR | RADIN | CALCRR | URFRR | NSWPRR | - | RESORR |
| O ₂ | OX | HEDOX | INPRO | OXIN | PROPS | - | - | - | - |
| CO ₂ | CO2 | HEDCO2 | INPRO | - | PROPS | - | - | - | - |
| H ₂ O | H2O | HEDH2O | INPRO | - | PROPS | - | - | - | - |
| O | O1 | HEDO | INCALC | - | EQUAL | - | - | - | - |
| N | AN1 | HEDN | INCLNO | - | EQUAL | - | - | - | - |
| N ₂ | AN2 | HEDNI | INPRO | PRIN | PROPS | - | - | - | - |
| H ₂ | H2 | HEDH2 | INRPO | - | PROPS | - | - | - | - |

TABLE VII

EFFECT OF RADIATION HEAT TRANSFER OF RADIAL TEMPERATURE DISTRIBUTION
AT AXIAL LOCATIONS; SWIRL NUMBER = 0.332

| Location | $\frac{x}{D} = 1.078$ | | $\frac{x}{D} = 1.948$ | | $\frac{x}{D} = 4.742$ | |
|----------|-----------------------|----------------|-----------------------|----------------|-----------------------|----------------|
| r/r_o | Without Radiation | With Radiation | Without Radiation | With Radiation | Without Radiation | With Radiation |
| | T°K | | T°K | | T°K | |
| 0.96 | 577 | 571 | 720 | 1055 | 834 | 815 |
| 0.88 | 564 | 569 | 912 | 1067 | 1292 | 1253 |
| 0.81 | 560 | 569 | 1101 | 1147 | 1458 | 1407 |
| 0.73 | 558 | 573 | 1231 | 1236 | 1539 | 1482 |
| 0.65 | 561 | 584 | 1330 | 1318 | 1585 | 1526 |
| 0.58 | 572 | 611 | 1408 | 1391 | 1615 | 1555 |
| 0.50 | 602 | 671 | 1472 | 1453 | 1636 | 1576 |
| 0.42 | 667 | 792 | 1524 | 1503 | 1650 | 1590 |
| 0.35 | 796 | 1035 | 1564 | 1542 | 1660 | 1600 |
| 0.27 | 1042 | 1232 | 1594 | 1572 | 1667 | 1607 |
| 0.19 | 1227 | 1352 | 1616 | 1592 | 1671 | 1612 |
| 0.12 | 1345 | 1440 | 1629 | 1605 | 1674 | 1615 |
| 0.04 | 1399 | 1475 | 1636 | 1612 | 1676 | 1617 |

TABLE VIII

EFFECT OF RADIATION HEAT TRANSFER ON RADIAL TEMPERATURE DISTRIBUTION
AT AXIAL LOCATIONS; SWIRL NUMBER = 0.721

| Location | $\frac{x}{D} = 1.078$ | | $\frac{x}{D} = 1.948$ | | $\frac{x}{D} = 4.742$ | |
|----------|-----------------------|----------------|-----------------------|----------------|-----------------------|----------------|
| r/r_o | Without Radiation | With Radiation | Without Radiation | With Radiation | Without Radiation | With Radiation |
| | T°K | | T°K | | T°K | |
| 0.96 | 821 | 847 | 1344 | 1365 | 818 | 837 |
| 0.88 | 1144 | 1251 | 1548 | 1540 | 1179 | 1213 |
| 0.81 | 1336 | 1440 | 1608 | 1587 | 1325 | 1361 |
| 0.73 | 1466 | 1534 | 1641 | 1613 | 1403 | 1437 |
| 0.65 | 1548 | 1583 | 1662 | 1631 | 1452 | 1485 |
| 0.58 | 1601 | 1612 | 1677 | 1645 | 1488 | 1517 |
| 0.50 | 1636 | 1630 | 1688 | 1655 | 1514 | 1541 |
| 0.42 | 1659 | 1642 | 1695 | 1662 | 1534 | 1558 |
| 0.35 | 1675 | 1650 | 1701 | 1668 | 1549 | 1570 |
| 0.27 | 1685 | 1656 | 1705 | 1672 | 1560 | 1580 |
| 0.19 | 1691 | 1660 | 1707 | 1675 | 1568 | 1586 |
| 0.12 | 1695 | 1663 | 1709 | 1677 | 1573 | 1591 |
| 0.04 | 1697 | 1664 | 1709 | 1678 | 1575 | 1593 |

TABLE IX
EFFECT OF RADIATION HEAT TRANSFER ON NITROGEN OXIDE
CONCENTRATIONS; SWIRL NUMBER = 0.720

| Location | $\frac{x}{D} = 1.078$ | | $\frac{x}{D} = 1.948$ | | $\frac{x}{D} = 4.742$ | |
|----------|-----------------------|----------------|-----------------------|----------------|-----------------------|----------------|
| r/r_0 | Without Radiation | With Radiation | Without Radiation | With Radiation | Without Radiation | With Radiation |
| | NO PPM | | NO PPM | | NO PPM | |
| 0.96 | .01 | .02 | .05 | .04 | .29 | .18 |
| 0.88 | .02 | .03 | .09 | .07 | .36 | .23 |
| 0.81 | .02 | .04 | .14 | .09 | .42 | .27 |
| 0.73 | .04 | .06 | .20 | .13 | .46 | .31 |
| 0.65 | .05 | .09 | .27 | .17 | .51 | .35 |
| 0.58 | .09 | .13 | .34 | .21 | .55 | .38 |
| 0.50 | .13 | .17 | .42 | .25 | .60 | .42 |
| 0.42 | .18 | .21 | .50 | .30 | .63 | .45 |
| 0.35 | .24 | .26 | .58 | .34 | .67 | .48 |
| 0.27 | .29 | .29 | .64 | .38 | .70 | .50 |
| 0.19 | .33 | .32 | .69 | .41 | .72 | .52 |
| 0.12 | .37 | .34 | .73 | .43 | .74 | .53 |
| 0.04 | .38 | .35 | .75 | .44 | .75 | .54 |

APPENDIX B

FIGURES

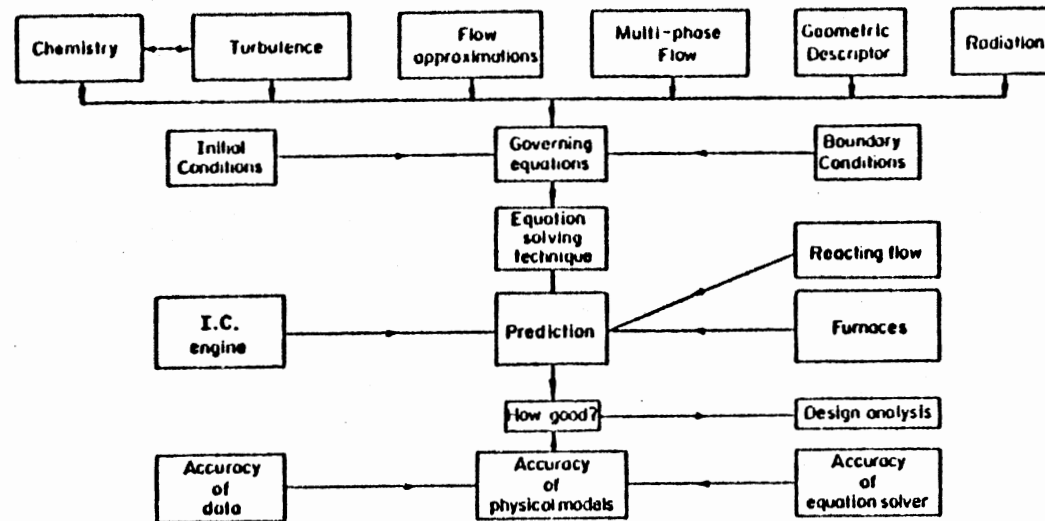


Figure 1. Structure of a Numerical Model

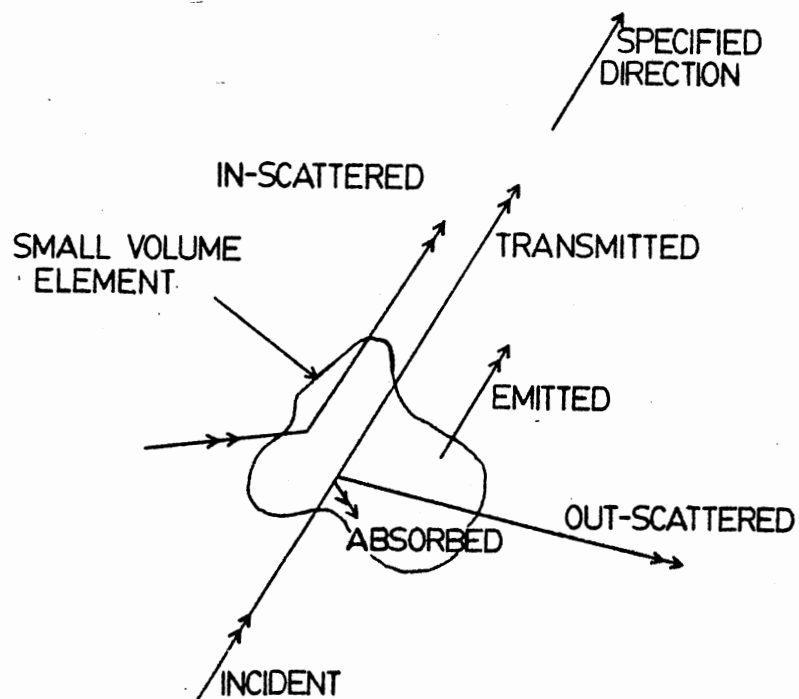


Figure 2. Radiant Energy Balance in a Specified Direction

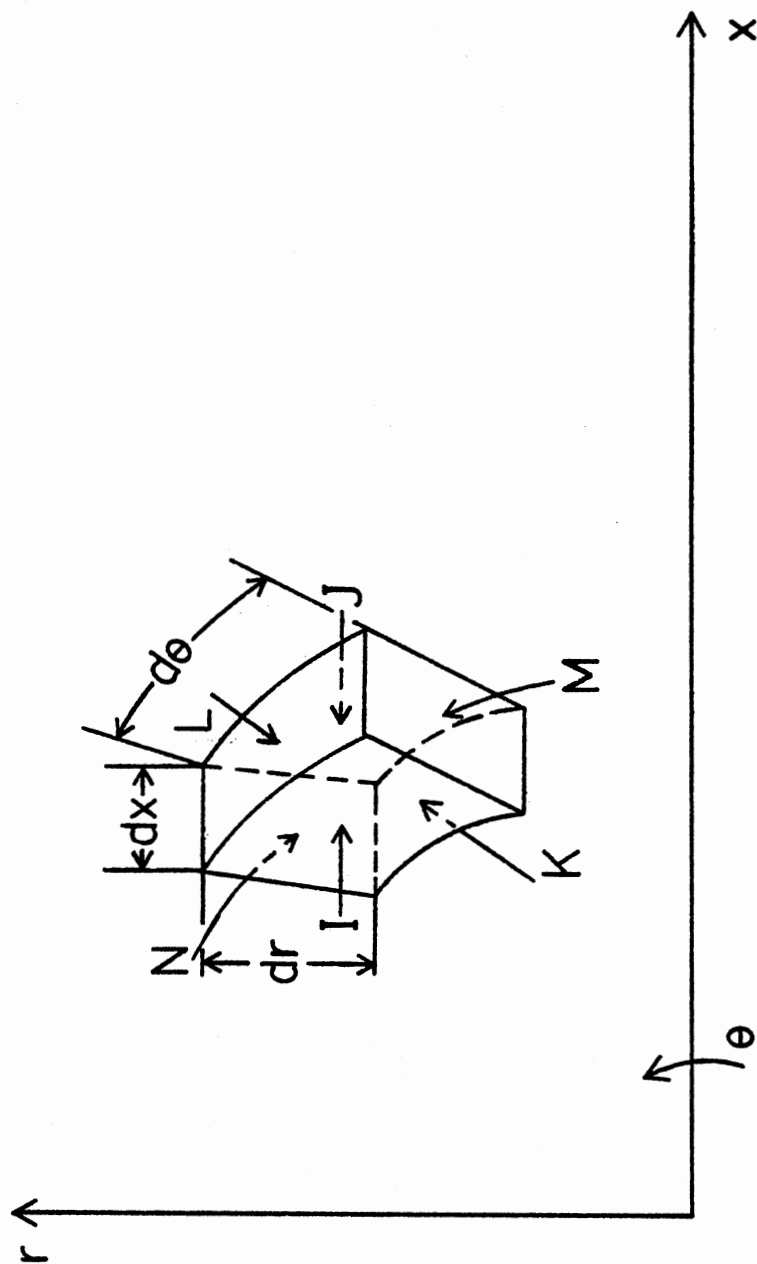


Figure 3. Flux Model for Cylindrical Coordinates

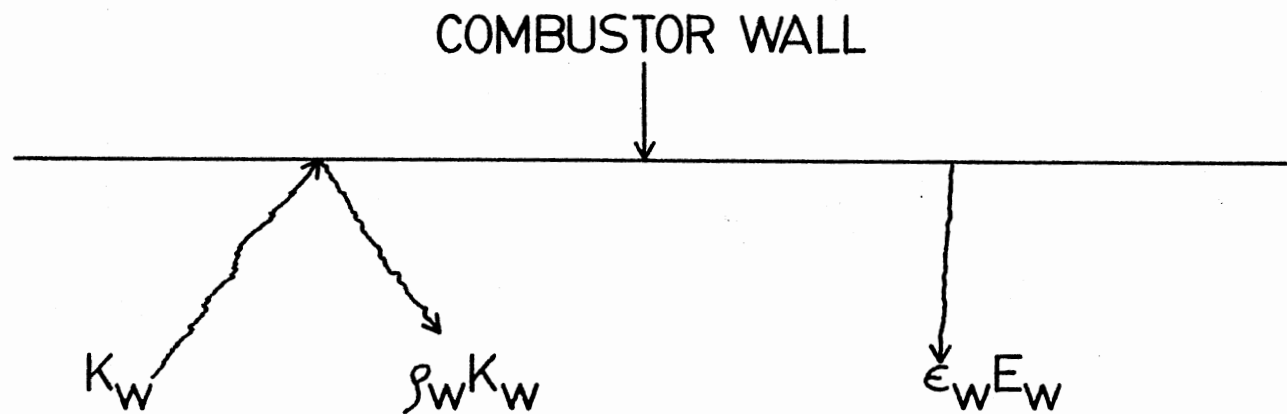


Figure 4. Radiation Balance at an Inside Combustor Wall

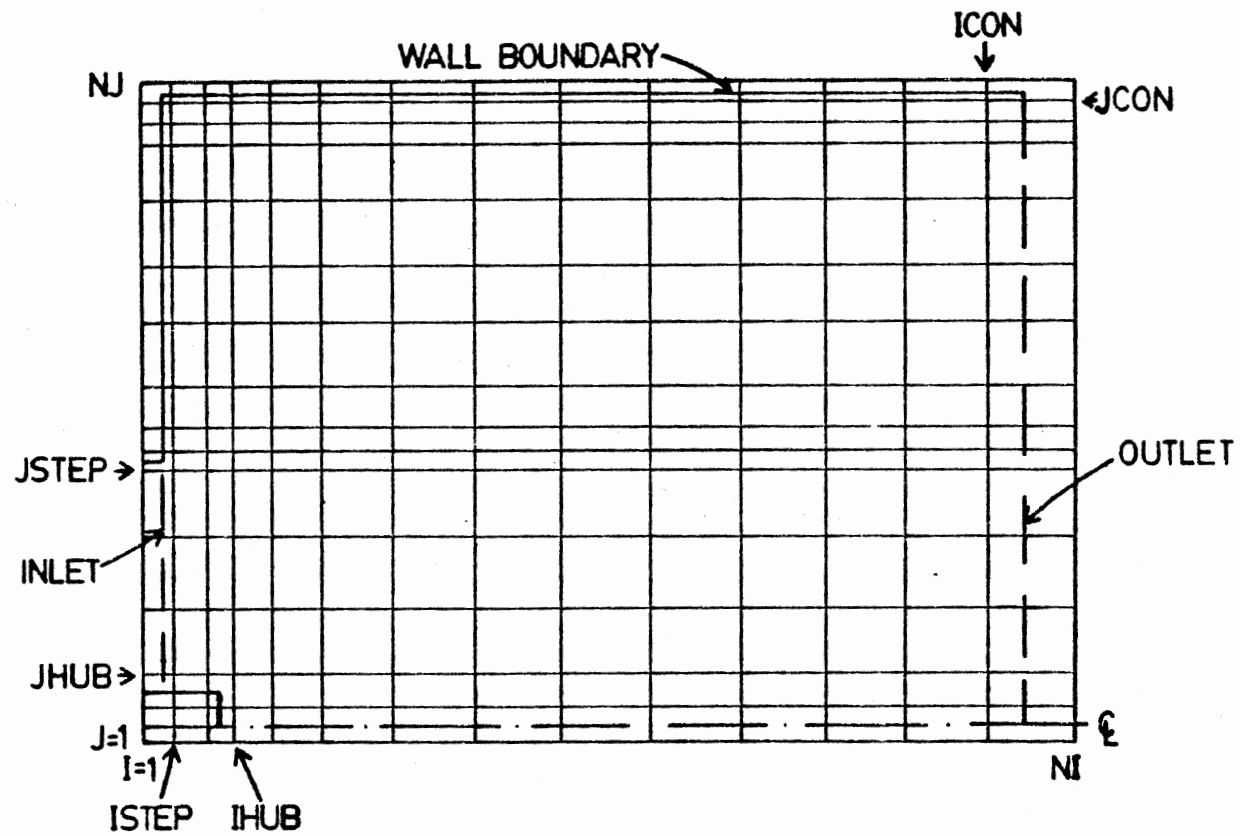
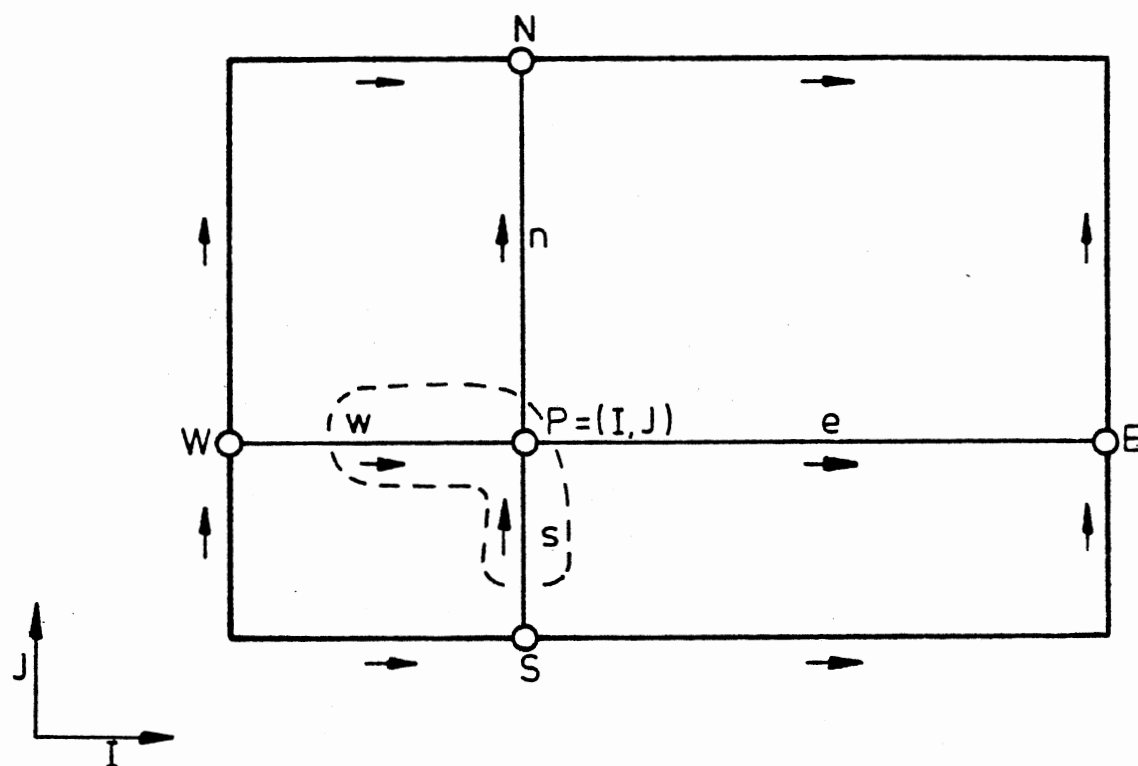
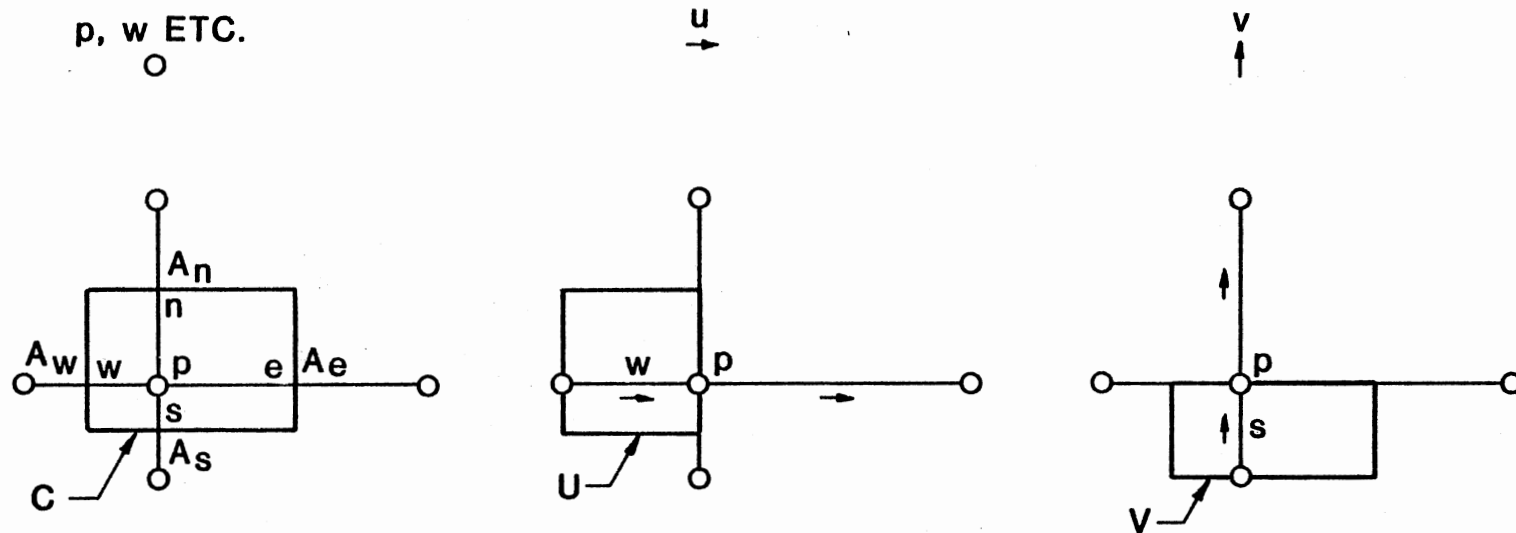


Figure 5. Irregularly Spaced Grid System with Flow Domain Fitted Inside



THREE GRIDS : FOR p, w ETC. - AT POSITION MARKED (O)
 FOR u VELOCITY - AT POSITION MARKED (\rightarrow)
 FOR v VELOCITY - AT POSITION MARKED (\uparrow)

Figure 6. Staggered Grid and Notation for the Rectangular Computational Mesh



CONTROL VOLUMES C, U, V FACE
 AREAS A_n , A_s , A_e AND A_w FOR C, SIMILAR FOR U AND V

Figure 7. The Three Control Volumes Associated with Points of the Three Grids

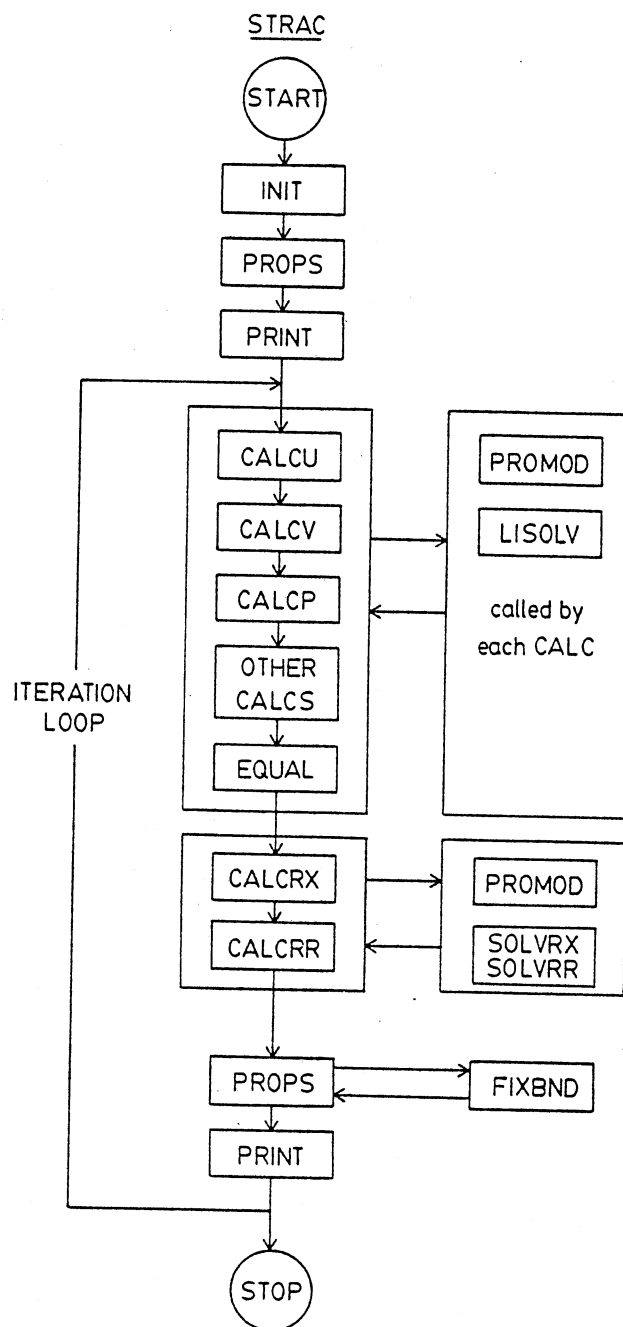


Figure 8. Flow Chart of Computer Program Showing the Subroutine Arrangement.

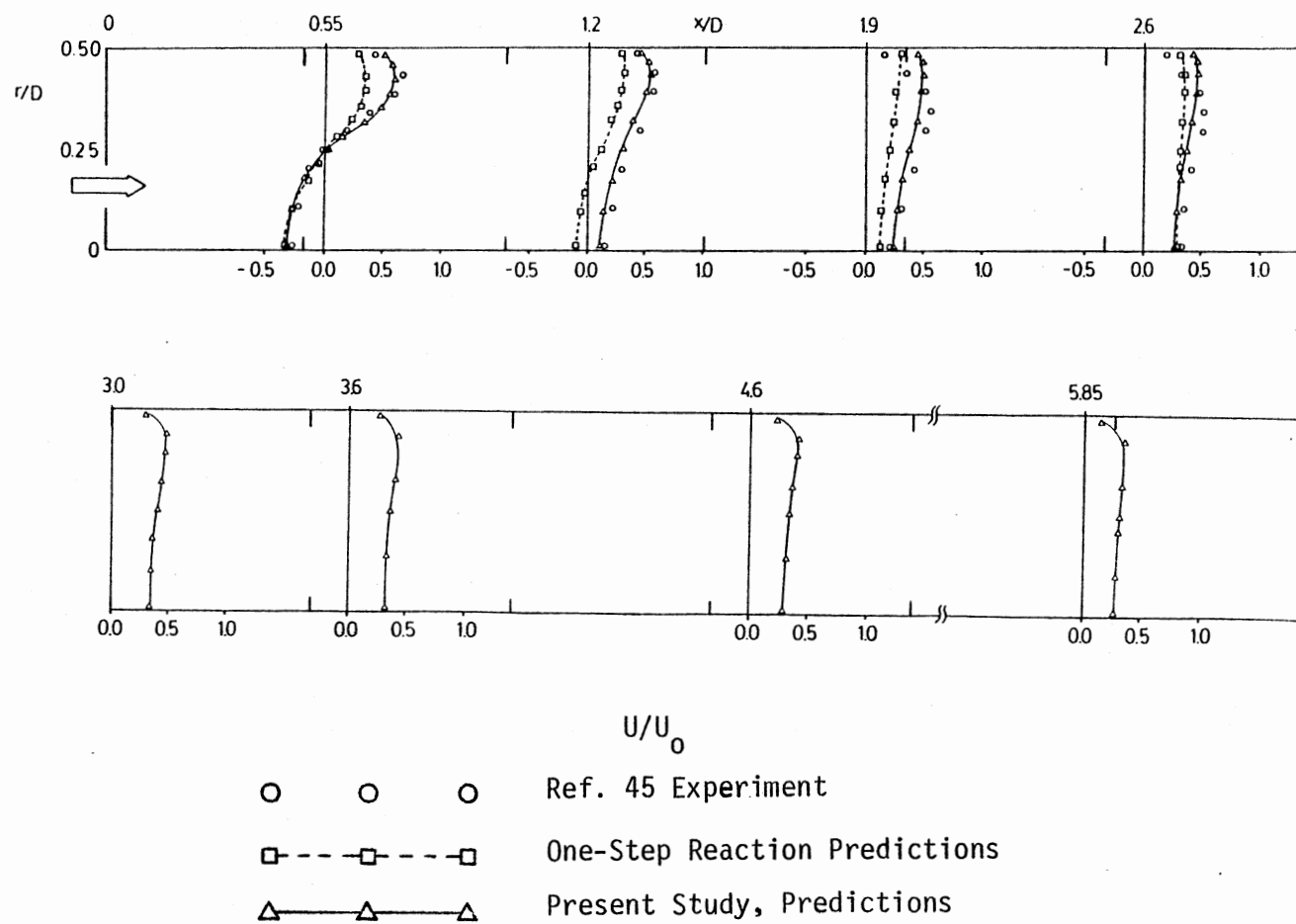


Figure 9. Axial Velocity Profiles for $S = 0.721$

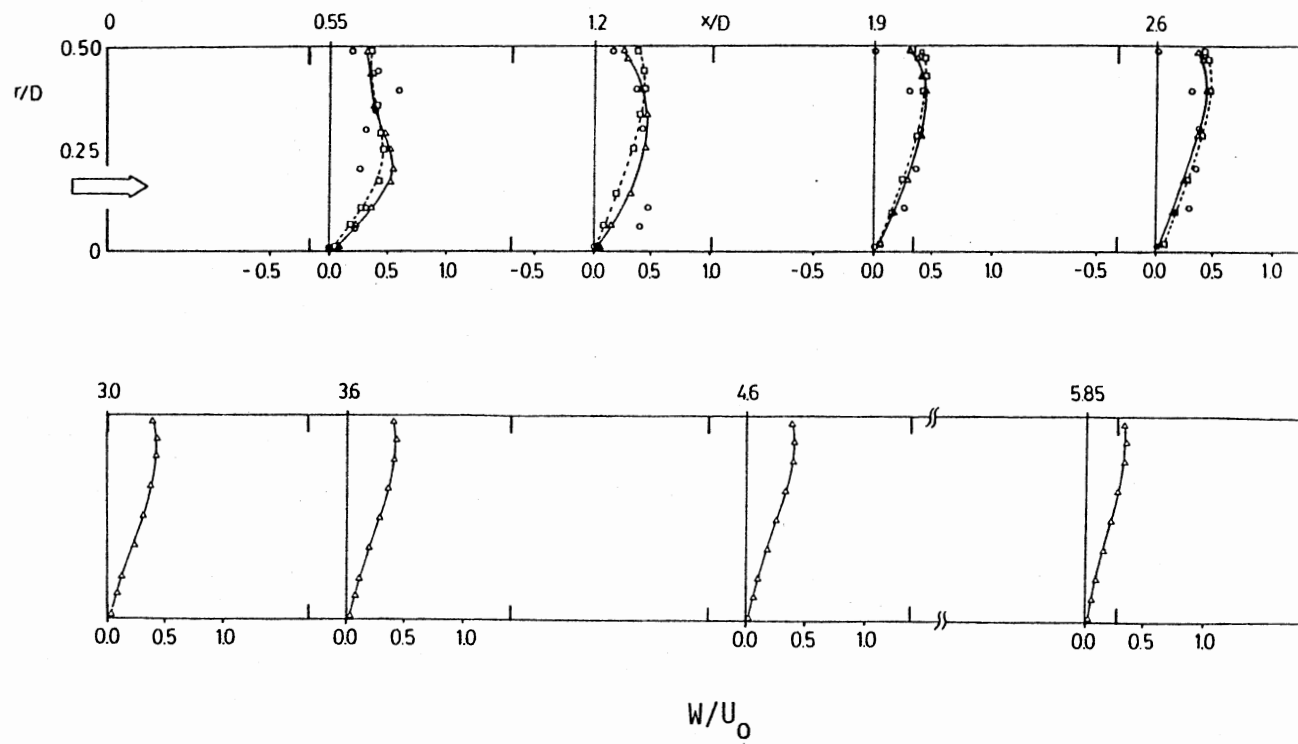
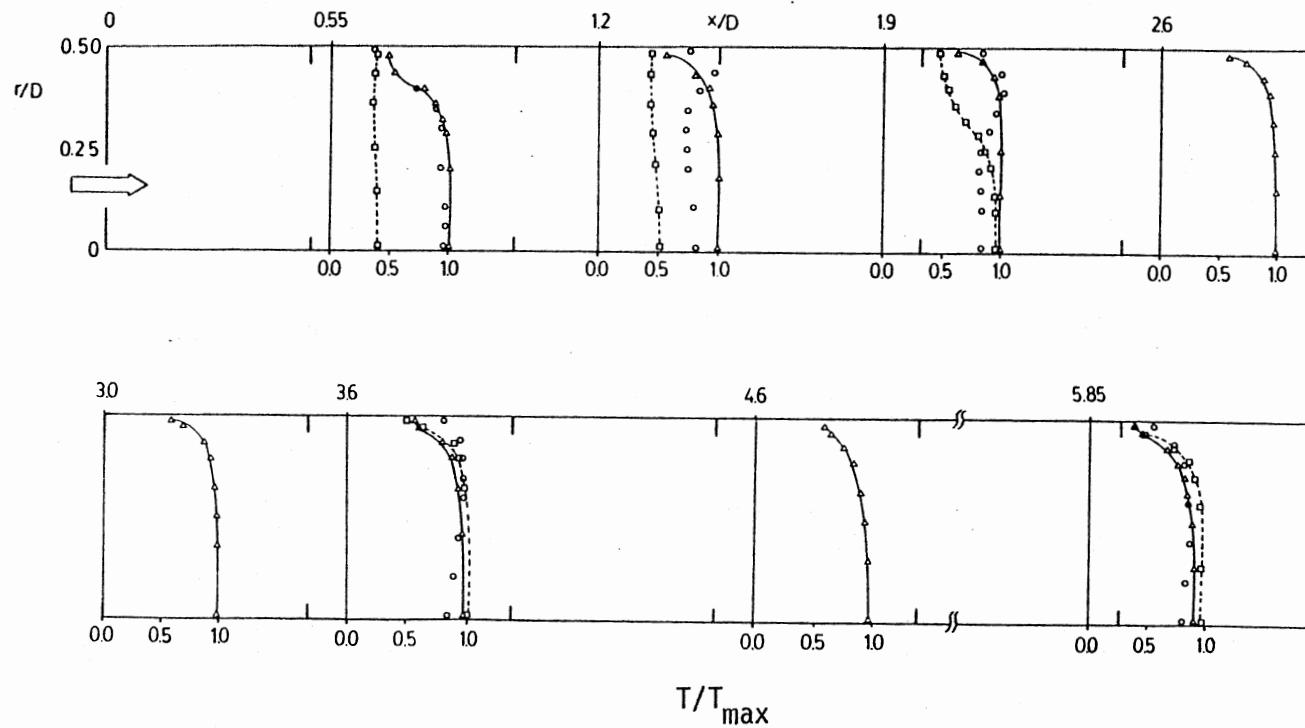
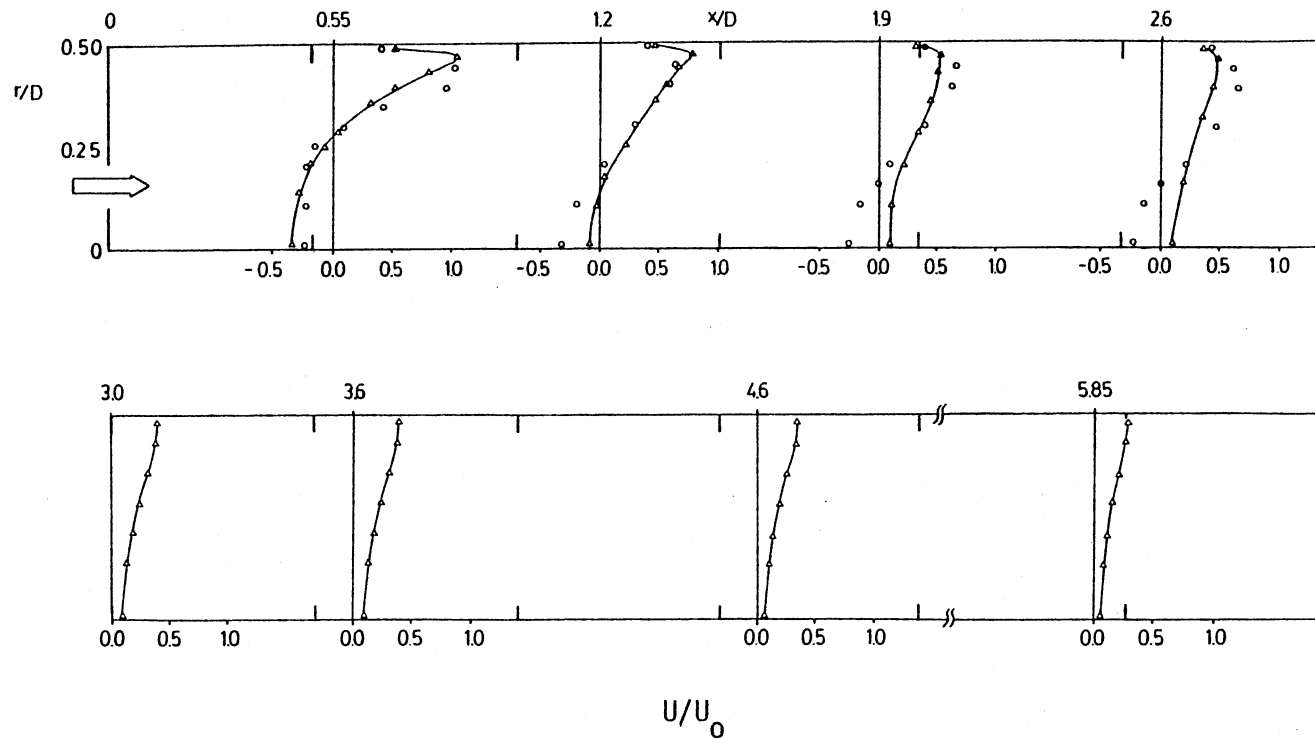


Figure 10. Swirl Velocity Profiles for $S = 0.721$



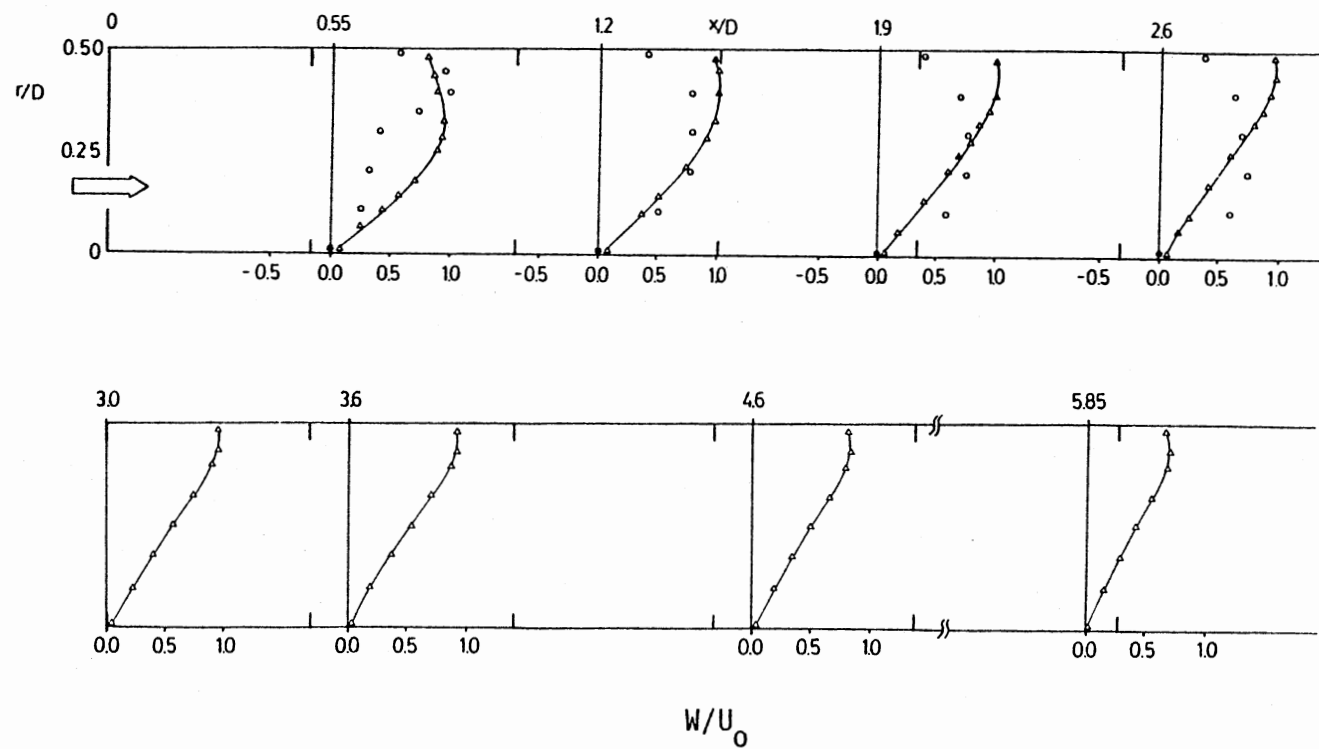
○ ○ ○ Ref. 45 Experiment
 □ --- □ --- □ One-Step Reaction Predictions
 △ — △ — △ Present Study, Predictions

Figure 11. Temperature Profiles for $S = 0.721$



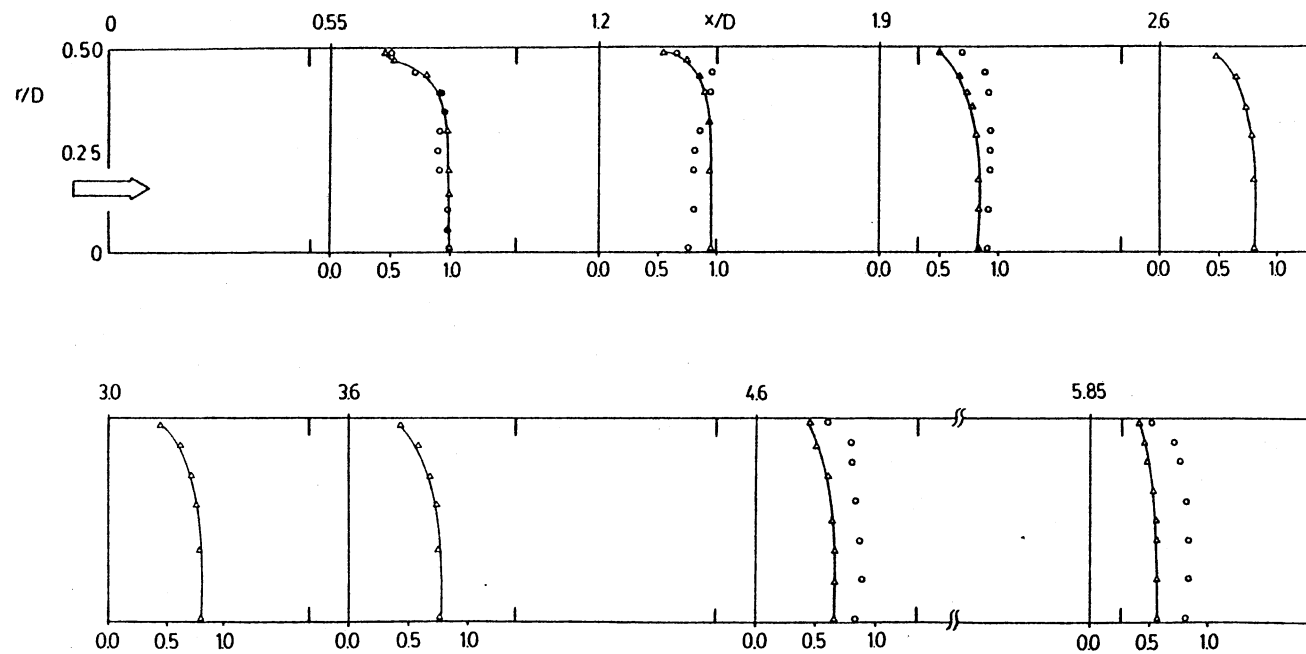
○ ○ ○ Ref. 45, Experiment
 ▲ ▲ ▲ Present Study, Predictions

Figure 12. Axial Velocity Profiles for $S = 1.980$



○ ○ ○ Ref. 45, Experiment
 △—△—△ Present Study, Predictions

Figure 13. Swirl Velocity Profiles for $S = 1.980$



T/T_{\max}

- ○ ○ Ref. 45, Experiment
- △ — △ — △ Present Study, Predictions

Figure 14. Temperature for $S = 1.980$

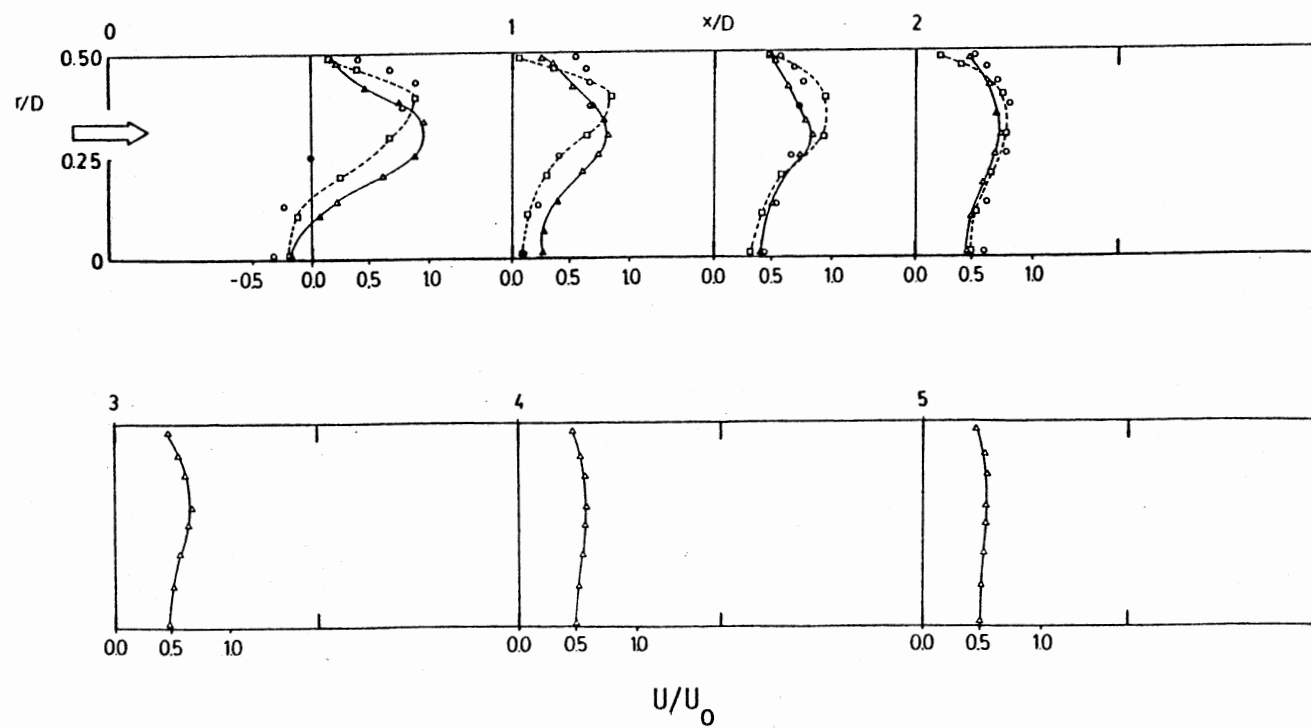


Figure 15. Axial Velocity Profiles for $S = 0.0$ and Pressure at 3.8 atm

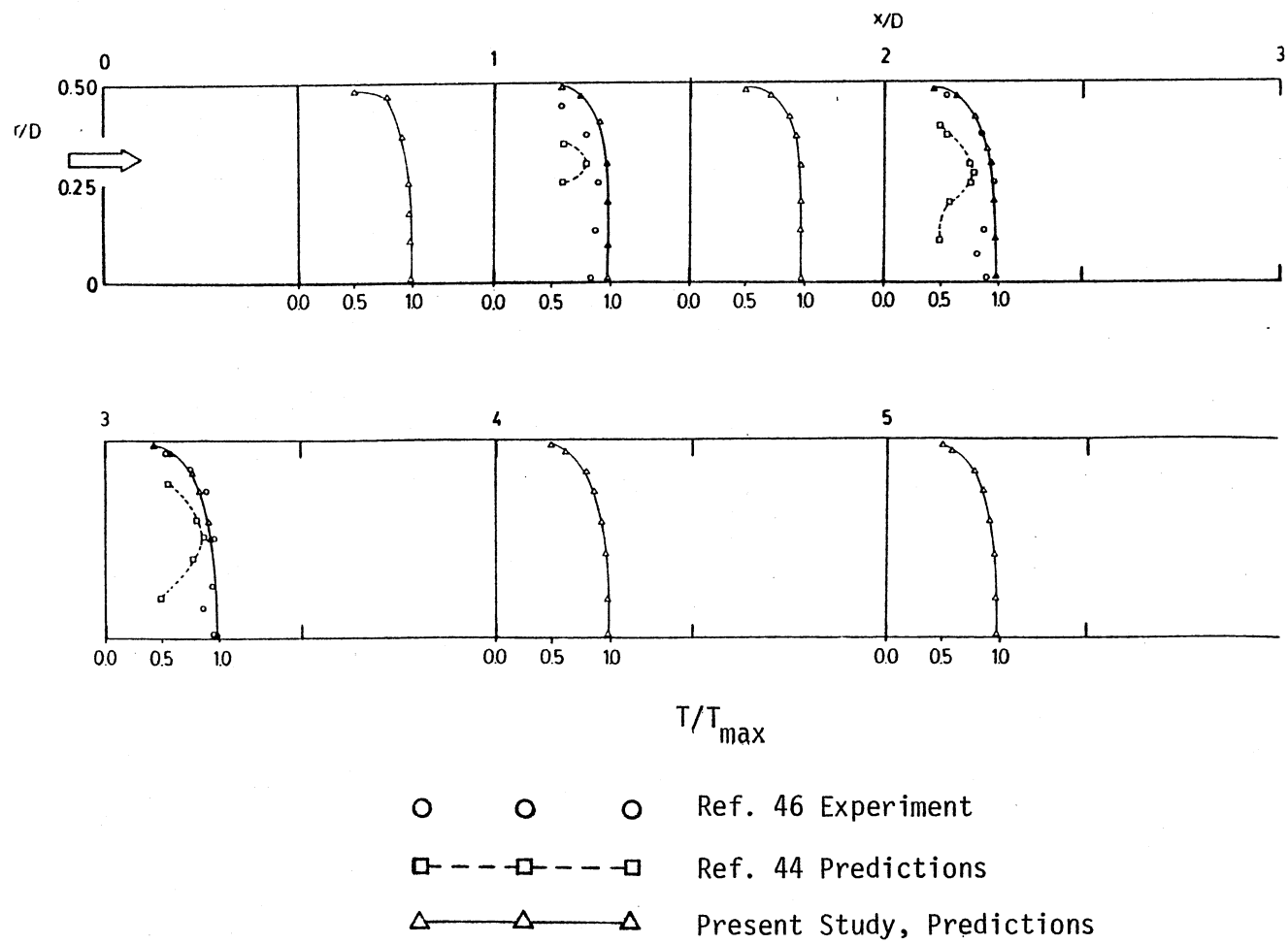


Figure 16. Temperature Profiles for $S = 0.0$ and Pressure at 3.8 atm

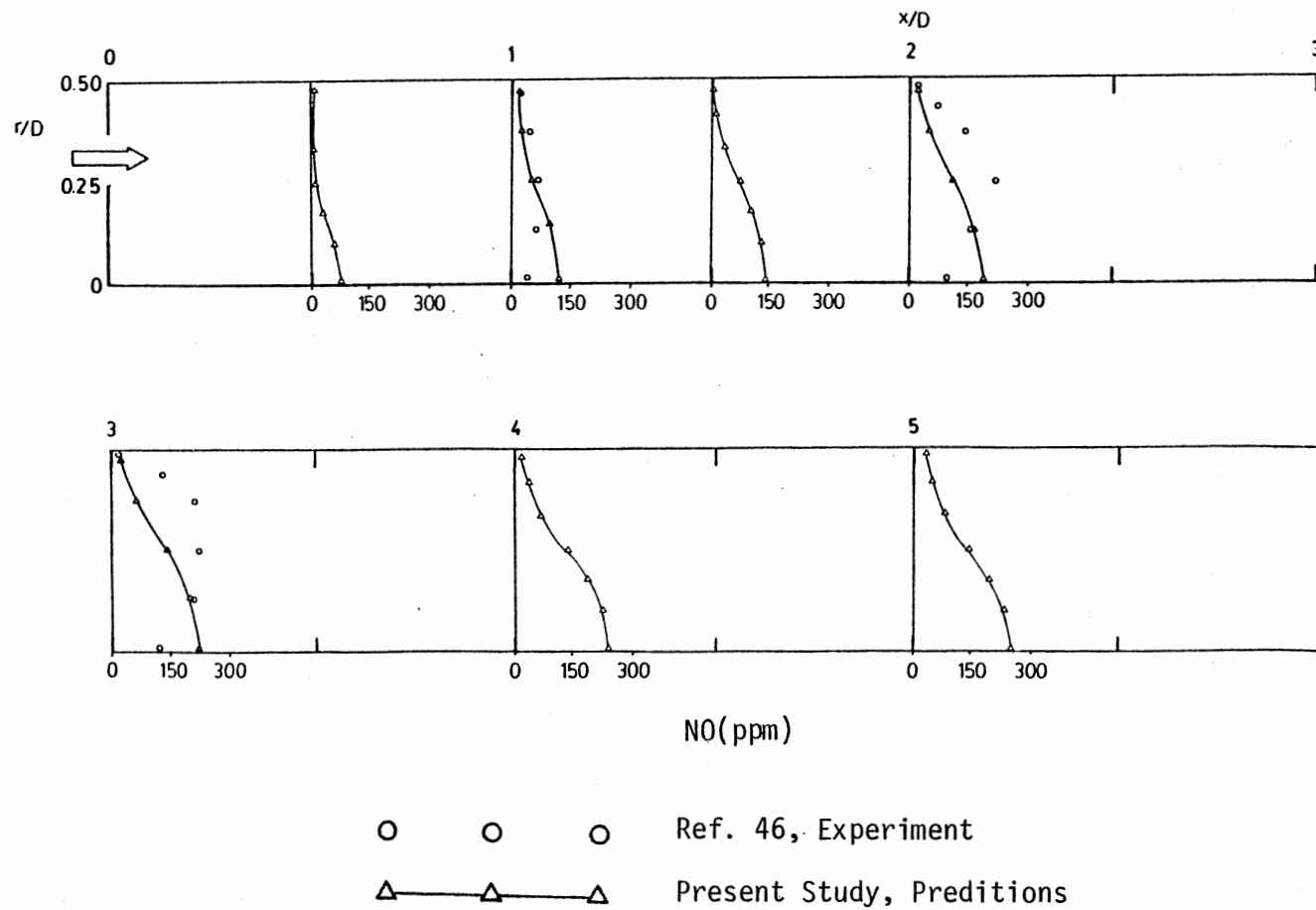


Figure 17. Nitrogen Oxide Profiles for $S = 0.0$ and Pressure at 3.8 atm

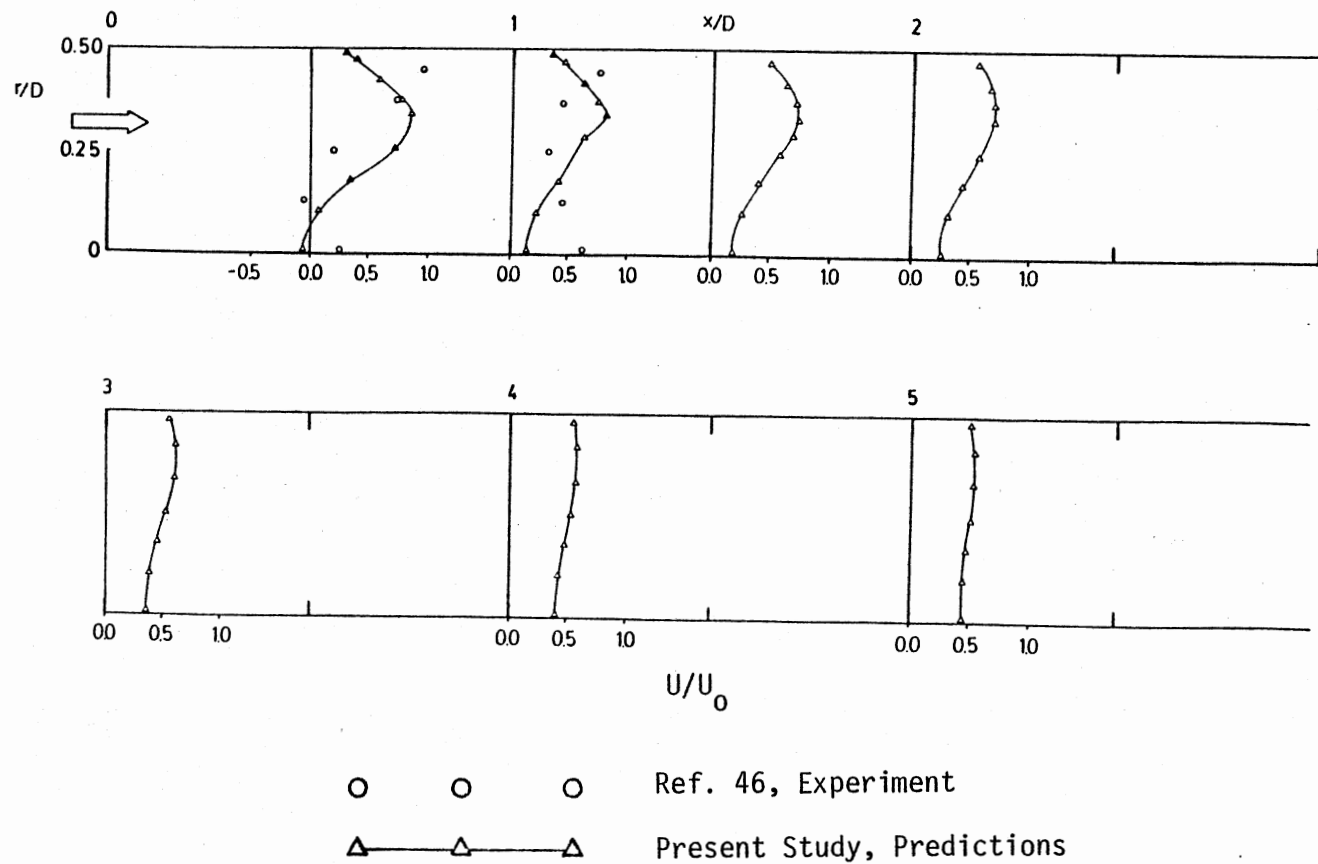


Figure 18. Axial Velocity Profiles for $S = 0.3$ and Pre-sure at 3.8 atm

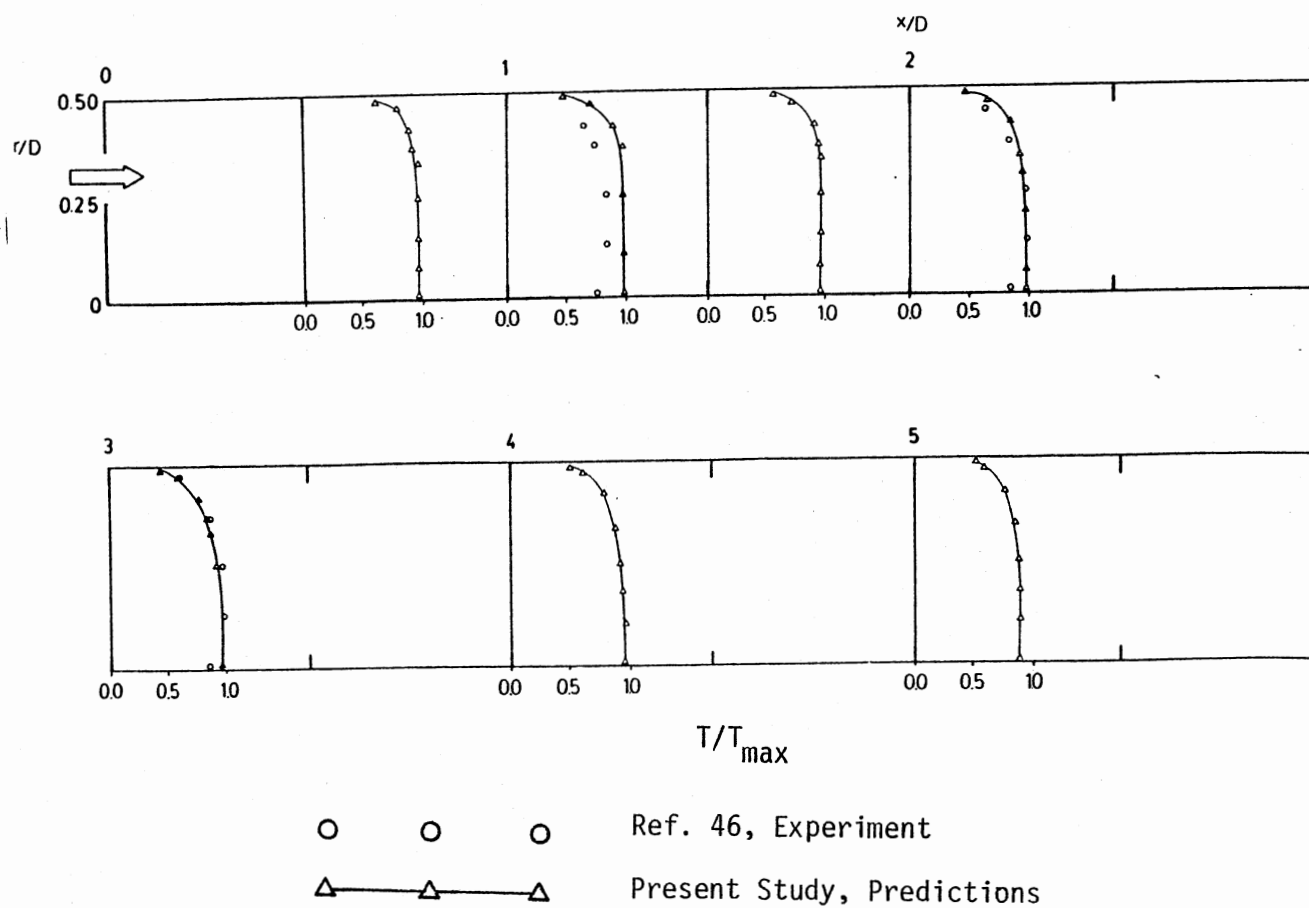


Figure 19. Temperature Profiles for $S = 0.3$ and Pressure at 3.8 atm

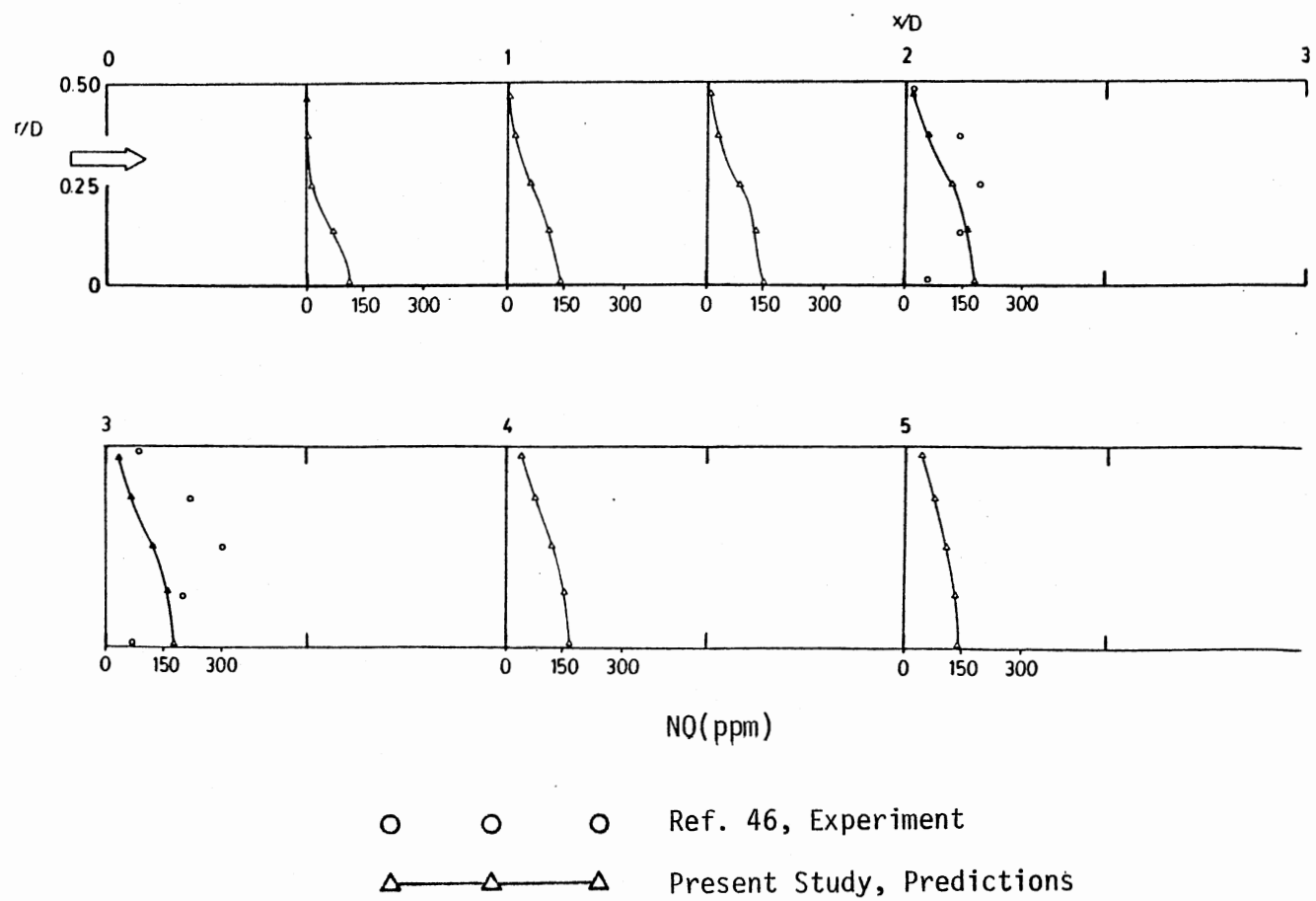
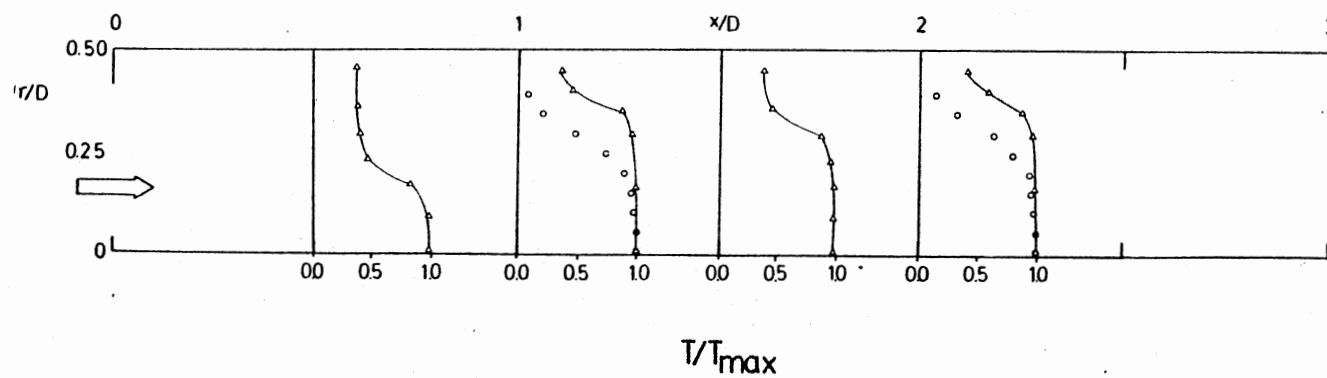
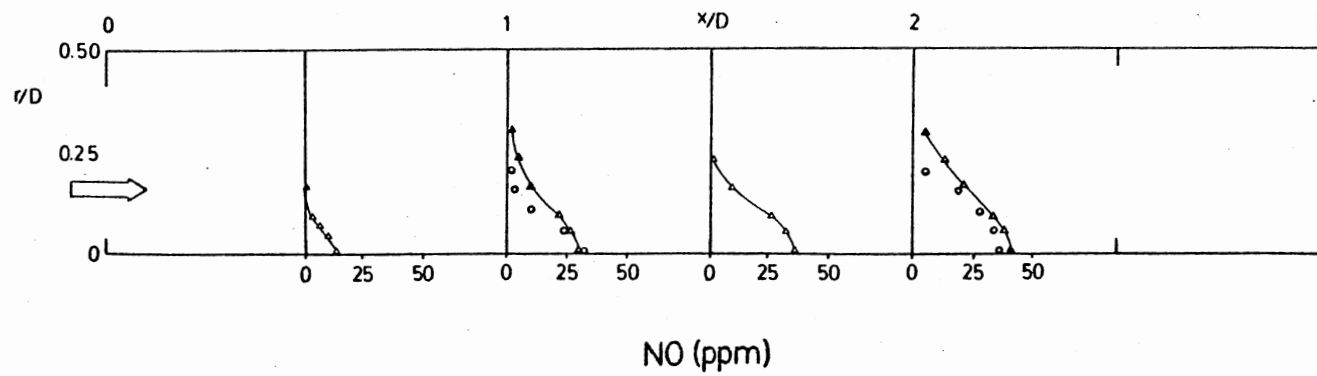


Figure 20. Nitrogen Oxide Profiles for $S = 0.3$ and Pressure at 3.8 atm.



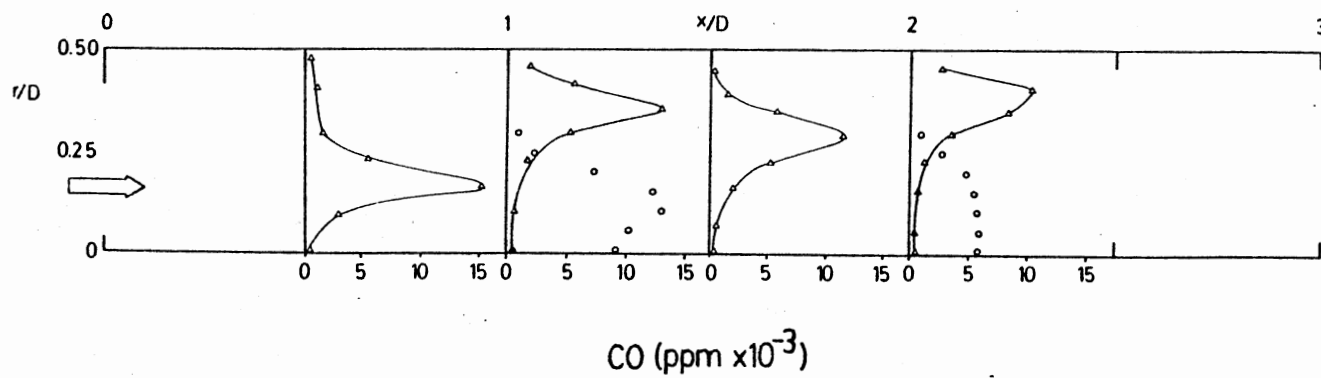
○ ○ ○ Ref. 47, Experiment
 △—△—△ Present Study, Predictions

Figure 21. Temperature Profiles for $S = 0.53$



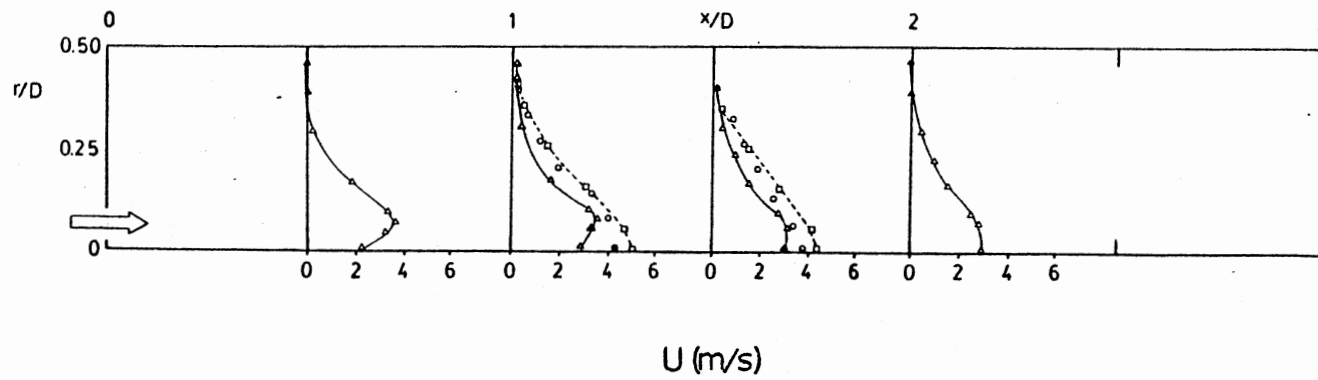
○ ○ ○ Ref. 47, Experiment
 △—△—△ Present Study, Predictions

Figure 22. Nitrogen Oxide Profiles and $S = 0.53$



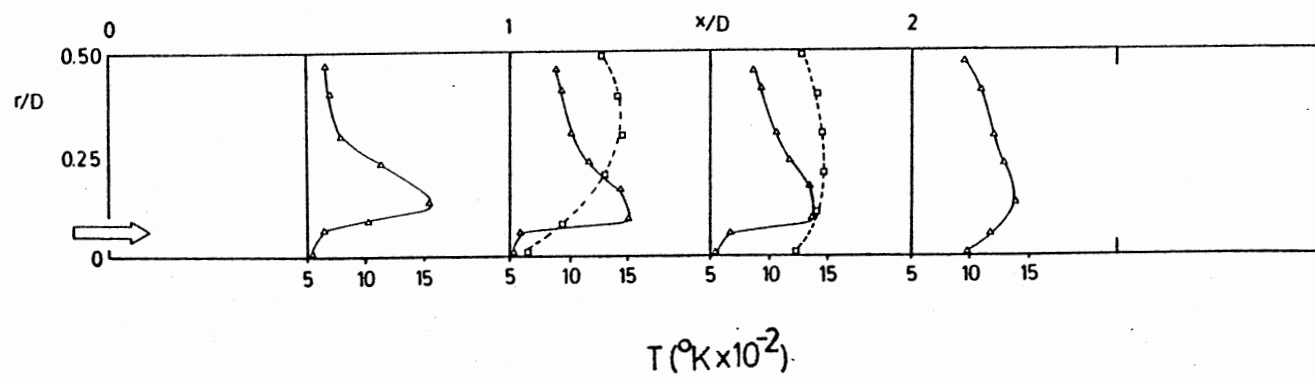
○ ○ ○ Ref. 47, Experiment
 △—△—△ Present Study, Predictions

Figure 23. Carbon Monoxide Profiles for $S = 0.53$



- ○ ○ Ref. 34, Selected Experimental Data
- --- □ --- □ Ref. 34, Predictions
- △ — △ — △ Present Study, Predictions

Figure 24. Axial Velocity Profiles for $S = 0.0$



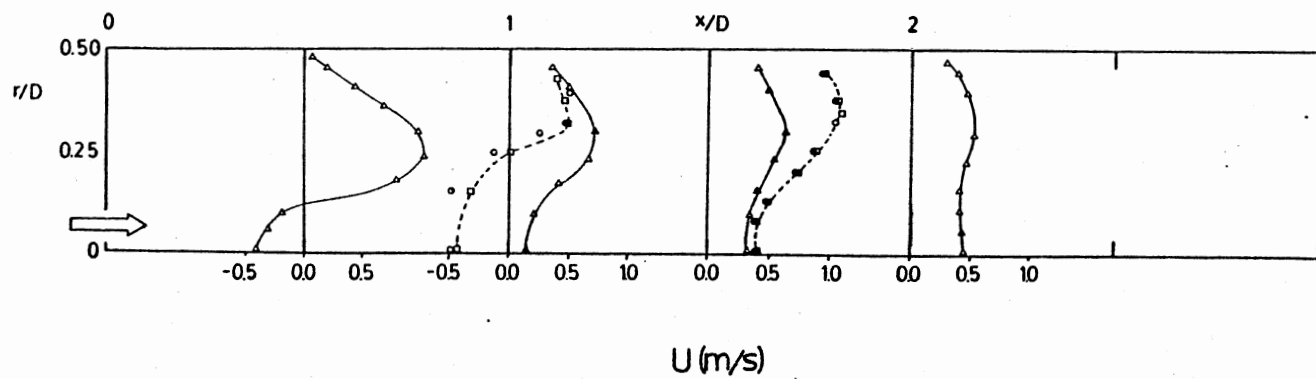
□ --- □ --- □

Ref. 34, Predictions

△ — △ — △

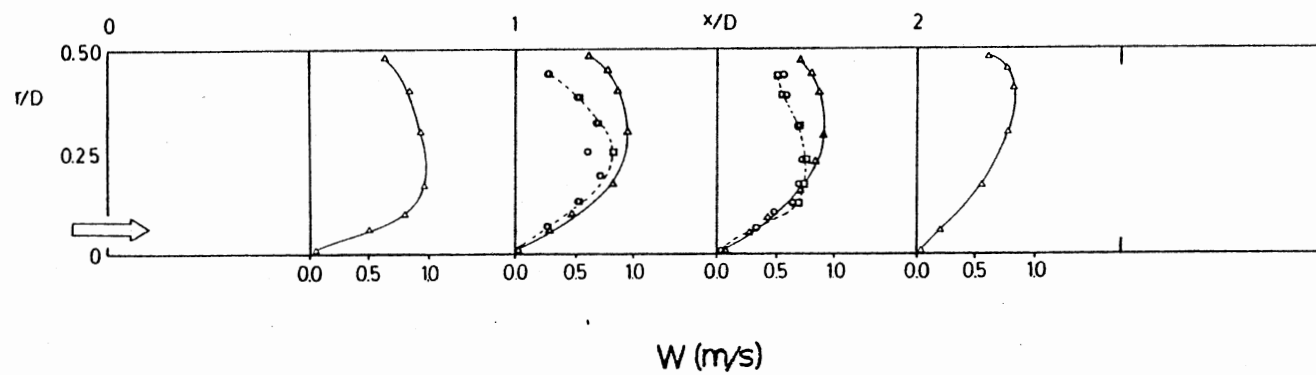
Present Study, Predictions

Figure 25, Temperature Profiles for $S = 0.0$



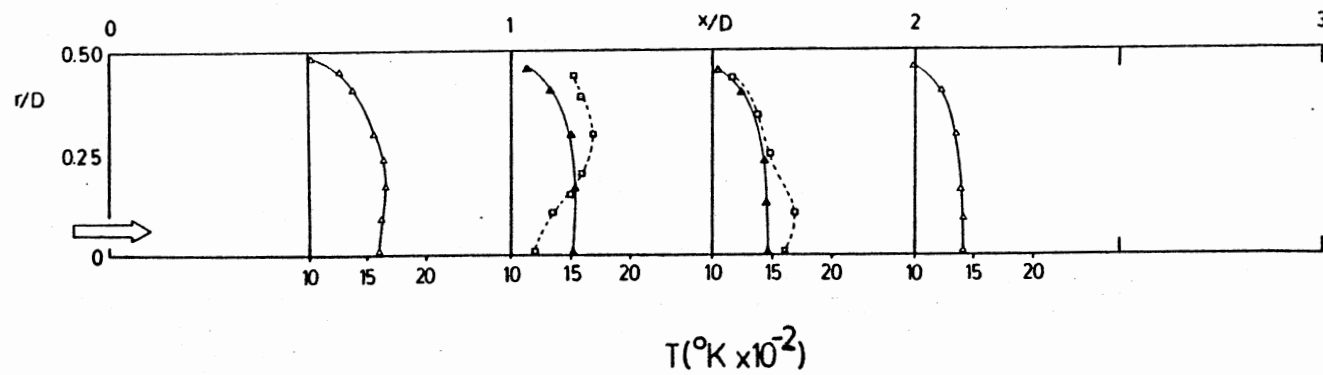
- ○ ○ Ref. 34, Selected Experimental Data
- --- □ --- □ Ref. 34, Predictions
- △ — △ — △ Present Study, Predictions

Figure 26. Axial Velocity Profiles for $S = 0.52$



- ○ ○ Ref. 34, Selected Experimental Data
- --- □ --- □ Ref. 34, Predictions
- △ — △ — △ Present Study, Predictions

Figure 27. Swirl Velocity Profiles for $S = 0.52$



\square --- \square --- \square Ref. 34, Predictions
 \triangle — \triangle — \triangle Present Study, Predictions

Figure 28. Temperature Profiles for $S = 0.52$

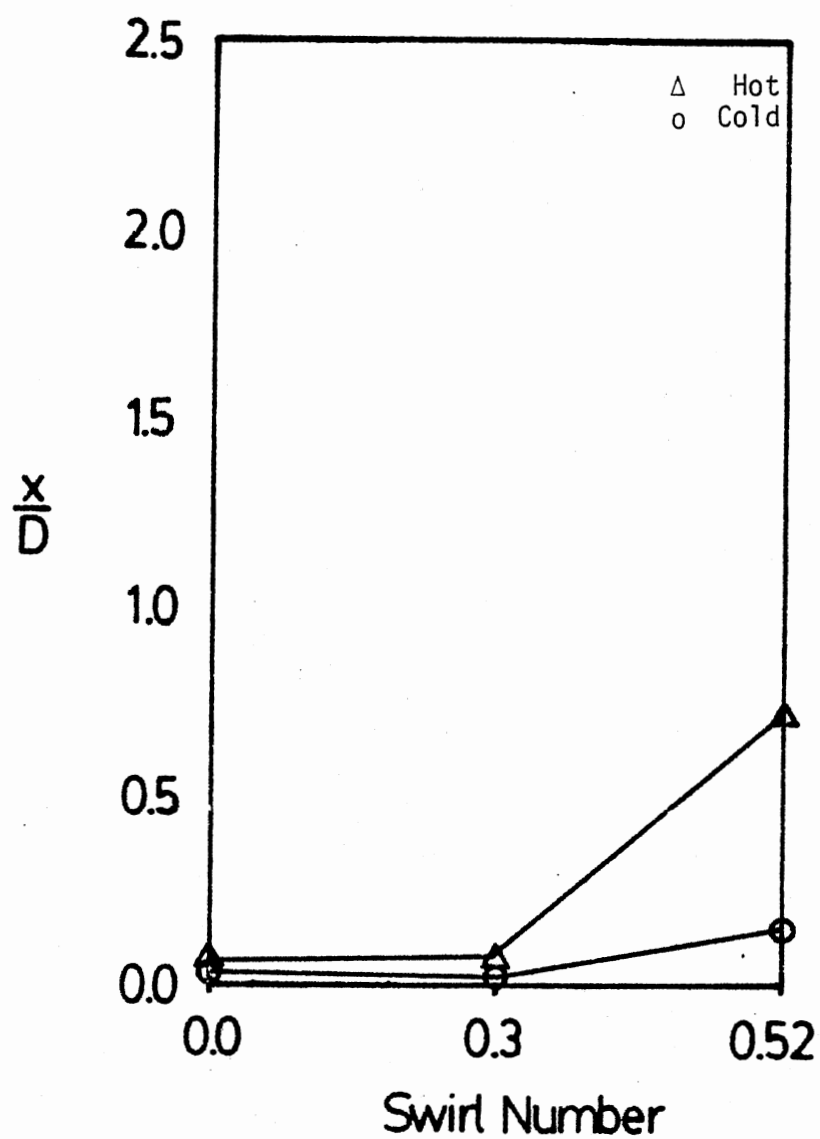


Figure 29. Predicted Central Toroidal Recirculation Zone for Hot and Cold Cases.

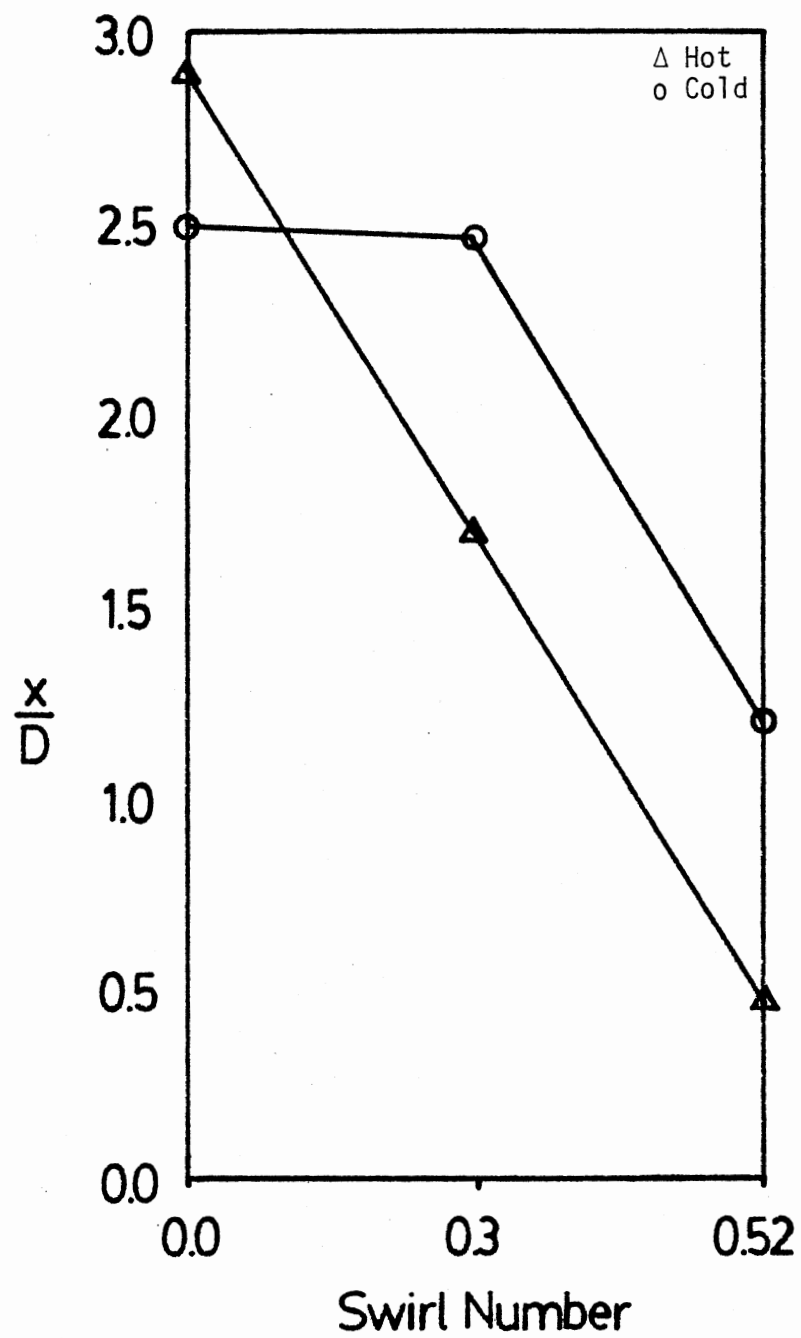


Figure 30. Predicted Corner Recirculation Zone for Hot and Cold Cases.

APPENDIX C

DEVELOPMENT OF THE SECOND-ORDER RADIATION FLUX EQUATIONS

C.1 Axial Components of Radiation Flux

Consider the first-order differential equations for radiation flux in the axial (x) direction:

$$\frac{dI}{dx} = -(a + s)I + \frac{s}{4} (I + J + K + L) + aE_B \quad (C.1)$$

$$\frac{dJ}{dx} = (a + s)J - \frac{s}{4} (I + J + K + L) - aE_B \quad (C.2)$$

Add (C.1) to (C.2) and obtain

$$\frac{d(I + J)}{dx} = (a + s) (J - I) \quad (C.3)$$

Define the total heat flux in the axial direction, Q_x as:

$$Q_x = I - J \quad (C.4)$$

and the flux sum in the axial direction, R_x as:

$$R_x = (I + J)/2 \quad (C.5)$$

Substitute (C.4) and (C.5) into (C.3) producing

$$\frac{2dR_x}{dx} = (a + s) (-Q_x) \quad (C.6)$$

and solve (C.6) for Q_x

$$Q_x = \frac{-2}{(a + s)} \frac{dR_x}{dx} \quad (C.7)$$

The exchange coefficient in the axial direction, Γ_x , is defined as

$$\Gamma_x = \frac{1}{(a + s)} \quad (C.7)$$

and is substituted into (C.7) above resulting in Equation (C.9).

$$Q_x = -2 \Gamma_x \frac{dR_x}{dx} \quad (C.9)$$

Addition of Equations (C.1) and (C.2) has produced the exchange coefficient and a relationship between the total heat flux and the flux sum. These relations are used to develop the final form of the flux equation. Subtraction of Equation (C.2) from (C.1) produces Equation (C.10)

$$d(I - J) = -(a + s)(I + J) + \frac{s}{2} (I + J + K + L) + 2 a E_B \quad (C.10)$$

Introducing the total heat flux and flux sums for both the axial and radial directions, where the radial (r direction) flux sum is

$$R_r = (K + L)/2 \quad (C.11)$$

results in

$$\frac{dQ_x}{dx} = - (a + s) 2R_x + \frac{s}{2} (2R_x + 2R_r) + 2 a E_B \quad (C.12)$$

Utilizing Q_x from (C.9) and dividing by -2 yields

$$\frac{d}{dx} \left[\Gamma_x \frac{dR_x}{dx} \right] = (a + s) R_x - \frac{s}{2} (R_x + R_r) - aE_B \quad (C.13)$$

and upon combining common factor yields the final working equation

$$\frac{d}{dx} \left[\Gamma_x \frac{dR_x}{dx} \right] = a(R_x - E_B) + \frac{s}{2} (R_x - R_r) \quad (C.14)$$

Equation (C.14) is the working equation to be used for the axial radiation flux sum, R_x . Note that this equation is loosely coupled to the radial flux due to the scattering to adjacent radial locations.

C.2 Radial Components of Radiation Flux

A similar series of algebraic manipulations produces a working equation for radial radiation flux, R_r . Here the total heat flux, Q_r , is defined by

$$Q_r = (K - L) \quad (C.15)$$

The initial first-order equations for cylindrical coordinates in the radial (r) direction are

$$\frac{1}{r} \frac{d(rK)}{dr} = -(a + s)K + \frac{L}{r} + \frac{s}{4} (I + J + K + L) + aE_B \quad (C.16)$$

and

$$\frac{1}{r} \frac{d(rL)}{dr} = (a + s)L + \frac{L}{r} - \frac{s}{4} (I + J + K + L) - aE_B \quad (C.17)$$

The final form of the working equation in the radial direction is

$$\frac{1}{r} \frac{d}{dr} \left(r \left[\Gamma_r \frac{dR_r}{dr} \right] \right) = a(R_r - E_B) + \frac{s}{2} (R_r - R_x) \quad (C.18)$$

where the exchange coefficient, Γ_r , is defined as

$$\Gamma_r = \frac{1}{(a + s + \frac{1}{r})} \quad (C.19)$$

Here again, the differential equation for the variation in radial flux is loosely coupled to the axial variation. The final working equations are ready to be cast into finite difference form for inclusion in TEACH.

C.3 Top Wall Boundary Condition

Beginning with the expression for the radiation emitted from the top wall, for example,

$$L_w = (1 - \epsilon_w)K_w + \epsilon_w E_w \quad (C.20)$$

the necessary differential expression for the boundary condition can be developed. Equation (C.20) is amended by multiplying by two, adding and subtracting $\epsilon_w L_w$ and rearranging to produce Equation (C.21),

$$2L_w - 2K_w + \epsilon_w K_w + \epsilon_w L_w + \epsilon_w K_w - \epsilon_w L_w - 2\epsilon_w E_w = 0 \quad (C.21)$$

Substituting Equations (C.11) and (C.15) into Equation (C.21) above and rearranging provides

$$-2Q_r + \epsilon_w Q_r + 2\epsilon_w - 2\epsilon_w E_w = 0, \quad (C.22)$$

and

$$-Q_r + \frac{2\epsilon_w}{2 - \epsilon_w} (R_r - E_w) = 0 \quad (C.23)$$

Recall that Q_r can also be defined as

$$Q_r = \frac{-1}{a + s + \frac{1}{r}} \frac{dR_r}{dr} \quad (C.24)$$

Using this relation and Equation (C.23) yields the final form of the boundary condition

$$\left[\Gamma_r \frac{dR_r}{dr} + \frac{\epsilon_w}{2 - \epsilon_w} (R_r - E_w) \right]_w = 0 \quad (C.25)$$

Equation (C.25) is the differential form which will be used in the final computer code. Other boundary conditions, of similar form, can be developed for the eastern, western, and southern walls as required.

APPENDIX D

DEVELOPMENT OF THE FINITE DIFFERENCE CODE

D.1 General Solution Format

The turbulent flux equations for conservation of mass, momentum, stagnation enthalpy, chemical species mass fraction, turbulent kinetic energy, and turbulent dissipation rate, govern the two-dimensional steady flow of the turbulent chemically reacting multi-component combustion reaction (64). Each of these equations contain similar terms for the convection and diffusion of the variables along with a source term S_ϕ for the general variable ϕ . The equations are of the general form

$$\frac{1}{r} \left\{ \frac{\partial}{\partial x} (\rho u r \phi) + \frac{\partial}{\partial r} (\rho v r \phi) - \frac{\partial}{\partial x} (r \Gamma_\phi \frac{\partial \phi}{\partial x}) - \frac{\partial}{\partial r} (r \Gamma_\phi \frac{\partial \phi}{\partial r}) \right\} = S_\phi \quad (D.1)$$

where ϕ is the variable in question. Each variable has a source term which when integrated over the volume produces, in the linearized form,

$$\int_V S_\phi dV = S_p^\phi \phi_p + S_u^\phi \quad (D.2)$$

where S_p is the source term associated with the variable at the central nodal point and S_u contains all other terms not dealing specifically with the variable at that point. To aid in convergence, the S_p term is usually negative and S_u is positive, thus increasing the diagonal dominance of the solution matrix.

The convection and diffusion terms are handled in the control volume by applying Gauss's divergence theorem and integrating over the area through which the transport occurs. Handling the differential equations in this manner results in the following general equation

$$a_p^\phi \phi_p = \sum_j a_j^\phi \phi_j + S_u^\phi \quad (D.3)$$

where

$$a_p^\phi = \sum_j a_j^\phi - S_p^\phi$$

and \sum_j = sum over N, S, E, W neighbors. Here a_j is called the coupling coefficient for the direction (face) specified. The goal here is to take the radiation equation and put it into the form of Equation (D.3).

Boundary conditions for the general variable ϕ necessitate variations of the formulation used for the internal mesh points. Generally this is done by setting the coupling coefficient to zero at the boundary and applying the boundary condition via the source term. Lilley (64) explains the application of the various boundary conditions in great detail. Some or all of these methods will be utilized in specifying the boundary conditions for the flux problem.

D.2 Development of the Finite Difference Form of the Radiation Flux Equations

To demonstrate the solution technique, Equation (3.14) will be put into difference form. Recall that this equation has been arranged to include the diffusion term and the accompanying source term. There is no convection and diffusion is only in the axial direction, leaving

$$\frac{d}{dx} \left[\Gamma_x \frac{dR_x}{dx} \right] = S_x \quad (D.4)$$

where the source term

$$S_x = a(R_x - E_B) + \frac{S}{2} (R_x - R_r) \quad (D.5)$$

Equation (D.1) is the general form which is to be solved. In order to put Equation (D.4) into this form, it must be multiplied by (-1), producing

$$-\frac{d}{dx} \left[\Gamma_x \frac{dR_x}{dx} \right] = -a(R_x - E_B) - \frac{S}{2} (R_x - R_r) \quad (D.6)$$

Equation (D.6) will be manipulated to produce the finite difference form. Looking first at the left-hand side (LHS). Integrating the LHS over the volume and applying Gauss's divergence theorem to go from a volume to an area integral yields

$$\int_V -\frac{d}{dx} \left[\Gamma_x \frac{dR_x}{dx} \right] dV = \int_{A_E}^{A_W} -\Gamma_x \frac{dR_x}{dx} dA \quad (D.7)$$

The exchange coefficient, Γ_x , is a constant and can be moved outside of the integral and

$$\text{LHS} = -\Gamma_x \int_{A_E}^{A_W} \frac{dR_x}{dx} dA \quad (D.8)$$

Integration yields

$$\text{LHS} = -\Gamma_x \left[\frac{\Delta R_{xE}}{\Delta x_E} A_E - \frac{\Delta R_{xW}}{\Delta x_W} A_W \right]$$

then

$$\text{LHS} = -\Gamma_x \left[\left(\frac{R_{xE} - R_{xP}}{\Delta x_E} \right) A_E - \left(\frac{R_{xP} - R_{xW}}{\Delta x_W} \right) A_W \right]$$

and

$$\text{LHS} = -\Gamma_x \frac{R_{xE}}{\Delta x_E} A_E + \Gamma_x \frac{R_{xP}}{\Delta x_E} A_E + \Gamma_x \frac{R_{xP}}{\Delta x_W} A_W - \Gamma_x \frac{R_{xW}}{\Delta x_W} A_W \quad (\text{D.9})$$

where E is the eastern face node, W is the western face node and P is the node within the control volume which is to be solved. Define the diffusion coefficient D for each face as

$$D = \Gamma_x \frac{A}{\Delta x} \quad (\text{D.10})$$

with subscripts E and W for the axial flux. Rewrite Equation (D.9) as

$$\text{LHS} = -D_E R_{xE} + D_E R_{xP} + D_W R_{xP} - D_W R_{xW} \quad (\text{D.11})$$

Looking next at the right-hand side (RHS). Adding and subtracting $S/2 R_x$ to the RHS produces

$$\text{RHS} = -a R_{xP} - s R_{xP} + a E_B + \frac{S}{2} (R_{xP} + R_{rP}) \quad (\text{D.12})$$

This procedure has been tested, both with and without this step and yields no discernible difference in the final results. It mainly cleans up the overall equation set.

Integration of the RHS over the cell volume is like multiplying by the volume since all the variables are independent of the coordinate frame and yields

$$\text{RHS} = -a R_{xP} \text{ vol} - s R_{xP} \text{ vol} + a E_B \text{ vol} + \frac{S}{2} (R_{xP} + R_{rP}) \text{ vol} \quad (\text{D.13})$$

Equating the RHS to the LHS

$$\begin{aligned} -D_E R_{xE} + D_E R_{xP} + D_W R_{xP} - D_W R_{xW} = & -(a + s) R_{xP} \text{ vol} + \\ & [a E_B + \frac{S}{2} (R_{xP} + R_{rP})] \text{ vol} \end{aligned} \quad (\text{D.14})$$

Equation (D.14) must now be put into the form of Equation (D.3). This is accomplished by defining the corresponding parts of Equations (D.3) and (D.14) as

$$S_p = - (a + s) \text{ vol}$$

and

$$S_u = [a E_B + \frac{s}{2} (R_{x_p} + R_{r_p})] \text{ vol}$$

and

$$\sum_j a_j \phi_j = a_E R_{x_E} + a_W R_{x_W} = D_E R_{x_E} + D_W R_{x_W}$$

and in a similar manner

$$\sum_j a_j = D_E + D_W$$

The single final equation to be solved is of the form

$$a_p \phi_p = \sum_j a_j \phi_j + S_u \phi$$

Using the definitions above,

$$\begin{aligned} (D_E + D_W + [-(a + s) \text{ vol}]) R_{x_p} &= D_E R_{x_E} + D_W R_{x_W} + \\ &[a E_B + \frac{s}{2} (R_{x_p} + R_{r_p})] \text{ vol} \end{aligned} \quad (D.15)$$

Application of Equation (D.15) to the basic code is via the same procedures used for other variables. Several notable exceptions do exist and are:

- 1 - There are no convection terms in the axial flux subroutine.
- 2 - The requirement for hybrid differencing is eliminated since

radiation is diffusion controlled.

3 - Diffusion is directional and utilizes either the E-W or N-S transport directions. In the case of the axial flux, references to N-S are unnecessary and are eliminated. Any reference to N-S coupling coefficients is unnecessary and will be removed.

4 - As previously mentioned, the flux equations cannot be solved using the standard TDMA in TEACH. A modified TDMA has been developed to accomodate 1-3 above. The new solvers are essentially the same with variations to insure a viable solution of the matrix. Further implementation details will be discussed later.

D.3 Boundary Conditions

As was shown in Appendix C, the boundary conditions are developed from the basic physical situation. The radial boundary condition at the top wall (N) is

$$\left[\frac{1}{a + s + \frac{1}{r}} \frac{dR_r}{dr} + \frac{\epsilon_W}{2 - \epsilon_W} (R_r - E_W) \right]_W = 0 \quad (D.17)$$

Rearrangement of Equation (D.17) yields the following familiar equation,

$$\Gamma_x \frac{dR_x}{dx} = \frac{\epsilon_W}{2 - \epsilon_W} (E_W - R_x) \quad (D.18)$$

It must be remembered at this point that the boundary condition is applied between the node being considered, the P node, and the boundary node at the eastern face. This eastern node is the combustor wall which has in this problem a constant temperature.

In applying the boundary condition the axial radiation flux will be used as the example. Consider the eastern face previously cited. Since

the boundary condition contains the derivative of the radiation flux between the P node and the eastern boundary. This derivative allows for the breaking of the link (coupling coefficient, a_E) between the internal mesh and the boundary in question. In its stead, the boundary condition is applied by modifying the source terms, S_u and S_p . Looking at Equation (D.18) it can be determined that these source term supplements should be

$$S_u = \frac{\epsilon_W}{2 - \epsilon_W} (E_W) \quad (D.19)$$

and

$$S_p = - \frac{\epsilon_W}{2 - \epsilon_W} \quad (D.20)$$

Thus the boundary conditions have been applied for the differential form and through S_p , contain the value of the radiative flux at the P node. Similar applications can be made at each boundary, N, S, E, and W.

D.4 Implementing Instructions

The radiation equations have several implementing steps which are somewhat different from those of other variables. Most importantly is that of initialization of the flux field. Since the temperature field is initialized to be the same as the inlet temperature, so also is the radiation field. Other variables which are prespecified are the absorptivity, a , the scattering coefficient, S , and the wall emissivity, ϵ_W . These initializations occur early on in the program, allowing INIT to be reserved for dimensional variables.

Two separate routines are used to calculate the axial and radial fluxes. Each subroutine calls a separate solver as previously mention-

ed. Within each of the routines is a call to the subroutine where the boundary conditions are applied and passed back to the original calculation routine. A degree of underrelaxation is used to aid in solution. From literature survey and practice this value has been set to 1. The radiation scheme is quite stable and little under relaxation is required.

After solution of the radiation fluxes, these values are passed to the enthalpy subroutines for application in the enthalpy source term. This term is defined as

$$S_h = 2a(R_x + R_r - 2E_B) \text{ vol} \quad (\text{D.21})$$

As previously mentioned, the magnitude of this term determines the net radiative effect on the temperature field, therefore, if R_x and R_r compare favorably with $2E_B$, the temperature variation may be small.

After all other calculations are complete, the net radiation heat flux is calculated for the axial and radial cases. This is accomplished by utilizing Equation (D.9) from Appendix C. This is the final result which is required.

Finally the decision to include radiation is made by establishing logical variables. When these are set to TRUE, the entire series of radiation calculations are completed. When these are set to FALSE, all the radiation portions in the calculation portion of TEACH are eliminated and enthalpy source term returns to its original form. This capability allows for inclusion or exclusion of radiation to aid in comparative analysis.

APPENDIX E

STRAC CODE LISTING

```

C      SUBROUTINE CONTRO
C      IMPLICIT REAL*8(A-H,O-Z)
C
C*****
C
C      STRAC
C
C      * A COMPUTER PROGRAM FOR THE CALCULATION OF PLANE OR AXISYMMETRIC
C      STEADY TWO-DIMENSIONAL RECIRCULATING FLOWS WITH COMBUSTION
C
C      J W SAMPLES,  VERSION OF MAY,1983
C
C*****
C
C      CHAPTER  0  0  0  0  0  0  0  0  0  PRELIMINARIES  0  0  0  0  0  0  0  0
C
C      CHARACTER*36 HEDU(9),HEDV(9),HEDW(9),HEDP(9),HEDTEM(9),HEDNDI(9),
C      1HEDED(9),HEDVIS(9),HEDKP(9),HEDLS(9),HEDH(9),HEDFU(9),HEDOF(9),
C      2HEDNI(9),HEDDEN(9),HEDEBU(9),HEDARR(9),HEDFUP(9),HEDRX(9),
C      3HEDCO2(9),HEDH2O(9),HEDCO(9),HEDH2(9),HEDO(9),HEDN(9),HEDNO(9),
C      4HEDNDU(9),HEDNDV(9),HEDNDW(9),HEDKE(9),HEDOX(9),HEDRR(9)
C      DIMENSION PD(40,15),VANB(5),SWNB(5)
C      COMMON
C      1/UVEL/RESORU,NSWPU,URFU,DXEPU(40),DXPWU(40),SEWU(40)
C      1/VVEL/RESORV,NSWPV,URFV,DYNPV(40),DYPSV(40),SNSV(40),RCV(40)
C      */WVEL/ RESORW, NSWPW, URFW
C      1/PCOR/RESORM,NSWPP,URFP,DU(40,15),DV(40,15),IPREF,JPREF
C      1/TENDIS/RESORK,NSWPK,URFK,RESORE,NSWPD,URFE
C      */VAR/U(40,15),V(40,15),W(40,15),P(40,15),PP(40,15),TE(40,15),
C      1ED(40,15),H(40,15),FU(40,15),OF(40,15)
C      1/ALL/IT,JT,NI,NJ,NIM1,NJM1,GREAT
C      1/GEOM1/INDCOS,X(40),Y(40),DXEP(40),DXPW(40),DYNP(40),DYPS(40),
C      1      SNS(40),SEW(40),XU(40),YV(40),R(40),RV(40),LABRUPT
C      1/FLUPR/URFVIS,VISCOS,DENSIT,PRANDT,DEN(40,15),VIS(40,15)
C      1      ,OX(40,15),AN2(40,15),T(40,15),RFUP(40,15),RCOP(40,15)
C      1,CO(40,15),H2O(40,15),H2(40,15),CO2(40,15),FUOLD(40,15),C1(40,15)
C      1/DIMTEM/TT(40,15)
C      1/KASE T1/UIN,TEIN,EDIN,FLOWIN,ALAMDA,
C      2      RSMALL,RLARGE,AL1,AL2,JSTEP,ISTEP,JSTP1,JSTM1,ISTP1,ISTM1,J
C      3INC,ICUT,ICTP1
C      1/TURB/GEN(40,15),CD,CMU,C1,C2,CAPPA,ELOG,PRED,PRTE
C      1/WALLF/YPLUSN(40),XPLUSW(40),TAUN(40),TAUW(40)
C      1      ,TAUE(40),TAUS(40),YPLUSS(40),XPLUSE(40)
C      1/COEF/AP(40,15),AN(40,15),AS(40,15),AE(40,15),AW(40,15),SU(40,15),
C      1      SP(40,15)
C      1/SWEN/PRW,WWALL,RESORH,NSWPH,URFH,PRH,TWALL
C      1/FUOF/RESORF,NSWPF,URFF,PRFU,FUWALL,RESORO,NSWPO,URFO,PROF,OFWALL
C      1/CHEM/URFDEN,GASCON,CFU,COX,CPR,WFU,WOX,WPR,HFU,HCO,OXDFU,PRESS
C      1,CCO,CCO2,CH2O,CAN2,RESORC,NSWPC,URFCO,PRCO,OXDCO,OXDFU1,WCO
C      1,WH2O,WCO2,WAN2,PERSTO,WH2,CH2,W01,CO1
C      COMMON
C      1/GEOM2/IHUB,JHUB,IHBP1,JHBP1,IHBM1,JHBM1,ICON,JCON,ICNP1,JCNP1
C      1/GEOM3/IEN1M,IEN1P,IEN2M,IEN2P

```

```

1/CHEM2/FUIN,AX,AY,AO
1/REAC/RFUEBU(40,15),RFUARR(40,15),NITER,RCOARR(40,15),
1RCOEBU(40,15)
1/RADT/RADX(40,15),RADR(40,15),RADIN
2      ,EMIW,NSWPRX,NSWPRR,URFRX,URFRR,SIGMA,ABSOR,SCATT
3      ,RESORR,RESORX
1/QRAD/QX(40,15),QR(40,15),Q(40,15)
COMMON
1/NITRO1/WN1,WNO,CN1,CNO,URFNO,AN1(40,15),ANO(40,15),NSWPNO
2,URFN1,PRNO,RESRNO,RNOF1(40,15),RNOF2(40,15)
3,RNOR2(40,15),RNOR1(40,15)
1/GEOM5/XND(40),XUND(40),YND(40),YVND(40)
1/NODIMV/USTAR(40,15),VSTAR(40,15),WSTAR(40,15)
EQUIVALENCE(PD(1),SU(1))
LOGICAL INCALU,INCALV,INCALW,INCALP,INPRO,INCALK,INCALD,
1LABRUPT,INCALH,INCALF,INCALO,INCOLD,INHOT,
1INCOOL,INOTPT,INCLRX,INCLRR,INCALC,INLET,INCLNO
C-----ALL PRIMARY USER INPUTS ARE LOCATED HERE
DATA VANB/0.0D0,25.0D0,38.D0,55.D0,60.D0/
1,SWNB/0.D0,0.30D0,0.52D0,1.0D0,1.25D0/
C-----IF 90 DEGREE EXPANSION, SET LABRUPT=.TRUE.
LABRUPT=.TRUE.
LFS=1
LFSMAX=3
NSBR=0
MAXIT=300
IT=40
JT=15
GREAT=1.E30
NSWPU=2
NSWPV=2
NSWPW=2
NSWPP=2
NSWPK=1
NSWPD=1
NSWPH=2
NSWPF=1
NSWPC=3
NSWPO=1
NSWPNO=2
NSWPRX=3
NSWPRR=3
C-----READ INCOLD AS TRUE FOR COLD RUN OR FALSE OTHERWISE
C-----NO UPDATE OF SPECIES ENTHALPY OR DENSITY
READ(10,011) INCOLD
011 FORMAT(L5)
C-----READ INCOOL AS TRUE FOR COOL RUN - LOW HEAT RELEASE
READ(10,011) INCOOL
C-----READ INFUPR AS 1,2 OR 3 FOR UNIFORM, 1- OR 2- PEAK
C-----FUEL INLET PROFILE
READ(10,509) INFUPR,IURF,INTERM
C-----READ AO=AY TO ELIMINATE HYDROGEN FROM THE PRODUCTS
READ(10,509) AX,AY,AO,HFU,HCO,PERSTO,FUIN
WFU=AX*12.+AY

```

```

OXDFU1=(32.*(AX/2.+AO/4.)/(12.*AX+AY))*PERSTO
OXDCO=0.5714*PERSTO
OXDFU=(32.*(AX+AY/4.)/(12.*AX+AY))*PERSTO
READ(10,509) TIN,TWALL
TWLMAX=TWALL
TWALL=TIN
C-----READ INOTPT AS FALSE IF INTERMEDIATE OUTPUT IS TO BE ELIMINATED
READ(10,011) INOTPT
C-----READ INLET=FALSE IF INITIAL OUTPUT IS TO BE ELIMINATED
READ(10,011) INLET
READ(10,010) HEDU,HEDV,HEDW,HEDP,HEDTEM,HEDNDT,HEDKE,HEDED,HEDVIS
1,HEDKP,HEDLS,HEDH,HEDFU,HEDOF,HEDOX,HEDNI,HEDDEN,HEDEBU,HEDARR
2,HEDFUP,HEDRX,HEDRR,HEDCO2,HEDH2O,HEDCO,HEDH2,HEDO,HEDN,HEDNO
3,HEDNDU,HEDNDV,HEDNDW
WRITE(6,499)
WRITE(6,500) WFU
WRITE(6,501) HFU
WRITE(6,502) OXDFU
WRITE(6,503) FUIN
WRITE(6,504) TIN
WRITE(6,505) TWLMAX
499 FORMAT(/////15X,33HTHE INLET VALUES ARE LISTED BELOW)
500 FORMAT( //15X,33HTHE WEIGHT OF THE FUEL IS ,1PE12.3)
501 FORMAT( //15X,33HTHE HEAT RELEASE IS ,1PE12.3)
502 FORMAT( //15X,33HTHE STOICHIOMETRIC RATIO IS ,1PE12.3)
503 FORMAT( //15X,33HTHE FUEL FLOW RATE (KG/S) IS ,1PE12.3)
504 FORMAT( //15X,33HTHE INLET TEMPERATURE IS ,1PE12.3)
505 FORMAT( //15X,33HTHE WALL TEMPERATURE IS ,1PE12.3)
010 FORMAT(9A4)
509 FORMAT(V)
C
CHAPTER 1 1 1 1 1 PARAMETERS AND CONTROL INDICES 1 1 1 1 1 1
C
C-----GRID
C-----ISTEP MUST BE GREATER THAN OR EQUAL TO IHUB
ISTEP=2
JSTEP=11
JINC=1
NSTEPS=7
IF(.NOT.LABRUPT) GO TO 9
JINC=3
NSTEP=1
9 CONTINUE
NI=40
NJ=JSTEP+NSTEPS*JINC+1
IF(LABRUPT) ICUT=ISTEP
IF(.NOT.LABRUPT) ICUT=ISTEP+NSTEPS-1
INDCOS=2
NIM1=NI-1
NJM1=NJ-1
ISTP1=ISTEP+1
ISTM1=ISTEP-1
JSTP1=JSTEP+1
JSTM1=JSTEP-1

```



```

      ICTP1=ICUT+1
C-----SETTING IHUB=2 APPROXIMATES THE NO HUB CASE
      IHUB=2
      JHUB=9
      IHBP1=IHUB+1
      JHBP1=JHUB+1
      IHBM1=IHUB-1
      JHBM1=JHUB-1
C-----LATERAL ENTRY
C-----SET NEXT FOUR VALUES TO ZERO IF NO LATERAL ENTRY
      IEN1M=0
      IEN1P=0
      IEN2M=0
      IEN2P=0
      RLARGE=0.061
      ALTOT=1.7
C-----ABSCISSA
      EPSX=1.09
      IF(EPSX-1.) 12,12,13
13      SUMX=0.5*EPSX**(NI-4)+(EPSX**(NI-3)-1.)/(EPSX-1.)+0.5
      GO TO 15
12      CONTINUE
      SUMX=NIM1-1
15      DX=ALTOT/SUMX
      X(1)=-0.5*DX
      X(2)=-X(1)
      DO 100 I=3,NIM1
      X(I)=X(I-1)+DX
100     DX=EPSX*DX
      X(NI)=X(NIM1)-X(NJ-2)+X(NJM1)
      AL1=0.5*(X(ISTEP)+X(ISTM1))
      AL2=ALTOT-AL1
C-----CONSTRICTED OUTLET CAN BE MADE TO HAVE NO EFFECT BY USING LARGE
C-----VALUES OF ICON AND JCON
C-----THESE VALUES SHOULD EQUAL NIM1 AND NJ IF NO CONTRACTION
C-----NO CONTRACTION FOR NOW
      ICON=NIM1
      JCON=NJ
      ICNP1=ICON+1
      JCNP1=JCON+1
C-----ORDINATES
      DY=RLARGE/FLOAT(NJ-2)
      Y(1)=-0.5*DY
      DO 101 J=2,NJ
101     Y(J)=Y(J-1)+DY
      Y(9)=0.031
      Y(10)=0.036
      Y(11)=0.042
      Y(12)=0.046
      Y(13)=0.052
      RSMALL=0.5*(Y(JSTEP)+Y(JSTP1))
C-----DEPENDENT VARIABLE SELECTION
      INCALU=.TRUE.
      INCALV=.TRUE.

```

```

    INCALW=.TRUE.
    INCALP=.TRUE.
    INCALK=.TRUE.
    INCALD=.TRUE.
    INPRO=.TRUE.
    INCALH=.TRUE.
    INCALF=.TRUE.
    INCALO=.TRUE.
    INCALC=.TRUE.
    INCLNO=.TRUE.
    INCLRX=.TRUE.
    INCLRR=.TRUE.
C-----INCOLD HAS BEEN READ IN ABOVE
    IF(INCOLD) INCALH=.FALSE.
    IF(INCOLD) INCALF=.FALSE.
    IF(INCOLD) INCALO=.FALSE.
    IF(INCOLD) INCALC=.FALSE.
    IF(INCOLD) INCLNO=.FALSE.
    IF(INCOLD) INCLRX=.FALSE.
    IF(INCOLD) INCLRR=.FALSE.
    INHOT=.TRUE.
    IF(INCOLD) INHOT=.FALSE.
C-----FLUID PROPERTIES
C-----DENSITY CALCULATIONS AFTER INLET BOUNDARY CONDITIONS
    PRW=1.0
    PRH=1.0
    PRFU=1.0
    PROF=1.0
    PRCO=1.0
    PRNO=1.0
C-----SI UNITS
    GASCON=8314.0
C-----SET INITIAL SPECIFIC HEATS
    CFU=2260.0
    COX=(42.27-6635.4/TIN)*1000.0/32.0
    CPR=(37.46-4559.3/TIN)*1000.0/28.0
    CAN2=1000.0
    CCO=1000.0
    CCO2=1000.0
    CH2O=1000.0
    CH2=1000.0
    CO1=1000.0
    CN1=1000.0
    CNO=1000.0
    WOX=32.0
C-----SET MOLECULAR WEIGHTS
    WPR=28.0
    WCO=28.0
    WCO2=44.0
    WH2O=18.0
    WAN2=28.0
    WH2=2.0
    WO1=16.0
    WN1=14.0

```

```

      WNO=30.0
C-----ESTABLISH INITIAL VISCOSITIES
      VISFU=4.85E-6
      VISOX=4.85E-6
      VISPR=4.85E-6
      VISAN2=4.85E-6
      VISCO=4.85E-6
      VISCO2=4.85E-6
      VISH20=4.85E-6
      VIS01=4.85E-6
      VISN1=4.85E-6
      VISMO=4.85E-6
C
      IF(HFU.EQ.0.0) GO TO 22
      IF(INCOOL) HFU=1000000.0
      IF(INCOLD) HFU=0.90
      22 CONTINUE
C-----RADIATION CONSTANTS
C-----ABSORPTIVITY
      ABSOR=0.1
C-----SCATTERING COEFFICIENT
      SCATT=0.01
      EMISIN=1.
C-----WALL EMISSIVITY
      EMISW=0.8
      EMIW=EMISW/(2.-EMISW)
C-----STEFAN BOLTZMAN CONSTANT
      SIGMA=5.6693E-08
C-----SET INITIAL PRESSURE
      PRESS=101325.0*1.0
C-----TURBULENCE CONSTANTS
      CMU=0.09
      CD=1.00
      C1=1.44
      C2=1.92
      CAPP=0.4187
      ELOG=9.793
      PRED=CAPP*CAPP/(C2-C1)/(CMU**.5)
      PRTE=1.0
C-----BOUNDARY VALUES
      UIN=17.0
      ULARGE=UIN*(RSMALL/RLARGE)**2
      TURBIN=.03
      TEIN=TURBIN*UIN**2
      ALAMDA=0.005
      EDIN=TEIN**1.5/(ALAMDA*RLARGE)
      IF(INCOLD) TIN=300.0
      IF(INCOLD) FUIN=0.0
      OXIN=(1.-FUIN)*.232
C-----HERE PRIN IS AN2(NITROGEN)
      PRIN=1.0-FUIN-OXIN
      OXIN=OXIN*PERSTO
      PRIN=PRIN*PERSTO
      OFIN=OXIN-OXDFU*FUIN

```

```

      DIN=OXIN+PRIN+FUIN
      CMIX=CFU*(FUIN/DIN)+COX*(OXIN/DIN)+CPR*(PRIN/DIN)
C-----STAGNATION ENTHALPY IS EQUATED TO ENTHALPY
      HIN=CMIX*TIN+HFU*FUIN
      RECIPM=FUIN/WFU+OXIN/WOX+PRIN/WPR
      DENSIT=PRESS/(GASCON*TIN*RECIPM)
      VISCOS=(FUIN/DIN)*VISFU+(OXIN/DIN)*VISOX+(PRIN/DIN)*VISPR
      REYN=(DENSIT*UIN*2*RSMALL)/VISCOS
      RADIN=EMISIN*SIGMA*TIN**4.
      WWALL=0.0

C
C-----LATERAL ENTRY-SET SIDE INLET RADIAL VELOCITIES-USUALLY NEG
      VIEN1=0.0
      VIEN2=0.0

C
C*****      SWIRL MODEL SELECTION
C      PROGRAM USUALLY USES SOLID BODY ROTATION MODEL FOR W UNLESS A
C      FLAT=.TRUE.      CARD IS INSERTED IN HERE
C
C-----PRESSURE CALCULATION
      IPREF=IHBP1
      JPREF=JHBP1
      IF (JHUB.GT.2) JPREF=JHBP1
C-----PROGRAM CONTROL AND MONITOR
      IMON=10
      JMON=8
      URFU=0.25
      URFV=0.25
      IF (IEN1P.NE.0) URFV=0.1
      URFW=0.25
      URFP=1.0
      URFE=0.7
      URFK=0.7
      URFVIS=0.7
      UFRX=1.
      UFRR=1.
      URFH=0.7
      URFV=0.7
      URFNO=0.5
      URFDEN=0.7
      IF (INHOT) URFDEN=0.25
      INDPRI=190

C
CHAPTER 2 2 2 2 2 2 INITIAL OPERATIONS 2 2 2 2 2 2 2 2 2
C
C-----CALCULATE GEOMETRICAL QUANTITIES AND SET VARIABLES TO ZERO
      CALL INIT
C-----NONDIMENSIONALIZE X+Y COORDINATES
      DO 50 I=1,NI
      XND(I)=X(I)/(2.*RLARGE)
50 XUND(I)=XU(I)/(2.*RLARGE)

```

```

      DO 60 J=1,NJ
      YND(J)=Y(J)/(2.*RLARGE)
60    YVND(J)=YV(J)/(2.*RLARGE)
C-----INITIALISE VARIABLE FIELDS
1000  CONTINUE
      SORMAX=0.50E-2
      NITER=0
      FLOWIN=0.0
      ARDEN=0.0
      ARDENT=0.0
      XMONIN=0.0
      WMONIN=0.0

C
C*****      INLET SWIRL VELOCITY PROFILE
C
C*****      W, USE SOLID BODY ROTATION MODEL
      WINST=2.*SWNB(LFS)/(1.+SWNB(LFS))*UIN
      DO 206 J=JHUB,JSTEP
206    W(1,J)=WINST*R(J)/R(JSTEP)
C-----NSER=0 - FLAT SWIRL VELOCITY PROFILE FROM SWIRL VANES
C-----NSBR=1 - SOLID BODY ROTATION FROM SWIRL GENERATOR
      IF(NSER.EQ.1) GO TO 208
C*****      W, FLAT PROFILE
      WIN=UIN*DSIN(VANB(LFS)*3.14159/180.)/DCOS(VANB(LFS)*3.14159/180.)
      DO 207 J=JHUB,JSTEP
207    W(1,J)=WIN
208  CONTINUE
      DO 200 J=JHUB,JSTEP
      U(2,J)=UIN
      TE(1,J)=TEIN
      ED(1,J)=EDIN
      H(1,J)=HIN
      FU(1,J)=FUIN
      OF(1,J)=OFIN
      OX(1,J)=OXIN
      AN2(1,J)=PRIN
      RADR(1,J)=RADIN
      RADX(1,J)=RADIN
      T(1,J)=TIN
      ARDEN=0.5*(DEN(1,J)+DEN(2,J))*R(J)*SNS(J)
      XMONIN=XMONIN+ARDEN*U(2,J)*U(2,J)
      WMONIN=WMONIN+ARDEN*U(2,J)*W(1,J)
      ARDENT=ARDENT+ARDEN
200  FLOWIN=FLOWIN+ARDEN*U(2,J)
      UMEAN=FLOWIN/ARDENT
C      SORMAX=SORMAX*FLOWIN
      IF(W(1,JSTEP).EQ.0.0) WMONIN=1.0
C-----INLET FUEL PROFILE IF NONUNIFORM
      IF(INFUPR.EQ.1) GO TO 214
      IF(INFUPR.EQ.2) GO TO 215
C-----THIS FOR INFUPR=3 - 2-PEAK FUEL PROFILE
      FU(1,5)=0.5*FUIN
      FU(1,6)=1.5*FUIN
      FU(1,7)=1.5*FUIN

```

```

      FU(1,8)=0.5*FUIN
      GO TO 214
215 CONTINUE
C-----THIS FOR INFUPR=2 - 1-PEAK FUEL PROFILE
      FU(1,5)=1.6*FUIN
      FU(1,6)=1.2*FUIN
      FU(1,7)=0.8*FUIN
      FU(1,8)=0.4*FUIN
214 CONTINUE
C
C-----LATERAL ENTRY
      IF(IEN1P.EQ.0) GO TO 211
      J=NJ
      DO 201 I=IEN1M,IEN1P
      V(I,J)=VIEN1
      TE(I,J)=TEIN*VIEN1**2/UIT**2
      ED(I,J)=EDIN
      H(I,J)=(COX*0.232+CPR*0.768)*TIN
      OF(I,J)=0.232
      ARDEN=0.5*(DEN(I,J)+DEN(I,J-1))*RV(J)*SEW(I)
      FLOWIN=FLOWIN-ARDEN*VIEN1
201 CONTINUE
211 CONTINUE
      IF(IEN2P.EQ.0) GO TO 212
      J=JCNPI
      DO 209 I=IEN2M,IEN2P
      V(I,J)=VIEN2
      TE(I,J)=TEIN*VIEN2**2/UIT**2
      ED(I,J)=EDIN
      H(I,J)=(COX*0.232+CPR*0.768)*TIN
      OF(I,J)=0.232
      ARDEN=0.5*(DEN(I,J)+DEN(I,J-1))*RV(J)*SEW(I)
      FLOWIN=FLOWIN-ARDEN*VIEN2
209 CONTINUE
212 CONTINUE
C-----INTERIOR VARIABLE FIELDS
      JFIN=JSTPI
      DO 202 I=2,NI
      IF(I.GE. ISTEP .AND. I.LE. ICUT) JFIN=JFIN+JINC
      IF(I.GT. ICUT) JFIN=NJ
      IF(I.GT. ICON) JFIN=JCON
      JEND=JFIN-1
      JSTA=2
      IF(I.LT. IHUB .AND. JHUB.GT.2) JSTA=JHUB
      DO 202 J=JSTA,JEND
      FACTOR=((YV(JSTPI)-YV(JHUB))*(RV(JSTPI)-RV(JHUB)))/
      1((YV(JFIN)-YV(JSTA))*(RV(JFIN)-RV(JSTA)))
      TE(I,J)=TEIN
      ED(I,J)=EDIN
      W(I,J)=0.0
      H(I,J)=HIN
      FU(I,J)=FUIN
      IF(I.EQ.NI) FU(I,J)=1.E-8
      OF(I,J)=-OXDFU*FUIN

```

```

      T(I,J)=TIN
      IF(I.EQ.2)GO TO 202
      IF(I.EQ.ISTEP.AND.J.GT.JSTEP) GO TO 202
      IF(I.EQ.IHUB.AND.J.LT.JHUB) GO TO 202
      U(I,J)=UIN*FACTOR
      IF(I.EQ.ISTEP.AND.I.EQ.IHUB) U(I,J)=U(I-1,J)
202  CONTINUE
C
      IF(NSBR .EQ. 0) GO TO 219
      JFIN=JSTP1
      DO 218 I=2,NI
      IF(I .GE. ISTEP .AND. I .LE. ICUT) JFIN=JFIN+JINC
      IF(I .GT. ICUT) JFIN=NJ
      IF(I.GT.ICON) JFIN=JCNP1
      JEND=JFIN-1
      JSTA=2
      IF(I.LT.IHUB.AND.JHUB.GT.2) JSTA=JHUB
      DO 218 J=JSTA,JEND
      WINST=2.*SWNB(LFS)/(1.+SWNB(LFS))*U(I,2)
      W(I,J)=WINST*R(J)/R(JEND)
218  CONTINUE
      GO TO 223
C
219  CONTINUE
      JFIN=JSTP1
      DO 220 I=2,NI
      IF(I .GE. ISTEP .AND. I .LE. ICUT) JFIN=JFIN+JINC
      IF(I .GT. ICUT) JFIN=NJ
      IF(I.GT.ICON) JFIN=JCNP1
      JSTA=2
      IF(I.LT.IHUB.AND.JHUB.GT.2) JSTA=JHUB
      JEND=JFIN-1
      DO 220 J=JSTA,JEND
      W(I,J)=WIN
220  CONTINUE
223  CONTINUE
C
C-----WALL FUNCTIONS
      DO 203 I=2,NIM1
      YPLUSN(I)=11.0
      YPLUSS(I)=11.0
203  IF(I.GE.IHUB)YPLUSS(I)=0.0
      DO 204 J=2,NJ
      XPLUSE(J)=11.0
      XPLUSW(J)=11.0
      IF(J.LE.JCON)XPLUSE(J)=0.0
204  IF(J.GE.JHUB.AND.J.LE.JSTEP)XPLUSW(J)=0.0
      CALL PROPS(NITER)
216  CONTINUE
C-----INITIAL OUTPUT
      WRITE(6,231)
      WRITE(6,221) UIN
      RE=UIN*RSMALL*2.0*DENSIT/VISCOS
      WRITE(6,230) RE

```

```

RSDRL=RSMALL/RLARGE
DO 295 I=1,NI
DO 205 J=1,NJ
205 PD(I,J)=P(I,J)-PRESS
295 CONTINUE
WRITE(6,240) RSDRL
WRITE(6,250) VISCOS
WRITE(6,260) DENSIT
WRITE(6,315) NI,NJ,ISTEP,JSTEP,IHUB,JHUB,ICON,JCON,IEN1M,IEN1P,
1IEN2M,IEN2P
IF(.NOT.INLET) GO TO 2999
IF(INCALU) CALL PRINT(1,1,NI,NJ,IT,JT,XU,Y,U,HEDU)
IF(INCALV) CALL PRINT(1,1,NI,NJ,IT,JT,X,YV,V,HEDV)
IF(INCALW) CALL PRINT(1,1,NI,NJ,IT,JT,X,Y,W,HEDW)
IF(INCALP) CALL PRINT(1,1,NI,NJ,IT,JT,X,Y,P,HEDP)
IF(INCALK) CALL PRINT(1,1,NI,NJ,IT,JT,X,Y,TE,HEDKE)
IF(INCald) CALL PRINT(1,1,NI,NJ,IT,JT,X,Y,ED,HEDED)
IF(INCALH) CALL PRINT(1,1,NI,NJ,IT,JT,X,Y,H,HEDH)
IF(INCALF) CALL PRINT(1,1,NI,NJ,IT,JT,X,Y,FU,HEDFU)
IF(INCALO) CALL PRINT(1,1,NI,NJ,IT,JT,X,Y,OF,HEDOF)
IF(INHOT ) CALL PRINT(1,1,NI,NJ,IT,JT,X,Y,OX,HEDOX)
IF(INHOT ) CALL PRINT(1,1,NI,NJ,IT,JT,X,Y,AN2,HEDNI)
IF(INHOT ) CALL PRINT(1,1,NI,NJ,IT,JT,X,Y,CO2,HEDCO2)
IF(INHOT ) CALL PRINT(1,1,NI,NJ,IT,JT,X,Y,H2O,HEDH2O)
IF(INHOT ) CALL PRINT(1,1,NI,NJ,IT,JT,X,Y,CO,HEDCO)
IF(INHOT ) CALL PRINT(1,1,NI,NJ,IT,JT,X,Y,T,HEDTEM)
IF(INHOT) CALL TEMPND
IF(INHOT) CALL PRINT(1,1,NI,NJ,IT,JT,X,Y,TT,HEDNDT)
IF(INHOT ) CALL PRINT(1,1,NI,NJ,IT,JT,X,Y,RADX,HEDRX)
IF(INHOT ) CALL PRINT(1,1,NI,NJ,IT,JT,X,Y,RADR,HEDRR)
IF(INHOT ) CALL PRINT(1,1,NI,NJ,IT,JT,X,Y,DEN,HEDDEN)
IF(INPRO ) CALL PRINT(1,1,NI,NJ,IT,JT,X,Y,VIS,HEDVIS)
IF(INHOT ) CALL PRINT(1,1,NI,NJ,IT,JT,X,Y,RFUP,HEDFUP)
IF(INHOT ) CALL PRINT(1,1,NI,NJ,IT,JT,X,Y,RFUARR,HEDARR)
IF(INHOT ) CALL PRINT(1,1,NI,NJ,IT,JT,X,Y,RFUEBU,HEDEBU)
2999 CONTINUE
WRITE(6,312)
RESORV=0.005
RESORU=0.005
RESORW=0.005
C
CHAPTER 3 3 3 3 3 3 3 ITERATION LOOP 3 3 3 3 3 3 3 3
C
WRITE(6,310) IMON,JMON
WRITE(6,313)
WRITE(6,316)
300 NITER=NITER+1
C-----UPDATE MAIN DEPENDENT VARIABLES
IF(INCALU) CALL CALCU
IF(INCALV) CALL CALCV
IF(INCALP) CALL CALCP
IF(INCALW) CALL CALCW
IF(INCALK) CALL CALCTE
IF(INCald) CALL CALCED

```



```

      IF(INCALH) CALL CALCH(INCLRX)
      IF(NITER.LE.(MAXIT/2))GO TO 306
      IF(INCLRX) CALL CALCRX
      IF(INCLRR) CALL CALCRR
306  CONTINUE
      IF(INCALF) CALL CALCFU
      IF(INCALO) CALL CALCOF
      IF(INCALC) CALL CALCCO
      IF(INCALC)CALL EQUAL(1)
      IF(INCLNO) CALL CALCNO
      IF(INCLNO)CALL EQUAL(2)
C-----UPDATE FLUID PROPERITIES
      IF(INPRO) CALL PROPS(NITER)
      IF(.NOT.(T(IMON,JMON).GT.TWALL.AND.TWALL.LT.TWLMAX))GO TO 307
      TWALL=TWALL+50.
307  CONTINUE
C-----INTERMEDIATE OUTPUT
      RESORM=RESORM/FLOWIN
      RESORU=RESORU/XMONIN
      RESORV=RESORV/XMONIN
      RESORW=RESORW/WMONIN
      RESORK=RESORK/(.5*FLOWIN*UMEAN*UMEAN)
      IF(.NOT.INOTPT) GO TO 555
      D=0.0
      WRITE(6,311) NITER,RESORU,RESORV,RESORW,RESORM,RESORK,
      *RESORE,U(IMON,JMON),V(IMON,JMON),W(IMON,JMON),P(IMON,JMON),
      *TE(IMON,NJM1),ED(IMON,NJM1)
      WRITE(6,314) RESORH,RESORF,RESORO,D,D,D,H(IMON,JMON),T(IMON,JMON),
1      FU(IMON,JMON),OF(IMON,JMON),OX(IMON,JMON),AN2(IMON,JMON)
      WRITE(6,317) RESORX,RESORR,RADX(IMON,JMON),RADR(IMON,JMON)
      IF(MOD(NITER,INDPRI).NE.0)GO TO 301
      WRITE(6,312)
      DO 304 I=1,NI
      DO 303 J=1,NJ
303  PD(I,J)=P(I,J)-PRESS
304  CONTINUE
      IF(INCALU) CALL PRINT(1,1,NI,NJ,IT,JT,XU,Y,U,HEDU)
      IF(INCALV) CALL PRINT(1,1,NI,NJ,IT,JT,X,YV,V,HEDV)
      IF(INCALW) CALL PRINT(1,1,NI,NJ,IT,JT,X,Y,W,HEDW)
      IF(INCALP) CALL PRINT(1,1,NI,NJ,IT,JT,X,Y,P,HEDP)
      IF(INCALK) CALL PRINT(1,1,NI,NJ,IT,JT,X,Y,TE,HEDKE)
      IF(INCald) CALL PRINT(1,1,NI,NJ,IT,JT,X,Y,ED,HEDED)
      IF(INCALH) CALL PRINT(1,1,NI,NJ,IT,JT,X,Y,H,HEDH)
      IF(INCALF) CALL PRINT(1,1,NI,NJ,IT,JT,X,Y,FU,HEDFU)
      IF(INCALO) CALL PRINT(1,1,NI,NJ,IT,JT,X,Y,OF,HEDOF)
      IF(INHOT) CALL PRINT(1,1,NI,NJ,IT,JT,X,Y,OX,HEDOX)
      IF(INHOT) CALL PRINT(1,1,NI,NJ,IT,JT,X,Y,AN2,HEDNI)
      IF(INHOT) CALL PRINT(1,1,NI,NJ,IT,JT,X,Y,CO2,HEDCO2)
      IF(INHOT) CALL PRINT(1,1,NI,NJ,IT,JT,X,Y,CO,HEDCO)
      IF(INHOT) CALL PRINT(1,1,NI,NJ,IT,JT,X,Y,H2O,HEDH2O)
      IF(INHOT) CALL PRINT(1,1,NI,NJ,IT,JT,X,Y,T,HEDTEM)
      IF(INHOT) CALL TEMPND
      IF(INHOT) CALL PRINT(1,1,NI,NJ,IT,JT,X,Y,TT,HEDNDT)
      IF(INHOT) CALL PRINT(1,1,NI,NJ,IT,JT,X,Y,RADX,HEDRX)

```

```

      IF(INHOT ) CALL PRINT(1,1,NI,NJ,IT,JT,X,Y,RADR,HEDRR)
      IF(INHOT ) CALL PRINT(1,1,NI,NJ,IT,JT,X,Y,DEN,HEDDEN)
      IF(INPRO ) CALL PRINT(1,1,NI,NJ,IT,JT,X,Y,VIS,HEDVIS)
      IF(INHOT ) CALL PRINT(1,1,NI,NJ,IT,JT,X,Y,RFUP,HEDFUP)
      IF(INHOT ) CALL PRINT(1,1,NI,NJ,IT,JT,X,Y,RFUARR,HEDARR)
      IF(INHOT ) CALL PRINT(1,1,NI,NJ,IT,JT,X,Y,RFUEBU,HEDEBU)
      WRITE(6,312)
      WRITE(6,310) IMON,JMON
      WRITE(6,313)
301  CONTINUE
555  CONTINUE
C-----TERMINATION TESTS
C      SORCE=RESORM
      SORCE=AMAX1(RESORM,RESORU,RESORV,RESORW,RESORK)
      IF(NITER .GE. MAXIT)GO TO 302
      IF(SORCE.GT.SORMAX.OR.NITER.LT.20) GO TO 300
302  CONTINUE
      IF(SORCE .GT. SORMAX) WRITE (6,320) SORMAX
C
CHAPTER 4 4 4 4 4 4 FINAL OPERATIONS AND OUTPUT 4 4 4 4 4 4
C
C-----NONDIMENSIONALIZE PROBLEM SOLUTION
      DO 700 I=1,NI
      DO 600 J=1,NJ
      USTAR(I,J)=U(I,J)/UIN
      VSTAR(I,J)=V(I,J)/UIN
      WSTAR(I,J)=W(I,J)/UIN
600  CONTINUE
700  CONTINUE
      WRITE(6,312)
      WRITE(6,410) LFS,NSBR,SWNB(LFS),VANB(LFS)
      DO 405 I=1,NI
      DO 404 J=1,NJ
404  PD(I,J)=P(I,J)-PRESS
405  CONTINUE
      IF(INCALU) CALL PRINT(1,1,NI,NJ,IT,JT,XU,Y,U,HEDU)
      IF(INCALV) CALL PRINT(1,1,NI,NJ,IT,JT,X,YV,V,HEDV)
      IF(INCALW) CALL PRINT(1,1,NI,NJ,IT,JT,X,Y,W,HEDW)
      IF(INCALP) CALL PRINT(1,1,NI,NJ,IT,JT,X,Y,PD,HEDP)
      IF(INCALK) CALL PRINT(1,1,NI,NJ,IT,JT,X,Y,TE,HEDKE)
      IF(INCald) CALL PRINT(1,1,NI,NJ,IT,JT,X,Y,ED,HEDED)
      IF(INCALH) CALL PRINT(1,1,NI,NJ,IT,JT,X,Y,H,HEDH)
      IF(INCALF) CALL PRINT(1,1,NI,NJ,IT,JT,X,Y,FU,HEDFU)
      IF(INCALO) CALL PRINT(1,1,NI,NJ,IT,JT,X,Y,OF,HEDOF)
      IF(INHOT ) CALL PRINT(1,1,NI,NJ,IT,JT,X,Y,OX,HEDOX)
      IF(INHOT ) CALL PRINT(1,1,NI,NJ,IT,JT,X,Y,AN2,HEDNI)
      IF(INCALC ) CALL PRINT(1,1,NI,NJ,IT,JT,X,Y,CO2,HEDCO2)
      IF(INCALC ) CALL PRINT(1,1,NI,NJ,IT,JT,X,Y,H2O,HEDH2O)
      IF(INCALC ) CALL PRINT(1,1,NI,NJ,IT,JT,X,Y,CO,HEDCO)
      IF(AO.NE.AY ) CALL PRINT(1,1,NI,NJ,IT,JT,X,Y,H2,HEDH2)
      IF(INCALC ) CALL PRINT(1,1,NI,NJ,IT,JT,X,Y,O1,HEDO)
      IF(INCLNO ) CALL PRINT(1,1,NI,NJ,IT,JT,X,Y,AN1,HEDN)
      IF(INCLNO ) CALL PRINT(1,1,NI,NJ,IT,JT,X,Y,ANO,HEDNO)
      IF(INHOT ) CALL TPRINT(1,1,NI,NJ,IT,JT,X,Y,T,HEDTEM)

```

```

IF(INHOT) CALL TEMPND
IF(INHOT) CALL TPRINT(1,1,NI,NJ,IT,JT,X,Y,TT,HEDNDT)
IF(INCLRX) CALL PRINT(1,1,NI,NJ,IT,JT,X,Y,RADX,HEDRX)
IF(INCLRR) CALL PRINT(1,1,NI,NJ,IT,JT,X,Y,RADR,HEDRR)
IF(INHOT) CALL PRINT(1,1,NI,NJ,IT,JT,X,Y,DEN,HEDDEN)
IF(INPRO) CALL PRINT(1,1,NI,NJ,IT,JT,X,Y,VIS,HEDVIS)
IF(INHOT) CALL PRINT(1,1,NI,NJ,IT,JT,X,Y,RFUP,HEDFUP)
IF(INHOT) CALL PRINT(1,1,NI,NJ,IT,JT,X,Y,RFUARR,HEDARR)
IF(INHOT) CALL PRINT(1,1,NI,NJ,IT,JT,X,Y,RFUEBU,HEDEBU)
IF(INCALU) CALL PRINT(1,1,NI,NJ,IT,JT,XUND,YND,USTAR,HEDNDU)
IF(INCALV) CALL PRINT(1,1,NI,NJ,IT,JT,XND,YVND,VSTAR,HEDNDV)
IF(INCALW) CALL PRINT(1,1,NI,NJ,IT,JT,XND,YND,WSTAR,HEDNDW)
IF(INHOT) CALL PRINT(1,1,NI,NJ,IT,JT,X,Y,RCOARR,HEDARR)
IF(INHOT) CALL PRINT(1,1,NI,NJ,IT,JT,X,Y,RCOEBU,HEDEBU)
C-----CALCULATION OF NON DIMENSIONAL TURBULENCE ENERGY AND LENGTH SCALE
IF(INCLRX) CALL CALCQ
IF(INCLRX) CALL PRINT(1,1,NI,NJ,IT,JT,X,Y,Q,HEDRX)
JEND=JSTEP
DO 411 I=2,NIM1
  JSTA=2
  IF(I.LT.IHUB) JSTA=JHUB
  IF(I.GE. ISTEP .AND. I.LE. ICUT) JEND=JEND+JINC
  IF(I.GT.ICON) JEND=JCON
  DO 400 J=JSTA,JEND
    SU(I,J)=TE(I,J)*DEN(I,J)/DABS(TAUN(I))
400 SP(I,J)=TE(I,J)**1.5/ED(I,J)/RLARGE
411 CONTINUE
    CALL PRINT(2,2,NI,NJ,IT,JT,X,Y,SU,HEDKP)
    CALL PRINT(2,2,NI,NJ,IT,JT,X,Y,SP,HEDLS)
C-----CALCULATION OF SHEAR-STRESS COEFFICIENT ALONG LARGE DUCT WALL
WRITE(6,402)
DO 401 I=ISTEP,NIM1
  SSC=TAUN(I)/(1.0*DENSIT*ULARGE*ULARGE)
  XUD=XU(I)/RLARGE/2.
  WRITE(6,403) I,XUD,SSC
401 CONTINUE
  WRITE(6,312)
C-----RESET INITIAL SWIRL VELOCITY PROFILE FOR ANOTHER SWIRL CASE
IF(LFS.GE. LFSMAX) GO TO 409
LFS=LFS+1
WINST=2.*SWNB(LFS)/(1.+SWNB(LFS))*UIN
DO 406 J=JHUB,JSTEP
406 W(1,J)=WINST*R(J)/R(JSTEP)
  IF(NSBR.EQ. 1) GO TO 408
  WIN=UIN*DSIN(VANB(LFS)*3.14159/180.)/DCOS(VANB(LFS)*3.14159/180.)
  DO 407 J=JHUB,JSTEP
407 W(1,J)=WIN
408 NITER=3
  WRITE(6,310) IMON,JMON
  WRITE(6,313)
  IF(LFS.GT.1) MAXIT=300
  GO TO 300
409 CONTINUE
C-----FORMAT STATEMENTS

```

```

231  FORMAT(1H1,15X,51HKASE T1 - TURBULENT FLOW THROUGH SUDDEN ENLARGEM
      IENT////)
221  FORMAT(////15X,33HINLET FLUID VELOCITY ,1PE11.3)
230  FORMAT( //15X,33HREYNOLDS NUMBER ,1PE11.3)
240  FORMAT( //15X,33HDIAMETER RATIO ,1PE11.3)
250  FORMAT( //15X,33HLAMINAR VISCOSITY ,1PE11.3)
260  FORMAT( //15X,33HFLUID DENSITY ,1PE11.3)
310  FORMAT(13HOITER I---, 9X,29HABSOLUTE RESIDUAL SOURCE SUMS,9X,
      111H---I I---,37H FIELD VALUES AT MONITORING LOCATION(,12,1H,,12,
      26H) ---I/14H NO UMON,5X,4HVMON,5X,4HMASS,5X,4HWMON,5X,4HTKIN
      3,5X,4HDISP,9X,1HU,8X,1HV,8X,1HP,8X,1HW,8X,1HK,8X,1HD)
311  FORMAT(1H ,13,5X,1P6E9.2,3X,1P6E9.2)
312  FORMAT (1H0,59(2H- ))
313  FORMAT(10X,4HENTH,5X,4HFUEL,5X,4HO-IF,36X,1HH,8X,1HT,8X,2HFU,7X,
      24HO-IF,5X,2HOF,7X,2HPR/)
314  FORMAT(9X,1P6E9.2,3X,1P6E9.2)
315  FORMAT(//5X,73H NI NJ ISTEP JSTEP IHUB JHUB ICON JCON I
      1EN1M IEN1P IEN2M IEN2P//5X,12I6////)
316  FORMAT(10X,4HRADX,5X,4HRADR,5X,4HXRAD,5X,4HRRAD)
317  FORMAT(9X,1P4E9.2/)
320  FORMAT (5X,'SOLN. DID NOT CONVERGE SORMAX =',E15.5)
402  FORMAT(//5X,1HI,7X,5HXU(I),6X,10HS.S.COEFF.)
403  FORMAT(/5X,I5,2(1PE11.3))
410  FORMAT(//23H SWIRL CASE WITH LFS =,I3/
      1 23H AND NSBR =,I3//
      163H CORRESPONDS IF NSBR = 1 TO SWIRL GENERATOR WITH SWIRL NUMBER =
      1,F10.3//37H OR IF NSBR = 0 TO SWIRL VANE ANGLE =,F10.3////)
      STOP
      END
C START OF SF7.FOR
C
SUBROUTINE INIT
IMPLICIT REAL*8(A-H,O-Z)
C*****
C
CHAPTER 0 0 0 0 0 0 0 0 PRELIMINARIES 0 0 0 0 0 0 0 0
C
COMMON
1/UVEL/RESORU,NSWPU,URFU,DXEPU(40),DXPWU(40),SEWU(40)
1/VVEL/RESORV,NSWPV,URFV,DYNPV(40),DYPSV(40),SNSV(40),RCV(40)
*/WVEL/ RESORW, NSWPW, URFW
1/PCOR/RESORM,NSWPP,URFP,DJ(40,15),DV(40,15),IPREF,JPREF
*/VAR/U(40,15), V(40,15), W(40,15), P(40,15), PP(40,15), TE(40,15),
1ED(40,15),H(40,15),FU(40,15),OF(40,15)
1/ALL/IT,JT,NI,NJ,NIM1,NJM1,GREAT
1/GEOM1/INDCOS,X(40),Y(40),DXEP(40),DXPW(40),DYNP(40),DYPS(40),
1 SNS(40),SEW(40),XU(40),YV(40),R(40),RV(40),LABRUPT
1/FLUPR/URFVIS,VISCOS,DENSIT,PRANDT,DEN(40,15),VIS(40,15)
1 ,OX(40,15),AN2(40,15),T(40,15),RFUP(40,15),RCOP(40,15)
1,CO(40,15),H2O(40,15),H2(40,15),CO2(40,15),FUOLD(40,15),OI(40,15)
1/KASE T1/UIN,TEIN,EDIN,FLOWIN,ALAMDA,
2 RSMALL,RLARGE,AL1,AL2,JSTEP,ISTEP,JSTP1,JSTM1,ISTP1,ISTM1,J
3INC,ICUT,ICTP1
1/DIMTEM/TT(40,15)

```

```

1/TURB/GEN(40,15),CD,CMU,C1,C2,CAPPA,ELOG,PRED,PRTE
1/COEF/AP(40,15),AN(40,15),AS(40,15),AE(40,15),AW(40,15),SU(40,15),
1      SP(40,15)
1/CHEM/URFDEN,GASCON,CFU,COX,CPR,WFU,WOX,WPR,HFU,HCO,OXDFU,PRESS
1,CCO,CCO2,CH2O,CAN2,RESORC,NSWPC,URFCO,PRCO,OXDCO,OXDFU1,WCO
1,WH2O,WCO2,WAN2,PERSTO,WH2,CH2,W01,CO1
1/RADT/RADX(40,15),RADR(40,15),RADIN
2      ,EMIW,NSWPRX,NSWPRR,URFRX,URFRR,SIGMA,ABSOR,SCATT
3      ,RESORR,RESORX
1/CHEM2/FUIN,AX,AY,AO
COMMON
1/NITRC1/WN1,WNO,CN1,CNO,URFNO,AN1(40,15),ANO(40,15),NSWPNO
2,URFN1,PRNO,RESRNO,RNOF1(40,15),RNOF2(40,15)
3,RNOR2(40,15),RNOR1(40,15)

```

C

CHAPTER 1 1 1 1 1 CALCULATE GEOMETRICAL QUANTITIES 1 1 1 1 1

C

```

      DO 100 J=1,NJ
      R(J)=Y(J)
100  IF (INDCOS.EQ.1) R(J)=1.0
      DXPW(1)=0.0
      DXEP(NI)=0.0
      DO 101 I=1,NIM1
      DXEP(I)=X(I+1)-X(I)
101  DXPW(I+1)=DXEP(I)
      DYPS(1)=0.0
      DYNP(NJ)=0.0
      DO 102 J=1,NJM1
      DYNP(J)=Y(J+1)-Y(J)
102  DYPS(J+1)=DYNP(J)
      SEW(1)=0.0
      SEW(NI)=0.0
      DO 103 I=2,NIM1
103  SEW(I)=0.5*(DXEP(I)+DXPW(I))
      SNS(1)=0.0
      SNS(NJ)=0.0
      DO 104 J=2,NJM1
104  SNS(J)=0.5*(DYNP(J)+DYPS(J))
      XU(1)=0.0
      DO 105 I=2,NI
105  XU(I)=0.5*(X(I)+X(I-1))
      DXPWU(1)=0.0
      DXPWU(2)=0.0
      DXEPU(1)=0.0
      DXEPU(NI)=0.0
      DO 106 I=2,NIM1
      DXEPU(I)=XU(I+1)-XU(I)
106  DXPWU(I+1)=DXEPU(I)
      SEWU(1)=0.0
      SEWU(2)=0.0
      DO 107 I=3,NIM1
107  SEWU(I)=0.5*(DXEPU(I)+DXPWU(I))
      YV(1)=0.0
      RV(1)=0.0

```

```

DO 108 J=2,NJ
RV(J)=0.5*(R(J)+R(J-1))
RCV(J)=0.5*(RV(J)+RV(J-1))
108 YV(J)=0.5*(Y(J)+Y(J-1))
DYPSV(1)=0.0
DYPSV(2)=0.0
DYNPV(NJ)=0.0
DO 109 J=2,NJM1
DYNPV(J)=YV(J+1)-YV(J)
109 DYPSV(J+1)=DYNPV(J)
SNSV(1)=0.0
SNSV(2)=0.0
SNSV(NJ)=0.0
DO 110 J=3,NJM1
110 SNSV(J)=0.5*(DYNPV(J)+DYPSV(J))
C
CHAPTER 2 2 2 2 2 2 SET VARIABLES TO ZERO 2 2 2 2 2 2
C
SMALL=1./GREAT
DO 200 I=1,NI
DO 200 J=1,NJ
U(I,J)=0.0
V(I,J)=0.0
W(I,J)=0.
P(I,J)=PRESS
PP(I,J)=0.0
TE(I,J)=0.0
ED(I,J)=0.0
H(I,J)=0.0
FU(I,J)=0.0
RFUP(I,J)=0.0
RCOP(I,J)=0.0
RNOF1(I,J)=0.0
RNOF2(I,J)=0.0
OF(I,J)=0.0
OX(I,J)=0.0
O1(I,J)=0.0
AN2(I,J)=0.0
CO(I,J)=0.0
CO2(I,J)=0.0
H2O(I,J)=0.0
FUOLD(I,J)=0.0
H2(I,J)=0.0
AN1(I,J)=0.0
ANO(I,J)=0.0
T(I,J)=0.0
TT(I,J)=0.0
DEN(I,J)=DENSIT
VIS(I,J)=VISCOS
RADX(I,J)=RADIN
RADR(I,J)=RADIN
DU(I,J)=0.0
DV(I,J)=0.0
SU(I,J)=0.0

```

```

      SP(I,J)=0.0
      AP(I,J)=0.0
200  CONTINUE
      RETURN
      END
C
      SUBROUTINE PROPS(NITER)
      IMPLICIT REAL*8(A-H,O-Z)
C*****
C
CHAPTER 0 0 0 0 0 0 0 0 0 PRELIMINARIES 0 0 0 0 0 0 0 0
C
      COMMON
      1/FLUPR/URFVIS,VISCOS,DENSIT,PRANDT,DEN(40,15),VIS(40,15)
      1,OX(40,15),AN2(40,15),T(40,15),RFUP(40,15),RCOP(40,15)
      1,CO(40,15),H2O(40,15),H2(40,15),CO2(40,15),FUOLD(40,15),O1(40,15)
      */VAR/U(40,15),V(40,15),W(40,15),P(40,15),PP(40,15),TE(40,15),
      1ED(40,15),H(40,15),FU(40,15),OF(40,15)
      1/ALL/IT,JT,NI,NJ,NIM1,NJM1,GREAT
      1/TURB/GEN(40,15).CD,CMU,C1,C2,CAPPA,ELOG,PRED,PRTE
      1/CHEM/URFDEN,GASCON,CFU,COX,CPR,WFU,WOX,WPR,HFU,HCO,OXDFU,PRESS
      1,CCO,CCO2,CH2O,CAN2,RESORC,NSWPC,URFCO,PRCO,OXDCO,OXDFU1,WCO
      1,WH2O,WCO2,WAN2,PERSTO,WH2,CH2,WO1,CO1
      1/CHEM2/FUIN,AX,AY,AO
      COMMON
      1/NITRO1/WN1,WNO,CN1,CNO,URFNO,AN1(40,15),ANO(40,15),NSWPNO
      2,URFN1,PRNO,RESRNO,RNOF1(40,15),RNOF2(40,15)
      3,RNOR2(40,15),RNOR1(40,15)
      OFLIM=-OXDFU*FUIN
C
CHAPTER 1 1 1 1 1 1 1 1 MIXTURE PROPERTIES 1 1 1 1 1 1 1 1
C
      IF(HFU.EQ.0.0) GO TO 101
      DO 100 I=2,NIM1
      DO 100 J=2,NJM1
      IF(NITER.LT.3)GO TO 15
C-----VARIABLE SPECIFIC HEAT CALCULATED HERE
      CCO=(37.85-4571.9/T(I,J))*1000.0/WCO
      CCO2=(66.27-11634.0/T(I,J))*1000.0/WCO2
      CH2O=(49.36-7940.8/T(I,J))*1000.0/WH2O
      CAN2=(37.46-4559.3/T(I,J))*1000.0/WPR
      COX=(42.27-6635.4/T(I,J))*1000.0/WOX
      CNO=(37.81-2874.8/T(I,J))*1000.0/WNO
      CO1=(24.6-2729.2/T(I,J))*1000.0/WO1
      CN1=(17.19+5371.4/T(I,J))*1000.0/WN1
      CH2=(40.35-8085.2/T(I,J))*1000.0/WH2
      CFU=2260.
15  CONTINUE
      DENOLD=DEN(I,J)
      IF(FU(I,J).LT.0.0) FU(I,J)=0.0
      IF(FU(I,J).GT.FUIN) FU(I,J)=FUIN
      IF(OF(I,J).LT.OFLIM) OF(I,J)=OFLIM
      IF(OF(I,J).GT.0.232*PERSTO) OF(I,J)=0.232*PERSTO
      OX(I,J)=OF(I,J)+OXDFU1*FU(I,J)+OXDCO*CO(I,J)-16./32.*O1(I,J)

```

```

1-ANO(I,J)*WO1/(WOX*WNO)
  IF(OX(I,J).LT.0.0) OX(I,J)=0.0
  IF(OX(I,J).GT.0.232*PERSTO) OX(I,J)=0.232*PERSTO
  CO2(I,J)=44.*AX*(FUIN-FU(I,J))/(12.+AY)
1-44./28.*CO(I,J)
  IF(CO2(I,J).LT.0.0) CO2(I,J)=0.0
  IF(CO2(I,J).GT.1.0) CO2(I,J)=1.0
  IF(CO(I,J).LT.0.0) CO(I,J)=0.0
  IF(CO(I,J).GT.1.0) CO(I,J)=1.0
  H2O(I,J)=H2O(I,J)+18.*AO*(FUOLD(I,J)-FU(I,J))/(2.*(12.+AY))
  IF(H2O(I,J).LT.0.0) H2O(I,J)=0.0
  IF(H2O(I,J).GT.1.0) H2O(I,J)=1.0
  H2(I,J)=H2(I,J)+2.*(AY-AO)*(FUOLD(I,J)-FU(I,J))/(2.*(12.+AY))
  IF(H2(I,J).LT.0.0) H2(I,J)=0.0
  IF(H2(I,J).GT.1.0) H2(I,J)=1.0
  AN2(I,J)=1.-(CO(I,J)+FU(I,J)+OX(I,J)+CO2(I,J)+H2O(I,J)+H2(I,J)
1+O1(I,J)+AN1(I,J)+ANO(I,J))
  AN2(I,J)=AN2(I,J)*PERSTO
  IF(AN2(I,J).LT.0.0) AN2(I,J)=0.0
  IF(AN2(I,J).GT.1.0) AN2(I,J)=1.0
  DN=AN2(I,J)+CO(I,J)+FU(I,J)+OX(I,J)+CO2(I,J)+H2O(I,J)+H2(I,J)
1+O1(I,J)+AN1(I,J)+ANO(I,J)
  CMIX=(CFU*FU(I,J)+CAN2*AN2(I,J)+CCO*CO(I,J)+CCO2*CO2(I,J)+
1COX*OX(I,J)+CH2O*H2O(I,J)+CH2*H2(I,J)+CO1*O1(I,J)
2+CN1*AN1(I,J)+CNO*ANO(I,J))/DN
  T(I,J)=(H(I,J)-HFU*FU(I,J)-HCO*CO(I,J))/CMIX
  IF(NITER.GE.75)GO TO 90
  T(I,J)=(H(I,J)-HFU*FU(I,J))/CMIX
90 CONTINUE
  IF(T(I,J).GT.3500.0) T(I,J)=3500.0
  IF(T(I,J).LT.300.0) T(I,J)=300.0
  RECIPM=FU(I,J)/WFU+OX(I,J)/WOX+AN2(I,J)/WPR
1+CO(I,J)/WCO+CO2(I,J)/WCO2+H2O(I,J)/WH2O+H2(I,J)/WH2
  DEN(I,J)=P(I,J)/(GASCON*T(I,J)*RECIPM)
C-----UNDER-RELAX DENSITY
  DEN(I,J)=URFDEN*DEN(I,J)+(1.0-URFDEN)*DENOLD
  IF(J.EQ.2)DEN(I,1)=DEN(I,J)
  FUOLD(I,J)=FU(I,J)
100 CONTINUE
101 CONTINUE
C
CHAPTER 2 2 2 2 2 2 2 VISCOSITY 2 2 2 2 2 2 2
C
  DO 200 I=2,NIM1
  DO 200 J=2,NJM1
  VISOLD=VIS(I,J)
  IF(ED(I,J).EQ.0.) GO TO 202
  VIS(I,J)=DEN(I,J)*TE(I,J)**2*CMU/ED(I,J)+VISCOS
  GO TO 201
202 VIS(I,J)=VISCOS
C-----UNDER-RELAX VISCOSITY
201 VIS(I,J)=URFVIS*VIS(I,J)+(1.-URFVIS)*VISOLD
  IF(J.EQ.2)VIS(I,1)=VIS(I,J)
200 CONTINUE

```



```

C
CHAPTER 3 3 3 3 3 3 3 PROBLEM MODIFICATIONS 3 3 3 3 3 3 3
C
      CALL PROMOD(1)
C
C***** FIX VALUES OF BOUNDARY PROPERTIES *****
      CALL FIXBND
C***** END FIX *****
      RETURN
      END
C
      SUBROUTINE CALCU
      IMPLICIT REAL*8(A-H,O-Z)
C*****
C
CHAPTER 0 0 0 0 0 0 0 PRELIMINARIES 0 0 0 0 0 0 0
C
      COMMON
      1/UVEL/RESGRU,NSWPU,URFU,DXEPU(40),DXPWU(40),SEWU(40)
      1/PCOR/RESORM,NSWPF,URFP,DU(40,15),DV(40,15),IPREF,JPREF
      */VAR/U(40,15),V(40,15),W(40,15),P(40,15),PP(40,15),TE(40,15),
      1ED(40,15),H(40,15),FU(40,15),OF(40,15)
      1/ALL/IT,JT,NI,NJ,NIM1,NJM1,GREAT
      1/GEOM1/INDCOS,X(40),Y(40),DXEP(40),DXPW(40),DYNP(40),DYPS(40),
      1      SNS(40),SEW(40),XU(40),YV(40),R(40),RV(40),LABRUPT
      1/FLUPR/URFVIS,VISCOS,DENSIT,PRANDT,DEN(40,15),VIS(40,15)
      1      ,OX(40,15),AN2(40,15),T(40,15),RFUP(40,15),RCOP(40,15)
      1,CO(40,15),H2O(40,15),H2(40,15),CO2(40,15),FUOLD(40,15),OI(40,15)
      1/COEF/AP(40,15),AN(40,15),AS(40,15),AE(40,15),AW(40,15),SU(40,15),
      1      SP(40,15)
      1/KASE T1/UIN,TEIN,EDIN,FLOWIN,ALAMDA,
      2      RSMALL,RLARGE,AL1,AL2,JSTEP,ISTEP,JSTP1,JSTM1,ISTP1,ISTM1,J
      3INC,ICUT,ICTP1
      1/GEOM2/IHUB,JHUB,IHBP1,JHBP1,IHBM1,JHBM1,ICON,JCON,ICNP1,JCNP1
C
CHAPTER 1 1 1 1 1 1 ASSEMBLY OF COEFFICIENTS 1 1 1 1 1 1 1
C
      DO 100 I=3,NIM1
      DO 101 J=2,NJM1
C-----COMPUTE AREAS AND VOLUME
      AREAN=RV(J+1)*SEWU(I)
      AREAS=RV(J)*SEWU(I)
      AREAEW=R(J)*SNS(J)
      VOL=R(J)*SEWU(I)*SNS(J)
C-----CALCULATE CONVECTION COEFFICIENTS
      GN=0.5*(DEN(I,J+1)+DEN(I,J))*V(I,J+1)
      GNW=0.5*(DEN(I-1,J)+DEN(I-1,J+1))*V(I-1,J+1)
      GS=0.5*(DEN(I,J-1)+DEN(I,J))*V(I,J)
      GSW=0.5*(DEN(I-1,J)+DEN(I-1,J-1))*V(I-1,J)
      IF(I.EQ.NIM1)GE=DEN(I,J)*U(I,J)
      GE=0.5*(DEN(I+1,J)+DEN(I,J))*U(I+1,J)
      GP=0.5*(DEN(I,J)+DEN(I-1,J))*U(I,J)
      GW=0.5*(DEN(I-1,J)+DEN(I-2,J))*U(I-1,J)
      CN=0.5*(GN+GNW)*AREAN

```

```

      CS=0.5*(GS+GSW)*AREAS
      CE=0.5*(GE+GP)*AREA EW
      CW=0.5*(GP+GW)*AREA EW
C-----CALCULATE DIFFUSION COEFFICIENTS
      VISN=0.25*(VIS(I,J)+VIS(I,J+1)+VIS(I-1,J)+VIS(I-1,J+1))
      VISS=0.25*(VIS(I,J)+VIS(I,J-1)+VIS(I-1,J)+VIS(I-1,J-1))
      DN=VISN*AREAN/DYNP(J)
      DS=VISS*AREAS/DYPS(J)
      DE=VIS(I,J)*AREA EW/DXEPU(I)
      DW=VIS(I-1,J)*AREA EW/DXPWU(I)
C-----CALCULATE COEFFICIENTS OF SOURCE TERMS
      SMP=CN-CS+CE-CW
      CP=DMAX1(0.0,SMP)
      CPO=CP
C-----ASSEMBLE MAIN COEFFICIENTS
      AN(I,J)=DMAX1(DABS(0.5*CN),DN)-0.5*CN
      AS(I,J)=DMAX1(DABS(0.5*CS),DS)+0.5*CS
      AE(I,J)=DMAX1(DABS(0.5*CE),DE)-0.5*CE
      AW(I,J)=DMAX1(DABS(0.5*CW),DW)+0.5*CW
      DU(I,J)=AREA EW
      SU(I,J)=CPO*U(I,J)+DU(I,J)*(P(I-1,J)-P(I,J))
      SP(I,J)=-CP
101 CONTINUE
100 CONTINUE
C
CHAPTER 2 2 2 2 2 2 2 PROBLEM MODIFICATIONS 2 2 2 2 2 2 2
C
      NCHAP=2
      CALL PROMOD (NCHAP)
C
CHAPTER 3 FINAL COEFF. ASSEMBLY AND RESIDUAL SOURCE CALCULATION 3 3
C
      RESORU=0.0
      DO 300 I=3,NIM1
      DO 301 J=2,NJM1
      AP(I,J)=AN(I,J)+AS(I,J)+AE(I,J)+AW(I,J)-SP(I,J)
      IF (AP(I,J).LT.1E-30) DU(I,J)=0.0
      IF (AP(I,J).LT.1E-30) GO TO 302
      DU(I,J)=DU(I,J)/AP(I,J)
302 RESOR=AN(I,J)*U(I,J+1)+AS(I,J)*U(I,J-1)+AE(I,J)*U(I+1,J)
1    +AW(I,J)*U(I-1,J)-AP(I,J)*U(I,J)+SU(I,J)
      VOL=R(J)*SEW(I)*SNS(J)
      SORVOL=GREAT*VOL
      IF (-SP(I,J).GT.0.5*SORVOL) RESOR=0.0
      RESORU=RESORU+DABS(RESOR)
C-----UNDER-RELAXATION
      AP(I,J)=AP(I,J)/URFU
      SU(I,J)=SU(I,J)+(1.-URFU)*AP(I,J)*U(I,J)
      DU(I,J)=DU(I,J)*URFU
301 CONTINUE
300 CONTINUE
C
CHAPTER 4 4 4 SOLUTION OF DIFFERENCE EQUATION 4 4 4 4 4 4 4
C

```

```

      DO 400 N=1,NSWPU
400  CALL LISOLV(3,2,NI,NJ,IT,JT,U,NCHAP)
      RETURN
      END
C
      SUBROUTINE CALCV
      IMPLICIT REAL*8(A-H,O-Z)
C*****
C
CHAPTER 0 0 0 0 0 0 0 0 PRELIMINARIES 0 0 0 0 0 0 0 0
C
      COMMON
      1/VVEL/RESORV,NSWPV,URFV,DYNPV(40),DYPSV(40),SNSV(40),RCV(40)
      1/PCOR/RESORM,NSWPP,URFP,DU(40,15),DV(40,15),IPREF,JPREF
      */VAR/U(40,15),V(40,15),W(40,15),P(40,15),PP(40,15),TE(40,15),
      1ED(40,15),H(40,15),FU(40,15),OF(40,15)
      1/ALL/IT,JT,NI,NJ,NIM1,NJM1,GREAT
      1/GEOM1/INDCOS,X(40),Y(40),DXEP(40),DXPW(40),DYNP(40),DYPS(40),
      1      SNS(40),SEW(40),XU(40),YV(40),R(40),RV(40),LABRUPT
      1/FLUPR/URFVIS,VISCOS,DENSIT,PRANDT,DEN(40,15),VIS(40,15)
      1      ,OX(40,15),AN2(40,15),T(40,15),RFUP(40,15),RCOP(40,15)
      1,CO(40,15),H2O(40,15),H2(40,15),CO2(40,15),FUOLD(40,15),OI(40,15)
      1/COEF/AP(40,15),AN(40,15),AS(40,15),AE(40,15),AW(40,15),SU(40,15),
      1      SP(40,15)
      1/KASE T1/UIN,TEIN,EDIN,FLOWIN,ALAMDA,
      2      RSMALL,RLARGE,AL1,AL2,JSTEP,ISTEP,JSTP1,JSTM1,ISTP1,ISTM1,J
      3INC,ICUT,ICTP1
      1/GEOM2/IHUB,JHUB,IHBP1,JHBP1,IHBM1,JHBM1,ICON,JCON,ICNP1,JCNF1
C
CHAPTER 1 1 1 1 1 1 ASSEMBLY OF COEFFICIENTS 1 1 1 1 1 1 1 1
C
      DO 100 I=2,NIM1
      DO 101 J=3,NJM1
C-----COMPUTE AREAS AND VOLUME
      AREAN=RCV(J+1)*SEW(I)
      AREAS=RCV(J)*SEW(I)
      AREAEW=RV(J)*SNSV(J)
      VOL=RV(J)*SEW(I)*SNSV(J)
C-----CALCULATE CONVECTION COEFFICIENTS
      GN=0.5*(DEN(I,J+1)+DEN(I,J))*V(I,J+1)
      GP=0.5*(DEN(I,J)+DEN(I,J-1))*V(I,J)
      GS=0.5*(DEN(I,J-1)+DEN(I,J-2))*V(I,J-1)
      GE=0.5*(DEN(I+1,J)+DEN(I,J))*U(I+1,J)
      GSE=0.5*(DEN(I,J-1)+DEN(I+1,J-1))*U(I+1,J-1)
      GW=0.5*(DEN(I,J)+DEN(I-1,J))*U(I,J)
      GSW=0.5*(DEN(I,J-1)+DEN(I-1,J-1))*U(I,J-1)
      CN=0.5*(GN+GP)*AREAN
      CS=0.5*(GP+GS)*AREAS
      CE=0.5*(GE+GSE)*AREAEW
      CW=0.5*(GW+GSW)*AREAEW
C-----CALCULATE DIFFUSION COEFFICIENTS
      VISE=0.25*(VIS(I,J)+VIS(I+1,J)+VIS(I,J-1)+VIS(I+1,J-1))
      VISW=0.25*(VIS(I,J)+VIS(I-1,J)+VIS(I,J-1)+VIS(I-1,J-1))
      DN=VIS(I,J)*AREAN/DYNPV(J)

```

```

      DS=VIS(I,J-1)*AREAS/DYPSV(J)
      DE=VISE*AREAWE/DXEP(I)
      DW=VISW*AREAWE/DXPW(I)
C-----CALCULATE COEFFICIENTS OF SOURCE TERMS
      SMP=CN-CS+CE-CW
      CP=DMAX1(0.0,SMP)
      CPO=CP
C-----ASSEMBLE MAIN COEFFICIENTS
      AN(I,J)=DMAX1(DABS(0.5*CN),DN)-0.5*CN
      AS(I,J)=DMAX1(DABS(0.5*CS),DS)+0.5*CS
      AE(I,J)=DMAX1(DABS(0.5*CE),DE)-0.5*CE
      AW(I,J)=DMAX1(DABS(0.5*CW),DW)+0.5*CW
      DV(I,J)=0.5*(AREAN+AREAS)
      SU(I,J)=CPO*V(I,J)+DV(I,J)*(P(I,J-1)-P(I,J))
      *      +VOL*(DEN(I,J)+DEN(I,J-1))*(W(I,J)+W(I,J-1))**2)/(8.*RV(J))
      SP(I,J)=-CP
      IF(INDCOS.EQ.2) SP(I,J)=SP(I,J)-2.*VIS(I,J)*VOL/RV(J)**2
101 CONTINUE
100 CONTINUE

C
CHAPTER 2 2 2 2 2 2 2 PROBLEM MODIFICATIONS 2 2 2 2 2 2
C
      NCHAP=3
      CALL PROMOD (NCHAP)

C
CHAPTER 3 FINAL COEFF. ASSEMBLY AND RESIDUAL SOURCE CALCULATION 3 3
C
      RESORV=0.0
      DO 300 I=2,NIM1
      DO 301 J=3,NJM1
      AP(I,J)=AN(I,J)+AS(I,J)+AE(I,J)+AW(I,J)-SP(I,J)
      IF(AP(I,J).LT.1E-30) DV(I,J)=0.0
      IF(AP(I,J).LT.1E-30) GO TO 302
      DV(I,J)=DV(I,J)/AP(I,J)
302 RESOR=AN(I,J)*V(I,J+1)+AS(I,J)*V(I,J-1)+AE(I,J)*V(I+1,J)
1      +AW(I,J)*V(I-1,J)-AP(I,J)*V(I,J)+SU(I,J)
      VOL=R(J)*SEW(I)*SNS(J)
      SCRVOL=GREAT*VOL
      IF(-SP(I,J).GT.0.5*SCRVOL) RESOR=0.0
      RESORV=RESORV+DABS(RESOR)
C-----UNDER-RELAXATION
      AP(I,J)=AP(I,J)/URFV
      SU(I,J)=SU(I,J)+(1.-URFV)*AP(I,J)*V(I,J)
      DV(I,J)=DV(I,J)*URFV
301 CONTINUE
300 CONTINUE

C
CHAPTER 4 4 4 SOLUTION OF DIFFERENCE EQUATION 4 4 4 4 4 4
C
      DO 400 N=1,NSWPV
400 CALL LISOLV(2,3,NI,NJ,IT,JT,V,NCHAP)
      RETURN
      END

C

```

[illegible]

[illegible]

C***** SOLUTION OF DIFFERENCE EQUATIONS

C

```
DO 400 N=1, NSWPW
400 CALL LISOLV(2, 2, NI, NJ, IT, JT, W,NCHAP)
RETURN
END
```

C

```
SUBROUTINE CALCP
IMPLICIT REAL*8(A-H,O-Z)
```

C*****

C

CHAPTER 0 0 0 0 0 0 0 0 PRELIMINARIES 0 0 0 0 0 0 0 0

C

COMMON

```
1/PCOR/RESORM,NSWPP,URFP,DU(40,15),DV(40,15),IPREF,JPREF
*/VAR/U(40,15),V(40,15),W(40,15),P(40,15),PP(40,15),TE(40,15),
1ED(40,15),H(40,15),FU(40,15),OF(40,15)
1/ALL/IT,JT,NI,NJ,NIM1,NJM1,GREAT
1/GEOM1/INDCOS,X(40),Y(40),DXEP(40),DXPW(40),DYNP(40),DYPS(40),
1SNS(40),SEW(40),XU(40),YV(40),R(40),RV(40),LABRUPT
1/FLUPR/URFVIS,VISCOS,DENSIT,PRANDT,DEN(40,15),VIS(40,15)
1,OX(40,15),AN2(40,15),T(40,15),RFUP(40,15),RCOP(40,15)
1,CO(40,15),H2O(40,15),H2(40,15),CO2(40,15),FUOLD(40,15),OI(40,15)
1/COEF/AP(40,15),AN(40,15),AS(40,15),AE(40,15),AW(40,15),SU(40,15),
1SP(40,15)
1/GEOM2/IHUB,JHUB,IHBP1,JHBP1,IHBM1,JHBM1,ICON,JCON,ICNP1,JCNP1
1/KASE T1/UIN,TEIN,EDIN,FLOWIN,ALAMDA,
2RSMALL,RLARGE,AL1,AL2,JSTEP,ISTEP,JSTP1,JSTM1,ISTP1,ISTM1,J
3INC,ICUT,ICTP1
RESORM=0.0
```

C

CHAPTER 1 1 1 1 1 1 ASSEMBLY OF COEFFICIENTS 1 1 1 1 1 1 1 1

C

```
DO 100 I=2,NIM1
DO 101 J=2,NJM1
```

C-----COMPUTE AREAS AND VOLUME

```
AREAN=RV(J+1)*SEW(I)
AREAS=RV(J)*SEW(I)
AREAEW=R(J)*SNS(J)
VOL=R(J)*SNS(J)*SEW(I)
```

C-----CALCULATE COEFFICIENTS

```
DENN=0.5*(DEN(I,J)+DEN(I,J+1))
DENS=0.5*(DEN(I,J)+DEN(I,J-1))
DENE=0.5*(DEN(I,J)+DEN(I+1,J))
DENW=0.5*(DEN(I,J)+DEN(I-1,J))
AN(I,J)=DENN*AREAN*DV(I,J+1)
AS(I,J)=DENS*AREAS*DV(I,J)
AE(I,J)=DENE*AREAEW*DU(I+1,J)
AW(I,J)=DENW*AREAEW*DU(I,J)
```

C-----CALCULATE SOURCE TERMS

```
CN=DENN*V(I,J+1)*AREAN
CS=DENS*V(I,J)*AREAS
CE=DENE*U(I+1,J)*AREAEW
CW=DENW*U(I,J)*AREAEW
```

```

      SMP=CN-CS+CE-CW
      SP(I,J)=0.0
      SU(I,J)=-SMP
C-----COMPUTE SUM OF ABSOLUTE SOURCES
      RESORM=RESORM+DABS(SMP)
      101 CONTINUE
      100 CONTINUE
C
CHAPTER  2  2  2  2  2  2  2  PROBLEM MODIFICATIONS  2  2  2  2  2  2
C
      NCHAP=4
      CALL PROMOD (NCHAP)
C
CHAPTER  3  3  3  3  3  FINAL COEFFICIENT ASSEMBLY  3  3  3  3  3  3
C
      DO 300 I=2,NIM1
      DO 301 J=2,NJM1
      301 AP(I,J)=AN(I,J)+AS(I,J)+AE(I,J)+AW(I,J)-SP(I,J)
      300 CONTINUE
C
CHAPTER  4  4  4  4  4  SOLUTION OF DIFFERENCE EQUATIONS  4  4  4  4  4
C
      DO 400 N=1,NSWPP
      400 CALL LISOLV(2,2,NI,NJ,IT,JT,PP,NCHAP)
C
CHAPTER  5  5  5  5  5  CORRECT VELOCITIES AND PRESSURE  5  5  5  5  5
C
C-----VELOCITIES
      JFIN=JSTEP
      DO 500 I=2,NIM1
      JSTA=2
      IF(I.LE.IHUB) JSTA=JHUB
      IF(I.LT.ISTEP) JFIN=JSTEP
      IF(I.GE.ISTEP.AND.I.LE.ICUT) JFIN=JFIN+JINC
      IF(I.GT.ICUT) JFIN=NJM1
      IF(I.GT.ICON) JFIN=JCON
      DO 500 J=JSTA,JFIN
      500 IF(I.NE.2) U(I,J)=U(I,J)+DU(I,J)*(PP(I-1,J)-PP(I,J))
      JFIN=JSTEP
      DO 501 I=2,NIM1
      JSTA=2
      IF(I.LT.IHUB) JSTA=JHBP1
      IF(I.LT.ISTEP) JFIN=JSTEP
      IF(I.GE.ISTEP.AND.I.LE.ICUT) JFIN=JFIN+JINC
      IF(I.GT.ICUT) JFIN=NJM1
      IF(I.GT.ICON) JFIN=JCON
      DO 501 J=JSTA,JFIN
      501 IF(J.NE.2) V(I,J)=V(I,J)+DV(I,J)*(PP(I,J-1)-PP(I,J))
C-----PRESSURE (WITH PROVISION FOR UNDER-RELAXATION)
      PPRF=PP(IPREF,JPREF)
      JFIN=JSTEP
      DO 502 I=2,NIM1
      JSTA=2
      IF(I.LT.IHUB) JSTA=JHUB

```



```

      IF(I.LT.ISTEP) JFIN=JSTEP
      IF(I.GE.ISTEP.AND.I.LE.ICUT) JFIN=JFIN+JINC
      IF(I.GT.ICUT) JFIN=NJM1
      IF(I.GT.ICON) JFIN=JCON
      DO 503 J=JSTA,JFIN
      P(I,J)=P(I,J)+URFP*(PP(I,J)-PPREF)
      PP(I,J)=0.0
503  CONTINUE
502  CONTINUE
      RETURN
      END
C
      SUBROUTINE CALCTE
      IMPLICIT REAL*8(A-H,O-Z)
C*****
C
CHAPTER 0 0 0 0 0 0 0 PRELIMINARIES 0 0 0 0 0 0 0
C
      COMMON
      1/TENDIS/RESORK,NSWPK,URFK,RESORE,NSWPD,URFE
      */VAR/U(40,15), V(40,15), W(40,15), P(40,15), PP(40,15), TE(40,15),
      1ED(40,15),H(40,15),FU(40,15),OF(40,15)
      1/ALL/IT,JT,NI,NJ,NIM1,NJM1,GREAT
      1/GEOM1/INDCOS,X(40),Y(40),DXEP(40),DXPW(40),DYNP(40),DYPS(40),
      1      SNS(40),SEW(40),XU(40),YV(40),R(40),RV(40),LABRUFT
      1/FLUPR/URFVIS,VISCOS,DENSIT,PRANDT,DEN(40,15),VIS(40,15)
      1      ,OX(40,15),AN2(40,15),T(40,15),RFUP(40,15),RCOP(40,15)
      1,CO(40,15),H2O(40,15),H2(40,15),CO2(40,15),FUOLD(40,15),OI(40,15)
      1/COEF/AP(40,15),AN(40,15),AS(40,15),AE(40,15),AW(40,15),SU(40,15),
      1      SP(40,15)
      1/TURB/GEN(40,15),CD,CMU,C1,C2,CAPPA,ELOG,PRED,PRTE
      1/WALLF/YPLUSN(40),XPLUSW(40),TAUN(40),TAUW(40)
      1      ,TAUE(40),TAUS(40),YPLUSS(40),XPLUSE(40)
      1/KASE T1/UIN,TEIN,EDIN,FLOWIN,ALAMDA,
      2      RSMALL,RLARGE,AL1,AL2,JSTEP,ISTEP,JSTP1,JSTM1,ISTP1,ISTM1,J
      3INC,ICUT,ICTP1
      1/SUSP/SUKD(40,15),SPKD(40,15)
      1/GEOM2/IHUB,JHUB,IHBP1,JHBP1,IHBM1,JHBM1,ICON,JCON,ICNP1,JCNP1
C
CHAPTER 1 1 1 1 1 1 ASSEMBLY OF COEFFICIENTS 1 1 1 1 1 1
C
      PRTE=1.0
      DO 100 I=2,NIM1
      DO 101 J=2,NJM1
      IF((I.LT.IHUB.AND.J.LT.JHUB).OR.(I.LT.ISTEP.AND.J.GT.JSTEP))
      1GO TO 101
C-----COMPUTE AREAS AND VOLUME
      AREAN=RV(J+1)*SEW(I)
      AREAS=RV(J)*SEW(I)
      AREAEW=R(J)*SNS(J)
      VOL=R(J)*SNS(J)*SEW(I)
C-----CALCULATE CONVECTION COEFFICIENTS
      GN=0.5*(DEN(I,J)+DEN(I,J+1))*V(I,J+1)
      GS=0.5*(DEN(I,J)+DEN(I,J-1))*V(I,J)

```

```

GE=0.5*(DEN(I,J)+DEN(I+1,J))*U(I+1,J)
GW=0.5*(DEN(I,J)+DEN(I-1,J))*U(I,J)
CN=GN*AREAN
CS=GS*AREAS
CE=GE*AREAEW
CW=GW*AREAEW
C-----CALCULATE DIFFUSION COEFFICIENTS
GAMN=0.5*(VIS(I,J)+VIS(I,J+1))/PRTE
GAMS=0.5*(VIS(I,J)+VIS(I,J-1))/PRTE
GAME=0.5*(VIS(I,J)+VIS(I+1,J))/PRTE
GAMW=0.5*(VIS(I,J)+VIS(I-1,J))/PRTE
DN=GAMN*AREAN/DYNP(J)
DS=GAMS*AREAS/DYPS(J)
DE=GAME*AREAEW/DXEP(I)
DW=GAMW*AREAEW/DXPW(I)
C-----SOURCE TERMS
SMP=CN-CS+CE-CW
CP=DMAX1(0.0,SMP)
CPO=CP
DUDX=(U(I+1,J)-U(I,J))/SEW(I)
DV DY=(V(I,J+1)-V(I,J))/SNS(J)
DUDY=((U(I,J)+U(I+1,J)+U(I,J+1)+U(I+1,J+1))/4.-(U(I,J)+U(I+1,J)+
1U(I,J-1)+U(I+1,J-1))/4.)/SNS(J)
DV DX=((V(I,J)+V(I,J+1)+V(I+1,J)+V(I+1,J+1))/4.-(V(I,J)+V(I,J+1)+V(
1I-1,J)+V(I-1,J+1))/4.)/SEW(I)
DWDR=(W(I,J+1)-W(I,J-1))/(DYNP(J)+DYPS(J))-W(I,J)/R(J)
DWDX=(W(I+1,J)-W(I-1,J))/(DXPW(I)+DXEP(I))
GEN(I,J)=(2.*(DUDX**2+DV DY**2)+(DUDY+DV DX)**2)*VIS(I,J)
IF(INDCOS.EQ.2) GEN(I,J)=GEN(I,J)+VIS(I,J)*(DWDR**2+DWDX**2)
IF(J.GT.2) VDR=V(I,J)/RV(J)
IF(J.EQ.2) VDR=0.0
IF(INDCOS.EQ.2) GEN(I,J)=GEN(I,J)+2.*VIS(I,J)*0.5*(VDR+V(I,J+1)/
1RV(J+1))**2
C-----ASSEMBLE MAIN COEFFICIENTS
AN(I,J)=DMAX1(DABS(0.5*CN),DN)-0.5*CN
AS(I,J)=DMAX1(DABS(0.5*CS),DS)+0.5*CS
AE(I,J)=DMAX1(DABS(0.5*CE),DE)-0.5*CE
AW(I,J)=DMAX1(DABS(0.5*CW),DW)+0.5*CW
SU(I,J)=CPO*TE(I,J)
SUKD(I,J)=SU(I,J)
SU(I,J)=SU(I,J)+GEN(I,J)*VOL
SP(I,J)=-CP
SPKD(I,J)=SP(I,J)
SP(I,J)=SP(I,J)-CD*CMU*DEN(I,J)**2*TE(I,J)*VOL/VIS(I,J)
101 CONTINUE
100 CONTINUE
C
CHAPTER 2 2 2 2 2 2 PROBLEM MODIFICATIONS 2 2 2 2 2 2
C
NCHAP=6
CALL PROMOD (NCHAP)
C
CHAPTER 3 FINAL COEFFICIENT ASSEMBLY AND RESIDUAL SOURCE CALCULATION 3
C

```

```

RESORK=0.0
DO 300 I=2,NIM1
DO 301 J=2,NJM1
AP(I,J)=AN(I,J)+AS(I,J)+AE(I,J)+AW(I,J)-SP(I,J)
RESOR=AN(I,J)*TE(I,J+1)+AS(I,J)*TE(I,J-1)+AE(I,J)*TE(I+1,J)
1      +AW(I,J)*TE(I-1,J)-AP(I,J)*TE(I,J)+SU(I,J)
VOL=R(J)*SEW(I)*SNS(J)
SORVOL=GREAT*VOL
IF(-SP(I,J).GT.0.5*SORVOL)RESOR=0.0
RESORK=RESORK+DABS(RESOR)
C-----UNDER-RELAXATION
AP(I,J)=AP(I,J)/URFK
SU(I,J)=SU(I,J)+(1.-URFK)*AP(I,J)*TE(I,J)
301 CONTINUE
300 CONTINUE
C
CHAPTER 4 4 4 4 4 SOLUTION OF DIFFERENCE EQUATIONS 4 4 4 4 4
C
DO 400 N=1,NSWPK
400 CALL LISOLV(2,2,NI,NJ,IT,JT,TE,NCHAP)
RETURN
END
C
SUBROUTINE CALCED
IMPLICIT REAL*8(A-H,O-Z)
C*****
C
CHAPTER 0 0 0 0 0 0 0 PRELIMINARIES 0 0 0 0 0 0 0
C
COMMON
1/TENDIS/RESORK,NSWPK,URFK,RESORE,NSWPD,URFE
1/ALL/IT,JT,NI,NJ,NIM1,NJM1,GREAT
1/GEOM1/INDCOS,X(40),Y(40),DXEP(40),DXPW(40),DYNP(40),DYPS(40),
1      SNS(40),SEW(40),XU(40),YV(40),R(40),RV(40),LABRUPT
1/GEOM2/IHUB,JHUB,IHBP1,JHBP1,IHBM1,JHBM1,ICON,JCON,ICNP1,JCNP1
1/FLUPR/URFVIS,VISCOS,DENSIT,PRANDT,DEN(40,15),VIS(40,15)
1      ,OX(40,15),AN2(40,15),T(40,15),RFUP(40,15),RCOP(40,15)
1,CO(40,15),H2O(40,15),H2(40,15),CO2(40,15),FUOLD(40,15),O1(40,15)
1/COEF/AP(40,15),AN(40,15),AS(40,15),AE(40,15),AW(40,15),SU(40,15),
1      SP(40,15)
*/VAR/U(40,15),V(40,15),W(40,15),P(40,15),PP(40,15),TE(40,15),
1ED(40,15),H(40,15),FU(40,15),OF(40,15)
1/TURB/GEN(40,15),CD,CMU,C1,C2,CAPPA,ELOG,PRED,PRTE
1/WALLF/YPLUSN(40),XPLUSW(40),TAUN(40),TAUW(40)
1      ,TAUE(40),TAUS(40),YPLUSS(40),XPLUSE(40)
1/SUSP/SUKD(40,15),SPKD(40,15)
1/KASE T1/UIN,TEIN,EDIN,FLOWIN,ALAMDA,
2      RSMALL,RLARGE,AL1,AL2,JSTEP,ISTEP,JSTP1,JSTM1,ISTP1,ISTM1,J
3INC,ICUT,ICTP1
C
CHAPTER 1 1 1 1 1 1 ASSEMBLY OF COEFFICIENTS 1 1 1 1 1 1
C
JEND=JSTEP
DO 100 I=2,NIM1

```

```

      IF(I .GE. ISTEP .AND. I .LE. ICUT) JEND=JEND+JINC
      DO 101 J=2, JEND
      IF((I.LT.IHUB.AND.J.LT.JHUB).OR.(I.LT.ISTEP.AND.J.GT.JSTEP))
1GO TO 101
C-----COMPUTE AREAS AND VOLUME
      AREAN=RV(J+1)*SEW(I)
      AREAS=RV(J)*SEW(I)
      AREAEW=R(J)*SNS(J)
      VOL=R(J)*SNS(J)*SEW(I)
C-----CALCULATE CONVECTION COEFFICIENTS
      GN=0.5*(DEN(I,J)+DEN(I,J+1))*V(I,J+1)
      GS=0.5*(DEN(I,J)+DEN(I,J-1))*V(I,J)
      GE=0.5*(DEN(I,J)+DEN(I+1,J))*U(I+1,J)
      GW=0.5*(DEN(I,J)+DEN(I-1,J))*U(I,J)
      CN=GN*AREAN
      CS=GS*AREAS
      CE=GE*AREAEW
      CW=GW*AREAEW
C-----CALCULATE DIFFUSION COEFFICIENTS
      GAMN=0.5*(VIS(I,J)+VIS(I,J-1))/PRED
      GAMS=0.5*(VIS(I,J)+VIS(I,J+1))/PRED
      GAME=0.5*(VIS(I,J)+VIS(I+1,J))/PRED
      GAMW=0.5*(VIS(I,J)+VIS(I-1,J))/PRED
      DN=GAMN*AREAN/DYNP(J)
      DS=GAMS*AREAS/DYPS(J)
      DE=GAME*AREAEW/DXEP(I)
      DW=GAMW*AREAEW/DXPW(I)
C-----SOURCE TERMS
      SMP=CN-CS+CE-CW
      CP=DMAX1(0.0,SMP)
      CPO=CP
C-----ASSEMBLE MAIN COEFFICIENTS
      AN(I,J)=DMAX1(DABS(0.5*CN),DN)-0.5*CN
      AS(I,J)=DMAX1(DABS(0.5*CS),DS)+0.5*CS
      AE(I,J)=DMAX1(DABS(0.5*CE),DE)-0.5*CE
      AW(I,J)=DMAX1(DABS(0.5*CW),DW)+0.5*CW
      SU(I,J)=CPO*ED(I,J)
      SUKD(I,J)=SU(I,J)
      SU(I,J)=SU(I,J)+C1*CMU*GEN(I,J)*VOL*DEN(I,J)*TE(I,J)/VIS(I,J)
      SP(I,J)=-CP
      SPKD(I,J)=SP(I,J)
      SP(I,J)=SP(I,J)-C2*DEN(I,J)*ED(I,J)*VOL/TE(I,J)
101 CONTINUE
100 CONTINUE
C
CHAPTER 2 2 2 2 2 2 PROBLEM MODIFICATIONS 2 2 2 2 2 2
C
      NCHAP=7
      CALL PROMOD (NCHAP)
C
CHAPTER 3 FINAL COEFFICIENT ASSEMBLY AND RESIDUAL SOURCE CALCULATION 3
C
      RESORE=0.0
      DO 300 I=2,NIM1

```

```

DO 301 J=2,NJM1
AP(I,J)=AN(I,J)+AS(I,J)+AE(I,J)+AW(I,J)-SP(I,J)
RESOR=AN(I,J)*ED(I,J+1)+AS(I,J)*ED(I,J-1)+AE(I,J)*ED(I+1,J)
1      +AW(I,J)*ED(I-1,J)-AP(I,J)*ED(I,J)+SU(I,J)
VOL=R(J)*SNS(J)*SEW(I)
SORVOL=GREAT*VOL
IF(-SP(I,J).GT.0.5*SORVOL) RESOR=0.0
RESORE=RESORE+DABS(RESOR)
C-----UNDER-RELAXATION
AP(I,J)=AP(I,J)/URFE
SU(I,J)=SU(I,J)+(1.-URFE)*AP(I,J)*ED(I,J)
301 CONTINUE
300 CONTINUE
C
CHAPTER 4 4 4 4 4 SOLUTION OF DIFFERENCE EQUATIONS 4 4 4 4 4
C
DO 400 N=1,NSWPD
400 CALL LISOLV(2,2,NI,NJ,IT,JT,ED,NCHAP)
RETURN
END
C
SUBROUTINE CALCH(INCLRX)
IMPLICIT REAL*8(A-H,O-Z)
C
CHAPTER 0 0 0 0 0 0 PRELIMINARIES 0 0 0 0 0 0 0 0 0
C
COMMON
C
1/SWEN/PRW,WWALL,RESORH,NSWPH,URFH,PRH,TWALL
*/VAR/U(40,15),V(40,15),W(40,15),P(40,15),PP(40,15),TE(40,15),
1ED(40,15),H(40,15),FU(40,15),OF(40,15)
1/FLUPR/URFVIS,VISCOS,DENSIT,PRANDT,DEN(40,15),VIS(40,15)
1      ,OX(40,15),AN2(40,15),T(40,15),RFUP(40,15),RCOP(40,15)
1,CO(40,15),H2O(40,15),H2(40,15),CO2(40,15),FUOLD(40,15),O1(40,15)
1/COEF/AP(40,15),AN(40,15),AS(40,15),AE(40,15),AW(40,15),SU(40,15),
1      SP(40,15)
1/ALL/IT,JT,NI,NJ,NIM1,NJM1,GREAT
1/GEOM1/INDCOS,X(40),Y(40),DXEP(40),DXPW(40),DYNP(40),DYPS(40),
1      SNS(40),SEW(40),XU(40),YV(40),R(40),RV(40),LABRUPT
1/GEOM2/IHUB,JHUB,IHBP1,JHBP1,IHBM1,JHBM1,ICON,JCON,ICNP1,JCNP1
1/CHEM/URFDEN,GASCON,CFU,COX,CPR,WFU,WOX,WPR,HFU,HCO,OXDFU,PRESS
1,CCO,CCO2,CH2O,CAN2,RESORC,NSWPC,URFCO,PRCO,OXDCO,OXDFU1,WCO
1,WH2O,WCO2,WAN2,PERSTO,WH2,CH2,W01,CO1
1/KASE T1/UIN,TEIN,EDIN,FLOWIN,ALAMDA,
2      RSMALL,RLARGE,AL1,AL2,JSTEP,ISTEP,JSTP1,JSTM1,ISTP1,ISTM1,J
3JNC,ICUT,ICTP1
1/RADT/RADX(40,15),RADR(40,15),RADIN
2      ,EMIW,NSWPRX,NSWPRR,URFRX,URFRR,SIGMA,ABSOR,SCATT
LOGICAL INCLRX
C
CHAPTER 1 1 1 1 1 1 1 ASSEMBLY OF COEFFICIENTS 1 1 1 1 1 1
C
DO 100 I=2,NIM1
DO 101 J=2,NJM1

```

```

C-----COMPUTE AREAS AND VOLUME
  AREAN=RV(J+1)*SEW(I)
  AREAS=RV(J)*SEW(I)
  AREAEW=0.5*(RV(J+1)+RV(J))*SNS(J)
  VOL=R(J)*SNS(J)*SEW(I)
C-----CALCULATE CONVECTION COEFFICIENTS
  GN=0.5*(DEN(I,J)+DEN(I,J+1))*V(I,J+1)
  GS=0.5*(DEN(I,J)+DEN(I,J-1))*V(I,J)
  GE=0.5*(DEN(I,J)+DEN(I+1,J))*U(I+1,J)
  GW=0.5*(DEN(I,J)+DEN(I-1,J))*U(I,J)
  CN=GN*AREAN
  CS=GS*AREAS
  CE=GE*AREAEW
  CW=GW*AREAEW
C-----CALCULATE DIFFUSION COEFFICIENTS
  GAMN=0.5*(VIS(I,J)+VIS(I,J+1))/PRH
  GAMS=0.5*(VIS(I,J)+VIS(I,J-1))/PRH
  GAME=0.5*(VIS(I,J)+VIS(I+1,J))/PRH
  GAMW=0.5*(VIS(I,J)+VIS(I-1,J))/PRH
  DN=GAMN*AREAN/DYNP(J)
  DS=GAMS*AREAS/DYPS(J)
  DE=GAME*AREAEW/DXEP(I)
  DW=GAMW*AREAEW/DXPW(I)
C-----SOURCE TERMS
  SMP=CN-CS+CE-CW
  CP=DMAX1(0.0,SMP)
  CPO=CP
C-----ASSEMBLE MAIN COEFFICIENTS
  AN(I,J)=DMAX1(DABS(0.5*CN),DN)-0.5*CN
  AS(I,J)=DMAX1(DABS(0.5*CS),DS)+0.5*CS
  AE(I,J)=DMAX1(DABS(0.5*CE),DE)-0.5*CE
  AW(I,J)=DMAX1(DABS(0.5*CW),DW)+0.5*CW
  SU(I,J)=CPO*H(I,J)
  IF(.NOT.INCLRX)GO TO 90
  SU(I,J)=CPO*H(I,J)+2.*ABSOR*(RADX(I,J)+RADR(I,J)-2.*SIGMA*
  1T(I,J)**4.)*VOL
  90 CONTINUE
  SP(I,J)=-CP
  101 CONTINUE
  100 CONTINUE
C
CHAPTER 2 2 2 2 2 2 PROBLEM MODIFICATIONS 2 2 2 2 2 2 2
C
  NCHAP=5
  CALL PROMOD (NCHAP)
C
CHAPTER 3 FINAL COEFFICIENT ASSEMBLY AND RESIDUAL SOURCE CALCULATION 3
C
  RESORH=0.0
  DO 300 I=2,NIM1
  DO 301 J=2,NJM1
    AP(I,J)=AN(I,J)+AS(I,J)+AE(I,J)+AW(I,J)-SP(I,J)
    RESOR=AN(I,J)*H(I,J+1)+AS(I,J)*H(I,J-1)+AE(I,J)*H(I+1,J)
    1 +AW(I,J)*H(I-1,J)-AP(I,J)*H(I,J)+SU(I,J)

```

```

      VOL=R(J)*SNS(J)*SEW(I)
      SORVOL=GREAT*VOL
      IF(-SP(I,J).GT.0.5*SORVOL) RESOR=0.0
      RESORH=RESORH+DABS(RESOR)
C-----UNDER-RELAXATION
      AP(I,J)=AP(I,J)/URFH
      SU(I,J)=SU(I,J)+(1.-URFH)*AP(I,J)*H(I,J)
      301 CONTINUE
      300 CONTINUE
C
CHAPTER 4 4 4 4 4 SOLUTION OF DIFFERENCE EQUATIONS 4 4 4 4 4
C
      DO 400 N=1,NSWPH
      400 CALL LISOLV(2,2,NI,NJ,IT,JT,H,NCHAP)
      RETURN
      END
C
      SUBROUTINE CALCFU
      IMPLICIT REAL*8(A-H,O-Z)
C
CHAPTER 0 0 0 0 0 0 PRELIMINARIES 0 0 0 0 0 0 0 0 0
C
      COMMON
C
      1/FUOF/RESORF,NSWPF,URFF,PRFU,FUWALL,RESORO,NSWPO,URFO,PROF,OFWALL
      */VAR/U(40,15), V(40,15), W(40,15), P(40,15), PP(40,15), TE(40,15),
      1ED(40,15),H(40,15),FU(40,15),OF(40,15)
      1/FLUPR/URFVIS,VISCOS,DENSIT,PRANDT,DEN(40,15),VIS(40,15)
      1 ,OX(40,15),AN2(40,15),T(40,15),RFUP(40,15),RCOP(40,15)
      1,CO(40,15),H2O(40,15),H2(40,15),CO2(40,15),FUOLD(40,15),O1(40,15)
      1/COEF/AP(40,15),AN(40,15),AS(40,15),AE(40,15),AW(40,15),SU(40,15),
      1 SP(40,15)
      1/ALL/IT,JT,NI,NJ,NIM1,NJM1,GREAT
      1/GEOM1/INDCOS,X(40),Y(40),DXEP(40),DXPW(40),DYNP(40),DYPS(40),
      1 SNS(40),SEW(40),XU(40),YV(40),R(40),RV(40),LABRUPT
      1/GEOM2/IHUB,JHUB,IHBP1,JHBP1,IHBM1,JHBM1,ICON,JCON,ICNP1,JCNP1
      1/CHEM/URFDEN,GASCON,CFU,COX,CPR,WFU,WOX,WPR,HFU,HCO,OXDFU,PRESS
      1,CCO,CCO2,CH2O,CAN2,RESORC,NSWPC,URFCO,PRCO,OXDCO,OXDFU1,WCO
      1,WH2O,WCO2,WAN2,PERSTO,WH2,CH2,W01,CO1
      1/CHEM2/FUIN,AX,AY,AO
      1/REAC/RFUEBU(40,15),RFUARR(40,15),NITER,RCOARR(40,15)
      1,RCOEBU(40,15)
      1/KASE T1/UIN,TEIN,EDIN,FLOWIN,ALAMDA,
      2 RSMALL,RLARGE,AL1,AL2,JSTEP,ISTEP,JSTP1,JSTM1,ISTP1,ISTM1,J
      3INC,ICUT,ICTP1
C
      DIMENSION RT(40,15)
      FITER=DMAX1(0.,DMIN1(1.,1.5-FLOAT(NITER)/50.))
C
CHAPTER 1 1 1 1 1 1 1 ASSEMBLY OF COEFFOCOENTS 1 1 1 1 1 1
C
      JFIN=JSTEP
      DO 100 I=2,NIM1
      DO 101 J=2,NJM1

```

```

C-----COMPUTE AREAS AND VOLUME
  AREAN=RV(J+1)*SEW(I)
  AREAS=RV(J)*SEW(I)
  AREAEW=R(J)*SNS(J)
  VOL=AREAEW*SEW(I)
C-----CALCULATE CONVECTION COEFFICIENTS
  GN=0.5*(DEN(I,J)+DEN(I,J+1))*V(I,J+1)
  GS=0.5*(DEN(I,J)+DEN(I,J-1))*V(I,J)
  GE=0.5*(DEN(I,J)+DEN(I+1,J))*U(I+1,J)
  GW=0.5*(DEN(I,J)+DEN(I-1,J))*U(I,J)
  CN=GN*AREAN
  CS=GS*AREAS
  CE=GE*AREAEW
  CW=GW*AREAEW
C-----CALCULATE DIFFUSION COEFFICIENTS
  GAMN=0.5*(VIS(I,J)+VIS(I,J+1))/PRFU
  GAMS=0.5*(VIS(I,J)+VIS(I,J-1))/PRFU
  GAME=0.5*(VIS(I,J)+VIS(I+1,J))/PRFU
  GAMW=0.5*(VIS(I,J)+VIS(I-1,J))/PRFU
  DN=GAMN*AREAN/DYNP(J)
  DS=GAMS*AREAS/DYPS(J)
  DE=GAME*AREAEW/DXEP(I)
  DW=GAMW*AREAEW/DXPW(I)
C-----SOURCE TERMS
  SMP=CN-CS+CE-CW
  CP=DMAX1(0.0,SMP)
  CPO=CP
C-----ASSEMBLE MAIN COEFFICIENTS
  AN(I,J)=DMAX1(DABS(0.5*CN),DN)-0.5*CN
  AS(I,J)=DMAX1(DABS(0.5*CS),DS)+0.5*CS
  AE(I,J)=DMAX1(DABS(0.5*CE),DE)-0.5*CE
  AW(I,J)=DMAX1(DABS(0.5*CW),DW)+0.5*CW
  SU(I,J)=CPO*FU(I,J)
  SP(I,J)=-CP
  IF (NITER.LT.25) RT(I,J)=T(I,J)
  IF (HFU.EQ.0.0) GO TO 102
  IF (I.LT.ISTEP) GO TO 102
  IF (FU(I,J).LT.1E-8.OR.OX(I,J).LT.1E-8) GO TO 102
C-----SOURCE TERM FOR RFU = CONSUMPTION OF FUEL
C-----ARRHENIUS MODEL
  TEMP=T(I,J)
  IF (NITER.GE.50) GO TO 104
  IF (I.NE.IHUB) GO TO 104
  IF (J.NE.(JHUB+2)) GO TO 104
  RT(I,J)=0.8*RT(I,J)+400.
  IF (TEMP.LT.RT(I,J)) TEMP=FITER*RT(I,J)+(1.-FITER)*TEMP
104 CONTINUE
  IF (TEMP.LT.400) GO TO 10
  RFUARR(I,J)=3.3E+14*DEN(I,J)**1.5*OX(I,J)*DSQRT(FU(I,J))*
  1DEXP(-27000/TEMP)
  GO TO 11
10    RFUARR(I,J)=0.0
11    CONTINUE
C-----EDDY-BREAK-UP MODEL

```



```

      RFUEBU(I,J)=3.0*DEN(I,J)*FU(I,J)*ED(I,J)/TE(I,J)
      RFUP(I,J)=DMIN1(RFUARR(I,J),RFUEBU(I,J))
      SP(I,J)=SP(I,J)-RFUP(I,J)*VOL/FU(I,J)
102 CONTINUE
101 CONTINUE
100 CONTINUE
C
CHAPTER 2 2 2 2 2 2 2 PROBLEM MODIFICATIONS 2 2 2 2 2 2
C
      NCHAP=9
      CALL PROMOD(NCHAP)
C
CHAPTER 3 FINAL COEFFICIENT ASSEMBLY AND RESIDUAL SOURCE CALCULATION 3
C
      RESORF=0.0
      DC 300 I=2,NIM1
      DO 301 J=2,NJM1
      AP(I,J)=AN(I,J)+AS(I,J)+AE(I,J)+AW(I,J)-SP(I,J)
      RESOR=AN(I,J)*FU(I,J+1)+AS(I,J)*FU(I,J-1)+AE(I,J)*FU(I+1,J)
1      +AW(I,J)*FU(I-1,J)-AP(I,J)*FU(I,J)+SU(I,J)
      VOL=R(J)*SNS(J)*SEW(I)
      SORVOL=GREAT*VOL
      IF(-SP(I,J).GT.0.5*SORVOL) RESOR=0.0
      RESORF=RESORF+DABS(RESOR)
C-----UNDER-RELAXATION
      AP(I,J)=AP(I,J)/URFF
      SU(I,J)=SU(I,J)+(1.-URFF)*AP(I,J)*FU(I,J)
301 CONTINUE
300 CONTINUE
C
CHAPTER 4 4 4 4 4 4 SOLUTION OF DIFFERENCE EQUATION 4 4 4 4
C
      DO 400 N=1,NSWPF
400 CALL LISOLV(2,2,NI,NJ,IT,JT,FU,NCHAP)
      RETURN
      END
C
      SUBROUTINE CALCOF
      IMPLICIT REAL*8(A-H,O-Z)
C
CHAPTER 0 0 0 0 0 0 0 PRELIMINARIES 0 0 0 0 0 0 0 0
C
      COMMON
C
1/FUOF/RESORF,NSWPF,URFF,PRFU,FUWALL,RESORO,NSWPO,URFO,PROF,OFWALL
*/VAR/U(40,15),V(40,15),W(40,15),P(40,15),PP(40,15),TE(40,15),
1ED(40,15),H(40,15),FU(40,15),OF(40,15)
1/FLUPR/URFVIS,VISCOS,DENSIT,PRANDT,DEN(40,15),VIS(40,15)
1,OX(40,15),AN2(40,15),T(40,15),RFUP(40,15),RCOF(40,15)
1,CO(40,15),H2O(40,15),H2(40,15),CO2(40,15),FUOLD(40,15),O1(40,15)
1/COEF/AP(40,15),AN(40,15),AS(40,15),AE(40,15),AW(40,15),SU(40,15),
1 SP(40,15)
1/ALL/IT,JT,NI,NJ,NIM1,NJM1,GREAT
1/GEOM1/INDCOS,X(40),Y(40),DXEP(40),DXPW(40),DYNP(40),DYPS(40),

```

```

1      SNS(40),SEW(40),XU(40),YV(40),R(40),RV(40),LABRUPT
1/GEOM2/IHUB,JHUB,IHBP1,JHBP1,IHBM1,JHBM1,ICON,JCON,ICNP1,JCNP1
1/KASE T1/UIN,TEIN,EDIN,FLOWIN,ALAMDA,
2      RSMALL,RLARGE,AL1,AL2,JSTEP,ISTEP,JSTP1,JSTM1,ISTP1,ISTM1,J
3INC,ICUT,ICTP1
C
CHAPTER 1 1 1 1 1 1 1 ASSEMBLY OF COEFFOCOENTS 1 1 1 1 1 1
C
      DO 100 I=2,NIM1
      DO 101 J=2,NJM1
C-----COMPUTE AREAS AND VOLUME
      AREAN=RV(J+1)*SEW(I)
      AREAS=RV(J)*SEW(I)
      AREAEW=R(J)*SNS(J)
      VOL=AREAEW*SEW(I)
C-----CALCULATE CONVECTION COEFFICIENTS
      GN=0.5*(DEN(I,J)+DEN(I,J+1))*V(I,J+1)
      GS=0.5*(DEN(I,J)+DEN(I,J-1))*V(I,J)
      GE=0.5*(DEN(I,J)+DEN(I+1,J))*U(I+1,J)
      GW=0.5*(DEN(I,J)+DEN(I-1,J))*U(I,J)
      CN=GN*AREAN
      CS=GS*AREAS
      CE=GE*AREAEW
      CW=GW*AREAEW
C-----CALCULATE DIFFUSION COEFFICIENTS
      GAMN=0.5*(VIS(I,J)+VIS(I,J+1))/PROF
      GAMS=0.5*(VIS(I,J)+VIS(I,J-1))/PROF
      GAME=0.5*(VIS(I,J)+VIS(I+1,J))/PROF
      GAMW=0.5*(VIS(I,J)+VIS(I-1,J))/PROF
      DN=GAMN*AREAN/DYNP(J)
      DS=GAMS*AREAS/DYPS(J)
      DE=GAME*AREAEW/DXEP(I)
      DW=GAMW*AREAEW/DXPW(I)
C-----SOURCE TERMS
      SMP=CN-CS+CE-CW
      CP=DMAX1(0.0,SMP)
      CPO=CP
C-----ASSEMBLE MAIN COEFFICIENTS
      AN(I,J)=DMAX1(DABS(0.5*CN),DN)-0.5*CN
      AS(I,J)=DMAX1(DABS(0.5*CS),DS)+0.5*CS
      AE(I,J)=DMAX1(DABS(0.5*CE),DE)-0.5*CE
      AW(I,J)=DMAX1(DABS(0.5*CW),DW)+0.5*CW
      SU(I,J)=CPO*OF(I,J)
      SP(I,J)=-CP
101 CONTINUE
100 CONTINUE
C
CHAPTER 2 2 2 2 2 2 2 PROBLEM MODIFICATIONS 2 2 2 2 2 2
C
      NCHAP=10
      CALL PROMOD(NCHAP)
C
CHAPTER 3 FINAL COEFFICIENT ASSEMBLY AND RESIDUAL SOURCE CALCULATION 3
C

```

```

RESORO=0.0
DO 300 I=2,NIM1
DO 301 J=2,NJM1
AP(I,J)=AN(I,J)+AS(I,J)+AE(I,J)+AW(I,J)-SP(I,J)
RESOR=AN(I,J)*OF(I,J+1)+AS(I,J)*OF(I,J-1)+AE(I,J)*OF(I+1,J)
1      +AW(I,J)*OF(I-1,J)-AP(I,J)*OF(I,J)+SU(I,J)
AREAEW=R(J)*SNS(J)
VOL=AREAEW*SEW(I)
SORVOL=GREAT*VOL
IF(-SP(I,J).GT.0.5*SORVOL) RESOR=0.0
RESORO=RESORO+DABS(RESOR)
C-----UNDER-RELAXATION
AP(I,J)=AP(I,J)/URFO
SU(I,J)=SU(I,J)+(1.-URFO)*AP(I,J)*OF(I,J)
301 CONTINUE
300 CONTINUE
C
CHAPTER 4 4 4 4 4 4 SOLUTION OF DIFFERENCE EQUATION 4 4 4 4 4
C
DO 400 N=1,NSWPO
400 CALL LISOLV(2,2,NI,NJ,IT,JT,OF,NCHAP)
RETURN
END
C
SUBROUTINE CALCRX
IMPLICIT REAL*8(A-H,O-Z)
C
CHAPTER 0 0 0 0 0 0 PRELIMINARIES 0 0 0 0 0 0 0 0 0
C
COMMON
C
1/SWEN/PRW,WWALL,RESORH,NSWPH,URFH,PRH,TWALL
*/VAR/U(40,15), V(40,15), W(40,15), P(40,15), PP(40,15), TE(40,15),
1ED(40,15),H(40,15),FU(40,15),OF(40,15)
1/FLUPR/URFVIS,VISCOS,DENSIT,PRANDT,DEN(40,15),VIS(40,15)
1      ,OX(40,15),AN2(40,15),T(40,15),RFUP(40,15),RCOP(40,15)
1,CO(40,15),H2O(40,15),H2(40,15),CO2(40,15),FUOLD(40,15),O1(40,15)
1/COEF/AP(40,15),AN(40,15),AS(40,15),AE(40,15),AW(40,15),SU(40,15),
1      SP(40,15)
1/ALL/IT,JT,NI,NJ,NIM1,NJM1,GREAT
1/GEOM1/INDCOS,X(40),Y(40),DXEP(40),DXPW(40),DYNP(40),DYPS(40),
1      SNS(40),SEW(40),XU(40),YV(40),R(40),RV(40),LABRUPT
1/GEOM2/IHUB,JHUB,IHBP1,JHBP1,IHBM1,JHBM1,ICON,JCON,ICNP1,JCNP1
1/CHEM/URFDEN,GASCON,CFU,COX,CPR,WFU,WOX,WPR,HFU,HCO,OXDFU,PRESS
1,CCO,CCO2,CH2O,CAN2,RESORC,NSWPC,URFCO,PRCO,OXDCO,OXDFU1,WCO
1,WH2O,WCO2,WAN2,PERSTO,WH2,CH2,W01,C01
1/KASE T1/UIN,TEIN,EDIN,FLOWIN,ALAMDA,
2      RSMALL,RLARGE,AL1,AL2,JSTEP,ISTEP,JSTP1,JSTM1,ISTP1,ISTM1,J
3INC,ICUT,ICTP1
1/RADT/RADX(40,15),RADR(40,15),RADIN
2      ,EMIW,NSWPRX,NSWPRR,URFRX,URFRR,SIGMA,ABSOR,SCATT
3      ,RESORR,RESORX
CHAPTER 1 1 1 1 1 1 1 ASSEMBLY OF COEFFICIENTS 1 1 1 1 1 1
C

```

```

      DO 100 I=2,NIM1
      DO 101 J=2,NJM1
C-----COMPUTE AREAS AND VOLUME
      AREAN=RV(J+1)*SEW(I)
      AREAS=RV(J)*SEW(I)
      AREAEW=R(J)*SNS(J)
      VOL=R(J)*SNS(J)*SEW(I)
C-----THERE IS NO CONVECTION IN THE RADIATION PROBLEM
C
C-----CALCULATE DIFFUSION COEFFICIENTS
      GAMN=0.0
      GAMS=0.0
      GAME=1./(ABSOR+SCATT)
      GAMW=GAME
      DN=GAMN*AREAN/DYNP(J)
      DS=GAMS*AREAS/DYPS(J)
      DE=GAME/DXEP(I)
      DW=GAMW/DXPW(I)
C-----SOURCE TERM CALCULATION
      SUTEM=ABSOR*SIGMA*T(I,J)**4.*SEW(I)+SCATT/2.*SEW(I)*
1 (RADX(I,J)+RADR(I,J))
      SPTEM=ABSOR+SCATT
C
C-----ASSEMBLE MAIN COEFFICIENTS
      AN(I,J)=DN
      AS(I,J)=DS
      AE(I,J)=DE
      AW(I,J)=DW
      SU(I,J)=0.0
      SP(I,J)=0.0
      SU(I,J)=SU(I,J)+SUTEM
      SP(I,J)=-SPTEM*SEW(I)
101 CONTINUE
100 CONTINUE
C
CHAPTER 2 2 2 2 2 2 PROBLEM MODIFICATIONS 2 2 2 2 2 2
C
      NCHAP=11
      CALL PROMOD (NCHAP)
C
CHAPTER 3 FINAL COEFFICIENT ASSEMBLY AND RESIDUAL SOURCE CALCULATION 3
C
      RESORX=0.0
      DO 300 I=2,NIM1
      DO 301 J=2,NJM1
      AP(I,J)=AN(I,J)+AS(I,J)+AE(I,J)+AW(I,J)-SP(I,J)
      RESOR=AN(I,J)*RADX(I,J+1)+AS(I,J)*RADX(I,J-1)+AE(I,J)*RADX(I+1,J)
1 +AW(I,J)*RADX(I-1,J)-AP(I,J)*RADX(I,J)+SU(I,J)
      VOL=R(J)*SNS(J)*SEW(I)
      SORVOL=GREAT*VOL
      IF(-SP(I,J).GT.0.5*SORVOL) RESOR=0.0
      RESORX=RESORX+DABS(RESOR)
C-----UNDER-RELAXATION
      AP(I,J)=AP(I,J)/URFRX

```

```

      SU(I,J)=SU(I,J)+(1.-URFRX)*AP(I,J)*RADX(I,J)
301 CONTINUE
300 CONTINUE
C
CHAPTER 4 4 4 4 4 SOLUTION OF DIFFERENCE EQUATION 4 4 4 4 4
C
      DO 400 N=1,NSWPRX
400 CALL SOLVRX(2,2,NI,NJ,IT,JT,RADX,NCHAP)
      RETURN
      END
C
      SUBROUTINE CALCRR
      IMPLICIT REAL*8(A-H,O-Z)
C
CHAPTER 0 0 0 0 0 0 PRELIMINARIES 0 0 0 0 0 0 0 0 0
C
      COMMON
C
      1/SWEN/PRW,WWALL,RESORH,NSWPH,URFH,PRH,TWALL
      */VAR/U(40,15), V(40,15), W(40,15), P(40,15), PP(40,15), TE(40,15),
      1ED(40,15),H(40,15),FU(40,15),OF(40,15)
      1/FLUPR/URFVIS,VISCOS,DENSIT,PRANDT,DEN(40,15),VIS(40,15)
      1      ,OX(40,15),AN2(40,15),T(40,15),RFUP(40,15),RCOP(40,15)
      1,CO(40,15),H2O(40,15),H2(40,15),CO2(40,15),FUOLD(40,15),O1(40,15)
      1/COEF/AP(40,15),AN(40,15),AS(40,15),AE(40,15),AW(40,15),SU(40,15),
      1      SP(40,15)
      1/ALL/IT,JT,NI,NJ,NIM1,NJM1,GREAT
      1/GEOM1/INDCOS,X(40),Y(40),DXEP(40),DXPW(40),DYNP(40),DYPs(40),
      1      SNS(40),SEW(40),XU(40),YV(40),R(40),RV(40),LABRUPT
      1/GEOM2/IHUB,JHUB,IHBP1,JHBP1,IHBM1,JHBM1,ICON,JCON,ICNP1,JCNP1
      1/CHEM/URFDEN,GASCON,CFU,COX,CPR,WFU,WOX,WPR,HFU,HCO,OXDFU,PRESS
      1,CCO,CCO2,CH2O,CAN2,RESORC,NSWPC,URFCO,PRCO,OXDCO,OXDFU1,WCO
      1,WH2O,WCO2,WAN2,PERSTO,WH2,CH2,W01,CO1
      1/KASE T1/UIN,TEIN,EDIN,FLOWIN,ALAMDA,
      2      RSMALL,RLARGE,AL1,AL2,JSTEP,ISTEP,JSTP1,JSTM1,ISTP1,ISTM1,J
      3INC,ICUT,ICTP1
      1/RADT/RADX(40,15),RADR(40,15),RADIN
      2      ,EMIW,NSWPRX,NSWPRR,URFRX,URFRR,SIGMA,ABSOR,SCATT
      3      ,RESORR,RESORX
      LOGICAL LABRUPT
CHAPTER 1 1 1 1 1 1 1 ASSEMBLY OF COEFFICIENTS 1 1 1 1 1 1
C
      DO 100 I=2,NIM1
      DO 101 J=2,NJM1
C-----COMPUTE AREAS AND VOLUME
      AREAN=RV(J+1)*SEW(I)
      AREAS=RV(J)*SEW(I)
      AREAEW=R(J)*SNS(J)
      VOL=R(J)*SNS(J)*SEW(I)
C-----THERE IS NO CONVECTION IN THE RADIATION PROBLEM
C
C-----CALCULATE DIFFUSION COEFFICIENTS
      GAMND=ABSOR+SCATT
      IF(INDCOS.EQ.2) GAMND=GAMND+1./RV(J+1)

```

```

      GAMN=1./GAMND
      GAMSD=ABSOR+SCATT
      IF (INDCOS.EQ.2) GAMSD=GAMSD+1./(RV(J)+1.E-30)
      GAMS=1./GAMSD
      GAME=0.0
      GAMW=GAME
      DN=GAMN*RV(J+1)/DYNP(J)
      DS=GAMS*RV(J)/DYPS(J)
      DE=GAME*AREAWE/DXEP(I)
      DW=GAMW*AREAWE/DXPW(I)
C-----SOURCE TERM CALCULATION
      SUTEM=ABSOR*SIGMA*T(I,J)**4.*R(J)+SCATT/2.*R(J)*
      1 (RADX(I,J)+RADR(I,J))
      SPTEM=ABSOR+SCATT
C
C-----ASSEMBLE MAIN COEFFICIENTS
      AN(I,J)=DN
      AS(I,J)=DS
      AE(I,J)=DE
      AW(I,J)=DW
      SU(I,J)=0.0
      SP(I,J)=0.0
      SU(I,J)=SU(I,J)+SUTEM
      SP(I,J)=-SPTEM*R(J)
      101 CONTINUE
      100 CONTINUE
C
CHAPTER 2 2 2 2 2 2 PROBLEM MODIFICATIONS 2 2 2 2 2 2
C
      NCHAP=12
      CALL PROMOD (NCHAP)
C
CHAPTER 3 FINAL COEFFICIENT ASSEMBLY AND RESIDUAL SOURCE CALCULATION 3
C
      RESORR=0.0
      DO 300 I=2,NIM1
      DO 301 J=2,NJM1
      AP(I,J)=AN(I,J)+AS(I,J)+AE(I,J)+AW(I,J)-SP(I,J)
      RESOR=AN(I,J)*RADR(I,J+1)+AS(I,J)*RADR(I,J-1)+AE(I,J)*RADR(I+1,J)
      1 +AW(I,J)*RADR(I-1,J)-AP(I,J)*RADR(I,J)+SU(I,J)
      VOL=R(J)*SNS(J)*SEW(I)
      SORVOL=GREAT*VOL
      IF (-SP(I,J).GT.0.5*SORVOL) RESOR=0.0
      RESORR=RESORR+DABS(RESOR)
C-----UNDER-RELAXATION
      AP(I,J)=AP(I,J)/URFRR
      SU(I,J)=SU(I,J)+(1.-URFRR)*AP(I,J)*RADR(I,J)
      301 CONTINUE
      300 CONTINUE
C
CHAPTER 4 4 4 4 4 SOLUTION OF DIFFERENCE EQUATION 4 4 4 4 4
C
      DO 400 N=1,NSWPRR
      400 CALL SOLVRR(2,2,NI,NJ,IT,JT,RADR,NCHAP)

```

```

      RETURN
      END
C
      SUBROUTINE CALCCO
      IMPLICIT REAL*8(A-H,O-Z)
C
CHAPTER 0 0 0 0 0 0 PRELIMINARIES 0 0 0 0 0 0 0 0 0
C
      COMMON
C
      1/FUOF/RESORF,NSWPF,URFF,PRFU,FUWALL,RESORO,NSWFO,URFO,PROF,OFWALL
      */VAR/U(40,15), V(40,15), W(40,15), P(40,15), PP(40,15), TE(40,15),
      1ED(40,15),H(40,15),FU(40,15),OF(40,15)
      1/FLUPR/URFVIS,VISCOS,DENSIT,PRANDT,DEN(40,15),VIS(40,15)
      1      ,OX(40,15),AN2(40,15),T(40,15),RFUP(40,15),RCOP(40,15)
      1,CO(40,15),H2O(40,15),H2(40,15),CO2(40,15),FUOLD(40,15),OI(40,15)
      1/COEF/AP(40,15),AN(40,15),AS(40,15),AE(40,15),AW(40,15),SU(40,15),
      1      SP(40,15)
      1/ALL/IT,JT,NI,NJ,NIM1,NJM1,GREAT
      1/GEOM1/INDCOS,X(40),Y(40),DXEP(40),DXPW(40),DYNP(40),DYPS(40),
      1      SNS(40),SEW(40),XU(40),YV(40),R(40),RV(40),LABRUPT
      1/GEOM2/IHUB,JHUB,IHBP1,JHBP1,IHBM1,JHBM1,ICON,JCON,ICNP1,JCNP1
      1/CHEM/URFDEN,GASCON,CFU,COX,CPR,WFU,WOX,WPR,HFU,HCO,OXDFU,PRESS
      1,CCO,CCO2,CH2O,CAN2,RESORC,NSWPC,URFCO,PRCO,OXDCO,OXDFU1,WCO
      1,WH2O,WCO2,WAN2,PERSTO,WH2,CH2,WO1,CO1
      1/CHEM2/FUIN,AX,AY,AO
      1/REAC/RFUEBU(40,15),RFUARR(40,15),NITER,RCOARR(40,15)
      1,RCOEBU(40,15)
      1/KASE T1/UIN,TEIN,EDIN,FLOWIN,ALAMDA,
      2      RSMALL,RLARGE,AL1,AL2,JSTEP,ISTEP,JSTP1,JSTM1,ISTP1,ISTM1,J
      3INC,ICUT,ICTP1
C
C
CHAPTER 1 1 1 1 1 1 1 ASSEMBLY OF COEFFOCOENTS 1 1 1 1 1 1
C
      RAT4=AX*WCO/WFU
      JFIN=JSTEP
      DO 100 I=2,NIM1
      DO 101 J=2,NJM1
C-----COMPUTE AREAS AND VOLUME
      AREAN=RV(J+1)*SEW(I)
      AREAS=RV(J)*SEW(I)
      AREAEW=R(J)*SNS(J)
      VOL=AREAEW*SEW(I)
C-----CALCULATE CONVECTION COEFFICIENTS
      GN=0.5*(DEN(I,J)+DEN(I,J+1))*V(I,J+1)
      GS=0.5*(DEN(I,J)+DEN(I,J-1))*V(I,J)
      GE=0.5*(DEN(I,J)+DEN(I+1,J))*U(I+1,J)
      GW=0.5*(DEN(I,J)+DEN(I-1,J))*U(I,J)
      CN=GN*AREAN
      CS=GS*AREAS
      CE=GE*AREAEW
      CW=GW*AREAEW
C-----CALCULATE DIFFUSION COEFFICIENTS

```

```

GAMN=0.5*(VIS(I,J)+VIS(I,J+1))/PRCO
GAMS=0.5*(VIS(I,J)+VIS(I,J-1))/PRCO
GAME=0.5*(VIS(I,J)+VIS(I+1,J))/PRCO
GAMW=0.5*(VIS(I,J)+VIS(I-1,J))/PRCO
DN=GAMN*AREAN/DYNP(J)
DS=GAMS*AREAS/DYPS(J)
DE=GAME*AREA EW/DXEP(I)
DW=GAMW*AREA EW/DXPW(I)
C-----SOURCE TERMS
SMP=CN-CS+CE-CW
CP=DMAX1(0.0,SMP)
CPO=CP
C-----ASSEMBLE MAIN COEFFICIENTS
AN(I,J)=DMAX1(DABS(0.5*CN),DN)-0.5*CN
AS(I,J)=DMAX1(DABS(0.5*CS),DS)+0.5*CS
AE(I,J)=DMAX1(DABS(0.5*CE),DE)-0.5*CE
AW(I,J)=DMAX1(DABS(0.5*CW),DW)+0.5*CW
SU(I,J)=CPO*CO(I,J)
SP(I,J)=-CP
IF(I.LT.ISTEP) GO TO 102
IF(CO(I,J).LT.1E-8.OR.OX(I,J).LT.1E-8) GO TO 102
C-----SOURCE TERM FOR RCO = CONSUMPTION OF FUEL
C-----EDDY-BREAK-UP MODEL
RCOEBU(I,J)=4.0*DEN(I,J)*CO(I,J)*ED(I,J)/TE(I,J)
C-----ARRHENIUS MODEL
TEMP=T(I,J)
RCOARR(I,J)=6.0E+8*DEN(I,J)**2.*CO(I,J)*DEXP(-12500./TEMP)
1*OX(I,J)
IF(RCOEBU(I,J).LT.RCOARR(I,J))GO TO 999
RCOP(I,J)=RCOARR(I,J)
GO TO 998
999 RCOP(I,J)=RCOEBU(I,J)
998 CONTINUE
RCO=RCOP(I,J)
SP(I,J)=SP(I,J)-RCO*VOL/CO(I,J)
102 SU(I,J)=SU(I,J)+RFUP(I,J)*VOL*RAT4
101 CONTINUE
100 CONTINUE
C
CHAPTER 2 2 2 2 2 2 2 PROBLEM MODIFICATIONS 2 2 2 2 2 2
C
NCHAP=9
CALL PROMOD(NCHAP)
C
CHAPTER 3 FINAL COEFFICIENT ASSEMBLY AND RESIDUAL SOURCE CALCULATION 3
C
RESORC=0.0
DO 300 I=2,NIM1
DO 301 J=2,NJM1
AP(I,J)=AN(I,J)+AS(I,J)+AE(I,J)+AW(I,J)-SP(I,J)
RESOR=AN(I,J)*CO(I,J+1)+AS(I,J)*CO(I,J-1)+AE(I,J)*CO(I+1,J)
1 +AW(I,J)*CO(I-1,J)-AP(I,J)*CO(I,J)+SU(I,J)
VOL=R(J)*SNS(J)*SEW(I)
SORVOL=GREAT*VOL

```



```

      IF(-SP(I,J).GT.0.5*SORVOL) RESOR=0.0
      RESORC=RESORC+DABS(RESOR)
C-----UNDER-RELAXATION
      AP(I,J)=AP(I,J)/URFCO
      SU(I,J)=SU(I,J)+(1.-URFCO)*AP(I,J)*CO(I,J)
      301 CONTINUE
      300 CONTINUE
C
CHAPTER 4 4 4 4 4 4 SOLUTION OF DIFFERENCE EQUATION 4 4 4 4
C
      DO 400 N=1,NSWPC
      400 CALL LISOLV(2,2,NI,NJ,IT,JT,CO,NCHAP)
      RETURN
      END
C
C
      SUBROUTINE EQUAL (NREACT)
      IMPLICIT REAL*8 (A-H,O-Z)
      COMMON
      1/FLUPR/URFVIS,VISCOS,DENSIT,PRANDT,DEN(40,15),VIS(40,15)
      1 ,OX(40,15),AN2(40,15),T(40,15),RFUP(40,15),RCOP(40,15)
      1,CO(40,15),H2O(40,15),H2(40,15),CO2(40,15),FUOLD(40,15),O1(40,15)
      1/KASE T1/UIN,TEIN,EDIN,FLOWIN,ALAMDA,
      2 RSMALL,RLARGE,AL1,AL2,JSTEP,ISTEP,JSTP1,JSTM1,ISTP1,ISTM1,J
      3INC,ICUT,ICTP1
      1/CHEM/URFDEN,GASCON,CFU,COX,CPR,WFU,WOX,WPR,HFU,HCO,OXDFU,PRESS
      1,CCO,CCO2,CH2O,CAN2,RESORC,NSWPC,URFCO,PRCO,OXDCO,OXDFU1,WCC
      1,WH2O,WCO2,WAN2,PERSTO,WH2,CH2,W01,CO1
      1/ALL/IT,JT,NI,NJ,NIM1,NJM1,GREAT
      COMMON
      1/NITRO1/WN1,WNO,CN1,CNO,URFNO,AN1(40,15),ANO(40,15),NSWPNO
      2,URFN1,PRNO,RESRNO,RNOF1(40,15),RNOF2(40,15)
      3,RNOR2(40,15),RNOR1(40,15)
      GO TO (1,2),NREACT
      1 CONTINUE
      DO 100 I=2,NIM1
      DO 101 J=2,NJM1
          IF(T(I,J).LT.700) GO TO 10
          AKO1=905.0*DEXP(-29710./T(I,J))
          GO TO 9
      10 AKO1=0.0
      9 CONTINUE
      O1(I,J)=0.8*AKO1*OX(I,J)**.5
      101 CONTINUE
      100 CONTINUE
      RETURN
C-----THIS REGION FOR FURTHER KINETICS
      2 CONTINUE
      DO 200 I=2,NIM1
      DO 201 J=2,NJM1
          IF((ANO(I,J)*RNOR1(I,J)).LT.1E-30.AND.(OX(I,J)*RNOF2(I,J))
      1.LT.1E-30) GO TO 201
          IF((O1(I,J)*RNOF1(I,J)*AN2(I,J)).LT.1E-37.OR.(O1(I,J)*
      1RNOR2(I,J)*ANO(I,J)).LT.1E-37) GO TO 201

```

```

      IF((RNOF1(I,J)*AN2(I,J)).LT.1E-32) GO TO 201
      IF((RNOR2(I,J)*ANO(I,J)).LT.1E-32) GO TO 201
      AN1(I,J)=O1(I,J)*(RNOF1(I,J)*AN2(I,J)+RNOR2(I,J)*ANO(I,J))
      1/(RNOR1(I,J)*ANO(I,J)+RNOF2(I,J)*OX(I,J))
201 CONTINUE
200 CONTINUE
      RETURN
      END
C
      SUBROUTINE LISOLV(ISTART,JSTART,NI,NJ,IT,JT,PHI,NCHAP)
      IMPLICIT REAL*8(A-H,O-Z)
C*****
C
CHAPTER 0 0 0 0 0 0 0 0 PRELIMINARIES 0 0 0 0 0 0 0 0
C
      DIMENSION PHI(IT,JT),A(40),B(40),C(40),D(40)
      COMMON
      1/COEF/AP(40,15),AN(40,15),AS(40,15),AE(40,15),AW(40,15),SU(40,15),
      1 SP(40,15)
      1/GEOM2/IHUB,JHUB,IHBP1,JHBP1,IHBM1,JHBM1,ICON,JCON,ICNP1,JCNP1
      1/KASE T1/UIN,TEIN,EDIN,FLOWIN,ALAMDA,
      2 RSMALL,RLARGE,AL1,AL2,JSTEP,ISTEP,JSTP1,JSTM1,ISTP1,ISTM1,J
      3INC,ICUT,ICTP1
      NIM1=NI-1
      NJM1=NJ-1
C-----COMMENCE W-E SWEEP
      JEND=JSTEP
      DO 100 I=ISTART,NIM1
      IF(NCHAP.EQ. 2) GO TO 50
      IF(I.GE. ISTEP .AND. I.LE. ICUT) JEND=JEND+JINC
      GO TO 70
50 CONTINUE
      IF(I.GE. ISTP1 .AND. I.LE. ICTP1) JEND=JEND+JINC
70 CONTINUE
      JSTA=JSTART
      IF(I.LT. (IHUB+ISTART-2)) JSTA=JHUB+JSTART-2
      JSM1=JSTA-1
      JENDP1=JEND+1
      A(JSM1)=0.0
      C(JSM1)=PHI(I,JSM1)
C-----COMMENCE S-N TRAVERSE
      DO 101 J=JSTA,JEND
      IF((I.LT.IHUB.AND.J.LT.JHUB).OR.(I.LT.ISTEP.AND.J.GT.JSTEP))
      1GO TO 101
C-----ASSEMBLE TDMA COEFFICIENTS
      A(J)=AN(I,J)
      B(J)=AS(I,J)
      C(J)=AE(I,J)*PHI(I+1,J)+AW(I,J)*PHI(I-1,J)+SU(I,J)
      D(J)=AP(I,J)
C-----CALCULATE COEFFICIENTS OF RECURRENCE FORMULA
      TERM=1./(D(J)-B(J)*A(J-1))
      A(J)=A(J)*TERM
      C(J)=(C(J)+B(J)*C(J-1))*TERM
101 CONTINUE

```

```

C-----OBTAIN NEW PHI)S
      DO 102 JJ=JSTA,JEND
      J=JENDP1+JSM1-JJ
102 PHI(I,J)=A(J)*PHI(I,J+1)+C(J)
100 CONTINUE
      RETURN
      END

C
      SUBROUTINE PRINT(ISTART,JSTART,NI,NJ,IT,JT,X,Y,PHI,HEAD)
      IMPLICIT REAL*8(A-H,O-Z)
C*****
C
      CHARACTER*36 HEAD(9)
      DIMENSION PHI(IT,JT),X(IT),Y(JT),STORE(50)
      ISKIP=1
      JSKIP=1
      WRITE(6,110)HEAD
      ISTA=ISTART-12
100 CONTINUE
      ISTA=ISTA+12
      IEND=ISTA+11
      IF(NI.LT.IEND) IEND=NI
      WRITE(6,111)(I,I=ISTA,IEND,ISKIP)
      WRITE(6,114)(X(I),I=ISTA,IEND,ISKIP)
      WRITE(6,112)
      DO 101 JJ=JSTART,NJ,JSKIP
      J=JSTART+NJ-JJ
      DO 120 I=ISTA,IEND
      A=PHI(I,J)
      IF(DABS(A).LT.1.E-20) A=0.0
120 STORE(I)=A
      101 WRITE(6,113)J,Y(J),(STORE(I),I=ISTA,IEND,ISKIP)
C-----
      IF(IEND.LT.NI)GO TO 100
      RETURN
110 FORMAT(1H0,17(2H*-),7X,9A4,7X,17(2H*-))
111 FORMAT(1H0,13H      I =      ,I2,11I9)
112 FORMAT(8H0 J      Y)
113 FORMAT(I3,0PF7.3,1X,1P12E9.2)
114 FORMAT(11H      X = ,F6.3,11F9.3)
      END

C      START OF SF8.FOR
C
      SUBROUTINE PROMOD (NCHAP)
      IMPLICIT REAL*8(A-H,O-Z)
C*****
C
CHAPTER 0 0 0 0 0 0 0 PRELIMINARIES 0 0 0 0 0 0 0 0 0
C
      COMMON
      1/UVEL/RESORU,NSWPU,URFU,DXEPU(40),DXPWU(40),SEWU(40)
      1/VVEL/RESORV,NSWPV,URFV,DYNPV(40),DYPSV(40),SNSV(40),RCV(40)
      */WVEL/ RESORW, NSWPW, URFW
      */VAR/U(40,15), V(40,15), W(40,15), P(40,15), PP(40,15), TE(40,15),

```

```

1ED(40,15),H(40,15),FU(40,15),OF(40,15)
1/PCOR/RESORM,NSWPP,URFP,DU(40,15),DV(40,15),IPREF,JPREF
1/ALL/IT,JT,NI,NJ,NIM1,NJM1,GREAT
1/GEOM1/INDCOS,X(40),Y(40),DXEP(40),DXPW(40),DYNP(40),DYPS(40),
1    SNS(40),SEW(40),XU(40),YV(40),R(40),RV(40),LABRUPT
1/FLUPR/URFVIS,VISCOS,DENSIT,PRANDT,DEN(40,15),VIS(40,15)
1    ,OX(40,15),AN2(40,15),T(40,15),RFUP(40,15),RCOP(40,15)
1,CO(40,15),H2O(40,15),H2(40,15),CO2(40,15),FUOLD(40,15),OI(40,15)
1/KASE T1/UIN,TEIN,EDIN,FLOWIN,ALAMDA,
2    RSMALL,RLARGE,AL1,AL2,JSTEP,ISTEP,JSTP1,JSTM1,ISTP1,ISTM1,J
3INC,ICUT,ICTP1
1/SUSP/SUKD(40,15),SPKD(40,15)
1/COEF/AP(40,15),AN(40,15),AS(40,15),AE(40,15),AW(40,15),SU(40,15),
1    SF(40,15)
1/TURB/GEN(40,15),CD,CMU,C1,C2,CAPPA,ELOG,PRED,PRTE
1/WALLF/YPLUSN(40),XPLUSW(40),TAUN(40),TAUW(40)
1    ,TAUE(40),TAUS(40),YPLUSS(40),XPLUSE(40)
1/SWEN/PRW,WWALL,RESORH,NSWPH,URFH,PRH,TWALL
1/FUOF/RESORF,NSWPF,URFF,PRFU,FUWALL,RESORO,NSWPO,URFO,PROF,OFWALL
COMMON
1/CHEM/URFDEN,GASCON,CFU,COX,CPR,WFU,WOX,WPR,HFU,HCO,OXDFU,PRESS
1,CCO,CCO2,CH2O,CAN2,RESORC,NSWPC,URFCO,PRCO,OXDCO,OXDFU1,WCO
1,WH2O,WCO2,WAN2,PERSTO,WH2,CH2,WO1,CO1
1/GEOM2/IHUB,JHUB,IHBP1,JHBP1,IHBM1,JHBM1,ICON,JCON,ICNP1,JCNP1
1/GEOM3/IEN1M,IEN1P,IEN2M,IEN2P
1/RADT/RADX(40,15),RADR(40,15),RADIN
2    ,EMIW,NSWPRX,NSWPRR,URFRX,URFRR,SIGMA,ABSOR,SCATT
3    ,RESORR,RESORX
LOGICAL LABRUPT
IF(NCHAP.EQ.2)GO TO 1100
C-----OUT OF RANGE VALUES
JFIN=JSTEP
DO 2101 I=1,NIM1
IF(I.GE.ISTEP.AND.I.LT.ICUT) JFIN=JFIN+JINC
DO 2102 J=1,NJM1
IF(I.LT.IHUB.AND.J.LT.JHUB) SP(I,J)--GREAT
IF(I.LT.ISTEP.AND.J.GT.JSTEP) SP(I,J)--GREAT
IF(I.GT.ICON.AND.J.GT.JCON) SP(I,J)--GREAT
IF(I.GE.ISTEP.AND.I.LT.ICUT.AND.J.GT.JFIN) SP(I,J)--GREAT
2102 CONTINUE
2101 CONTINUE
1100 CONTINUE
GO TO (1,2,3,4,5,6,7,8,9,10,11,12),NCHAP
C
C
C
CHAPTER 1 1 1 1 1 1 1 1 1 PROPERTIES 1 1 1 1 1 1 1 1 1
C
1 CONTINUE
DO 100 J=1,NJ
100 DEN(NI,J)=DEN(NIM1,J)
RETURN
C
CHAPTER 2 2 2 2 2 2 2 2 2 U MOMENTUM 2 2 2 2 2 2 2 2 2

```

```

C
  2 CONTINUE
C-----OUT OF RANGE VALUES
  JFIN=JSTEP
  DO 200 I=2,NIM1
    IF(I.GE.ISTEP.AND.I.LE.ICUT) JFIN=JFIN+JINC
  DO 202 J=2,NJM1
    IF(I.LE.IHUB.AND.J.LT.JHUB) SP(I,J)=-GREAT
    IF(I.LT.ISTEP.AND.J.GT.JSTEP) SP(I,J)=-GREAT
    IF(I.GT.ICON.AND.J.GT.JCON) SP(I,J)=-GREAT
    IF(I.GE.ISTEP.AND.I.LE.ICUT.AND.J.GE.JFIN) SP(I,J)=-GREAT
    IF((.NOT.LABRUPT).AND.I.GE.ISTEP.AND.I.LE.ICUT.AND.J.GT.(JFIN-JINC
1)) SP(I,J)=-GREAT
    IF(LABRUPT.AND.I.EQ.ISTEP.AND.J.GT.JSTEP) SP(I,J)=-GREAT
  202 CONTINUE
  200 CONTINUE
C-----TOP WALL
  CDTERM=CMU**0.25
  J=JSTEP
  DO 210 I=3,NIM1
    IF(I.GE.IEN1M.AND.I.LE.(IEN1P+1)) GO TO 216
    IF(I.GE.IEN2M.AND.I.LE.(IEN2P+1)) GO TO 216
    IF(I.GE.ISTP1.AND.I.LE.ICTP1) J=J+JINC
    IF(I.GT.ICON) J=JCON
    YP=YV(J+1)-Y(J)
    SQRTK=DSQRT(0.5*(TE(I,J)+TE(I-1,J)))
    DENU=0.5*(DEN(I,J)+DEN(I-1,J))
    YPLUSA=0.5*(YPLUSN(I)+YPLUSN(I-1))
    IF(YPLUSA.LE.11.63) GO TO 211
    TMULT=DENU*CDTERM*SQRTK*CAPPA/DLOG(ELOG*YPLUSA)
    GO TO 212
  211 TMULT=VISCOS/YP
  212 CONTINUE
    WAVG=DABS((W(I,J)+W(I-1,J))/2.)
    UEFF=DSQRT(U(I,J)*U(I,J) + WAVG*WAVG)
    IF(U(I,J) .LT. 0.) UEFF=-UEFF
    IF((LABRUPT .AND.I.NE. ISTEP) .OR. I .LT. ISTEP .OR. I .GE. ICTP1
2.OR.I.GT.ICON) GO TO 205
  204 SP(I,J)=SP(I,J)-TMULT*(XU(I)-XU(I-1))/2.*RV(J+1)
    GO TO 210
  205 SP(I,J)=SP(I,J)-TMULT*SEWU(I)*RV(J+1)
  210 AN(I,J)=0.
  216 CONTINUE
C-----SIDE WALLS 1 AND 2
  JFIN=JSTEP
  DO 213 I=2,ICTP1
    IF(I.GE.ISTP1.AND.I.LE.ICTP1) JFIN=JFIN+JINC
  DO 213 J=2,JFIN
    IF(J.GE.JHUB.AND.J.LE.(JFIN-JINC)) GO TO 213
    IF(J.LT.JHUB.AND.I.EQ.IHBP1) AW(I,J)=0.0
    IF(I.LT.ISTP1) GO TO 213
    AW(I,J)=0.0
  213 CONTINUE
C-----SYMMETRY AXIS

```

```

      DO 203 I=IHUB,NI
203  AS(I,2)=0.
C-----OUTLET
      ARDENT=0.0
      FLOW=0.0
      JEND=NJM1
      IF(JCON.LT.NJM1) JEND=JCON
      DO 209 J=2, JEND
      ARDEN=0.50*(DEN(NIM1,J)+DEN(NIM1-1,J))*R(J)*SNS(J)
      ARDENT=ARDENT+ARDEN
209  FLOW=FLOW+ARDEN*U(NIM1,J)
      UINC=(FLOWIN-FLOW)/ARDENT
      DO 215 J=2,NJM1
215  U(NI,J)=U(NIM1,J)+UINC
C-----SIDE WALL 3
      IF(JCON.EQ.NJ) GO TO 251
      DO 250 J=JCNP1,NJM1
250  AE(ICON,J)=0.0
251  CONTINUE
C-----BOTTOM WALL
      IF(IHUB.LE.3) GO TO 275
      J=JHUB
      CDTERM=CMU**0.25
      YP=Y(J)-YV(J)
      DO 260 I=3, IHBM1
      SQRTK=DSQRT(0.5*(TE(I,J)+TE(I-1,J)))
      DENU=0.5*(DEN(I,J)+DEN(I-1,J))
      YPLUSA=0.5*(YPLUSS(I)+YPLUSS(I-1))
      IF(YPLUSA.LE.11.63) GO TO 261
      TMULT=DENU*CDTERM*SQRTK*CAPPA/DLOG(ELOG*YPLUSA)
      GO TO 262
261  TMULT=VISCOS/YP
262  TAUS(I)=-TMULT*U(I,J)
      SP(I,J)=SP(I,J)-TMULT*SEWU(I)*RV(J)
260  AS(I,J)=0.0
      TAUS(2)=TAUS(3)
275  CONTINUE
      RETURN

C
CHAPTER 3 3 3 3 3 3 3 3 3 V MOMENTUM 3 3 3 3 3 3 3 3
C
      3 CONTINUE
C-----SIDE WALLS 1 AND 2
      CDTERM=CMU**0.25
      JFIN=JSTEP
      IEND=ICUT
      IF(LABRUPT) IEND=ISTEP
      DO 310 I=2, IEND
      IF(I.GE.ISTEP.AND.I.LE.ICUT) JFIN=JFIN+JINC
      DO 310 J=2, JFIN
      IF(J.GE.JHUB.AND.J.LE.(JFIN-JINC)) GO TO 310
      IF(J.LT.JHUB.AND.I.EQ.IHUB) GO TO 333
      IF(I.LT.ISTEP) GO TO 310
      XP=X(I)-XU(I)

```

```

      SQRTK=DSQRT(0.5*(TE(I,J)+TE(I,J-1)))
      DENV=0.5*(DEN(I,J)+DEN(I,J-1))
      XPLUSA=0.5*(XPLUSW(J)+XPLUSW(J-1))
      IF(XPLUSA.LE.11.63)      GO TO 311
      TMULT=DENV*CDTERM*SQRTK*CAPPA/DLOG(ELOG*XPLUSA)
      GO TO 312
311  TMULT=VISCOS/XP
312  CONTINUE
      WAVG=DABS((W(I,J)+W(I,J-1))/2.)
      VEFF=DSQRT(V(I,J)*V(I,J) + WAVG*WAVG)
      IF(V(I,J) .LT. 0.) VEFF=-VEFF
      IF(J.GT.JFIN.OR.(LABRUPT.AND.J.NE.JSTP1).OR.J.LT.JHUB) GO TO 305
      SP(I,J)=SP(I,J)-TMULT*SNSV(J)/2.*.5*(RCV(J+1)+RCV(J))
      GO TO 333
305  SP(I,J)=SP(I,J)-TMULT*SNSV(J)*0.5*(RCV(J+1)+RCV(J))
333  AW(I,J)=0.0
310  CONTINUE
C-----TOP WALL
      J=JSTEP
      DO 313 I=2,NIM1
      IF(I.GE.IEN1M.AND.I.LE.IEN1P) GO TO 313
      IF(I.GE.IEN2M.AND.I.LE.IEN2P) GO TO 313
      IF(I .GE. ISTEP .AND. I .LE. ICUT) J=J+JINC
      IF(I.GT.ICON) J=JCON
      AN(I,J)=0.0
313  CONTINUE
C-----SYMMETRY AXIS
      DO 320 I=IHUB,NIM1
320  AS(I,3)=0.
      IF(JCON.EQ.NJ)GO TO 321
      CDTERM=CMU**0.25
      I=ICON
      DO 340 J=JCNP1,NJM1
      XP=XU(I+1)-X(I)
      SQRTK=DSQRT(0.5*(TE(I,J)+TE(I,J-1)))
      DENV=0.5*(DEN(I,J)+DEN(I,J-1))
      XPLUSE=0.5*(XPLUSE(J)+XPLUSE(J-1))
      IF(XPLUSE.LE.11.63) GO TO 341
      TMULT=DENV*CDTERM*SQRTK*CAPPA/DLOG(ELOG*XPLUSE)
      GO TO 342
341  TMULT=VISCOS/XP
342  SP(I,J)=SP(I,J)-TMULT*SNSV(J)*0.5*(RCV(J+1)+RCV(J))
      AE(I,J)=0.0
340  CONTINUE
321  CONTINUE
C-----BOTTOM WALL
      IF(IHUB.LE.2)GO TO 355
      DO 350 I=2,IHBM1
350  AS(I,JHBP1)=0.0
355  CONTINUE
      RETURN

```

C
 CHAPTER 4 4 4 4 4 4 PRESSURE CORRECTION 4 4 4 4 4 4 4
 C

```

      4 CONTINUE
C-----SIDE WALLS 1 AND 2
      JFIN=JSTEP
      IEND=ICUT
      IF(LABRUPT) IEND=ISTEP
      DO 401 I=2,IEND
      IF(I.GE.ISTEP.AND.I.LE.ICUT) JFIN=JFIN+JINC
      DO 401 J=2,JFIN
      IF(J.GE.JHUB.AND.J.LE.(JFIN-JINC))GO TO 401
      IF(J.LT.JHUB.AND.I.EQ.IHUB)GO TO 433
      IF(I.LT.ISTEP)GO TO 401
      433 AW(I,J)=0.0
      401 CONTINUE
C-----TOP WALL
      J=JSTEP
      DO 420 I=2,NIM1
      IF(I.GE.ISTEP.AND.I.LE.ICUT) J=J+JINC
      IF(I.GT.ICON) J=JCON
      420 AN(I,J)=0.0
C-----SYMMETRY AXIS
      DO 403 I=IHUB,NIM1
      403 AS(I,2)=0.0
C-----OUTLET
      DO 404 J=2,JCON
      404 AE(NIM1,J)=0.0
C-----SIDE WALL 3
      IF(JCON.EQ.NJ)GO TO 406
      DO 405 J=JCNP1,NJM1
      405 AE(ICON,J)=0.0
      406 CONTINUE
C-----BOTTOM WALL
      IF(IHUB.LE.2)GO TO 475
      DO 407 I=2,IHBM1
      407 AS(I,JHUB)=0.0
      475 CONTINUE
      RETURN
C
CHAPTER 5 5 5 5 5 5 5 THERMAL ENERGY 5 5 5 5 5 5 5 5
C
      5 CONTINUE
      COX=1132.0
      CPR=1189.0
      CFU=2260.0
C-----SIDE WALLS 1 AND 2
      JFIN=JSTEP
      IEND=ICUT
      IF(LABRUPT) IEND=ISTEP
      DO 501 I=2,IEND
      IF(I.GE.ISTEP.AND.I.LE.ICUT) JFIN=JFIN+JINC
      DO 501 J=2,JFIN
      IF(J.GE.JHUB.AND.J.LE.(JFIN-JINC))GO TO 501
      IF(J.LT.JHUB.AND.I.EQ.IHUB)GO TO 533
      IF(I.LT.ISTEP)GO TO 501
      533 AW(I,J)=0.0

```



```

501 CONTINUE
C-----TOP WALL
  J=JSTEP
  DO 502 I=2,NIM1
    IF(I.GE.IEN1M.AND.I.LE.IEN1P) GO TO 502
    IF(I.GE.IEN2M.AND.I.LE.IEN2P) GO TO 502
    IF(I.GE.ISTEP.AND.I.LE.ICUT) J=J+JINC
    IF(I.GT.ICON) J=JCON
    RDY=RV(J+1)/((YV(J+1)-Y(J))*PRH)
    AN(I,J)=0.0
    CMIX=CFU*FU(I,J)+COX*OX(I,J)+CPR*AN2(I,J)
    HWALL=CMIX*TWALL+HFU*FU(I,J)+HCO*CO(I,J)
    TERM=VIS(I,J)*SEW(I)*RDY
    SU(I,J)=SU(I,J)+TERM*HWALL
    SP(I,J)=SP(I,J)-TERM
  502 CONTINUE
C-----SYMMETRY AXIS
  DO 503 I=IHUB,NIM1
    503 AS(I,2)=0.0
C-----OUTLET
C-----SIDE WALL
  IF(JCON.EQ.NJ)GO TO 508
  DO 506 J=JCNF1,NJM1
    506 AE(ICON,J)=0.0
  508 CONTINUE
C-----BOTTOM WALL
  IF(IHUB.LE.2)GO TO 575
  DO 507 I=2,IHBM1
    507 AS(I,JHUB)=0.0
  575 CONTINUE
  RETURN

C
C
CHAPTER 6 6 6 6 6 TURBULENT KINETIC ENERGY 6 6 6 6 6 6 6 6
C
  6 CONTINUE
C-----TOP WALL
  CDTERM=CMU**0.25
  J=JSTEP
  DO 610 I=2,NIM1
    IF(I.GE.IEN1M.AND.I.LE.IEN1P) GO TO 610
    IF(I.GE.IEN2M.AND.I.LE.IEN2P) GO TO 610
    IF(I.GT.ICON) J=JCON
    IF(I .GE. ISTEP .AND. I .LE. ICUT) J=J+JINC
    DWDR=(W(I,J+1)-W(I,J-1))/(DYNP(J)+DYPS(J))-W(I,J)/R(J)
    UAVG=DABS((U(I,J)+U(I+1,J))/2.)
    UEFF=DSQRT(UAVG*UAVG + W(I,J)*W(I,J))
    IF((U(I,J)+U(I+1,J))/2. .LT. 0.) UEFF=-UEFF
    YP=YV(J+1)-Y(J)
    DENU=DEN(I,J)
    SQRTK=DSQRT(TE(I,J))
    VOL=0.5*(RV(J+1)+RV(J))*SNS(J)*SEW(I)
    GENCOU=DABS(TAUN(I)*UEFF)/YP
    YPLUSN(I)=DENU*SQRTK*CDTERM*YP/VISCOS

```

```

      DUDY=((U(I,J)+U(I+1,J)+U(I,J+1)+U(I+1,J+1))/4.-(U(I,J)+U(I+1,J)+U(
41I,J-1)+U(I+1,J-1))/4.)/SNS(J)
      GENRES=GEN(I,J)-VIS(I,J)*(DUDY**2+DWDR**2)
      GEN(I,J)=GENRES+GENCOU
      IF (YPLUSN(I) .LE. 11.63) GO TO 611
      DITERM=DEN(I,J)*(CMU**.75)*SQRTK*DLOG(ELOG*YPLUSN(I))/(CAPPA*YP)
      GO TO 612
611 CONTINUE
      DITERM=DEN(I,J)*(CMU**.75)*SQRTK*YPLUSN(I)/YP
612 CONTINUE
      SU(I,J)=GEN(I,J)*VOL+SUKD(I,J)
      SP(I,J)=-DITERM*VOL+SPKD(I,J)
      AN(I,J)=0.0
610 CONTINUE
C-----SIDE WALLS 1 AND 2
      JFIN=JSTEP
      IEND=ICUT
      IF (LABRUPT) IEND=ISTEP
      DO 620 I=2,IEND
      IF (I.GE.ISTEP.AND.I.LE.ICUT) JFIN=JFIN+JINC
      DO 620 J=2,JFIN
      IF (J.GE.JHUB.AND.J.LE.(JFIN-JINC)) GO TO 620
      IF (I.LT.ISTEP) GO TO 620
      DWDX=(W(I+1,J)-W(I-1,J))/(DXPW(I)+DXEP(I))
      VAVG=DABS((V(I,J)+V(I,J+1))/2.)
      VEFF=DSQRT(VAVG*VAVG + W(I,J)*W(I,J))
      IF ((V(I,J)+V(I,J+1))/2. .LT. 0.) VEFF=-VEFF
      XP=X(I)-XU(I)
      DENV=DEN(I,J)
      SQRTK=DSQRT(TE(I,J))
      VOL=0.5*(RV(J+1)+RV(J))*SNS(J)*SEW(I)
      XPLUSW(J)=DENV*SQRTK*CDTERM*XP/VISCOS
      GENCOU=DABS(TAUW(J)*VEFF)/XP
      DVDX=((V(I,J)+V(I,J+1)+V(I+1,J)+V(I+1,J+1))/4.-(V(I,J)+V(I,J+1)+V(
3I-1,J)+V(I-1,J+1))/4.)/SEW(I)
      GENRES=GEN(I,J)-VIS(I,J)*(DVDX**2+DWDX**2)
      GEN(I,J)=GENRES+GENCOU
      IF (XPLUSW(J) .LE. 11.63) GO TO 621
      DITERM=DEN(I,J)*(CMU**.75)*SQRTK*DLOG(ELOG*XPLUSW(J))/(CAPPA*XP)
      GO TO 622
621 CONTINUE
      DITERM=DEN(I,J)*(CMU**.75)*SQRTK*XPLUSW(J)/XP
622 CONTINUE
      SU(I,J)=SU(I,J)+SUKD(I,J)+GEN(I,J)*VOL
      SP(I,J)=SP(I,J)+SPKD(I,J)-DITERM*VOL
      AW(I,J)=0.0
620 CONTINUE
C-----SYMMETRY AXIS
      J=2
      DO 630 I=IHUB,NIM1
      DUDY=((U(I,J)+U(I+1,J)+U(I,J+1)+U(I+1,J+1))/4.-(U(I,J)+U(I+1,J)+
3U(I,J-1)+U(I+1,J-1))/4.)/SNS(J)
      VOL=0.5*(RV(J+1)+RV(J))*SNS(J)*SEW(I)
      GEN(I,J)=GEN(I,J)-VIS(I,J)*DUDY**2

```

```

      SU(I,J)=SUKD(I,J)+GEN(I,J)*VOL
630 AS(I,2)=0.0
C-----SIDE WALL 3
      IF(JCON.EQ.NJ)GO TO 631
      I=ICON
      DO 640 J=JCNF1,NJM1
      XP=XU(I+1)-X(I)
      DENV=DEN(I,J)
      SQRTK=DSQRT(TE(I,J))
      VOL=0.5*(RV(J+1)+RV(J))*SNS(J)*SEW(I)
      XPLUSE(J)=DENV*SQRTK*CDTERM*XP/VISCOS
      GENCOU=0.5*(DABS(TAUE(J+1)*V(I,J+1))+DABS(TAUE(J)*V(I,J)))/XP
      DVDX=((V(I,J)+V(I,J+1)+V(I+1,J)+V(I+1,J+1))/4.-
1 (V(I,J)+V(I,J+1)+V(I-1,J)+V(I-1,J+1))/4.)/SEW(I)
      GENRES=GEN(I,J)-VIS(I,J)*DVDX**2
      GEN(I,J)=GENRES+GENCOU
      IF(XPLUSE(J).LE.11.63) GO TO 641
      DITERM=DEN(I,J)*(CMU**.75)*SQRTK*DLOG(ELOG*XPLUSE(J))/(CAPPA*XP)
      GO TO 642
641 DITERM=DEN(I,J)*(CMU**.75)*SQRTK*XPLUSE(J)/XP
642 CONTINUE
      SU(I,J)=SU(I,J)+SUKD(I,J)+GEN(I,J)*VOL
      SP(I,J)=SP(I,J)+SPKD(I,J)-DITERM*VOL
      AE(I,J)=0.0
640 CONTINUE
631 CONTINUE
      IF(IHUB.LE.2)GO TO 675
C-----BOTTOM WALL
      J=JHUB
      CDTERM=CMU**.25
      YP=Y(J)-YV(J)
      DO 650 I=2,IHBM1
      DENU=DEN(I,J)
      SQRTK=DSQRT(TE(I,J))
      VOL=0.5*(RV(J+1)+RV(J))*SNS(J)*SEW(I)
      GENCOU=0.5*(DABS(TAUS(I+1)*U(I+1,J))+DABS(TAUS(I)*U(I,J)))/XP
      YPLUSS(I)=DENU*SQRTK*CDTERM*YP/VISCOS
      DUDY=((U(I,J)+U(I+1,J)+U(I,J+1)+U(I+1,J+1))/4.-
1 (U(I,J)+U(I+1,J)+U(I,J-1)+U(I+1,J-1))/4.)/SNS(J)
      GENRES=GEN(I,J)-VIS(I,J)*DUDY**2
      GEN(I,J)=GENRES+GENCOU
      IF(YPLUSS(I).LE.11.63) GO TO 651
      DITERM=DEN(I,J)*(CMU**.75)*SQRTK*DLOG(ELOG*YPLUSS(I))/(CAPPA*YP)
      GO TO 652
651 DITERM=DEN(I,J)*(CMU**.75)*SQRTK*YPLUSS(I)/YP
652 SU(I,J)=GEN(I,J)*VOL+SUKD(I,J)
      SP(I,J)=-DITERM*VOL+SPKD(I,J)
650 AS(I,J)=0.0
675 CONTINUE
      RETURN

```

C
CHAPTER 7 7 7 7 7 7 7 7 DISSIPATION 7 7 7 7 7 7 7 7
C

7 CONTINUE

```

C-----TOP WALL
  J=JSTEP
  DO 710 I=2,NIM1
    IF(I.GE.IEN1M.AND.I.LE.IEN1P) GO TO 710
    IF(I.GE.IEN2M.AND.I.LE.IEN2P) GO TO 710
    IF(I.GT.ICON) J=JCON
    IF(I .GE. ISTEP .AND. I .LE. ICUT) J=J+JINC
    YP=YV(J+1)-Y(J)
    TERM=(CMU**.75)/(CAPPA*YP)
    IF(TE(I,J).LT.0.0) TE(I,J)=DABS(TE(I,J))
    SU(I,J)=GREAT*TERM*TE(I,J)**1.5
  710 SP(I,J)=-GREAT
C-----SIDE WALLS 1 AND 2
  JFIN=JSTEP
  IEND=ICUT
  IF(LABRUPT) IEND=ISTEP
  DO 720 I=2,IEND
    IF(I.GE.ISTEP.AND.I.LE.ICUT) JFIN=JFIN+JINC
    DO 720 J=2,JFIN
      IF(J.GE.JHUB.AND.J.LE.(JFIN-JINC)) GO TO 720
      IF(J.LT.JHUB.AND.I.EQ.IHUB) GO TO 733
      IF(I.LT.ISTEP) GO TO 720
      IF(J.EQ.JFIN) GO TO 720
  733 XP=X(I)-XU(I)
    TERM=(CMU**.75)/(CAPPA*XP)
    IF(TE(I,J).LT.0.0) TE(I,J)=DABS(TE(I,J))
    SU(I,J)=GREAT*TERM*TE(I,J)**1.5
    SP(I,J)=-GREAT
  720 CONTINUE
C-----SYMMETRY AXIS
  DO 730 I=IHUB,NIM1
    730 AS(I,2)=0.0
C-----SIDE WALL 3
  IF(JCON.EQ.NJ) GO TO 731
  I=ICON
  NJM2=NJ-2
  DO 740 J=JCNP1,NJM2
    XP=XU(I+1)-X(I)
    TERM=(CMU**.75)/(CAPPA*XP)
    IF(TE(I,J).LT.0.0) TE(I,J)=DABS(TE(I,J))
    SU(I,J)=GREAT*TERM*TE(I,J)**1.5
    SP(I,J)=-GREAT
  740 CONTINUE
  731 CONTINUE
C-----BOTTOM WALL
  IF(IHUB.LE.2) GO TO 775
  J=JHUB
  YP=Y(J)-YV(J)
  TERM=(CMU**.75)/(CAPPA*YP)
  DO 750 I=2,IHBM1
    IF(TE(I,J).LT.0.0) TE(I,J)=DABS(TE(I,J))
    SU(I,J)=GREAT*TERM*TE(I,J)**1.5
  750 SP(I,J)=-GREAT
  775 CONTINUE

```

[illegible]

```

      AW(I,J)=0.0
      850 CONTINUE
      TAUW(JSTEP)=TAUW(JSTP1)
      TAUW(NJ)=TAUW(NJM1)
C-----SYMMETRY AXIS
      DO 860 I=IHUB,NI
C60   AS(I,2)=0.
          TERM=W(I,3)*R(2)/R(3)
          SU(I,2)=GREAT*TERM
      860   SP(I,2)=-GREAT
C-----OUTLET
      DO 870 J=1, NJ
      870   AE(NIM1,J)=0.
C-----SIDE WALL 3
      IF(JCON.EQ.NJ)GO TO 807
      DO 805 J=JCNP1,NJM1
      805   AE(ICON,J)=0.0
      807 CONTINUE
C-----BOTTOM WALL
      IF(IHUB.LE.2)GO TO 875
      DO 806 I=2,IHBM1
      806   AS(I,JHUB)=0.0
      875 CONTINUE
      RETURN

C
CHAPTER 9 9 9 9 9 9 9 9 FUEL 9 9 9 9 9 9 9 9 9
C
      9 CONTINUE
C-----SIDE WALLS 1 AND 2
      JFIN=JSTEP
      IEND=ICUT
      IF(LABRUPT) IEND=ISTEP
      DO 901 I=2, IEND
      IF(I.GE.ISTEP.AND.I.LE.ICUT) JFIN=JFIN+JINC
      DO 901 J=2, JFIN
      IF(J.GE.JHUB.AND.J.LE.(JFIN-JINC))GO TO 901
      IF(J.LT.JHUB.AND.I.EQ.IHUB)GO TO 933
      IF(I.LT.ISTEP)GO TO 901
      933 AW(I,J)=0.0
      901 CONTINUE
C-----TOP WALL
      J=JSTEP
      DO 902 I=2,NIM1
      IF(I.GE.IEN1M.AND.I.LE.IEN1P) GO TO 902
      IF(I.GE.IEN2M.AND.I.LE.IEN2P) GO TO 902
      IF(I.GE.ISTEP.AND.I.LE.ICUT) J=J+JINC
      IF(I.GT.ICON) J=JCON
      AN(I,J)=0.0
      902 CONTINUE
C-----SYMMETRY AXIS
      DO 903 I=IHUB,NIM1
      903 AS(I,2)=0.0
C-----OUTLET
C

```

```

C-----SIDE WALL 3
  IF(JCON.EQ.NJ) GO TO 907
  DO 905 J=JCNP1,NJM1
    905 AE(ICON,J)=0.0
  907 CONTINUE
C-----BOTTOM WALL
  IF(IHUB.LE.2)GO TO 975
  DO 906 I=2,IHBM1
    906 AS(I,JHUB)=0.0
  975 CONTINUE
  RETURN

C
CHAPTER 10 10 10 10 10 OXFU = OX - I * FU 10 10 10 10 10 10 10 10
C
  10 CONTINUE
C-----SIDE WALLS 1 AND 2
  JFIN=JSTEP
  IEND=ICUT
  IF(LABRUPT) IEND=ISTEP
  DO 1001 I=2,IEND
    IF(I.GE.ISTEP.AND.I.LE.ICUT) JFIN=JFIN+JINC
    DO 1001 J=2,JFIN
      IF(J.GE.JHUB.AND.J.LE.(JFIN-JINC))GO TO 1001
      IF(J.LT.JHUB.AND.I.EQ.IHUB)GO TO 1033
      IF(I.LT.ISTEP)GO TO 1001
    1033 AW(I,J)=0.0
  1001 CONTINUE
C-----TOP WALL
  J=JSTEP
  DO 1002 I=2,NIM1
    IF(I.GE.IEN1M.AND.I.LE.IEN1P) GO TO 1002
    IF(I.GE.IEN2M.AND.I.LE.IEN2P) GO TO 1002
    IF(I.GE.ISTEP.AND.I.LE.ICUT) J=J+JINC
    IF(I.GT.ICON) J=JCON
    AN(I,J)=0.0
  1002 CONTINUE
C-----SYMMETRY AXIS
  DO 1003 I=IHUB,NIM1
    1003 AS(I,2)=0.0
C-----OUTLET
C-----SIDE WALL 3
  IF(JCON.EQ.NJ)GO TO 1007
  DO 1005 J=JCNP1,NJM1
    1005 AE(ICON,J)=0.0
  1007 CONTINUE
C-----BOTTOM WALL
  IF(IHUB.LE.2)GO TO 1075
  DO 1006 I=2,IHBM1
    1006 AS(I,JHUB)=0.0
  1075 CONTINUE
  RETURN

C
C
CHAPTER 11 11 11 11 11 11 RADIATION-X-DIRECTION 11 11 11 11 11

```

```

C
  11 CONTINUE
C-----SIDE WALLS 1 AND 2
      JFIN=JSTEP
      IEND=ICUT
      IF(LABRUPT) IEND=ISTEP
      DO 1101 I=2,IEND
      IF(I.GE.ISTEP.AND.I.LE.ICUT) JFIN=JFIN+JINC
      DO 1102 J=2,JFIN
      IF(I.GT.ISTEP.AND.J.LT.(JFIN-JINC))GO TO 1102
      IF(.NOT.(I.EQ.ISTEP.AND.J.GE.JHUB.AND.J.LE.(JFIN-JINC)))GO TO 90
      SU(I,J)=SU(I,J)+RADIN
      SP(I,J)=SP(I,J)-1.
  90 CONTINUE
      IF(I.LT.ISTEP) GO TO 1102
      GAMW=1./(ABSOR+SCATT)
      VOL=R(J)*SNS(J)*SEW(I)
      SU(I,J)=SU(I,J)+EMIW*SIGMA*TWALL**4.
C      1+GAMW*RADX(I+1,J)/(X(I+1)-X(I))
      SP(I,J)=SP(I,J)-EMIW
C      1-GAMW/(X(I+1)-X(I))
      AW(I,J)=0.0
  1102 CONTINUE
  1101 CONTINUE
C-----SYMMETRY AXIS
C      SIDE WALL 3
      IF(JCON.EQ.NJ) GO TO 1105
      I=ICON
      DO 1104 J=JCNPL,NJM1
      VOL=R(J)*SNS(J)*SEW(I)
      GAME=1./(ABSOR+SCATT)
      SU(I,J)=SU(I,J)+EMIW*SIGMA*TWALL**4.
C      1+GAME*RADX(I-1,J)/(X(I)-X(I-1))
      SP(I,J)=SP(I,J)-EMIW
C      1-GAME/(X(I)-X(I-1))
  1104 AE(I,J)=0.0
  1105 CONTINUE
C-----TOP WALL
      DO 1111 J=2,JCON
      1111 AE(NIM1,J)=0.0
      RETURN
C
CHAPTER 12 12 12 12 12 RADIATION-R-DIRECTION 12 12 12 12 12
C
  12 CONTINUE
C-----SIDE WALLS 1 AND 2
C-----SYMMETRY AXIS
      J=2
      DO 1203 I=IHUB,NIM1
      1203 AS(I,J)=0.0
C      SIDE WALL 3
C-----TOP WALL
      J=JSTEP
      DO 1210 I=2,NIM1

```



```

      IF(I.GE.IEN1M.AND.I.LE.IEN1P) GO TO 1215
      IF(I.GE.IEN2M.AND.I.LE.IEN2P) GO TO 1215
      IF(I.GT.ICON) J=JCON
      IF(I.GE.ISTEP.AND.I.LE.ICUT) J=J+JINC
      GAMN=(ABSOR+SCATT)
      IF(INDCOS.EQ.2) GAMN=GAMN+1./(RV(J)+1.E-30)
      GAMN=1./GAMN
      VOL=R(J)*SNS(J)*SEW(I)
      SU(I,J)=SU(I,J)+EMIW*SIGMA*TWALL**4.*RV(J+1)
C      1+GAMN*RADR(I,J-1)/(R(J)-R(J-1))*RV(J+1)
      SP(I,J)=SP(I,J)-EMIW*RV(J+1)
C      1-GAMN/(R(J)-R(J-1))*RV(J+1)
      1210 AN(I,J)=0.0
      1215 CONTINUE
C-----BOTTOM WALL
      IF(IHUB.LE.1) GO TO 1275
      J=JHUB
      DO 1250 I=2,IHBM1
      VOL=R(J)*SNS(J)*SEW(I)
      GAMS=(ABSOR+SCATT)
      IF(INDCOS.EQ.2) GAMS=GAMS+1./(RV(J)+1.E-30)
      GAMS=1./GAMS
      SU(I,J)=SU(I,J)+EMIW*SIGMA*TWALL**4.*RV(J)
C      1+GAMS*RADR(I,J+1)/(R(J+1)-R(J))*RV(J+1)
      SP(I,J)=SP(I,J)-EMIW*RV(J)
C      1-GAMS/(R(J+1)-R(J))*RV(J+1)
      1250 AS(I,J)=0.0
      1275 CONTINUE
      DO 1211 I=IHUB,NIM1
      1211 AS(I,2)=0.0
      RETURN
      END
      SUBROUTINE TEMPND
      IMPLICIT REAL*8(A-H,O-Z)
C----- THIS NONDIMENSIONALIZES TEMPERATURE
      COMMON
      1/FLUPR/URFVIS,VISCOS,DENSIT,PRANDT,DEN(40,15),VIS(40,15)
      2      ,OX(40,15),AN2(40,15),T(40,15),RFUP(40,15),RCOP(40,15)
      1,CO(40,15),H2O(40,15),H2(40,15),CO2(40,15),FUGLD(40,15),O1(40,15)
      1/ALL/IT,JT,NI,NJ,NIM1,NJM1,GREAT
      1/DIMTEM/TT(40,15)
      TMAX=T(1,1)
      DO 1 I=2,NIM1
      DO 2 J=2,NJM1
      IF(T(I,J).GE.TMAX) TMAX=T(I,J)
      2 CONTINUE
      1 CONTINUE
      DO 3 I=1,NI
      DO 3 J=1,NJ
      TT(I,J)=T(I,J)/TMAX
      3 CONTINUE
      RETURN
      END
      SUBROUTINE SOLVRX(ISTART,JSTART,NI,NJ,IT,JT,PHI,NCHAP)

```

```

      IMPLICIT REAL*8(A-H,O-Z)
C*****
C
CHAPTER 0 0 0 0 0 0 0 0 PRELIMINARIES 0 0 0 0 0 0 0 0
C
      DIMENSION PHI(IT,JT),A(40),B(40),C(40),D(40)
      COMMON
      1/COEF/AP(40,15),AN(40,15),AS(40,15),AE(40,15),AW(40,15),SU(40,15),
      1      SP(40,15)
      1/GEOM2/IHUB,JHUB,IHBP1,JHBP1,IHEM1,JHEM1,ICON,JCON,ICNP1,JCNP1
      1/KASE T1/UIN,TEIN,EDIN,FLOWIN,ALAMDA,
      2      RSMALL,RLARGE,AL1,AL2,JSTEP,ISTEP,JSTP1,JSTM1,ISTP1,ISTM1,J
      3INC,ICUT,ICTP1
      1/GEOM1/INDCOS,X(40),Y(40),DXEP(40),DXPW(40),DYNP(40),DYPS(40),
      1      SNS(40),SEW(40),XU(40),YV(40),R(40),RV(40),LABRUPT
      LOGICAL LABRUPT
      NIM1=NI-1
      NJM1=NJ-1
C-----COMMENCE N-S SWEEP
      JSTA=JSTART
      JEND=NJM1
      IEND=NIM1
      IBEG=0
      JFIX=0
      ISTA=ISTART
      DO 200 J=JSTA,JEND
      IF(J.LT.JHUB) ISTA=IHUB
      IF(J.GT.JCON) IEND=ICON
      IF(LABRUPT.AND.J.GE.JSTP1) GO TO 70
      IF(J.EQ.JSTP1) ISTA=ISTEP
      IF(J.GT.JSTEP.AND.J.LE.NJM1) JFIX=JFIX+1
      IF(JFIX.GT.JINC) IBEG=ISTA+1
      IF(IBEG.GT.ISTA) GO TO 80
      GO TO 90
80    JFIX=1
      ISTA=IBEG
      GO TO 90
70    ISTA=ISTEP
90    CONTINUE
      ISM1=ISTA-1
      IENDP1=IEND+1
      A(ISM1)=0.0
      B(ISM1)=0.0
      DO 300 I=ISTA,IEND
      IF((I.LT.IHUB.AND.J.LT.JHUB).OR.(I.LT.ISTEP.AND.J.GT.JSTEP))
1GO TO 300
      STORE=AP(I,J)-AW(I,J)*A(I-1)
      A(I)=AE(I,J)/STORE
      B(I)=(SU(I,J)+AW(I,J)*B(I-1))/STORE
      CALL DVCHK (ILAS)
      IF(ILAS.EQ.1) PRINT ,I,J,AP(I,J),SP(I,J),AN(I,J),AS(I,J),AE(I,J),
1AW(I,J),NCHAP
300  CONTINUE
      ISUM=ISTA+IEND

```

```

      DO 301 IJ=ISTA,IEND
      I=ISUM-IJ
      PHI(I,J)=A(I)*PHI(I+1,J)+B(I)
301  CONTINUE
200  CONTINUE
      RETURN
      END
      SUBROUTINE SOLVRR(ISTART,JSTART,NI,NJ,IT,JT,PHI,NCHAP)
      IMPLICIT REAL*8(A-H,O-Z)
C*****
C
CHAPTER 0 0 0 0 0 0 0 0 PRELIMINARIES 0 0 0 0 0 0 0 0
C
      DIMENSION PHI(IT,JT),A(40),B(40),C(40),D(40)
      COMMON
      1/COEF/AP(40,15),AN(40,15),AS(40,15),AE(40,15),AW(40,15),SU(40,15),
      1      SP(40,15)
      1/GEOM2/IHUB,JHUB,IHBP1,JHBP1,IHBM1,JHBM1,ICON,JCON,ICNP1,JCNP1
      1/KASE T1/UIN,TEIN,EDIN,FLOWIN,ALAMDA,
      2      RSMALL,RLARGE,AL1,AL2,JSTEP,ISTEP,JSTP1,JSTM1,ISTP1,ISTM1,J
      3INC,ICUT,ICTP1
      NIM1=NI-1
      NJM1=NJ-1
C-----COMMENCE W-E SWEEP
      JEND=JSTEP
      DO 100 I=ISTART,NIM1
      IF(NCHAP.EQ. 2) GO TO 50
      IF(I.GE. ISTEP.AND. I.LE. ICUT) JEND=JEND+JINC
      GO TO 70
50  CONTINUE
      IF(I.GE. ISTP1.AND. I.LE. ICTP1) JEND=JEND+JINC
70  CONTINUE
      JSTA=JSTART
      IF(I.LT. (IHUB+ISTART-2)) JSTA=JHUB+JSTART-2
      JSM1=JSTA-1
      JENDP1=JEND+1
      A(JSM1)=0.0
      B(JSM1)=0.0
C-----COMMENCE S-N TRAVERSE
      DO 101 J=JSTA,JEND
      IF((I.LT.IHUB.AND.J.LT.JHUB).OR.(I.LT.ISTEP.AND.J.GT.JSTEP))
      1GO TO 101
C-----ASSEMBLE TDMA COEFFICIENTS
      STORE=AP(I,J)-AS(I,J)*A(J-1)
      A(J)=AN(I,J)/STORE
      B(J)=(SU(I,J)+AS(I,J)*B(J-1))/STORE
C-----CALCULATE COEFFICIENTS OF RECURRENCE FORMULA
      CALL DVCHK (ILAS)
      IF(ILAS.EQ.1)PRINT ,I,J,AP(I,J),SP(I,J),AN(I,J),AS(I,J),AE(I,J),
      1AW(I,J),NCHAP
      101 CONTINUE
C-----OBTAIN NEW PHI)S
      JSUM=JSTA+JEND
      DO 102 JJ=JSTA,JEND

```

```

      J=JSUM-JJ
102 PHI(I,J)=A(J)*PHI(I,J+1)+B(J)
100 CONTINUE
      RETURN
      END
      SUBROUTINE CALCQ
      IMPLICIT REAL*8(A-H,O-Z)

```

```

C
CHAPTER 0 0 0 0 0 0 PRELIMINARIES 0 0 0 0 0 0 0 0
C

```

```

COMMON

```

```

C
1/SWEN/PRW,WWALL,RESORH,NSWPH,URFH,PRH,TWALL
*/VAR/U(40,15),V(40,15),W(40,15),P(40,15),PP(40,15),TE(40,15),
1ED(40,15),H(40,15),FU(40,15),OF(40,15)
1/FLUPR/URFVIS,VISCOS,DENSIT,PRANDT,DEN(40,15),VIS(40,15)
1      ,OX(40,15),AN2(40,15),T(40,15),RFUP(40,15),RCOP(40,15)
1,CO(40,15),H2O(40,15),H2(40,15),CO2(40,15),FUOLD(40,15),OI(40,15)
1/COEF/AP(40,15),AN(40,15),AS(40,15),AE(40,15),AW(40,15),SU(40,15),
1      SP(40,15)
1/ALL/IT,JT,NI,NJ,NIM1,NJM1,GREAT
1/GEOM1/INDCOS,X(40),Y(40),DXEP(40),DXPW(40),DYNP(40),DYPS(40),
1      SNS(40),SEW(40),XU(40),YV(40),R(40),RV(40),LABRUPT
1/GEOM2/IHUB,JHUB,IHBP1,JHBP1,IHBM1,JHBM1,ICON,JCON,ICNP1,JCNP1
1/CHEM/URFDEN,GASCON,CFU,COX,CPR,WFU,WOX,WPR,HFU,HCO,OXDFU,PRESS
1,CCO,CCO2,CH2O,CAN2,RESORC,NSWPC,URFCO,PRCO,OXDCO,OXDFU1,WCO
1,WH2O,WCO2,WAN2,PERSTO,WH2,CH2,WO1,CO1
1/KASE T1/UIN,TEIN,EDIN,FLOWIN,ALAMDA,
2      RSMALL,RLARGE,AL1,AL2,JSTEP,ISTEP,JSTP1,JSTM1,ISTP1,ISTM1,J
3INC,ICUT,ICTP1
1/RADT/RADX(40,15),RADR(40,15),RADIN
2      ,EMIW,NSWPRX,NSWPRR,URFRX,URFRR,SIGMA,ABSOR,SCATT
3      ,RESORR,RESORX
1/QRAD/QX(40,15),QR(40,15),Q(40,15)
NIM2=NIM1-1
JFIN=JSTM1
DO 100 I=2,NIM1
JSTA=2
IF(I.LE.IHUB)JSTA=JHUB
IF(I.GE.ISTEP.AND.I.LE.ICUT)JFIN=JFIN+JINC
IF(I.GT.ICUT)JFIN=NJM1
IF(I.GT.ICON)JFIN=JCON-1
DO 101 J=JSTA,JFIN
QX(I,J)=-2./(ABSOR+SCATT)*(RADX(I+1,J)-RADX(I,J))/DXEP(I)
QR(I,J)=-2./(ABSOR+SCATT+1/R(J))*(RADR(I,J+1)-RADR(I,J))/DYNP(J)
THETA=DATAN(DABS(QR(I,J)/QX(I,J)))
Q(I,J)=QR(I,J)/DSIN(THETA)
101 CONTINUE
100 CONTINUE
      RETURN
      END
C
      SUBROUTINE CALCNO
      IMPLICIT REAL*8(A-H,O-Z)

```

```

C
CHAPTER 0 0 0 0 0 0 PRELIMINARIES 0 0 0 0 0 0 0 0
C
COMMON
C
1/FUOF/RESORF,NSWPF,URFF,PRFU,FUWALL,RESORO,NSWPO,URFO,PROF,OFWALL
*/VAR/U(40,15), V(40,15), W(40,15), P(40,15), PP(40,15), TE(40,15),
1ED(40,15),H(40,15),FU(40,15),OF(40,15)
1/FLUPR/URFVIS,VISCOS,DENSIT,PRANDT,DEN(40,15),VIS(40,15)
1      ,OX(40,15),AN2(40,15),T(40,15),RFUP(40,15),RCOP(40,15)
1.CO(40,15),H2O(40,15),H2(40,15),CO2(40,15),FUOLD(40,15),O1(40,15)
1/COEF/AP(40,15),AN(40,15),AS(40,15),AE(40,15),AW(40,15),SU(40,15),
1      SP(40,15)
1/ALL/IT,JI,NI,NJ,NIM1,NJM1,GREAT
1/GEOM1/INDCOS,X(40),Y(40),DXEP(40),DXPW(40),DYNP(40),DYPS(40),
1      SNS(40),SEW(40),XU(40),YV(40),R(40),RV(40),LABRUPT
1/GEOM2/IHUB,JHUB,IHBP1,JHBP1,IHBM1,JHBM1,ICON,JCON,ICNP1,JCNP1
1/CHEM/URFDEN,GASCON,CFU,COX,CPR,WFU,WOX,WPR,HFU,HCO,OXDFU,PRESS
1,CCC,CCO2,CH2O,CAN2,RESORC,NSWPC,URFCO,PRCO,OXDCO,OXDFU1,WCO
1,WH2O,WCO2,WAN2,PERSTO,WH2,CH2,WO1,CO1
1/CHEM2/FUIN,AX,AY,AO
1/REAC/RFUEBU(40,15),RFUARR(40,15),NITER,RCOARR(40,15)
1,RCOEBU(40,15)
1/KASE T1/UIN,TEIN,EDIN,FLOWIN,ALAMDA,
2      RSMALL,RLARGE,AL1,AL2,JSTEP,ISTEP,JSTP1,JSTM1,ISTP1,ISTM1,J
3INC,ICUT,ICTP1
COMMON
1/NITRO1/WN1,WNO,CN1,CNO,URFNO,AN1(40,15),ANO(40,15),NSWPN0
2,URFN1,PRNO,RESRNO,RNOF1(40,15),RNOF2(40,15)
3,RNOR2(40,15),RNOR1(40,15)
C
C
CHAPTER 1 1 1 1 1 1 1 ASSEMBLY OF COEFFOCOENTS 1 1 1 1 1 1
C
RAT1=WNO/WAN2
RAT2=WNO/WN1
JFIN=JSTEP
DO 100 I=2,NIM1
DO 101 J=2,NJM1
C-----COMPUTE AREAS AND VOLUME
AREAN=RV(J+1)*SEW(I)
AREAS=RV(J)*SEW(I)
AREAEW=R(J)*SNS(J)
VOL=AREAEW*SEW(I)
C-----CALCULATE CONVECTION COEFFICIENTS
GN=0.5*(DEN(I,J)+DEN(I,J+1))*V(I,J+1)
GS=0.5*(DEN(I,J)+DEN(I,J-1))*V(I,J)
GE=0.5*(DEN(I,J)+DEN(I+1,J))*U(I+1,J)
GW=0.5*(DEN(I,J)+DEN(I-1,J))*U(I,J)
CN=GN*AREAN
CS=GS*AREAS
CE=GE*AREAEW
CW=GW*AREAEW
C-----CALCULATE DIFFUSION COEFFICIENTS

```

```

      GAMN=0.5*(VIS(I,J)+VIS(I,J+1))/PRNO
      GAMS=0.5*(VIS(I,J)+VIS(I,J-1))/PRNO
      GAME=0.5*(VIS(I,J)+VIS(I+1,J))/PRNO
      GAMW=0.5*(VIS(I,J)+VIS(I-1,J))/PRNO
      DN=GAMN*AREAN/DYNP(J)
      DS=GAMS*AREAS/DYPS(J)
      DE=GAME*AREAEW/DXEP(I)
      DW=GAMW*AREAEW/DXPW(I)
C-----SOURCE TERMS
      SMP=CN-CS+CE-CW
      CP=DMAX1(0.0,SMP)
      CPO=CP
C-----ASSEMBLE MAIN COEFFICIENTS
      AN(I,J)=DMAX1(DABS(0.5*CN),DN)-0.5*CN
      AS(I,J)=DMAX1(DABS(0.5*CS),DS)+0.5*CS
      AE(I,J)=DMAX1(DABS(0.5*CE),DE)-0.5*CE
      AW(I,J)=DMAX1(DABS(0.5*CW),DW)+0.5*CW
      SU(I,J)=CPO*ANO(I,J)
      SP(I,J)=-CP
      IF(I.LT.ISTEP) GO TO 106
C      IF(ANO(I,J).LT.1E-20.OR.OX(I,J).LT.1E-8) GO TO 102
C-----SOURCE TERM FOR RAN2 = CONSUMPTION OF FUEL
C-----ARRHENIUS MODEL
      TEMP=T(I,J)
      FLAG=0.0
      FLAG1=0.0
      IF(TEMP.LT.700)GO TO 10
      RNOF1(I,J)=6.192E+10*TEMP**0.1*DEXP(-37888/TEMP)/28.
      GO TO 9
10      RNOF1(I,J)=0.0
9      CONTINUE
      RNOF2(I,J)=6.43E+06*TEMP**1.0*DEXP(-3150/TEMP)/14.
      IF(ANO(I,J).LT.1E-20.AND.AN1(I,J).LT.1E-20)FLAG=1.
      IF(FLAG.EQ.1.)GO TO 103
      MIXF1=(AN1(I,J)*WN1+ANO(I,J)*WNO)/(ANO(I,J)+AN1(I,J))
      RNOR1(I,J)=3.1E+10*DEXP(-168.2/TEMP)/MIXF1
103 IF(ANO(I,J).LT.1E-20.AND.O1(I,J).LT.1E-20)FLAG1=1.
      IF(FLAG1.EQ.1.)GO TO 104
      MIXF2=(O1(I,J)*WO1+ANO(I,J)*WNO)/(O1(I,J)+ANO(I,J))
      RNOR2(I,J)=3.661E+05*TEMP**1.16*DEXP(-19077/TEMP)/MIXF2
104 IF(FLAG.EQ.1.0.AND.FLAG1.EQ.1.)GO TO 106
      IF(FLAG.NE.1.)SP(I,J)=SP(I,J)-RNOR1(I,J)*VOL*AN1(I,J)
      IF(FLAG1.NE.1.)SP(I,J)=SP(I,J)-RNOR2(I,J)*VOL*O1(I,J)
106 SU(I,J)=SU(I,J)+RNOF1(I,J)*VOL*RAT1*AN2(I,J)*O1(I,J)
      1+RNOF2(I,J)*VOL*RAT2*AN1(I,J)*OX(I,J)
101 CONTINUE
100 CONTINUE
C
CHAPTER 2 2 2 2 2 2 2 PROBLEM MODIFICATIONS 2 2 2 2 2 2 2
C
      NCHAP=9
      CALL PROMOD(NCHAP)
C
CHAPTER 3 FINAL COEFFICIENT ASSEMBLY AND RESIDUAL SOURCE CALCULATION 3

```

```

C
  RESRNO=0.0
  DO 300 I=2,NIM1
  DC 301 J=2,NJM1
  AP(I,J)=AN(I,J)+AS(I,J)+AE(I,J)+AW(I,J)-SP(I,J)
  RESOR=AN(I,J)*ANO(I,J+1)+AS(I,J)*ANO(I,J-1)+AE(I,J)*ANO(I+1,J)
1    +AW(I,J)*ANO(I-1,J)-AP(I,J)*ANO(I,J)+SU(I,J)
  VOL=R(J)*SNS(J)*SEW(I)
  SORVOL=GREAT*VOL
  IF(-SP(I,J).GT.0.5*SORVOL) RESOR=0.0
  RESRNO=RESRNO+DABS(RESOR)
C-----UNDER-RELAXATION
  AP(I,J)=AP(I,J)/URFNO
  SU(I,J)=SU(I,J)+(1.-URFNO)*AP(I,J)*ANO(I,J)
  301 CONTINUE
  300 CONTINUE
C
CHAPTER 4 4 4 4 4 4 SOLUTION OF DIFFERENCE EQUATION 4 4 4 4
C
  DO 400 N=1,NSWPNO
  400 CALL LISOLV(2,2,NI,NJ,IT,JT,ANO,NCHAP)
  RETURN
  END
  SUBROUTINE TPRINT(ISTART,JSTART,NI,NJ,IT,JT,X,Y,PHI,HEAD)
  IMPLICIT REAL*8(A-H,O-Z)
C*****
C
  CHARACTER*36 HEAD(9)
  DIMENSION PHI(IT,JT),X(IT),Y(JT),STORE(50)
  ISKIP=1
  JSKIP=1
  WRITE(6,110)HEAD
  ISTA=ISTART-11
100 CONTINUE
  ISTA=ISTA+11
  IEND=ISTA+10
  IF(NI.LT.IEND) IEND=NI
  WRITE(6,111)(I,I=ISTA,IEND,ISKIP)
  WRITE(6,114)(X(I),I=ISTA,IEND,ISKIP)
  WRITE(6,112)
  DO 101 JJ=JSTART,NJ,JSKIP
  J=JSTART+NJ-JJ
  DO 120 I=ISTA,IEND
  A=PHI(I,J)
  IF(DABS(A).LT.1.E-20) A=0.0
120 STORE(I)=A
  101 WRITE(6,113)J,Y(J),(STORE(I),I=ISTA,IEND,ISKIP)
C-----
  IF(IEND.LT.NI)GO TO 100
  RETURN
110 FORMAT(1H0,17(2H*-),7X,9A4,7X,17(2H*-))
111 FORMAT(1H0,14H I = ,I2,10I10)
112 FORMAT(8H0 J Y)
113 FORMAT(I3,0PF7.3,1X,1P11E10.3)

```

```

114 FORMAT(12H          X = ,F6.3,10F10.3)
      END
C***** BOUNDARY FIX SUBROUTINE*****
      SUBROUTINE FIXBND
      IMPLICIT REAL*8(A-H,O-Z)
C*****
      COMMON
C
      1/SWEN/PRW,WWALL,RESORH,NSWPH,URFH,PRH,TWALL
      1/FLUPR/URFVIS,VISCOS,DENSIT,PRANDT,DEN(40,15),VIS(40,15)
      1      ,OX(40,15),AN2(40,15),T(40,15),RFUP(40,15),RCOP(40,15)
      1,CO(40,15),H2O(40,15),H2(40,15),CO2(40,15),FUOLD(40,15),O1(40,15)
      1/ALL/IT,JT,NI,NJ,NIM1,NJM1,GREAT
      1/GEOM2/IHUB,JHUB,IHBP1,JHBP1,IHBM1,JHBM1,ICON,JCON,ICNP1,JCNP1
      1/KASE T1/UIN,TEIN,EDIN,FLOWIN,ALAMDA,
      2      RSMALL,RLARGE,AL1,AL2,JSTEP,ISTEP,JSTP1,JSTM1,ISTP1,ISTM1,J
      3INC,ICUT,ICTP1
      1/RADT/RADX(40,15),RADR(40,15),RADIN
      2      ,EMIW,NSWPRX,NSWPRR,URFRX,URFRR,SIGMA,ABSOR,SCATT
      3      ,RESORR,RESORX
      JFIN=JSTEP
      DO 1 I=1,NI
      IF(I.GE.ISTEP.AND.I.LE.ICUT) JFIN=JFIN+JINC
      IF(I.GT.ICON) JFIN=JCON
      DO 2 J=1,NJ
      IF(.NOT.(I.LT.IHUB.AND.J.LT.JHUB))GO TO 4
      T(I,J)=TWALL
      RADX(I,J)=SIGMA*T(I,J)**4.
      RADR(I,J)=RADX(I,J)
4 CONTINUE
      IF(J.LE.JFIN)GO TO 5
      T(I,J)=TWALL
      RADX(I,J)=SIGMA*T(I,J)**4.
      RADR(I,J)=RADX(I,J)
5 CONTINUE
2 CONTINUE
1 CONTINUE
      RETURN
      END

```


APPENDIX F

MAJOR FORTRAN VARIABLES

| | |
|----------|---|
| A(J) | = Coefficient of recurrence relation |
| ABSOR | = Absorptivity (= 0.1) |
| AE(I,J) | = Coefficient of combined convective/diffusive flux through east-wall of control volume |
| AL1 | = X-coordinate of inlet boundary of flow domain |
| AL2 | = X-coordinate of outlet boundary of flow domain |
| ALAMDA | = Length scale factor at inlet of flow domain |
| ALTOT | = Total length of pipe of larger diameter |
| AN(I,J) | = Coefficient of combined convective/diffusive flux through north-wall of control volume |
| ANO(I,J) | = Mass fraction of Nitrogen Oxide, NO |
| AN1(I,J) | = Mass fraction of Nitrogen, N |
| AN2(I,J) | = Mass fraction of Nitrogen, N ₂ |
| AP(I,J) | = Sum of coefficients of combined convective/diffusive fluxes through all four walls of control volume |
| AREAEW | = Area of east/west wall of control volume |
| AREAN | = Area of north-wall of control volume |
| AREAS | = Area of south-wall of control volume |
| ARDEN | = Area of east/west cell-wall times density of fluid |
| ARDENT | = Sum of all east/wall ARDEN at a cross-section |
| AS(I,J) | = Coefficient of combined convective/diffusive flux through south-wall of control volume |

| | |
|------------------|---|
| AW(I,J) | = Coefficient of combined convective/diffusive flux through west-wall of control volume |
| B(J) | = Coefficient of recurrence formulae |
| C(J) | = Coefficient of recurrence relation |
| C1 | = Constant of turbulence model (= 1.44) |
| C2 | = Constant of turbulence model (= 1.92) |
| CAN2 | = Specific heat of N ₂ |
| CAPPA | = Von Karman constant (= 0.4187) |
| CCO | = Specific heat of CO |
| CCO ₂ | = Specific heat of CO ₂ |
| CD | = Constant of turbulence model (= 1.0) |
| CDTERM | = CMU * * 0.25 |
| CE | = Coefficient of convective flux through east-wall of control volume |
| CFU | = Specific heat of fuel |
| CH2 | = Specific heat of H ₂ |
| CH2O | = Specific heat of H ₂ O |
| CMIX | = Mixture specific heat |
| CMU | = Constant of turbulence model (= 0.09) |
| CN | = Coefficient of convective flux through north-wall of control volume |
| CN1 | = Specific heat of N |
| CNO | = Specific heat of NO |
| CO(I,J) | = Mass fraction of CO |
| CO1 | = Specific heat of O |
| CO2(I,J) | = Mass fraction of CO ₂ |
| COX | = Specific heat of O ₂ |

| | |
|----------|---|
| CP | = Maximum of zero and net outflow (SMP) from control volume |
| CPR | = Specific heat of N_2 (Initial Value) |
| CPO | = CP |
| CS | = Coefficient of convective flux through south-wall of control volume |
| CW | = Coefficient of convective flux through west-wall of control volume |
| D(J) | = Coefficient of recurrence formulae |
| DE | = Coefficient of diffusive flux through east-wall of control volume |
| DEN(I,J) | = Density of fluid |
| DENSIT | = Density of fluid at inlet of the calculation domain |
| DITERM | = Coefficient of volume intergral of energy dissipation rate in vicinity of walls |
| DN | = Coefficient of diffusive flux through north-wall of control volume |
| DS | = Coefficient of diffusive flux through south-wall of control volume |
| DU(I,J) | = Coefficient of velocity-correction term for U velocity |
| DUDX | = $\partial u / \partial x$ at main grid node (I,J) |
| DUDY | = $\partial u / \partial y$ at main grid node (I,J) |
| DV(I,J) | = Coefficient of velocity-correction term for V velocity |
| DVDX | = $\partial v / \partial x$ at main grid node (I,J) |
| DVDY | = $\partial v / \partial y$ at main grid node (I,J) |
| DW | = Coefficient of diffusive flux through west wall of control volume |

| | |
|----------|---|
| DWDX | = $\partial W / \partial x$ at main grid node (I,J) |
| DWDR | = $\partial W / \partial r$ at main grid node (I,J) |
| DXEP(I) | = $X(I + 1) - X(I)$ |
| DXEPU(I) | = $XU(I + 1) - XU(I)$ |
| DXPW(I) | = $X(I) - X(I - 1)$ |
| DYNP(J) | = $Y(J + 1) - Y(J)$ |
| DYNPV(J) | = $YV(J + 1) - YV(J)$ |
| DYPS(J) | = $Y(J) - Y(J - 1)$ |
| DYPSV(J) | = $YV(J) - YV(J - 1)$ |
| ED(I,J) | = Energy dissipation rate, ϵ |
| EDIN | = Energy dissipation rate at inlet of flow domain (ϵ_{in}) |
| ELOG | = Constant of P-function for heat transfer at walls (= 9.793) |
| EMISW | = Gray body emissivity at the wall (= 0.8) |
| EPSX | = Grid expansion factor in axial direction |
| FACTOR | = Area ratio of setting initial u-velocity field |
| FLOW | = Mass flow rate at a cross-section based on calculated velocity |
| FLOWIN | = Total mass flow rate entering pipes |
| FU(I,J) | = Mass fraction of fuel |
| FUIN | = Mass fraction of fuel at the inlet |
| GE | = Mass flux through east-wall of cell |
| GEN(I,J) | = Generation of turbulence by shear from mean flow |
| GENCOU | = Part of generation term modified in terms of wall shear stress |
| GENRES | = Total unmodified generation of turbulence (GEN(I,J) less $\mu_t (\partial v / \partial x)^2$). |

| | |
|----------|--|
| GN | = Mass flux through north-wall of cell |
| GNW | = Mass flux through north-wall of u-cell |
| GP | = Mass flux at location of velocity |
| GREAT | = A very large value (10^{30}) |
| GS | = Mass flux through south-wall of cell |
| GSW | = Mass flux through south-wall of u-cell |
| H(I,J) | = Enthalpy |
| H2(I,J) | = Mass fraction of H ₂ |
| H2O(I,J) | = Mass fraction of H ₂ O |
| HCO | = Heating value of CO |
| HEDARR | = Heading 'ARRHENIUS MODEL' |
| HEDCO | = Heading 'CO MASS FRACTION' |
| HEDCO2 | = Heading 'CO2 MASS FRACTION' |
| HEDDEN | = Heading 'DENSITY' |
| HEDED | = Heading 'ENERGY DISSIPATION' |
| HEDFU | = Heading 'FUEL MASS FRACTION' |
| HEDFUP | = Heading 'HEDFUP' |
| HEDH | = Heading 'STAGNATION ENTHALPY' |
| HEDH2 | = Heading 'H2 MASS FRACTION' |
| HEDH2O | = Heading 'H2O MASS FRACTION' |
| HEDKE | = Heading 'TURBULENT KINETIC ENERGY' |
| HEDKP | = Heading 'KPLUS = TE*RHO/TAUN' |
| HEDLS | = Heading 'LENGTH SCALE' |
| HEDN | = Heading 'N MASS FRACTION' |
| HEDNDT | = Heading 'NON DIMENSIONAL TEMPERATURE' |
| HEDNOU | = Heading 'NON DIMENSIONAL U VELOCITY' |
| HEDNDV | = Heading 'NON DIMENSIONAL V VELOCITY' |

| | |
|--------|--|
| HEDNDW | = Heading 'NON DIMENSIONAL W VELOCITY' |
| HEDNI | = Heading 'PRODUCT MASS FRACTION' |
| HEDNO | = Heading 'NO MASS FRACTION' |
| HEDO | = Heading 'O MASS FRACTION' |
| HEDOF | = Heading 'OXYGEN FUEL RATIO' |
| HEDOX | = Heading 'OXYGEN MASS FRACTION' |
| HEDP | = Heading 'PRESSURE' |
| HEDRR | = Heading 'R DIRECTION RADIATION' |
| HEDRX | = Heading 'X DIRECTION RADIATION' |
| HEDTEM | = Heading 'TEMPEATURE' |
| HEDU | = Heading 'U VELOCITY' |
| HEDV | = Heading 'V VELOCITY' |
| HEDVIS | = Heading 'VISCOSITY' |
| HEDW | = Heading 'W VELOCITY' |
| HFU | = Heating value of fuel |
| HIN | = Inelt stagnation enthalpy |
| I | = Index for dependent variables, and co-ordinates |
| ICNP1 | = ICON + 1 |
| ICON | = I-index of the constricted outlet |
| IHBM1 | = IHUB - 1 |
| IHBP1 | = HHUB + 1 |
| IHUB | = I-index of centerline hub |
| IMON | = I-index of monitoring location |
| INCALC | = Logical parameter for solution of CO-equation |
| INCALD | = Logical parameter for soluiton of ϵ -equation |
| INCALF | = Logical parameter for solution of FU-equation |
| INCALH | = Logical parameter for solution for H-equation |

| | |
|--------|---|
| INCALK | = Logical parameter for solution of k-equation |
| INCALO | = Logical parameter for solution of OF-equation |
| INCALP | = Logical parameter for solution of P-equation |
| INCALU | = Logical parameter for solution of U-equation |
| INCALV | = Logical parameter for solution of V-equation |
| INCALW | = Logical parameter for solution of W-equation |
| INCLNO | = Logical parameter for solution of NO-equation |
| INCLRR | = Logical parameter for solution of RADR-equation |
| INCLRX | = Logical parameter for solution of RADX-equation |
| INCOLD | = Logical parameter for cold flow solution |
| INDCOS | = Control index for definition of co-ordinate system (= 1 for plane flows; = 2 for axisymmetric flows) |
| INHOT | = Logical parameter for hot flow solution |
| INLET | = Logical parameter for printing initial conditions |
| INPRO | = Logical parameter for updating of fluid properties |
| IPREF | = I-index of location where pressure is fixed |
| ISTEP | = I-index of entrance plane, within calculation domain |
| ISTM1 | = ISTEP-1 |
| ISTP1 | = ISTEP+1 |
| IT | = I-index of maximum dimension of dependent variables |
| J | = Index for dependent variables, and co-ordinate |
| JCNPI | = JCON+1 |
| JCON | = J-index of the constricted outlet |
| JHBM1 | = JHUB-1 |
| JHBPI | = JHUB+1 |
| JHUB | = J-index of the centerline hub |
| JMON | = J-index of monitoring location |

| | |
|--------|--|
| JPREF | = J-index of location where pressure is fixed |
| JSTEP | = J-index of horizontal plane next to wall of, and within, smaller pipe |
| JSTM1 | = JSTEP-1 |
| JSTP1 | = JSTEP+1 |
| JT | = J-index of maximum dimension of dependent variables |
| LFS | = Index for counting loops for swirl |
| LFSMAX | = Number of swirl loops to be run |
| MAXIT | = Maximum number of iterations to be completed if iteration sequence is not stopped by test on value of SOURCE |
| NI | = Maximum value of I-index |
| NIM1 | = NI-1 |
| NITER | = Number of iterations completed |
| NJ | = Maximum value J-index |
| NJM1 | = NJ-1 |
| NSBR | = Zero value specifies flat W profile; the value one specifies solid body rotation |
| NSWPC | = Number of applications of line iteration for CO-equation |
| NSWPD | = Number of applications of line iteration for ε -equation |
| NSWPF | = Number of applications of line iteration for FU-equation |
| NSWPH | = Number of applications of line iteration for H-equation |
| NSWPK | = Number of applications of line iteration for K-equation |
| NSWPN0 | = Number of applications of line iteration for NO-equation |

| | |
|----------|---|
| NSWPO | = Number of applications of line iteration for OF-equation |
| NSWPO | = Number of applications of line iteration for P'-equation |
| NSWPRR | = Number of applications of line iteration for RADR-equation |
| NSWPRX | = Number of applications of line iteration for RADX-equation |
| NSWPU | = Number of applications of line iteration for U-equation |
| NSWPV | = Number of applications of line iteration for V-equation |
| NSWPW | = Number of applications of line iteration for W-equation |
| OI(I,J) | = Mass fraction of O |
| OF(I,J) | = Oxygen fuel ratio |
| OX(I,J) | = Mass fraction of O ₂ |
| OXDFU | = Stoichiometric oxygen to fuel ratio |
| OXDCO | = Stoichiometric oxygen to CO ratio |
| OXIN | = Inlet oxygen mass fraction |
| P(I,J) | = Pressure, P |
| PHI(I,J) | = General representation for all dependent variables, ϕ |
| PP(I,J) | = Pressure-correction, P' |
| PRANDT | = Turbulent Prandtl number |
| PRED | = Constant of turbulence model in ϵ -equation, σ_{ϵ} |
| PRIN | = Inlet concentration of N ₂ |
| PRTE | = Constant of turbulence model in k-equation, σ_{ϵ} |
| R(J) | = Radius of main grid node (I,J) from symmetry axis |
| RADIN | = Inlet radiation value |

| | |
|-------------|--|
| RADR(I,J) | = R-direction radiation flux |
| RADX(I,J) | = X-direction radiation flux |
| RCO | = Consumption rate for CO |
| RCOARR(I,J) | = Arrhenius consumption rate of CO |
| RCOEBU(I,J) | = Eddy-Break-Up consumption rate of CO |
| RCV(J) | = Radius of C- and U-cell center |
| RESOR | = Residual source for individual control volume |
| RESORC | = Sum of residual sources within calculation domain for CO-equation |
| RESORE | = Sum of residual sources within calculation domain for ϵ equation |
| RESORF | = Sum of residual sources within calculation domain for FU-equation |
| RESORH | = Sum of residual sources within calculation domain for H-equation |
| RESORK | = Sum of residual sources within calculation domain for k-equation |
| RESORM | = Sum of mass sources within calculation domain |
| RESORO | = Sum of residual sources within calculation domain for OF-equation |
| RESORR | = Sum of residual sources within calculation domain for RADR-equation |
| RESORX | = Sum of residual sources within calculation domain for RADX-equation |
| RESORU | = Sum of residual sources within calculation domain for U-equation |
| RESORV | = Sum of residual sources within calculation domain for |

| | |
|-------------|--|
| | V-equation |
| RESORW | = Sum of residual sources within calculation domain for W-equation |
| RESRNO | = Sum of residual sources within calculation domain for NO-equation |
| RFUARR(I,J) | = Arrhenius consumption rate of fuel |
| RFUEBU(I,J) | = Eddy-break-up consumption rate of fuel |
| RFUP(I,J) | = Minimum (RFUARR,RFUEBU) |
| RLARGE | = Radius of large pipe |
| RNOF1,2 | = Forward reaction rates for NO |
| RNPRI,2 | = Reverse reaction rates for NO |
| RSDRL | = RSMALL/RLARGE |
| RSMALL | = Radius of small pipe |
| RV(J) | = Radius of location of V(I,J) from symmetry axis |
| SCATT | = Scattering coefficient (= 0.01) |
| SEW(I) | = $0.5 \cdot (DXEP(I) + DXPW(I))$ |
| SEWU(I) | = $0.5 \cdot (DXEPU(I) + DXPWU(I))$ |
| SIGMA | = Stefan-Boltzman constant (= $5.6693 \text{ E} - 08$) |
| SMP | = Net outflow from control volume |
| SNS(J) | = $0.5 \cdot (DYNP(J) + DYPS(J))$ |
| SNSV(J) | = $0.5 \cdot (DYNPV(J) + DYPSV(J))$ |
| SORCE | = Maximum of RESORM, RESORVU, RESORV, RESORW, RESORK |
| SORMAX | = Maximum acceptable value of SORCE for converged solution |
| SORVOL | = GREAT * VOL |
| SP(I,J) | = Coefficient of linearized source treatment |
| SPKD(I,J) | = -CP, for k- and ϵ -equations |

| | |
|-----------|--|
| SSC | = Shear-stress coefficient |
| SU(I,J) | = Coefficient of linearized source treatment |
| SUKD(I,J) | = $CP0 * TE(I,J)$, for k-equation |
| | = $CP0 * ED(I,J)$, for ϵ -equation |
| SWNB(LFS) | = Inlet swirl number specification of WINST |
| T(I,J) | = Temperature |
| TAUN(I) | = Shear stress at north wall-boundary of flow domain |
| TAUS(I) | = Shear stress at south wall-boundary of flow domain |
| TAUW(J) | = Shear stress at west wall-boundary of flow domain |
| TE(I,J) | = Turbulence energy, k |
| TEIN | = Turbulence energy at inlet of flow domain (k_{in}) |
| TIN | = Inlet temperature |
| TMULT | = Coefficient of wall shear-stress expression |
| TT(I,J) | = Non-dimensional temperature |
| TURBIN | = Turbulence intensity factor at inlet of flow domain |
| U(I,J) | = Component of mean velocity in axial direction (u-velocity) |
| UEFF | = $SQRT[U(I,J)**2 + W(I,J)**2]$ |
| UIN | = U-velocity at inlet of flow domain |
| UINC | = Uniform increment of u-velocity at outlet of flow domain |
| ULARGE | = $UIN * (RSMALL/RLARGE)**2$ |
| UMEAN | = Mean u-velocity at inlet |
| URFCO | = Under-relaxation factor for carbon monoxide |
| URFDEN | = Under-relaxation factor for density |
| URFE | = Under-relaxation factor for energy-dissipation |
| URFF | = Under-relaxation factor for fuel consumption |

| | |
|------------|---|
| URFH | = Under-relaxation factor for enthalpy |
| URFK | = Under-relaxation factor for turbulence energy |
| URFNO | = Under-relaxation factor for nitrogen oxide |
| URFO | = Under-relaxation factor for oxygen-fuel ratio |
| URFP | = Under-relaxation factor for pressure-correction |
| URFRR | = Under-relaxation factor for r-radiation |
| URFRX | = Under-relaxation factor for x-radiation |
| URFU | = Under-relaxation factor for u-velocity |
| URFV | = Under-relaxation factor for v-velocity |
| URFVIS | = Under-relaxation factor for viscosity |
| URFW | = Under-relaxation factor for w-velocity |
| USTAR(I,J) | = Dimensionless u-velocity |
| V(I,J) | = Component of mean velocity in radial direction (v-velocity) |
| VANB(LFS) | = Swirl vane angle |
| VAVG | = Average v-velocity between nodes (I,J) and (I,J + 1) |
| VDR | = $V(I,J)/RV(J)$ |
| VIS(I,J) | = Effective viscosity |
| VISCOS | = Laminar viscosity |
| WISE | = Effective viscosity at mid-point of east-wall of cell |
| VISOLD | = Value of effective viscosity before underrelaxation |
| VISN | = Effective viscosity of mid-point of north-wall of cell |
| VISS | = Effective viscosity of mid-point of south-wall of cell |
| VISW | = Effective viscosity at mid-point of west-wall of cell |
| VOL | = Volume of cell or control-volume |
| VSTAR(I,J) | = Dimensionless v-velocity |
| W(I,J) | = w-velocity |

| | |
|------------|--|
| WAN2 | = Molecular weight of N_2 (also WPR) |
| WCO | = Molecular weight of CO |
| WC02 | = Molecular weight of CO_2 |
| WH2 | = Molecular weight of H_2 |
| WH20 | = Molecular weight of H_2O |
| WIN | = Inlet w-velocity from swirl vanes |
| WINST | = Inlet w-velocity at JSTEP from solid body rotation swirl generator |
| WMONIN | = Inlet swirl momentum |
| WN1 | = Molecular weight of N |
| WNO | = Molecular weight of NO |
| WO1 | = Molecular weight of O |
| WOX | = Molecular weight of O_2 |
| WSTAR(I,J) | = Dimensionless w-velocity |
| X(I) | = Distance from inlet plane in axial direction |
| XMONIN | = Momentum of fluid at inlet of flow domain |
| XND(I) | = Dimensionless X(I) |
| XPLUSW(I) | = Local Reynolds number based on friction velocity and distance from west wall-boundary of flow domain |
| XU(I) | = X-coordinate of storage location of U(I,J) |
| Y(J) | = Distance from symmetry axis in radial direction |
| YND(J) | = Dimensionless Y(J) |
| YPLUSN(J) | = Local Reynolds number based on friction velocity and distance from north wall-boundary of flow domain |
| YV(J) | = Y-coordinate of storage location of V(I,J) |
| YUND(J) | = Dimensionless YV(J) |

2
VITA

Jerry Wayne Samples

Candidate for the Degree of
Doctor of Philosophy

Thesis: PREDICTION OF AXISYMMETRIC CHEMICALLY-REACTING COMBUSTOR
FLOWFIELDS

Major Field: Mechanical Engineering

Biographical:

Personal Data: Born in Staunton, Virginia, July 18, 1947, the son
of Mr. and Mrs. Wilmer C. Samples.

Education: Graduated from Glen Cove High School, Glen Cove, New
York, in June, 1965; received Bachelor of Science in Chemical
Engineering degree from Clarkson College of Technology in
1969; received Master of Science degree from Oklahoma State
University in 1979; completed requirements for the Doctor of
Philosophy degree at Oklahoma State University in May, 1983.

Professional Experience: Laboratory Technician, Columbia Ribbon
and Carbon, Mfg., Co., 1969-1970; Combat Engineer, United
State Army, 1970-1977; Instructor and Assistant Professor,
United States Military Academy, West Point, 1979-1982.